Doctoral Thesis

Role of Mesenchymal Stromal Cells and their Extracellular Vesicles microRNAs in JAK2 Myeloproliferative Neoplasms

Supervisors

Profª. Dra. María Consuelo del Cañizo

Dr. Fermín Sánchez-Guijo

Dr. Luis Ignacio Sánchez-Abarca

Teresa da Conceição Lopes Ramos

Salamanca, 2016

Profª. Dra. María Consuelo del Cañizo Fernández-Roldán, con D.N.I. 03404639H, Profesora Catedrática de Hematología y Hemoterapia de la Universidad de Salamanca (USAL) y Jefa de Servicio de Hematología y Hemoterapia del Hospital Universitario de Salamanca (HUS).

Dr. Fermín Sánchez-Guijo Martín, con D.N.I. 07869479Y, Profesor Asociado de Ciencias de la Salud de la Universidad de Salamanca (USAL) y Responsable del Área de Terapia Celular y Hematopoyesis del Servicio de Hematología del Hospital Universitario de Salamanca (HUS).

Dr. Luis Ignacio Sánchez-Abarca Bernal con D.N.I. 07865299N Doctor en Farmacia e Investigador Posdoctoral en la Fundación Investigación del Cáncer de la Universidad de Salamanca (IBMCC)

CERTIFICAN

que han dirigido esta Tesis Doctoral titulada ***"Role of Mesenchymal Stromal Cells and their Extracellular Vesicles microRNAs in JAK2 Myeloproliferative Neoplasms"*** realizada por Dña. Teresa da Conceição Lopes Ramos, que obtuvo su Diploma de Estudios Avanzados en la Universidad de Salamanca (USAL), a través del programa de Programa de Doctorado en Biociencias: Biología y Clínica del Cáncer y Medicina Traslacional (CiC-IBMCC).

Y AUTORIZAN

la presentación de la misma, considerando que reúne las condiciones de originalidad y contenidos requeridos para optar al grado de Doctor por la Universidad de Salamanca.

En Salamanca, a 6 de Julio de 2016

Profª Dra. M. C. del Cañizo Dr. F. Sánchez-Guijo Dr. L.I. Sánchez-Abarca

Este proyecto de tesis ha sido financiado por:

- La Fundação para a Ciência e Tecnologia, Governo de Portugal, expediente, **SFRH/BD/86451/2012**.

- Proyecto de la Consejería de Sanidad de Castilla y León, expediente, **GRS 1034/A/14**.

- Red Temática de Investigación Cooperativa en Cáncer **(RTICC-**ISCIII), expediente**, (RD12/0036/0069)**

- Fondo de Investigación Sanitaria, Instituto de Salud Carlos III, Ministerio de Sanidad, expediente, **PI12/01775**

Los resultados obtenidos a lo largo de esta Tesis Doctoral han sido publicados como artículos en las siguientes revistas:

Ramos, T.L., Sanchez-Abarca, L.I., Muntion, S., Preciado, S., Puig, N., Lopez-Ruano, G., Hernandez-Hernandez, A., Redondo, A., Ortega, R., Rodriguez, C., Sanchez-Guijo, F. & del Canizo, C. (2016) *MSC surface markers (CD44, CD73, and CD90) can identify human MSC-derived extracellular vesicles by conventional flow cytometry.* Cell Commun Signal 2016; 14: 2.

Los resultados obtenidos a lo largo de esta Tesis Doctoral han sido presentados en los siguientes congresos:

Teresa L. Ramos; Luis Ignacio SánchezAbarca; Beatriz Rosón; Concepción Rodríguez Serrano; Alba Redondo; Rebeca Ortega; Ángel HernándezHernández; Sandra Muntión; Silvia Preciado; José Ramón GonzálezPorras; Fermín Sánchez Guijo; Consuelo Del Cañizo. *HDAC8 Overexpression in Mesenchymal Stromal Cells from JAK2^{+} myeloproliferative Neoplasms: A New Therapeutic Target?* 57th ASH Annual Meeting and Exposition, Orlando, Florida, EUA. 2015. Póster

Teresa L. Ramos; Luis I. Sánchez-Albarca; Beatriz Rosón; Concepción Rodríguez Serrano; Alba Redondo; Rebeca Ortega; Ángel Hernández-Hernández; Sandra Muntión; Silvia Preciado; Javier de las Rivas; José Ramón González-Porras; Fermín Sánchez-Guijo; Consuelo del Cañizo**.** *Implications of HDAC8 overexpression in mesenchymal stromal cells of JAK2^{+} myeloproliferative neoplasm* Reunião Anual da SPH, Figueira da Foz, Portugal. 2015. Oral

Teresa L. Ramos; Luis Ignacio Sánchez-Abarca; Silvia Preciado; Beatriz Rosón; Ángel Hernández-Hernández; Sandra Muntión; Concepción Rodríguez Serrano; Rebeca Ortega; Alba Redondo; Fermín Sánchez-Guijo; Consuelo del Cañizo. La sobre-expressión de HDAC8 en células *Mesenquimales estromales de pacientes con neoplasias mieloproliferativas JAK2*$^{+}$ *¿Una nueva diana terapéutica?* LVII Congreso Nacional de la SEHH y del XXXI Congreso Nacional de la SETH, Valencia. 2015. Sesión Plenaria - Oral

Teresa Lopes Ramos; Luis Ignacio Sánchez-Albarca; Alba Redondo; Sandra Muntión; Beatriz Rosón; Silvia Preciado; Maria E. Alonso-Sarasquete; Fermín Sánchez-Guijo; Mª Consuelo Del Cañizo. *Differential gene expression analysis of mesenchymal stromal cells from patients with JAK2*$^{+}$ *Polycythemia Vera and Essential Thrombocytemia.* Reunião anual SPH 2014. Évora, Portugal Oral

Teresa Lopes Ramos; Luis I. Sánchez-Albarca; Alba Redondo; Beatriz Rosón; Silvia Preciado; Maria E. Alonso-Sarasquete; Fermín Sánchez-Guijo; Mª Consuelo Del Cañizo. *Análisis de expresión génica diferencial de las células mesenquimales de pacientes con neoplasias mieloproliferativas JAK2*$^{+}$*: Policitemia vera versus trombocitemia esencial.* LVI Congreso Nacional de la Sociedad Española de Hematología y Hemoterapia. Madrid, España. 2014. Póster

Acknowledgements / Agradecimientos

La realización de esta tesis doctoral fue posible gracias a la contribución de muchas personas. Por este motivo, me gustaría mostrar mi agradecimiento a todos los que de una manera u otra han contribuido en mi aprendizaje.

A mis directores de tesis:

- La Profesora Dra. Consuelo del Cañizo por permitirme formar parte de su grupo, por transmitirme su experiencia, su filosofía de trabajo y su pasión por la investigación. Ha sido un privilegio poder trabajar a su lado.

- Al Dr. Fermín Sánchez-Guijo, por su optimismo y entusiasmo, por los muchos conocimientos que me ha transmitido, y principalmente por depositar en mí la confianza necesaria para llevar a cabo este trabajo permitiéndome crecer como investigadora.

- Al Dr. Luis Ignacio Sánchez-Abarca, por sus consejos científicos y no tan científicos (los de la vida…), su tiempo, su paciencia, y su amistad en todo momento. Siempre me ha ayudado de forma desinteresada y me ha conducido por el buen camino.

A todos los miembros del Laboratorio de Terapia Celular, a los que están (Ana Gómez, Ana Rico, Alba Redondo, Haidy Moreno, Silvia Preciado, Sandra Muntión, Belén Blanco, Luis Alba, Olga López y a María Díez Campelo (siempre pendiente de mis muestras)), a los que estuvieron (Carmen Herrero, Soraya Carrancio, Teresa Caballero, Miryam Santos, Silvia Gutiérrez, Elena Martín y Carlos Romo) y a los que vinieron de paso, porque cada uno ha aportado su granito de arena.

A Conchi Rodríguez y Rebeca Ortega siempre han estado a mi lado en los buenos y en los malos momentos. Por este motivo, siempre las llevaré en mi corazón. También quiero agradecer a todo el personal de la sala blanca por su espíritu de colaboración.

A todos los Laboratorios y al Servicio de Hematología del Hospital Clínico Universitario de Salamanca: investigadores, personal técnico, personal médico, enfermeras, personal administrativo y de mantenimiento, porque todos hacen de este servicio, un servicio de referencia.

A todos los integrantes del laboratorio 12 del CIC, por vuestra ayuda y apoyo. Al equipo del profesor Ángel Hernández-Hernández por adoptarme, apoyarme como si fuera un miembro más de su laboratorio y aleccionarme en el interesante mundo del Western Blot. A Guillermo Ruano que ha tenido la paciencia de dedicarme su tiempo para “enseñar”.

Quiero también agradecer a Noemí Puig por su gran amistad y por convertirse en mi médico de cabecera.

Quiero agradecer a mis *tugas* Salmantinas, Teresa Amaral, Inês Mota y Patricia Domingues por facilitarme el camino, por escuchar y comprender en los momentos de dificultad.

“Si quieres ir rápido vas solo, pero si quieres ir lejos tienes que ir acompañado"…

¡Gracias a todos por acompañarme en este camino!

Agora, é a parte que dedico esta tese à minha Família e principalmente ao meu irmão Pedro. Tenho a certeza que estás muito orgulhoso de mim, TU que me ensinaste a encher o peito de ar e a encarar a vida como se fossemos os reis do mundo. Aos meus pais que estão sempre na retaguarda, para limparem as feridas e dar motivação. Ao Jun por fazer-me rir e ser o meu professor de inglês particular. Aos meus amigos, que mesmo longe, sempre transmitiram as suas boas vibrações.

“O valor das coisas não está no tempo em que elas duram, mas na intensidade com que acontecem. Por isso existem momentos inesquecíveis, coisas inexplicáveis e pessoas incomparáveis”

Fernando Pessoa

“Everything we hear is an opinion, not a fact!

Everything we see is a perspective, not the truth!”

Marcus Aurelius

Table of contents

Abstract

Background

Bone marrow-derived mesenchymal stromal cells (BM-MSC) are crucial for haematopoietic niche maintenance. There is evidence of continuous cross-talk between the neoplastic cells and BM-MSC, inducing the modulation of both populations, which may favour the emergence and progression of myeloproliferative neoplastic (MPN) disease. Extracellular vesicles (EV) have emerged as new players in cell-to-cell communication. These structures are associated with the bidirectional transfer of proteins, mRNA, microRNA between cancer cells and stromal cells, inducing functional and genetic alterations in neighbouring cells.

Objectives and methodology

- To characterise and compare BM-MSC from MPN patients ($JAK2^{V617F}$) with BM-MSC from HD and CML patients, population doubling, multilineage differentiation, immunophenotype, apoptosis and cell cycle assays were performed.

- To study the presence of genomic alterations in the BM-MSC from ET and PV patients, and compare to control MSC (HD), a global analysis of gene expression profile from the different experimental groups was performed, using Affymetrix Oligoarrays (Human Gene 1.0 ST arrays). RT-PCR and Western blot (WB) were performed to confirm the results.

- To evaluate if the alteration in the BM-MSC from JAK-2 MPN patients modifies the capacity to support normal and MPN haematopoietic progenitor cells, clonogenic (CFU-GM) and long-term BM culture (LTBMC) assays were performed.

- To identify altered genes and pathways in the MPN-MSC which could potentially be used as therapeutic targets, we selected from the previous experiments histone deacetylase 8 (HDAC8). Then we treated BM-MSC from HD and MPN patients with a specific inhibitor PCI34051 at concentration of 25µM during 48h. The effects of HDAC8i on the BM-MSC was evaluated by annexing V (apoptosis), cell cycle, RT-PCR and WB. To assess the impact of this inhibition on the capacity of MPN-MSC to support haematopoiesis, BM mononuclear cells (BM-MNC) were co-cultured in transwell for 48h, with PCI34051-treated and non-treated BM-MSC. After co-culture, cell viability, CFU-GM assays and TP53 expression were analysed.

- To compare the microRNA content in the MSC-derived extracellular vesicles (EV) from HD and MPN patients, and to study the functional alterations that may be induced when incorporated into haematopoietic progenitor cells. Firstly, EV were isolated from BM-MSC of MPN patients and HD, and were purified by ultracentrifugation. For EV characterisation, transmission electron microscopy (TEM), NanoSight, flow cytometry (MFC) and WB for CD63 were performed. To evaluate microRNA content into EV-MSC from both groups (patients and controls), expression of miRNA was analysed using 384-well microfluidic cards (TaqMan® MicroRNA Array A).

EV incorporation was demonstrated by fluorescence microscopy and MFC, where HPC (CD34+cells obtained by immunomagnetic selection) were co-cultured with EV previously labelled with Vybrant Dil. To study HPC modification induced by the incorporation of EV, apoptosis and clonogenic assays were performed.

Results

Compared to HD, BM-MSC from MPN patients showed similar morphology and differentiation capacity, with an increased proliferation rate with less apoptotic cells. BM-MSC from MPN expressed comparable levels of CD73, CD44, CD90 and CD166, whereas they were negative for haematopoietic markers. The median expression of CD105 was lower in BM-MSC from MPN patients ($p < 0.05$) when compared to controls. Gene expression profile of BM-MSC showed a total of 169 genes that were differentially expressed in BM-MSC from MPN patients compared to HD. RT-PCR was performed in two genes to confirm these results, demonstrating that HDAC8 and MYADM genes were up-regulated. Next, we observed a significant increase in the number of CFU-GM when MPN-HPC were co-cultured with MPN-MSC compared to HD-MSC. MPN-MSC also showed the ability to support healthy HPC in LTBMC. However, MPN-MSC showed alterations in the expression of genes associated to the maintenance of haematopoiesis.

The inhibition of HDAC8 in BM-MSC from MPN was confirmed by RT-PCR and WB assays, when the cells were treated with PCI34051. HDAC8-selective inhibition also induced a cell cycle arrest in the MPN BM-MSC, with an increase of the percentage of apoptotic cells. Co-cultures of BM-MNC from MPN patients with neoplastic stroma previously treated with HDAC8 inhibitor induced a decrease in MNC cell viability ($p=0.028$), CFU-GM ($p=0.018$) and an increase of TP53 expression.

Regarding the EV studies, we showed that the characterisation by TEM and NanoSight revealed that EV-MSC from both groups exhibited a size and morphology characteristic of EV, and were positive for CD63 (WB), the characteristic marker of EV. By MFC, EV released from BM-MSC of both groups (HD and JAK2) were defined as particles less than 1µM of diameter, positive for CD90, CD44 and CD73 and for EV markers. At the same time they were negative for CD34 and CD45, demonstrating the specificity of monoclonal labelling. When the content of microRNA was analysed (8 HD-MSC and 11 MPN-MSC), we observed an overall increase in the microRNA expression in the EV from patients, yet without reaching statistical significance.

Using RT-PCR, we observed a significant overexpression ($p=0.032$) of miR-155 in the EV derived from MPN-MSC. We also observed an increase of CD34+ cell viability, after the incorporation of EV from both groups (HD and JAK2). A significant increase ($p=0.04$) of miR-155 expression was observed in the HD CD34+ cells, after incorporating MPN-MSC-derived EV. In addition, an increase of CFU-GM was observed when neoplastic CD34+ cells incorporated the EV derived from MSC from MPN patients ($p=0.056$).

Conclusions

These results suggest that MPN-MSC display different proliferative rate, immunophenotypic markers, gene expression profile and HDAC8 overexpression compared to HD-MSC. The inhibition of HDAC8 expression by its specific inhibitor decreases the capacity of the stroma to support haematopoietic cells from MPN patients, suggesting that HDAC8 may be a potential therapeutic target. Furthermore, we suggest that EV released from MPN-MSC represent a mechanism of intercellular communication between malignant stromal and haematopoietic cells, through the transfer of genetic information that may be relevant in the pathophysiology of these diseases**.**

List of Abbreviations

A

AGM: aorta-gonad mesonephros

AML: Acute Myeloid Leukaemia

ANGPT1: Angiopoietin 1

APC: Allophycocyanin

B

BM: Bone marrow

BFU-e: Burst forming unit-erythroid

BMP: Bone morphogenetic protein

BCR-ABL: Breakpoint cluster region - Abelson murine leukaemia

BSA: Bovine serum albumin

BMP2: Bone morphogenetic proteín-2

C

CD: Cluster of Differentiation

CAR cells: CXCL12-abundant reticular cells

CXCR4: C-X-C chemokine receptor type 4

CARL: Gene encoding calreticulin

CFU-GEMM: Colony-forming unit-granulocyte, erythroid, macrophage, megakaryocyte

CXCL12: Chemokine (C-X-C Motif) Ligand 12 or stromal cell-derived factor 1 (SDF1)

CML: Chronic Myeloid Leukaemia

CM: Conditioned medium

CCL3: Chemokine (C-C motif) ligand 3

D

DNMT3A: DNA cytosine methyltransferase 3A

DNA: Deoxyribonucleic acid

DMEM: Dulbecco's Modified Eagle's medium

E

EC: Endothelial cells

ECM: Extracellular matrix

ET: Essential Thrombocythemia

EZH2: Enhancer of zeste homolog 2

EV: Extracellular Vesicles

EDTA: Ethylenediamine tetraacetic acid

F

FITC: Fluorescein isothiocyanate

FBS: Fetal bovine serum

G

GAPDH: Glyceraldehyde-3-phosphate dehydrogenase

H

HSC: Hematopoietic stem cells

HPC: Hematopoietic progenitor cells

HIF-1α: Hypoxia-inducible transcription factor 1-α

HDAC8: Histone Deacetylase 8

I

IDH1/2: Isocitrate dehydrogenase 1 and 2

IL: Interleukin

ISCT: International Society for Cellular Therapy

IMDM: Iscove's Modified Dulbecco's Medium

J

JAK2: Janus Kinase 2

JAG-1: Jagged 1

L

LSC: Leukemic stem cells (LSC)

LT-HSC: Long term – Haematopoietic Stem Cells

LTBMC: Long-term bone marrow cultures

M

MSC: Mesenchymal stromal cells

MPP: Multipotent progenitor cells

MPN: Myeloproliferative neoplasms

MKs: Megakaryocytes

MAPK: Mitogen-activated protein kinase

MDS: Myelodysplastic syndrome

MPL: MPL proto-oncogene - thrombopoietin receptor

MIF: Mean fluorescence intensity

MVB: Multivesicular bodies

MNC: Mononuclear cells

MFC: Multiparametric flow cytometry

N

NF-ƙB: Nuclear factor ƙB

NTB/BCIP: Nitroblue tetrazolium chloride / 5-bromo-4-chloro-3-indolyl-phosphate

NTA: Nano-particle tracking analysis

O

OSTB: Osteoblast

P

PL: Platelet lysate

PTH: Parathyroid hormone

Ph: Philadelphia chromosome

PB: Peripheral blood

PV: Polycythemia Vera

PMF: Primary Myelofibrosis

PD: Population doublings

PCR: Polymerase chain reaction

PE: Phycoerytrin

PerCP: Peridinin chlorophyll protein

PI3K: Phosphatidylinositol-3'-kinase

R

ROS: Reactive oxygen species

RUNX2: Runt-related transcription factor 2

RNA: Ribonucleic acid

RPMI: Roswell Park Memorial Institute

S

SCF: Stem Cell Factor

SPP1: Secreted phosphoprotein 1

SOCS: Suppressors of cytokines signalling

STAT3/5: Signal transducer and activator of transcription 3/5

T

THPO: Thrombopoietin

Tie-2: Receptor tyrosine kinase of the Tie family

TGF-ß: Transforming growth factor-ß ()

TET1: Tet Methylcytosine Dioxygenase 1

TNFα: Tumour necrosis factor α

TEM: Transmission electron microscopy

V

VCAM-1: Vascular cell adhesion protein 1

W

WHO: World Health Organization

List of Figures

List of Tables

1. Haematopoiesis

Blood is one of the most regenerative adult tissues in the human body. Mature blood cells have a short life span, and it is estimated that every day one trillion new blood cells are produced *(Emerson, et al 1987)*. This process is called haematopoiesis, and involves a complex network between hematopoietic stem cells (HSC), intrinsic biology processes, and their connection to the environment. The number of HSC is scarce (1 in every 20 million nucleated cells in the bone marrow (BM)), and the fate of these cells determines if they remain quiescent, proliferate or self-renew, depending on the balance between genetic and environmental mechanisms.

Whereas in adult mammals HSC reside in the BM, during embryogenesis the anatomic location of this process is variable *(Galloway and Zon 2003)*. Primitive haematopoiesis originates in the extra-embryonic yolk sac blood islands and then at the aorta-gonad mesonephros (AGM) region, placenta, fetal liver, and ultimately in the BM *(Costa, et al 2012).*

Hematopoietic stem cells are derived from mesoderm, one of the three primary germ layers of the embryo *(Kinder, et al 1999).* The properties of HSC in each spatial and temporal site presumably reflects the environmental cues that could influence the timing of hematopoietic cell appearance, and the type of hematopoietic cells that develops *(Huber 2010)*.

Different studies have described a population of stem cells that co-express haematopoietic and endothelial surface markers, referred to as hemangioblasts. The concept of a hemogenic endothelium has its origin in early histological studies showing the close spatial and temporal development of haematopoietic and endothelium lineages.

The concept that the entire spectrum of haematopoietic cells originate from a common precursor was first postulated at the end of the 19th century *(Ramalho-Santos and Willenbring 2007)*. The first experimental assays proving this hypothesis were performed in the early 1960s by Till and McCulloch, where they demonstrated a multipotential population in the murine BM *(Till and Mc 1961)*. However, it was with the single cell transplantation experiments that the capacity of a unique isolated long-term HSC (LT-HSC) to reconstitute the

haematopoiesis of lethally-irradiated recipients was demonstrated, showing the ability for the self-renewal and multilineage differentiation ability of the HSC *(Osawa, et al 1996)*.

Recent techniques using advanced cell sorting by flow cytometry and clonal/molecular assays facilitated the identification of human HSC, enabling their biological and functional characterisation at the single cell level. The CD34 antigen was the first and is still the most commonly used marker to recognize and quantitate human HSC and progenitor cells. However, it identifies a highly heterogeneous population that can be further enriched by the exclusion of CD38 and CD45RA, as markers of more differentiated haematopoietic cells. A single cell defined with the phenotype $Lin^{-}CD34^{+}CD38^{-}CD45RA^{-}Thy^{-}Rho^{lo}CD49f^{+}$, transplanted in immunodeficient mice, was capable of long-term multilineage reconstitution *(Notta, et al 2011)*. **Figure 1** represents the haematopoiesis hierarchy (mouse and human), where the loss of CD49f from the LT-HSC gives rise to a more committed human multipotent progenitor (MPP) cell population.

Regarding the hierarchy of human haematopoiesis, it continues to be controversial to understand how individual HSC contribute to lifetime haematopoiesis. Two models of clonal kinetics have been proposed, the first being the “clonal succession”, which is based on the sequential activation of a small number of HSC clones *(Abkowitz, et al 1990)*. The other model, “clonal maintenance”, advocates the average contribution of the entire HSC pool during steady-state haematopoiesis.

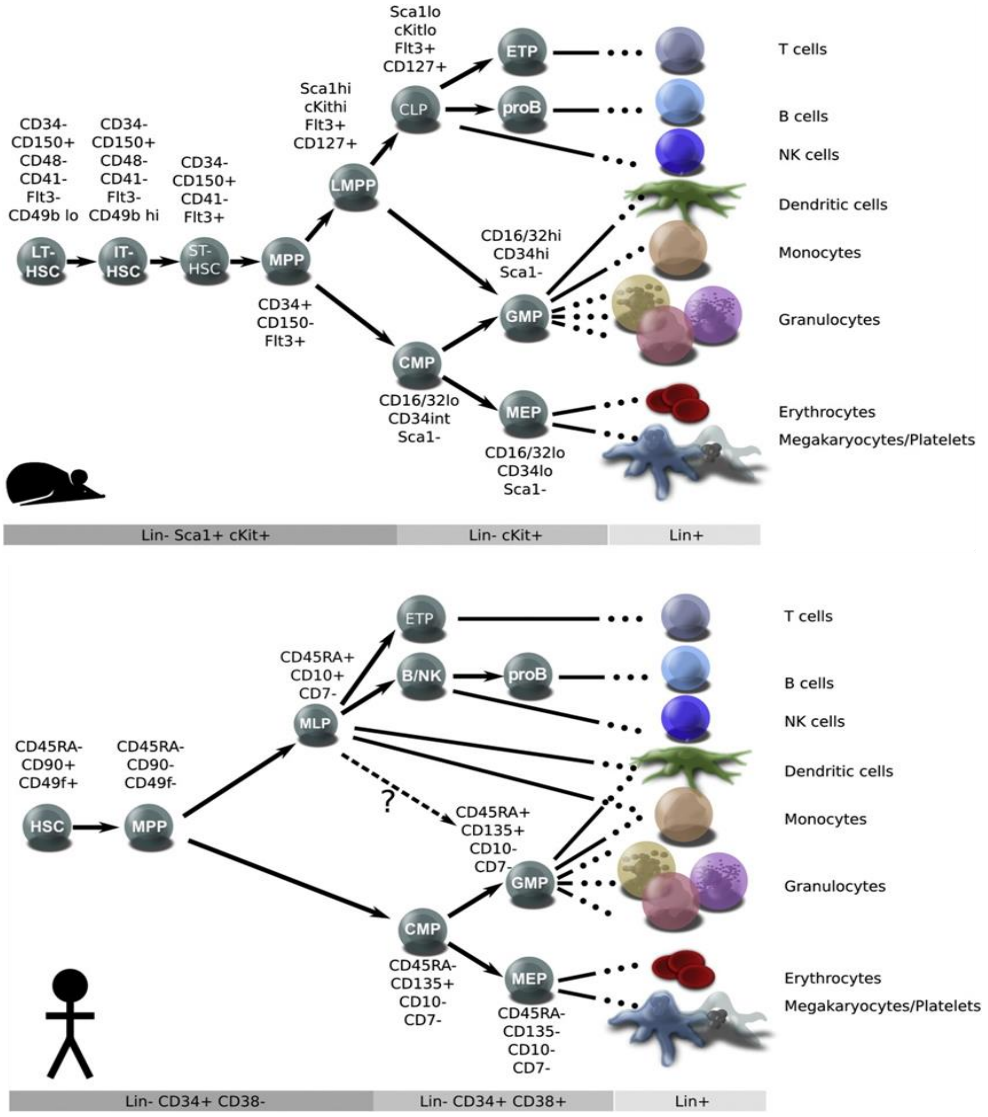

Figure 1: Haematopoietic hierarchy. Simplified schematic representation of adult mouse and human haematopoietic hierarchies. Figure illustrated in the work developed by Doulatov and co-workers. *Cell stem Cell (2012)* ***(Doulatov, et al 2012)***

1.1. Microenvironment cues that disturb haematopoiesis: *mapping the bone marrow*

HSC niche is a very dynamic system defined by their anatomy and function, and is allocated in diverse tissues during the development. After birth, BM represents the primary site of HSC maintenance and haematopoiesis. The work developed by Schofield *(Schofield 1978)* demonstrated the involvement of the BM stromal cells in the regulation and maintenance of HSC.

Determining which cells are responsible for maintaining the stem cell population has been challenging. In the first studies, HSC were observed in the endosteum after being transplanted into irradiated mice, showing the important role of this region in HSC maintenance. Based on these results, it was hypothesised the existence of two distinct BM niches with defined functions: the endosteal niche, and the vascular niche.

The endosteal niche, where osteoblasts represent the major cell type, are responsible for maintaining the HSC in a quiescent state. Osteoblasts provide crucial factors such as thrombopoietin (THPO), CXC chemokine ligand (CXCL12), and angiopoietin 1 (ANG1) *(Arai, et al 2004, Calvi, et al 2003)*. Other factors as the dynamic bone remodelling by osteoclasts, Ca^{2+} gradients, oxygen levels and reactive oxygen species (ROS) also play an important role in the endosteal niche *(Adams, et al 2006, Mansour, et al 2012)*. In the vascular niche, endothelial cells represent the main cell type to maintain the HSC, but inducing a proliferative state of HSC and differentiation.

Recent studies have challenged this concept of two separated niches, suggesting that primitive haematopoietic cells traffic in different and specific micro domains of BM. New stromal cell types have emerged as responsible for supporting the HSC.

In this section the different cues present in each particular cell type that constitute the BM microenvironment will be described (**Figure 2**).

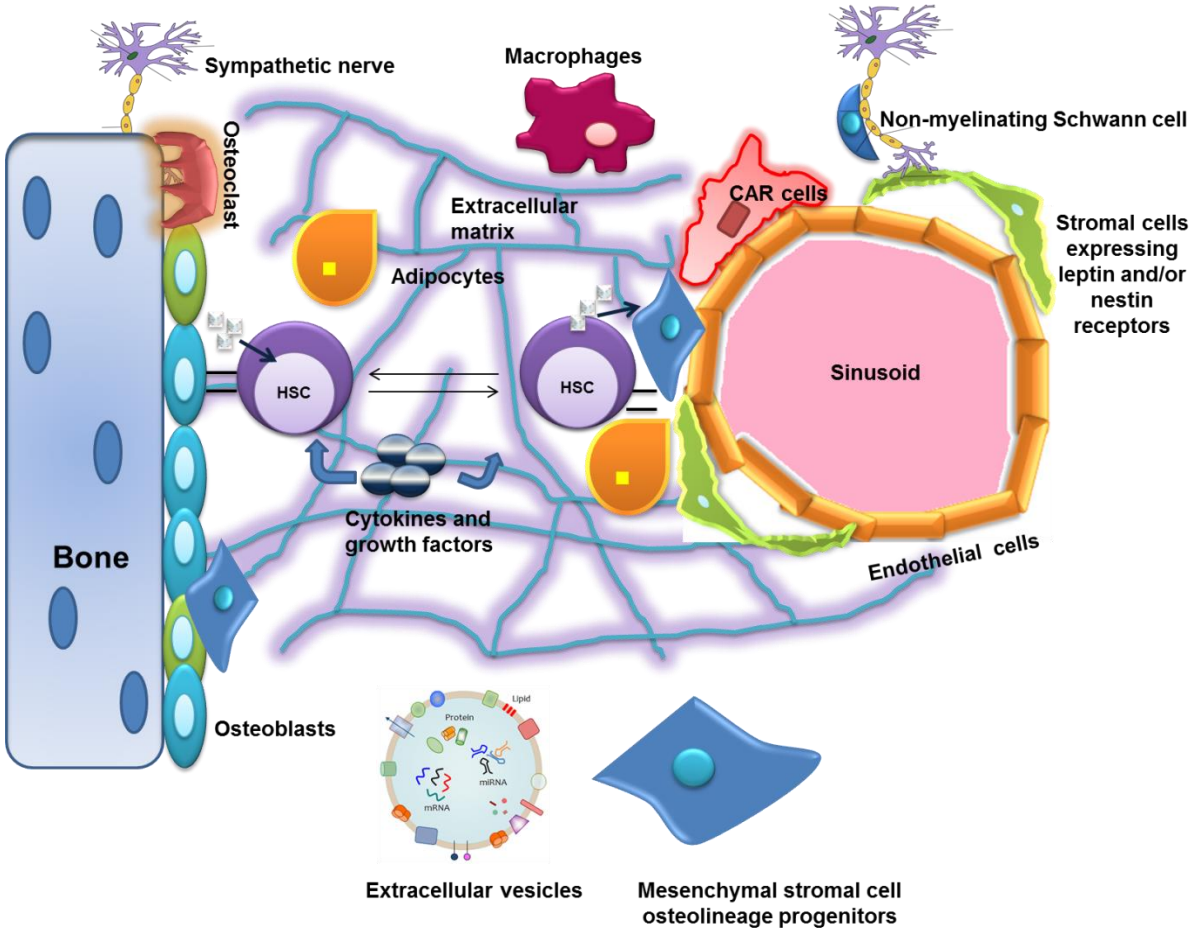

Figure 2: Haematopoietic stem cell niches (structure and function). Bone marrow microenvironment is composed of multiple cell populations that contribute directly or by cytokines and soluble factors to the regulation of haematopoiesis. Real-time imaging showed that HSC are found mainly adjacent to sinusoids through the bone marrow (BM), where two major components of the BM, endothelial cells and mesenchymal stromal cells (MSC), promote HSC maintenance by producing SCF and CXCL12. Extracellular vesicles released from MSC, macrophages, endothelial cells and HSC have gained notoriety in the cross-talk between the BM microenvironment and HSC.

1.1.1. Osteoblasts lineage cells (*endosteal niche*) – are a group of cells that includes mesenchymal progenitor cells, preosteoblasts, mature osteoblasts, bone lining cells and osteocytes. Osteoblasts are characterised by the expression of osteocalcin. The population between mesenchymal progenitor cells and mature osteoblasts (named pre-osteoblasts) is heterogeneous, characterised by the expression of the transcript factor RUNX2, which is maintained at a more advanced state of differentiation accompanied by the expression of osterix *(Fujita, et al 2004)*.

The endosteum is not only constituted by osteoblasts, but also by a diverse group of cells and anatomical elements, including arteriolar and sinusoidal blood vessels *(Lo Celso, et al 2009, Morrison and Scadden 2014).*

Results from *in vivo* studies demonstrating the capacity of osteoblasts to support the haematopoiesis are controversial. The first published results, from two independent groups, showed that transgenic mice genetically altered to produce osteoblastic cells by constitutively activated receptor for parathyroid hormone (PTH) and PTH-related peptide-PTH/ PTHrP receptors (PPRs), showed not only an increase of osteoblasts (number) but also an increase of the Notch ligand jagged 1 levels, that was associated with HSC proliferation *(Calvi, et al 2003).* The other *in vivo* study was published by Zhang *et al*., and suggested that the adhesion of HSC to osteoblasts may be mediated by N-cadherin. In this case, they developed a mouse genetically modified with conditional inactivation of bone morphogenetic protein (BMP) receptor type IA (BMPRIA), showing the correlation between an increase of spindle-shaped N-cadherin $CD45^-$ osteoblastic cells and HSC *(Zhang, et al 2003)*.

Recent results challenge the importance of the key adhesion molecule N-cadherin in promoting HSC maintenance. The deletion of the gene that encodes N-cadherin (cdh2) from HSC or from osteoblasts cells had no effect on HSC frequency and function *(Greenbaum, et al 2012, Kiel, et al 2009)*. The work of Calvi was also challenged in 2012 by herself, showing that PTH receptor activation increases not only the number of osteoblasts, but also osteocytes and osteoclasts in the trabecular bone. However, it was not enough to induce phenotypic and functional changes in the BM-HSC *(Calvi, et al 2012)*.

Although the role of osteoblast or osteolinage cells in the regulation of the hematopoietic system is not fully understood, several studies have suggested the relation between this two systems. Osteoblasts express important factors that regulate HSC quiescence, as osteopontin, THPO and Angp-1. The depletion of THPO in mice ($THPO^{-/-}$) increase HSC proliferation and reduce their number *(Yoshihara, et al 2007).* The expression of Angp-1 by osteoblasts can activate the receptor tyrosine kinase and EGF-like domain 1 (Tie-2) in HSC, promoting their adhesion by increasing ß1 integrin subunit and their quiescence *(Arai, et al 2004)*.

In addition to the direct influence of osteoblasts in the HSC, indirect effects like bone turnover also affects the HSC. The degradation and formation of osteolineage cells results in high local concentrations of ionic calcium, promoting the expression of calcium-sensing receptor in the HSC, that is important for the engraftment of these cells during the development or after transplantation *(Adams, et al 2006)*. Results from *in vivo* assays demonstrated that the depletion of osteocalcin from mature osteoblasts decrease the mobilisation of short-term repopulating cells *(Asada, et al 2013)*. Osteoblast lineage cells are the major constituents of the endosteum, even though the last results suggest that mature osteoblasts cells probably have an indirect role in modulating HSC.

Other cells that constitute the endosteum, as endothelial cells (arteriolar and sinusoidal blood vessels) *(Nombela-Arrieta, et al 2013)*, megakaryocytes (MKs) *(Lemieux, et al 2010)*, as well as mesenchymal cells with osteolineage potential, have been also demonstrate an important role in HSC homing and engraftment. Recent findings described a group of more immature and undifferentiated mesenchymal stromal cells (MSC) around blood vessels, responsible for maintaining HSC under homeostasis *(Mendez-Ferrer, et al 2010b, Sugiyama, et al 2006)*.

1.1.2. Endothelial cells (*perivascular niche*) – The BM is richly vascularised by specific structures termed sinusoids, which can also be found in the liver and spleen *(Kiel and Morrison 2008)*.

It has been demonstrated that endothelial cells (EC) are an important functional component of the HSC niche. These cells do not only promote chemotaxis, adhesion and differentiation of HSC /progenitors *(Li, et al 2004)*, but also provide important factors for maintaining the self-renewal of the HSC in situations of stress, like irradiation and chemotherapy *(Winkler, et al 2012)*. *In vitro* studies showed the capacity of EC to maintain the HSC in culture, and the capacity of BM sinusoidal endothelial cells to promote long-term reconstitution of HSC expansion *(Li, et al 2004, Rafii, et al 1995)*. *In vivo* models also support the notion that sinusoidal endothelial cells regulate haematopoiesis, in part by soluble factors and other by direct

contact *(Brandt, et al 1999, Salter, et al 2009)*. Some reports demonstrated the role of the adhesion molecule E-selectin (expressed in the endothelial cells) in promoting HSC proliferation. The knockout of this gene in the EC leads to an increase of quiescence and resistance to irradiation of HSC *(Winkler, et al 2012)*.

Endothelial cells are not the only cell type that regulates perivascular HSC niche. The co-localization of murine BM Nestin^{+} MSC and HSC into the blood vessels surroundings and adrenergic nerves, with the fact that the depletion of these cells led to reduction of HSC in the BM, provide strong evidence for the capacity of Nestin-MSC to maintain HSC *(Mendez-Ferrer, et al 2010a, Mendez-Ferrer, et al 2010b)*. However, several types of MSC have been identified: human perivascular MSC that express CD146 *(Sacchetti, et al 2007)*, CXCL12-MSC, Prx1^{+} MSC and Leptin receptor^{+} MSC.

Cells expressing high amounts of CXCL12, defined as CXCL12-abundant “reticular” (CAR) cells can also be found co-localised with HSC throughout the BM *(Sugiyama, et al 2006)*. The ablation of CXCL12 from CAR cells not only leads to a reduction of HSC, but also the capacity of bone marrow stromal cells to differentiate into adipocytes and osteoblasts *(Omatsu, et al 2010)*. Prx1^{+} and Leptin^{+} MSC also have been described as cells capable of maintaining HSC *(Ding and Morrison 2013, Greenbaum, et al 2013)*. Prx 1 is a transcription factor expressed in pre-osteoblasts, mature osteoblasts and osteoclasts. In vivo depletion of CXCL12 from these cells resulted in a decrease of HSC in the BM and increases extramedullary haematopoiesis *(Greenbaum, et al 2013)*. Additional studies showed that Leptin receptor^{+} MSC promotes HSC proliferation since they express high stem cell factor (SCF) *(Ding and Morrison 2013, Ding, et al 2012)*. Conditional deletion of SCF results in haematopoietic failure with decreased BM HSC content.

Other cells involved in the regulation of the perivascular HSC niche are those from the sympathetic nervous system localised around the blood vessels *(Mendez-Ferrer, et al 2009)*. Circulating HSC fluctuates in antiphase with the expression of CXCL12 in the bone marrow microenvironment, where high expression of CXCL12 leads to HSC retention in the BM *(Casanova-Acebes, et al 2013)*.

Noradrenaline-producing neurons activate ß2- and ß3- adrenergic receptors in osteoblasts and MSC (Nestin^{+} cells), decreasing the BM CXCL12 expression and promoting the mobilisation of HSC to the peripheral blood (PB) *(Lucas, et al 2008).*

Bone marrow monocytes and macrophages also modulate the expression CXCL12, a subpopulation of this cells secretes prostaglandin E2 that upregulates CXCL12 expression in the BM, changing the CXCR4 expression in haematopoietic progenitor cells. This modification limits the production of ROS in the HSC, which is essential to maintain this cell in a quiescence state *(Ludin, et al 2012)*. The depletion of this population reduces the production of supportive cytokines at the endosteum that regulates HSC retention and promotes their mobilisation to PB *(Winkler, et al 2010b)*.

BM neuron-wrapping non-myelinating Schwann cells seems to regulate haematopoiesis *(Yamazaki, et al 2011)*, endorsing HSC quiescence by the expression of transforming growth factor-ß (TGF-ß). Depletion of TGF-ß receptor II$^{-/-}$ mice leads to the reduction of long term HSC, increasing their proliferation *(Larsson and Karlsson 2005)*.

Extracellular matrix (ECM) is a complex and dynamic network of macromolecules (mainly glycosaminoglycans, proteoglycan, fibronectin and collagens), which represents an important component in stem cell niches *(Gattazzo, et al 2014)*, since it can directly or indirectly modulate the maintenance proliferation, self-renewal and differentiation of HSC *(Gordon, et al 1988, Saez, et al 2014)*.

Evidence that oxygen pressure influences haematopoiesis was first reported in the 19th century showing that in high altitudes, where oxygen pressure is low, erythropoiesis is stimulated *(Fisher 2010, Reissmann 1950)*. Hypoxia also promotes plasmacytoid dendritic cell differentiation, delaying megakaryocyte differentiation *(Cipolleschi, et al 1993, Mostafa, et al 2000)*. Recent methodology using bioprobe pimonidazole has allowed demonstrating *in vivo* that endosteum is a hypoxic region *(Levesque, et al 2007)*. However, it has been suggested that pimonidazole staining reflects the metabolic state of the cells rather oxygen levels in the microenvironment *(Nombela-Arrieta, et al 2013)*.

The mechanism, *in vivo*, by which hypoxia modulates haematopoiesis is believed to involve the expression of hypoxia-inducible transcription factor 1-α (HIF-1α) *(Takubo, et al 2010)*. In hypoxic conditions, HIF-α subunit is not degraded, and forms a dimer with the constitutive HIF-ß. This heterodimer binds to hypoxia regulated elements, present in promoters of several genes promoting its transcription *(Semenza, et al 1996)*. The idea that perivascular areas are not in hypoxic state has been questioned. Direct measurements of the local oxygen tension (pO_2) showed low pO_2 in the perisinusoidal regions with low blood flow rate (0-0.2 mm/sec) *(Simsek, et al 2010, Winkler, et al 2010a)*.

The balance between proliferation and differentiation is essential for the homeostasis in the haematopoietic system. Another set of questions concerns how the microenvironment participates in the haematological disorders. Are the changes in the niches being responsible but non-cell autonomous driver of neoplasia in humans? Or do haematological diseases modulate the niche to be hostile to normal progenitors and to support leukemic stem cells (LSC)?

2. Myeloproliferative Neoplasms (MPN)

The concept of myeloproliferative neoplasms was first proposed by Dameshek in 1951, by including a group of closely related entities characterised by excessive proliferation of myeloid cells from one or more lineages in peripheral blood *(Dameshek 1951)*. The description, of the Philadelphia chromosome (Ph) resulting from the reciprocal translocation t(9;22)(q34;q11) and, generating the oncoprotein BCR-ABL, the hallmark of Chronic Myeloid Leukaemia (CML), led to a reorganisation of these chronic diseases. They were subgrouped into Ph positive MPN (CML) and the classic Ph negative MPN *(Nowell 1962, Nowell and Hungerford 1960, Rowley 1973)*.

The classical Ph negative MPN include Polycythemia Vera (PV), Essential Thrombocythemia (ET) and Primary Myelofibrosis (PMF). In 2005, four independent research groups identified a somatic point mutation in the gene coding for the Janus Kinase 2 (JAK2) tyrosine kinase that was present in most cases of PV and in some cases of ET and PMF *(Baxter, et al 2005, James, et al 2005, Kralovics, et al 2005a, Levine, et al 2005)*.

Janus kinases (JAKs) comprise a family of four members: JAK1, JAK2, JAK3 and Tyk2 *(Yamaoka, et al 2004)*. The JAKs play an important role in the homeostasis of the cells, because they act as signal-transducers of cytokines involved in development, proliferation, survival and immune regulation *(Ihle, et al 1998, Parganas, et al 1998).*

Structurally JAK2 is a non-receptor tyrosine kinase and a member of the Janus kinase protein and, is composed of four domains: 1) the amino-terminal FERM (band 4.1, ezrin, radixin, and moesin) domains, 2) SH2 (the second domain), 3) JH2 is the third domain, which is presumed to be catalytically inactive due to the lack of residues required for tyrosine kinase activity, called “pseudo-kinase”, and lastly 4) JH1 being the fourth and c-terminal domain, having all the characteristic features of a catalytic tyrosine kinase, that is activated upon phosphorylation of tyrosine 1007 (Y1007) localised in the activation loop of JAK2 protein (**Figure 3)** *(Huang, et al 2001, Ungureanu, et al 2011)*.

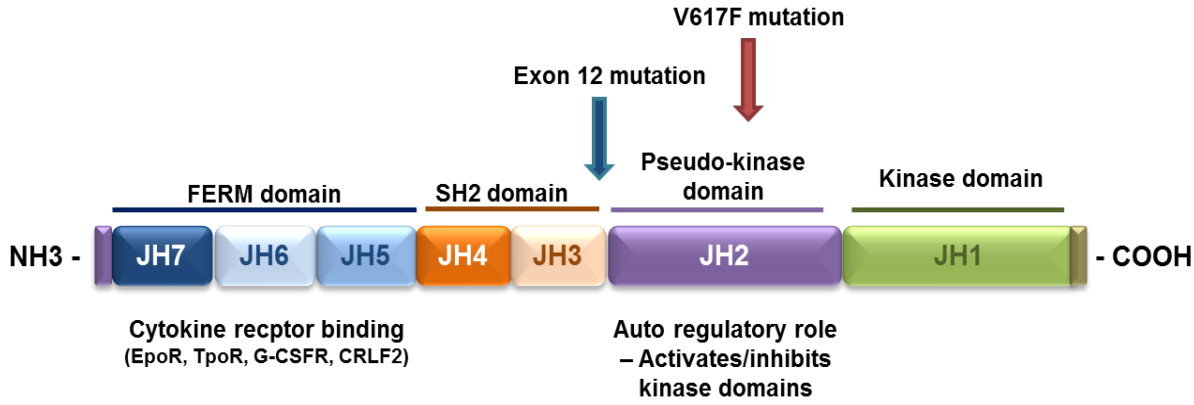

Figure 3: Domain structure of JAK2. JAK2 contains a tyrosine kinase domain (JAK homology 1 (JH1)), a pseudokinase domain (JH2), SH2-like domain, and amino-terminal FERM domain, responsible for attachment to the cytosolic domains of cytokine receptors. The pseudokinase domain, JH2, functionally prevents the activation of the kinase domain, JH1.

The somatic guanine-to-thymine (G>T) mutation encoding to a valine-to-phenylalanine substitution at the position 617 (V617F) of the auto inhibitory JH2 domain in JAK2, originates the activation of the tyrosine kinase that results in the downstream activation of different pathways leading to uncontrolled cell proliferation, survival and blocking of apoptosis *(Zhao, et al 2005)*.

Several growth factors (EPO, TPO, G-CSF, GM-CSF, SCF, IL-3 and IGF-1) are essential for normal haematopoiesis *(Gadina, et al 2001, Jatiani, et al 2010)*. These growth factors bind to cytokine receptors, which activate JAK proteins, setting off a cascade of signalling events. Once JAK molecules are activated induce downstream the activation of signal transducer and activator of transcription (STAT). The phosphorylation of STAT allows their homodimerization (mainly STAT3 and STAT5) and translocation into the nucleus, where they act as transcript factors *(Park, et al 1996, Staerk and Constantinescu 2012)*. Other signalling pathways are also activated due to JAK signalling activation, such as mitogen-activated protein kinase (MAPK), phosphatidylinositol-3'-kinase (PI3K) and AKT/mammalian target of rapamycin (mTOR), responsible also for cell proliferation *(Levy and Darnell 2002)*.

JAK-STAT signalling is controlled by several regulatory mechanisms that stress the suppressors of cytokines signalling (SOCS) proteins. These proteins acts as negative regulators binding to phosphotyrosine residues of either activated JAK or cytokine receptors *(Starr and Hilton 1999).*

JAK2^{V617F} mutation is a clonal mutation that can be detected in the haematopoietic progenitors as well as in mature hematopoietic cells. Microsatellite mapping allowed to demonstrate that the loss of heterozygosity from chromosome 9p (9p24) in individual cells resulted on a mitotic recombination. Over time, the number of cells homozygous for JAK2^{V617F} increases, suggesting a proliferative and survival advantage of mutant progenitor cells *(Kralovics, et al 2005b)*.

The frequency of JAK2^{V617F} mutation is estimated to be 97% in PV, 50-60% in ET and 55-65% in PMF. However, this mutation is not specific of MPN and can be also found in patients with Acute Myeloid Leukaemia (AML), Myelodysplastic Syndromes (MDS) (<5%) and CML *(Barbui, et al 2015, Steensma, et al 2005).* Despite the presence of this mutation in other haematological diseases, the JAK2 mutation screening was adapted as a useful clonal marker of MPN by the World Health Organization (WHO) system of hematopoietic tumour classifications in 2008 *(Tefferi, et al 2007, Vardiman, et al 2009)*.

Recently, another mutation involving the CALR gene (located in chromosome 19p13.2) was described for MPN patients. It represents the second most frequent mutation in this group of diseases *(Nangalia, et al 2013)*, being present in 20-50% in ET and PMF and almost absent in PV *(Barbui, et al 2015)*. Myeloproliferative leukaemia virus oncogene (MPL), also known as gene for the thrombopoietin receptor, localised on chromosome 1p34 it has been found mutated in 3% of patients with ET, 7% in PMF and in a very low percentage of patients with PV *(Gianelli, et al 2014)*. Additionally, a variety of mutations that modify the epigenetic regulation are found in MPN patients, including mutations in: TET (oncogene family member 2), IDH1/2 (isocitrate dehydrogenase 1 and 2), EZH2 (enhancer of zeste homolog 2), ASXL1 (additional sex combs-like 1), and DNMT3A (DNA cytosine methyltransferase 3a) *(Passamonti, et al 2011, Vannucchi, et al 2013)*.

The determination of allele burden in JAK2/CARL/MPL mutations can be useful to clarify the specific diagnosis and also to provide important prognostic information. For example, low $JAK2^{V617F}$ allele burden in PMF has been associated to worse prognosis and also higher than 50% $JAK2^{V617F}$ allele burden in PV has been associated to increased risk of fibrotic transformation *(Passamonti, et al 2010)*.

2.1. Leukemic bone marrow niche: *A partner in crime.*

HSC are maintained throughout life and, their genomic integrity is preserved to prevent leukemic transformation and ensure normal blood production. However, these cells are constantly exposed to both intrinsic and extrinsic stressing factors that can lead to genomic instability (DNA damage) and mutations *(Bakker and Passegue 2013)*. These mutations accumulate with age and, if not properly resolved, can result in loss of function or malignant transformation *(Welch, et al 2012).*

Different reports along the last decade have suggested that the alterations in the BM-MSC can lead to haematological abnormalities *(Schepers, et al 2015).* The first studies reported that genetic deletion of IKBα in mice induces a severe hematologic disorder, characterized by an increase of granulocyte/erythroid/monocytes macrophages colony-forming cells (CFU-GEMM). This particular myeloproliferative disturbance was mediated by the dysregulation of Jagged-1 expression in IKBα-deficient hepatocytes (*Rupec, et al 2005*). In 2007, Walkley and colleagues demonstrated that the loss of one the major receptor of vitamin A, retinoic acid receptor γ (RARγ), resulted in a murine myeloproliferative neoplasm (MPN), with an increase of granulocytes in PB, BM and spleen *(Walkley, et al 2007a)*. They suggested that microenvironment induces the myeloproliferative disease by increasing the expression levels of tumour necrosis factor α (TNFα). Transplantation of $TNF\alpha^{-/-}$ BM mice into $RAR\gamma^{-/-}$ mice had the capacity to revert the MPN-like phenotype. The same group also reported that Mx1-Cre-mediated deletion of the retinoblastoma (RB) gene in both haematopoietic and stromal cells resulted in MPN-like disease in the mice with splenomegaly. However, the develop-

ment of MPN in mice was dependent on the deletion of RB in both components, myeloid cells and BM microenvironment *(Walkley, et al 2007b).* In the same line, the development of a mice where the canonical Notch ligand receptor mind bomb1 (*Mib1*) in the stroma was inactive resulted in MPN- like disease, independently of *Mib1* status in haematopoietic system *(Kim, et al 2008)*.

The results described underscore the role of BM stromal niches in disease initiation. However, in these reports the hyper-proliferation was not accompanied by haematopoietic cell transformation or abnormal differentiation. Recent studies have suggested that altered microenvironment can serve as the initiating event in haematological malignances. The deletion of *Dicer 1* gene, required for microRNA processing in osteoprogenitor cells, was sufficient to drive a myelodysplastic-like syndrome, which was fully reverted upon transplantation into wild-type mice *(Raaijmakers, et al 2010).* Subsequently, it was demonstrated that the increase of ß-catenin expression stimulates the Notch ligand Jagged-1 in osteoblasts, which can increase Notch signalling in haematopoietic cells developing AML in mice *(Kode, et al 2014)*.

Another recent study suggests that Notch signalling plays an important role in HSC regulation. A conditional knockout model of RBPJ, a non-redundant downstream effector of the canonical Notch signalling cascade, induces the up-regulation of miR-155 expression on BM stromal cells and endothelial cells. The constitutive over-expression of the miR-155, which directly targets the nuclear factor ƙB (NF-ƙB) inhibitor ƙB-Ras1, induces NF-ƙB activation and a global state inflammation in the BM, increasing the production of pro-inflammatory cytokines including G-CSF and TNF-α. This inflammatory state altered the mechanisms in BM- stromal cells, leading to an uncontrolled expansion of myeloid cells and the development of a MPN-like disease in mice *(Wang, et al 2014).* They also studied the implications of miR-155 in human MPN patients, analysing 85 BM mononuclear cells (BM-MNC) of patients with myelofibrosis (MF) (characterized by a high inflammatory process), and found an over-expression of the miR-155 when compared to healthy donors.

Other controversial idea is that genetic changes could independently occur in BM stromal cells during the course of the disease or be already present at diagnosis *(Blau, et al 2011, Blau, et al 2007, Lopez-Villar, et al 2009)*, although it is not confirmed if this genomic changes are related to the development of the disease.

2.1.1. The tumour microenvironment as a key to MPN pathogenesis

In the last years, different groups have found evidence that the haematopoietic niche influences leukemic stem cell proliferation, survival and migration, contributing to the disease progression *(Mendez-Ferrer, et al 2015, Schmitt-Graeff, et al 2015)*. During neoplastic transformation, BM niches undergo a profound modulation with a disruption of their physiological architecture. Examples of that include the JAK-STAT pathway activation in malignant and non-malignant cells or the hyper-activation in pre-fibrotic MPN of the fibronectin secretory pathway in stromal cells *(Kleppe, et al 2015)*. A hallmark of profound alteration in the BM niche, with a progressive remodelling of the BM stroma, can be observed in PMF, a subset of PV and in a minority of ET patients resulting in fibrosis and osteosclerosis *(Gianelli, et al 2012, Thiele, et al 2005)*.

Various studies have suggested that the development and progression of MPN can be driven through mutated haematopoietic stem/progenitor cells (HSPC) and the BM-niche feedback loop (Figure 3), which include:

- *Neuroglial damage in the BM* - $JAK2^{V617F}$ MPN mouse model, where the excessive production of interleukin (IL)-1ß by mutant MPN HSC induced neural damage and depletion of $nestin^{+}$ MSC (apoptosis), leading to acceleration of MPN and subsequent disease progression. This phenotype was reverted by treatment with 4-methycatechol, a neuroprotective drug that signals through ß3-adregenic receptors *(Arranz, et al 2014)*.
- *Production of pro-inflammatory cytokines by leukemic and normal cells* – Some reports have shown that CML cells can generate an inflammatory environment by the production of IL- 6, IL-1α that can decrease the expression of CXCL12 in the stromal

niche with an increment of MSC proliferation *(Krause, et al 2013)*. Murine models of CML showed the role of THPO, the chemokine (C-C motif) ligand 3 (CCL3) and direct cell-cell interaction between the leukemic cell and the MSC, resulting in the overproduction of functionally altered osteoblasts *(Reynaud, et al 2011, Schepers, et al 2015)*. These models also demonstrated the capacity of MPN hematopoietic cells to remodel the endosteal BM niche, where the ability of osteoblasts to maintain normal HSC is severely compromised *(Schepers, et al 2013)*. Myelofibrotic osteoblasts also expressed pro-inflammatory cytokines (IL-1 and TNF-α) which likely amplify aberrant myeloid cell production, creating a vicious circle.

- *The capacity of leukemic cells to alter neighbouring non-transformed hematopoietic progenitor cells* - An *in vivo* model reported that normal cells exposed to leukemic cells (CML) acquired characteristics of the transformed cells. The production of abnormal cytokines (IL-6) by human CML can inhibit the proliferation of normal haematopoietic cells while sparing the transformed ones *(Welner, et al 2015).*

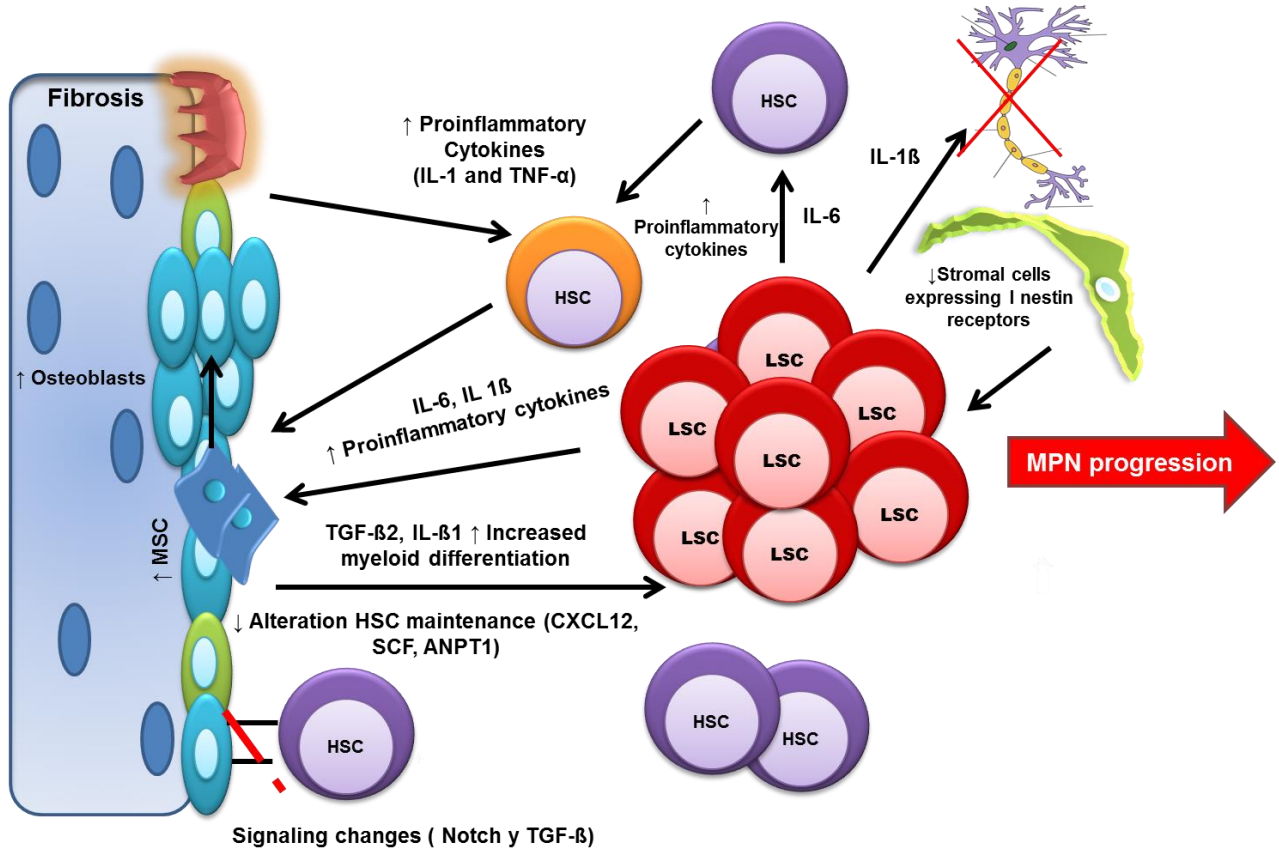

Figure 4: Scheme model for MPN BM niche. Myeloproliferative neoplasms (MPN) are haematological disorders from a clonal hematopoietic stem cell, which originates a population of leukemic stem cells (LSC) with increased survival and proliferative capacity. LCS secretes IL-1β, which damages sympathetic nervous system (SNS) nerve terminals and MSC apoptosis. LSC overproduce leukemic myeloid cells that secrete high levels of proinflammatory cytokines, thus creating a paracrine feedback loop that drives myeloid differentiation and also directly stimulate MSC to overproduce functionally altered osteoblasts, which accumulate in the BM cavity as inflammatory myelofibrotic cells (Myelofibrosis). With an altered stroma severely compromised in their ability to maintain normal HSC, but not LSC. The high production of IL-6 by the LSC transforms normal leukaemia-exposed progenitor cells (HSC) into “leukemic-like” cells, promoting myeloid differentiation.

2.1.2. Extracellular vesicles

In recent years, it has been widely recognised the cross-talk between neoplastic cells and the microenvironment in the progression of haematological neoplasms, where we have to highlight the role of extracellular vesicles (EV) *(Raimondo, et al 2015, S, et al 2013)*. Reprogramming of somatic cells requires a complex interaction between intracellular and extracellular signals leading to epigenetic changes. Cell fate is therefore determined by signals that can change the phenotype of the target cells. Cell-secreted vesicles were initially described nearly 30-40 years ago, where two independent groups observed the presence of multivesicular bodies in the reticulocytes and their capacity to release vesicles *(Pan, et al 1983, Pan and Johnstone 1983)*. Raposo and colleagues *(Raposo, et al 1996)* demonstrated that vesicles isolated from Epstein-Barr virus transformed B lymphocytes were able to stimulate adaptive immune response was a landmark in the EV research field.

Numerous studies have reported the role of EV in intracellular communication based on the presence of proteins, lipids and nucleic acids (RNA and microRNA) in their cargo. EV have been isolated from almost all biological fluids and cell types demonstrating the important role in normal and pathology processes *(Yanez-Mo, et al 2015)*.

Extracellular vesicles, it is a general term to describe all types of vesicles released by the cells and can be classified in different subtypes based on their cellular origin, biological function and biogenesis *(Yanez-Mo, et al 2015)*:

(a) Apoptotic bodies – vesicles released during the process of apoptosis;

(b) Cellular microparticles/microvesicles/ectosomes – generated from plasma membrane budding and thus, their membrane composition reflects the parental cells;

(c) Exosomes – derived from the endolysosomal pathway – exosomes are generated from the multivesicular bodies (MVB) as part of the endocytic machinery known as late endosomes, which are released to the extracellular environment upon the fusion of MVB with the plasma membrane.

Extracellular vesicles exert their effects on fundamental biological process, so the impact of EV in disease pathogenesis is not surprising. Numerous studies have implicated EV in the

bidirectional transfer of genetic information between cancer and stroma, leading to alterations that include cell proliferation, angiogenesis, matrix remodelling, metastasis and immune escape *(Webber, et al 2015)*.

Previous studies reported by our group showed that BCR-ABL cell release an EV containing the oncogene (mRNA), that can be incorporated into endothelial cells leading to the expression of the oncoprotein in negative BCR-ABL cells *(Ramos, et al 2015).* In the context of MPN, other groups also showed that vesicles released by CML cell lines induce the reduction of VCAM-1 and CXCL12 expression in endothelial cells, demonstrating the capacity of EV of reprogramming the microenvironment *(Taverna, et al 2014).*

The crosstalk is not unidirectional, incorrect signals from the microenvironment may lead to a destabilisation of haematopoietic system. Rocarro *et al* reported that BM-MSC from multiple-myeloma patients derived exosomes with a direct impact in multiple myeloma disease progression *in vivo* *(Roccaro, et al 2013)*. Work developed by our group *(Muntion, et al 2016)* also showed that BM-MSC from MDS patients release EV containing the microRNA-10a and microRNA-15a. The incorporation of these EV in haematopoietic progenitors had the ability to modify their behaviour, increasing their viability and clonogenic capacity.

Hypothesis and Main Objectives of the Thesis

Myeloproliferative neoplasms are caused by a clonal mutation in the haematopoietic stem cells. JAK2^{V617F} mutation is the main molecular marker in patients with Polycythemia Vera (PV) and Essential Thrombocythemia (ET). Different findings have demonstrated the importance of the bone marrow stromal microenvironment in the survival, proliferation and resistance to chemotherapy of the leukemic cells. It could be hypothesised that the BM microenvironment could be differentially altered in patients with PV and ET with JAK-2 mutation, and maybe this changes could play a role in the different clinical characteristics of both entities.

Thus, the main objective of this thesis was to compare the functional and genomic characteristics of bone marrow mesenchymal stromal cells of JAK2-MPN patients with PV and ET, and the interactions established between stromal and haematopoietic cells.

Specific Aims:

1. To compare ability to proliferate, to differentiate and the immunophenotype of the BM-MSC from MPN patients (JAK2^{V617F}), with that of BM-MSC from healthy donors (HD) and CML patients;
2. To study the presence of genomic alterations in the MSC from ET and PV patients, by conferring them with control MSC (HD);
3. To evaluate if the alteration in the MSC from JAK-2 MPN patients modifies the capacity to support normal and MPN haematopoietic progenitor cells;
4. To identify altered genes and pathways in the MPN-MSC which could potentially be used as therapeutic targets;
5. To compare the microRNA content in the MSC-derived extracellular vesicles from HD and MPN patients, and to study the functional alterations that may be induced when incorporated into haematopoietic progenitor cells.

1. Patient characteristics

Seventy-two MPN patients were included in the study (45 $JAK2^{V617}$, 4 CARL, 9 MPN JAK2/CARL/MPL negative and 14 CML). Median age of $JAK2^{V617}$ patients was 66 (range 31-85), 55 (range 43-82) for MPN patients without the mutation in JAK2 (JAK2 (negative)) and 51 (range 35-57) for CML patients. MPN diagnosis was established according to the WHO classification *(Tefferi, et al 2007)*. Patient´s characteristics are summarised in **Table 1**. Normal BM samples were obtained from 50 healthy donors, 32 men and 18 women, with a median age of 49 years (range, 31-73 years). Written informed consent was obtained from all healthy donors and patients according to the ethical guidelines of the *Hospital Universitário de Salamanca* and was also in accordance with the Helsinki Declaration.

Table 1: Patient's characteristics

Subject	Sex	Age (y)	Hb (g/dL)	Platelets 10^3/µL	WBC 10^3/µL	%$JAK2^{V617F}$	CARL	Other Mutation/Observations
PMF1	M	66	—-	—-	—-	60%	NO	NO
PMF2	M	75	—-	—-	—-	36%	NO	NO
PV1	F	46	16.9	775	11.1	17%	NO	NO
PV2	F	78	17.8	364	14.1	70%	NO	NO
PV3	M	53	13.9	262	4.01	49%	NO	NO
PV4	F	52	17.3	649	8.11	33%	NO	NO
PV5	M	74	15.7	233	4.19	40%	NO	NO
PV6	F	72	16.4	454	14.13	90%	NO	NO
PV7	M	66	16.9	1041	17.6	46%	NO	NO
PV8	M	67	17.3	485	12.9	33%	NO	NO
PV9	F	69	16.7	356	5.87	33%	NO	NO
PV10	F	79	17.8	557	11.6	57%	NO	NO
PV11	M	71	18.4	597	8.26	23%	NO	NO
PV12	F	70	16.8	387	17.3	75%	NO	NO
PV13	M	55	—-	—-	—-	NO	NO	NO
PV14	F	43	—-	—-	—-	NO	NO	NO
PV15	M	46	—-	—-	—-	NO	NO	NO
PV16	M	54	—-	—-	—-	NO	NO	NO
ET1	F	40	14.3	415	9.2	24%	NO	NO
ET2	F	51	14.1	596	9.17	16%	NO	NO
ET3	F	70	17.6	567	8.67	54%	NO	NO
ET4	M	52	13.5	567	8.96	11%	NO	NO
ET5	M	74	15.7	180	6.08	35%	NO	NO
ET6	F	37	14.7	484	6.56	21%	NO	NO
ET7	M	65	14.5	483	7.63	20%	NO	NO

ET8	M	85	15.5	98	8.82	90%	NO	NO
ET9	M	69	14.9	293	6.79	32%	NO	NO
ET10	F	51	13.5	644	7.41	13%	NO	NO
ET11	M	72	11.8	472	7.98	48%	NO	NO
ET12	F	74	14.3	636	5.83	22%	NO	NO
ET13	M	73	12.3	1167	13.7	25%	NO	NO
ET14	M	77	16.9	595	10.44	26%	NO	NO
ET15	F	45	15.5	648	10.5	12%	NO	NO
ET16	M	73	11.3	656	9.73	60%	NO	NO
ET17	F	56	16.1	856	8.5	20%	NO	NO
ET18	M	62	17	697	10.2	10%	NO	NO
ET19	M	31	16.6	168	3.78	30%	NO	NO
ET20	F	79	15.7	548	5.22	12%	NO	NO
ET21	F	68	14.7	571	6.92	18%	NO	NO
ET22	M	74	15.8	387	11.6	16%	NO	NO
ET23	M	70	14.1	224	3.8	22%	NO	NO
ET24	F	67	15.8	1027	11.1	24%	NO	NO
ET25	F	50	15.3	517	7.78	15%	NO	NO
ET26	F	78	15.9	640	11.97	80%	NO	NO
ET27	M	47	14	634	5.22	44%	NO	NO
ET28	F	76	15.5	523	9.23	22%	NO	NO
ET29	F	73	—-	—-	—-	NO	SI	NO
ET30	F	47	—-	—-	—-	NO	SI	NO
ET31	F	75	—-	—-	—-	NO	SI	NO
ET32	F	47	—-	—-	—-	NO	NO	NO
ET33	M	55	—-	—-	—-	NO	NO	NO
ET34	M	43	—-	—-	—-	NO	NO	NO
ET35	M	70	—-	—-	—-	NO	NO	NO
ET36	F	72	—-	—-	—-	NO	NO	NO
ET37	F	58	—-	—-	—-	NO	SI	NO
CML1	M	53	—-	—-	—-	NO	NO	BCR-ABL
CML2	M	58	—-	—-	—-	NO	NO	BCR-ABL
CML3	M	41	—-	—-	—-	NO	NO	BCR-ABL
CML4	F	68	—-	—-	—-	NO	NO	BCR-ABL
CML5	M	39	—-	—-	—-	NO	NO	BCR-ABL
CML6	F	47	—-	—-	—-	NO	NO	BCR-ABL
CML7	M	50	—-	—-	—-	NO	NO	BCR-ABL
CML8	F	74	—-	—-	—-	NO	NO	BCR-ABL
CML9	F	47	—-	—-	—-	NO	NO	BCR-ABL
CML10	M	35	—-	—-	—-	NO	NO	BCR-ABL
CML11	F	52	—-	—-	—-	NO	NO	BCR-ABL
CML12	F	87	—-	—-	—-	NO	NO	BCR-ABL
CML13	F	47	—-	—-	—-	NO	NO	BCR-ABL
CML14	M	64	—-	—-	—-	NO	NO	BCR-ABL

Y= years; M= Male; F= Female; PMF= Primary myelofibrosis; PV= Polycythemia Vera; ET= Essential thrombocythemia; Hb= Haemoglobin; WBC= White blood cells

2. Bone marrow mesenchymal stromal cells (BM-MSC) and cell lines

2.1 BM-MSC isolation and expansion

Bone marrow (BM) aspirates were obtained following institutional standard protocols *(Carrancio, et al 2008)*. BM was diluted in HBSS Hanks Solution (Gibco, Invitrogen^{TM}) and mononuclear cells (MNC) were separated by density gradient centrifugation using a solution of high density with low viscosity and low osmotic pressure - Ficoll-Paque (density: 1.077k; GE Healthcare BioSciences). MNC from buffy coat layer were recovered, washed and seeded at a density of 10^6 MNC/cm^2 on a plastic culture flask (Corning Incorporated) with an expansion medium consisting on Dulbecco's Modified Eagle Medium (DMEM) (Gibco, Invitrogen^{TM}) supplemented with 5% of platelet lysate, heparin (200 IU/mL) and 1% of penicillin/streptomycin (10^5U/mL/10^5µg/mL - Gibco, Invitrogen^{TM}) and cultured at 37ºC and 5% of CO_2 in a humidified atmosphere *(Carrancio, et al 2011, Carrancio, et al 2008)*. Platelet lysate (PL) were obtained from the University Hospital of Salamanca Blood Bank. Culture medium was replaced every 3-4 days and non-adherent cells were removed. BM-MSC were isolated due to their characteristic adherence to plastic surfaces. When cultures reached approximately 70-80% confluence, cells were detached by treatment with 0,05% trypsin/EDTA (Gibco, Invitrogen^{TM}) and replanted for culture expansion at a density between 3000-5000 cells/cm^2. The procedure has been schematically represented in **Figure 5.** In each expansion cycle, cells counts were performed applying Trypan Blue (Gibco, Invitrogen^{TM}) staining on Neubauer chamber. Cell growth rates were analysed calculating the population doublings (PD) at each passage, following the formula: $\log_{10}(N)/\log_{10}(2)$ where N represents the cells harvested/cells seeded *(Lu, et al 2006)*. Results were expressed as PD for each passage.

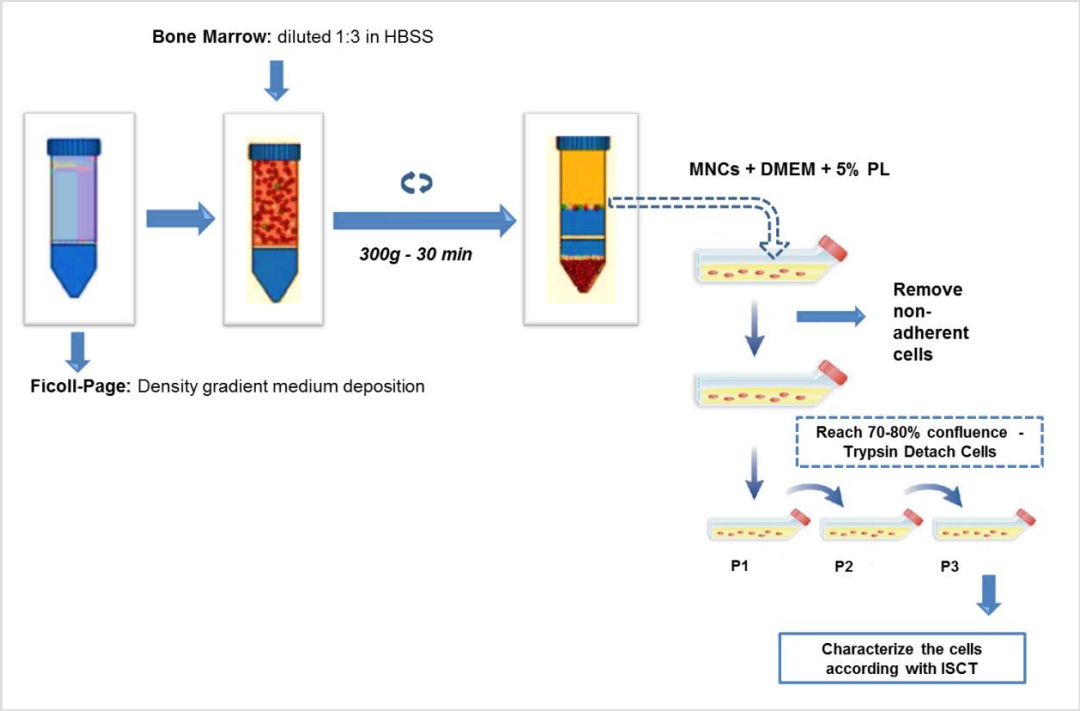

Figure 5: Protocol scheme of BM-MSC isolation and expansion

2.1.1 Multiparametric flow cytometry analysis (MFC)

For immunophenotypic characterisation, MSC were identified following the ISCT recommendations *(Dominici, et al 2006).* Adherent cells at passage 3 were harvested and incubated using the following conjugated monoclonal antibody combinations: CD34-FITC, CD73-PE, CD45-PerCPCy5.5, CD105-APC/ CD44-FITC, CD14-PE, CD19-PerCPCy5.5/ CD90-FITC, CD166-PE, HLA-DR-PerCPCy5.5 (FITC: fluorescein isothiocyanate, PE: phycoerytrin, PerCP: peridinin chlorophyll protein, APC: allophycocyanin.) **Table 2**. To control background fluorescence, unstained MSC were also acquired and used as negative control. Expression of individual markers was recorded both as percentage of positive cells and as mean fluorescence intensity (MIF) after subtracting the baseline auto-fluorescence levels observed for MSC.

Table 2: Panel of antibodies used for characterise BM-MSC by MFC

Antibody	Concentration	Clone	Commercial
CD90-FITC	0.5 mg/mL	5E10	Becton Dickinson, BioSciences
CD34-FITC	25 µg/mL	8G12	Becton Dickinson, BioSciences
CD44-FITC	12.5 µg/mL	L178	Becton Dickinson, BioSciences
CD73-PE	20 µl/per.Test.	Clone AD2	Becton Dickinson, BioSciences
CD14-PE	50 µg/mL	Clone MφP9	Becton Dickinson, BioSciences
CD166 PE	20 µl/per.Test	3A6	Becton Dickinson, BioSciences
CD45- PerCPCy5.5	6 µg/mL	Clone 2D1	Becton Dickinson, BioSciences
CD19- PerCPCy5.5	5 µg/mL	Clone SJ25C1	Becton Dickinson, BioSciences
HLA-DR- PerCPCy5.5	6.25 µg/mL	Clone L243	Becton Dickinson, BioSciences
CD105 APC	10 µL/10^6 cells	Monoclonal Mouse IgG1 Clone # 166707	R&D systems

Labelled cells were acquired immediately after the staining using a FACSCalibur flow cytometer (BD Biosciences) equipped with the CellQuestTM program (BD Biosciences). Data were analysed using the Infinicyt software (Cytognos, Salamanca, Spain), as previously described *(Del Canizo, et al 2003, Sanchez-Abarca, et al 2013, Sanchez-Guijo, et al 2009).*

2.1.2 Differentiation assays

Osteogenic and Adipogenic Differentiation

For *in vitro* differentiation the cells were cultured with specific medium - osteogenic medium (NH Osteodiff Medium, Miltenyi Biotec) and adipogenic medium (NH Adipodiff Medium, Miltenyi Biotec). Osteoblastic alkaline phosphatase activity was detected by staining with NTB/BCIP (nitro-blue tetrazolium chloride / 5-bromo-4-chloro-3-indolyl-phosphate) solution (Roche, Switzer-

land) and counterstained with hematoxylin (Merck, Germany). For adipocyte detection cells were stained with Oil-Red-O solution (Certistain Merk KGaA).

2.1.3 Cell cycle assays

BM-MSC from HD (n=10) and JAK2^{V617F} (n=15, 11 ET and 4 PV) or MNC from the different experimental conditions were stained with propidium iodide (PI), using the kit Cycle Tests (BD), according to manufacturer's instructions. A minimum of 20,000 events was acquired on a FACSCalibur flow cytometer using the CellQuest software program. The distribution of cells along the cell-cycle phases was analysed using ModFit LTTM Macintosh program (Verity Software House, Inc., Topsham, ME, USA).

2.1.4 Apoptosis assays

For apoptosis assessment, the BM-MSC and MNC from the different experimental conditions were stained with Annexin V-PE using the PE Annexin V Apoptosis Detection Kit I (BD) following the manufacturer's instructions. The samples were acquired on FACSCalibur and analysed using the Infinicyt software to determine the percentage of viable cells (both annexin-V and 7ADD negative).

2.2 Cell lines

2.2.1 BM-MSC stromal cell lines: hMSC-TERT, a human MSC cell line immortalised by the expression of the telomerase reverse transcriptase gene was used (generous gift of Dr. Enrique Ocio, Centro de Investigación del Cáncer, Universidad de Salamanca) as well as the fibroblastoid cell line HS-5 obtained from the ATCC (ATTC CRL11882). These cell lines were cultured in DMEM medium supplemented with 10% FBS and 1% penicillin/streptomycin (P/S).

2.2.2 MPN cell lines – Different JAK2^{V617F} cell lines derived from patients diagnosed with myeloproliferative diseases and BCR-ABL positive cell line were used.

- Hematopoietic cell lines K562 cells from ATCC (ATCC CCL243), a human cell derived from a patient with Ph^{+} blast crisis (BCR-ABL positive) was cultured in Roswell Park Memorial Institute (RPMI)-1640- medium (Gibco ® - Life Technologies-Invitrogen, UK) with 10% FBS and 1% P/S.

- UKE-1 is a cell line derived from an essential thrombocythemia (ET) patient transformed into acute leukaemia, homozygous for $JAK2^{V617F}$ mutation *(Buors, et al 2012)*. UKE-1 cell line was cultured in Iscove's Modified Dulbecco's Medium (IMDM) containing high glucose (4,500 mg/L), sodium pyruvate and HEPES buffer (Lonza, Belgium) supplemented with 20% of FBS, 1µM of hydrocortisone, 1% P/S and L-Glutamine (Life Technologies).

- SET-2 cell line was established from a patient with ET at megakaryoblastic leukemic transformation *(Uozumi, et al 2000)*. This megakaryoblastic leukemic cell line is heterozygous for the $JAK2^{V617F}$ mutation.

- HEL cell line was established from a patient with erythroleukemia, being homozygous for $JAK2^{V617F}$ mutation *(Papayannopoulou, et al 1983)*. SET-2 and HEL cell lines were cultured in Roswell Park Memorial Institute (RPMI-1640) medium with 10% FBS and 1% P/S. All cell lines were kindly donated by Prof. António de Almeida (Instituto Português de Oncologia de Lisboa, Portugal).

All cell types were cultured at 37ºC in a humidified atmosphere in the presence of 5% CO2-95% air.

3 RNA-related assays

3.1 RNA extraction and purification

BM-MSC from all groups, were trypsinized and frozen (-80ºC) in 1mL of TRIzol® (Invitrogen, CA) at passage 3 for eventual precipitation and purification. Briefly, to isolate the RNA chloroform was added (Sigma, Aldrich) and centrifuged. The aqueous phase was transferred in to a clean Eppendorf, 2-propanol (Merck, USA) was added and the final solution was centrifuged. RNA was cleaned with sterile ethanol (Sigma-Aldrich) 70% and re-suspended in sterile water.

For microarrays assays the RNA was submitted to a purification process using the RNA-extraction kit from Qiagen following manufacturer's instructions.

3.2 RNA quantification

RNA quantity was determined using a spectrophotometer NANOdrop and 260nM/280nM and 260nM/230nM ratios were analysed. In order to accept the RNA, both ratios should be as close 2.0 as possible.

RNA integrity was assessed by the RNA 6000 Lab Chip® kit using a 2100 Bioanalyzer (Agilent technologies, CA).

3.3 Gene Chip® Human Gene ST Arrays

Total and purified RNA extracted from BM-MSC were hybridized in the platform Gene Chip Gene 1.0 ST array system (Affymetrix, Santa Clara, CA). This platform uses a subset of 28,869 well-annotated genes with 764,885 distinct probes. Briefly, 100 ng of total RNA from each sample were reverse-transcripted to cDNA.

Microarrays were hybridized, washed, stained, and scanned according to the protocol described in WT sense target labelling assay manual from Affymetrix. The arrays were scanned using the Affymetrix Gene Chip scanner 3000 7G system. Gene- and exon-level expression signal estimates were derived from CEL files generated from Affymetrix GeneChip Exon 1.0 ST arrays using the multiarray analysis algorithm implemented from the Affymetrix Power Tools software.

3.4. Microarray data analysis: normalisation, signal calculation, differential gene expression and clustering

Microarray data analyses were performed in the R/Bioconductor statistical environment. Micorarrays were pre-processed and normalized with the RMA (Robust Multi-Array Average) algorithm (from R library affy) *(Irizarry, et al 2003)*. The expression signal at gene level was calculated applying a gene-centric redefinition of the Affymetrix probes to Ensembl genes (Ensembl IDs: “ENSG”). This alternative Chip Definition File (CDF) with complete unambiguous mapping of microarray probes to genes is available at GATExplorer (http://bioinfow.dep.usal.es/xgate/) *(Risueno, et al 2010)*. The algorithm LIMMA (from R library limma) was used for differential expression analyses *(Smyth, et al 2005).* Differential expression was considered statistically significant when adjusted p-value was under 0.05

(for multiple-testing adjustment, the FDR method of Benjamini-Hochberg was applied). Unsupervised sample to sample clustering and heatmap were produced based on Euclidean distances between micoroarrays.

3.4.1. Gene functional enrichment analysis

Selected sets of genes, that were differential expressed compared to control, were submitted to functional enrichment analysis using two bioinformatics tools: DAVID Bioinformatics Resources 6.7 (*http://david.abcc.ncifcrf.gov/*) *(Huang da, et al 2009)* and GeneTerm Linker (*http://gtlinker.dacya.ucm.es/*) *(Fontanillo, et al 2011).* The gene sets analysed for functional enrichment were the most significant from List I (up-regulated genes with FDR<0.03) and List II (up-regulated genes with FDR<0.02). The down-regulated significant genes were also analysed in separated runs.

3.5. Gene expression assays – Real-time PCR

Total RNA obtained from both BM-MSC and MNC with TRIzol and subsequent reverse transcription was carried out using the High Capacity cDNA Reverse Transcription Kit (Applied Biosystems, Foster City, CA, USA). The total RNA input was 1000ng in a final reaction volume of 20µL and the conditions for this reaction were as follows: 10 min at 25ºC, 120 min at 37ºC and 5 sec at 85ºC. To prepare the 2X RT Master mix (per 20µL reaction): - 10X RT Buffer: 2.0µL; - 25X dNTP Mix (100nM):0.8µL; - MultiScribe™ Reverse Transcriptase: 1.0µL; RNase Inhibitor: 1.0µL; - Nuclease-free H_2O: 3.2µL.

To analyse the expression of interesting genes (**Table 3**), RT-PCR after generation of cDNA was performed, using commercial TaqMan® Gene Expression Assays and MicroAmp 96 well optical plates on Step One Plus Real-Time PCR System (Applied Biosystems). Housekeeping gene Glyceraldehyde-3-phosphate dehydrogenase (GAPDH) was used to assess RNA quality and to normalise gene expression in the experiments.

All reactions were carried out in a 10µL final volume containing 5µL of 2X TaqMan FAST Universal Mastermix (Applied Biosystems), 200nM of probe and 300nM of each prime. A measure conditions were 15 sec at 95ºC and 50 cycles consisting of 1 sec denaturation at 95ºC,

and 20 sec at 60ºC for annealing/ extension. Reactions were carried out in a StepOnePlus Real-Time PCR System.

The expression level of each gene was analysed using the average of the duplicates. Reproducible amplification curves of both duplicates were analysed.

Relative quantification was calculated using the $2^{-\Delta Ct}$ values where:

$$\Delta Ct = Ct_{Gene} - Ct_{GAPDH}.$$

Table 3: Panel of genes used in RT-PCR assays

Gene symbol	Assay IDs	Gene symbol	Assay IDs
KIT	Hs00174029	MYADM	Hs00414763
SPP1	Hs00167093	CXCL12	Hs00171022
THPO	Hs00171458	HDAC8	HS00954353
JAG1	Hs01070032	BAD	Hs000188930
BMP2	Hs01055564	MYADM	Hs00414763
ANGPT1	Hs00181613	*hsa-miR-155-5p*	*2623*
NFKBIB	Hs00182115	*RNU6B*	*1093*
TNF	Hs00174128		
TP53	HS00153340		

All the genes were purchased from Applied Biosystems, Foster City, CA, USA

4. Protein assays

4.1. Western Blot assays

4.1.1. *Protein extraction:* BM-MSC proteins extractions were obtained re-suspended with lysis buffer and centrifuged to obtain the protein. To prepare lysis buffer we used milliQ H_2O complemented with 20mM of Tris-HCl pH=7.0, 140mM NaCl, 10mM EDTA, 1% of Nonidet P-40 and 10% glycerol (all purchase from Sigma-Aldrich), complemented with 0.1 mM sodium orthovanadate, 1mM PMSF and Protease Inhibitor Cocktail (Roche Diagnostics, Mannheim, Germany).

4.1.2. *Protein quantification:* The protein concentration was measured using Bradford assay (Bio-rad) using a solution of 3mg/mL BSA as standard. Samples and standards were prepared by adding 10µL of the extract to 790µL of MilliQ H_2O and 200µL of Bradford. The samples were reed in a spectrophotometer (Bio-Rad) at 595nm. Protein concentration was determined according to the Beer-Lambert Law.

4.1.2. *Electrophoresis and Transference*: The proteins extracts were subjected to SDS-PAGE under reducing conditions, using the method of Laemmli *(Laemmli 1970).* The samples were diluted in loading/sample buffer, which was prepared with 125mM Tris HCl pH 6.8, 2% SDS (p/v), 5% glycerol (v/v), 0.003% of bromophenol blue and 1% (v/v) of ß-mercaptoethanol. Then, were heated at 95ºC for 5 min, for their denaturation, and directly loaded on the acrylamide gel or stored at -20ºC. Finally, the proteins were loaded on a discontinuous acrylamide gel consisting of 7%-15% separating gel (depending on size of protein of interest) and 5% of stacking gel. Electrophoresis was run at 40V-90V until reaching the resolving gel and since them at 120V. As weight marker 3-5 µL Page Ruler Prestained Protein Ladder was used (Bio-Rad). After being resolved by SDS-PAGE the proteins were transferred to PVDF Immobilon-FL membranes (Millipore). In short, membranes were activated for 2 min in methanol and left in transference buffer (Tris 25mM, glycine 190mM and methanol 20% (v/v) pH 8.1-8.4). Transference ran for 4h at 40V at 4ºC. The quality of the transference was assessed by Ponceau (0.5g of red Ponceau in 1000mL of acetic acid (Merck)). Finally, the membranes were washed in MilliQ H_2O and in TBS-Tween (Tris 10mM and tween 20 0.05% (v/v))

4.1.3. *Blocking and incubation with the primary and secondary antibodies:* Membranes were left blocking for unspecific binding with 5% non-fat dry milk or 2% BSA in TBS-Tween for 1 hour. After membrane blockage, membranes were incubated with primary antibodies at the appropriate dilution (**Table 4**) was performed overnight at 4°C. The respective secondary antibody incubation was performed at room temperature for 1 h. Blots were visualised using chemiluminescence using ECL-Plus reagent (Thermo Fischer Scientific, United States of America).

Table 4: Panel of antibodies used in Western blot assays

Primary Antibody	MW (kDa)	Host species	Dilution	Commercial	Secondary	Block Solution
MYADM	30	Mouse	1:500	mAb2B12#was generated as previously described *Aranda et al 2011*	1:10000	Milk 5%
HDAC8	42	Rabbit	1:10000	Abcam#ab187139	1:10000	Milk 5%
CD73	73	Rabbit	1:1000	Abcam#ab124725	1:10000	Milk 5%
CD63	53		1:500	Biosciences (SBI system) #EXOAB-CD63A-1	1:1000	Milk 5%
GAPDH	37	Rabbit	1:2000	Cell Signaling	1:10000	Milk 5%
ß-Tubulin	55	Mouse	1:1000	Santa Cruz	1:10000	Milk 5%
pSTAT5$_{(Y694)}$	90	Mouse	1:2000	BD	1:20000	BSA 2%
STAT5	90	Rabbit	1:2000	Santa Cruz	1:20000	Milk 5%

4.2. Immunofluorescence assays

Cells were fixed for 30 minutes with 4% paraformaldehyde, rinsed in 1X PBS three times each for 10 min and finally blocked for 1 hour at room temperature with 0.2% Tripton X-100, 5% normal donkey serum (Jackson Immnuno Research) and 2% of BSA in PBS. Primary antibody (**Table 5**) was incubated overnight at 4ºC. Secondary antibody Alexa Fluor 488 donkey anti-rabbit or anti-mouse IgG and Alexa Fluor 555 donkey anti-rabbit or anti-mouse (all from Invitrogen, Paisley, UK) were incubated for 1 hour at room temperature. After the final washes, 1 µg/ml 4', 6-Diamidine-2' -phenyl indole, dihydrochloride (DAPI) in PBS was added. Slides were mounted using Vectashield H-1000 medium (Vector Labs) and examined images were captured using a TCS SP5 Confocal Laser Scanning Microscope (Leica Microsystems, Wetzlar, Germany) with the LAS AF acquisition program (version 2.6.0.7266). Fluorescence images were captured using a Leica DMI6000B microscope (Leica Microsystems). Captured images were handled using Adobe Photoshop CS6 (Adobe Systems, San Jose, CA, USA).

Table 5: **Panel of antibodies used in immunofluorescence assays**

Primary Antibody	Host species	Dilution	Commercial
Anti-HDAC8	Rabbit	1:1000	Abcam#ab187139
Anti-SDF1	Rabbit	1:1000	Abcam#ab187139
Tubulin	Mouse	1:1000	Santa Cruz

5. Functional studies

5.1. Isolation of $CD34^+$ cells

$CD34^+$ cells were isolated from BM (HD and MPN) and from leukapheresis of HD. MNC were counted with trypan blue and $CD34^+$ progenitor cells were sorted by magnetic labelling using the human CD34 MicroBead kit (Miltenyi Biotec, Germany) in accordance with manufactures protocol. The purity of $CD34^+$ cells after separation was assessed by flow cytometry using FITC-conjugated CD34 (BD, USA).

5.2. *Transwell* assays – haematopoiesis support

To analyse the capacity of $JAK2^{V617F}$-MSC (isolated at diagnosis) and HD-MSC to support normal and leukemic haematopoiesis *in vitro transwell* assays were performed. Briefly, confluent MSC at passage 3 were trypsinized and subculture at a concentration of $1X10^5$ MSC/well in 24-well plates. After overnight adhesion, $1X10^5$ $CD34^+$ cells were co-cultured using a *transwell* membrane of 0.04µm (Costar, Corning NY, USA) (**Figure 6**). Cultures were maintained for 48 hours. Thereafter, the persistence of primitive progenitors was assessed by transferring cells into a semi-solid medium to allow the development of hematopoietic colonies.

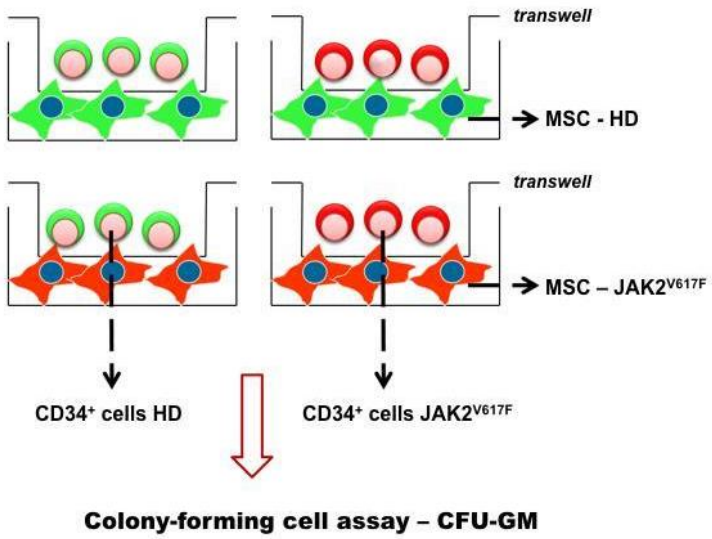

Figure 6: Protocol scheme of *transwell* assays. *In vitro* studies of haematopoiesis supporting ability of BM-MSC in *transwell* assays. JAK2^{V617F}-MSC and HD-MSC were co-culture with CD34^{+} cells from BM-HD and BM-JAK2$^{V617F.}$

5.3. Colony-forming cell assay

To study the capacity of the different stromal layers to support haematopoiesis, CD34^{+}cells recovered from the different culture experiments were washed and counted. 5X10^{3} cells were plated in a 24-well culture plate (Costar, Corning NY, USA) with 0.5mL complete methycellulose medium - MethoCult H4534 (Stem cell Technology, Vancouver, Canada) and recombinant cytokines, as previously described *(Lopez-Holgado, et al 2004)*. The cultures were incubated in a humidified atmosphere at 37ºC with 5% CO_2 cultured for 14 days. Colony-forming units in culture (CFU-C) were subsequently scored with an inverted microscope following standard criteria for colony counting. Colonies were defined as clusters consisting of 40 or more cells. Results were expressed as the number of progenitor produced (CFU-GM (Granulocyte/Macrophage)/10^{5} cells.

5.4 Long-term bone marrow cultures (LTBMC)

LTBMC were established according to the methods of Gartner and Kaplan with slight modifications *(Lopez-Holgado, et al 2005).* HD-MSC and JAK2^{V617F}-MSC were plated (concentration of 10^{3}) in a 48-well plate (Costar, Corning NY, USA) and were maintained in culture. When

confluence was achieved the expansion medium was changed for LTBMC medium (IMDM 350 mOsm/kg supplemented with 10% pre-selected FCS, 10% horse serum (BioWittaker) and 5×10−7 M hydrocortisone sodium succinate (Sigma). The cultures were incubated in a humidified atmosphere with 5% CO_2 in air at 33 ◦C for 5 weeks. Weekly stromal layer formation was analysed under an inverted microscope. For re-feeding, half of the supernatant was removed and replaced with fresh LTBMC medium. The harvested non-adherent cells were counted and $5x10^3$ were plated in a 24-well culture plate (Costar, Corning NY, USA) with 0.5 mL of methylcellulose medium - MethoCult™ H4434 Classic - with recombinant cytokines and EPO for human cells (Stem cells Technologies, Grenoble, France) to quantify erythroid progenitors (CFU-E and BFU-E), granulocyte-macrophage progenitors (CFU-GM, CFU-G and CFU-M) and multi-potential granulocyte, erythroid, macrophage and megakaryocyte progenitors (CFU-GEMM). After 14 days, the colonies were scored with an inverted microscope following standard criteria for colony counting (**Figure 7**). Results were expressed as the number of CFU per 10^5 cells seeded and the total number of CFU present in the culture.

Figure 7: Identification of the different colonies derived from human hematopoietic progenitors cells $5x10^3$ were plated in a 24-well culture plate with 0.5 mL of methylcellulose medium - MethoCult™ H4434 Classic - with recombinant cytokines and EPO for human cells. The different colonies type showed in an inverted microscope

6. BM-MSC HDAC8 inhibition (*in vitro* assays)

6.1. HDAC8 selective inhibitor

PCI34051 (1H-Indole-6-carboxamide, N-hydroxy-1-[(4-methoxyphenyl)methyl]-, N-Hydroxy-1-[(4-methoxyphenyl)methyl]-1H-indole-6-carboxamide) with the formula C17H16N2O3 (**Figure 8**) is a potent, specific inhibitor of histone deacetylase 8 (HDAC8) (IC50=0.01µM) with more than 200-fold selectivity over the other HDAC isoforms, such 1, 2, 3, 6 and 10. PCI34051 was supplied as crystalline solid (Cayman Chemical, Ann Arbor, USA) dissolved in DMSO in a stock solution of 10mM and stored at -20ºC for posterior use.

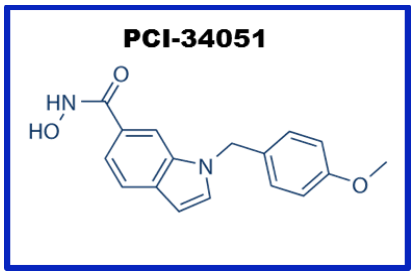

Figure 8: PCI34051 structure

6.2. *In vitro* studies in BM-MSC from HD and MPN patients after treatment with PCI 34051

To test if the PCI 34051 treatment affects the growth capacity of the BM-MSC from HD, ET and PV patients, the cells were seeded in 96-well or 24-well plates at a concentration of $3X10^3$ cells/well or 10^4 cells/well, respectively. AlamarBlue, apoptosis (Annexin-V) and cell cycle assays were performed to study the alterations on BM-MSC due to the inhibition of HDAC8.

RT-PCR, western blot and immunofluorescence assays were performed to study the expression of HDAC8 in the BM-MSC (HD and $JAK2^{V617F}$) after the treatment with PCI34051. The cells were seeded in 6 well-plates at a concentration of $2X10^5$/mL and treated with PCI34051 for 48 hours. Then, the cells were trypsinized and the different methodologies described above were performed (**Figure 9**).

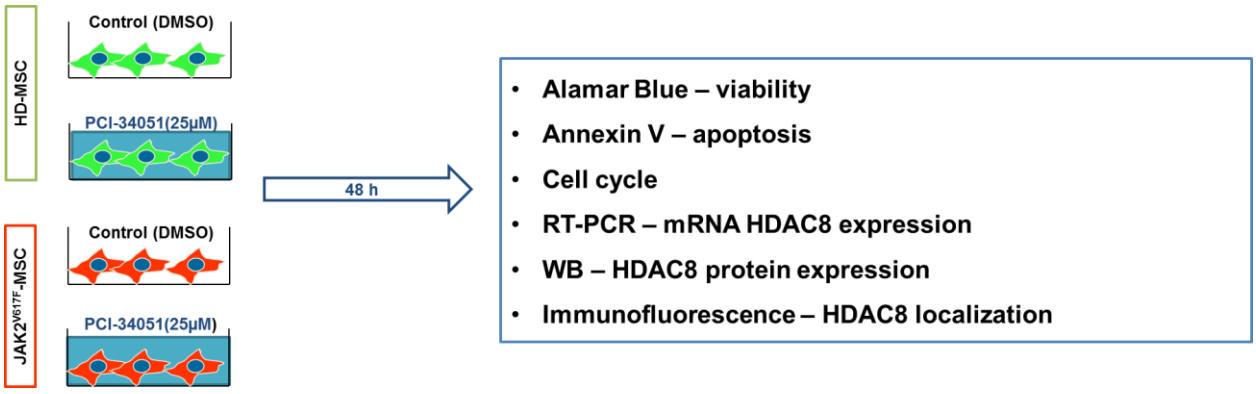

Figure 9*:* Scheme of the *in vitro* studies performed on BM-MSC treated with the HDAC8 specific inhibitor PCI 34051.

6.2.1. *AlamarBlue staining*

AlamarBlue staining (Invitrogen, UK) was performed according to the manufacturer´s instructions. The BM-MSC from -HD (n=3), -PV (n=3) and -ET (n=3) were plated and maintained in culture during 6 hours to allow cell attachment, then they were incubated for 6h, 24h, 48h and 72h with PCI34051 at different concentrations (0,5µM - 1µM - 2µM - 5µM - 10µM- 25µM - and 50µM).

After treatment, BM-MSC were incubated for 4-6 hours at 37ºC with a solution prepared with alamarBlue and fresh culture medium (with reduced serum) in a proportion 1:9 (v/v).

Absorbance was measured at 570 nm and 620 nm with a photometric microplane reader in an Infinite® F500 teach plate reader (Tecan; Maennedorf, Switzerland). Fluorescence was also measured using a fluorescence excitation wavelength of 540-570 nm (peak excitation is 570 nm). AlamarBlue activity was calculated subtracting the blank value (well with medium but not cells) and normalised with control (untreated cells).

6.3. Haematopoietic supportive capacity of BM-MSC treated with PCI 34051

To study the impact of HADC8 inhibition in the capacity to maintain haematopoiesis BM-MSC from HD and JAK2^{V617F} patients, co-culture experiments were performed. BM-MSC from both groups (passage 3-5) were tripsinized and plated at concentration of 10^5 cells/ well in a 6-well plate (Costar, Bodenheim, Germany) overnight. Then the BM-MSC were incubated

with PCI34051 at concentration of 25µM for 48 hours. After BM-MSC treatment, the CD34^{+}cells/MNC from BM of HD and JAK2^{V617F} patients were co-cultured by direct contact or in a *transwell* system constituted by a polycarbonate membrane (3.0µm pore size, Corning Incorporated, Costar). The MNC:MSC ratio was 10:1 and CD34^{+}cells:MSC was 2:1, according previous experiments *(Sanchez-Guijo, et al 2005, Villaron, et al 2004).* The cultures were maintained in a 5% CO_2, humidified atmosphere at 37ºC for 48 hours. After the time of co-culture the hematopoietic cells were recovered and different protocols were performed as showed in the **Figure 10**.

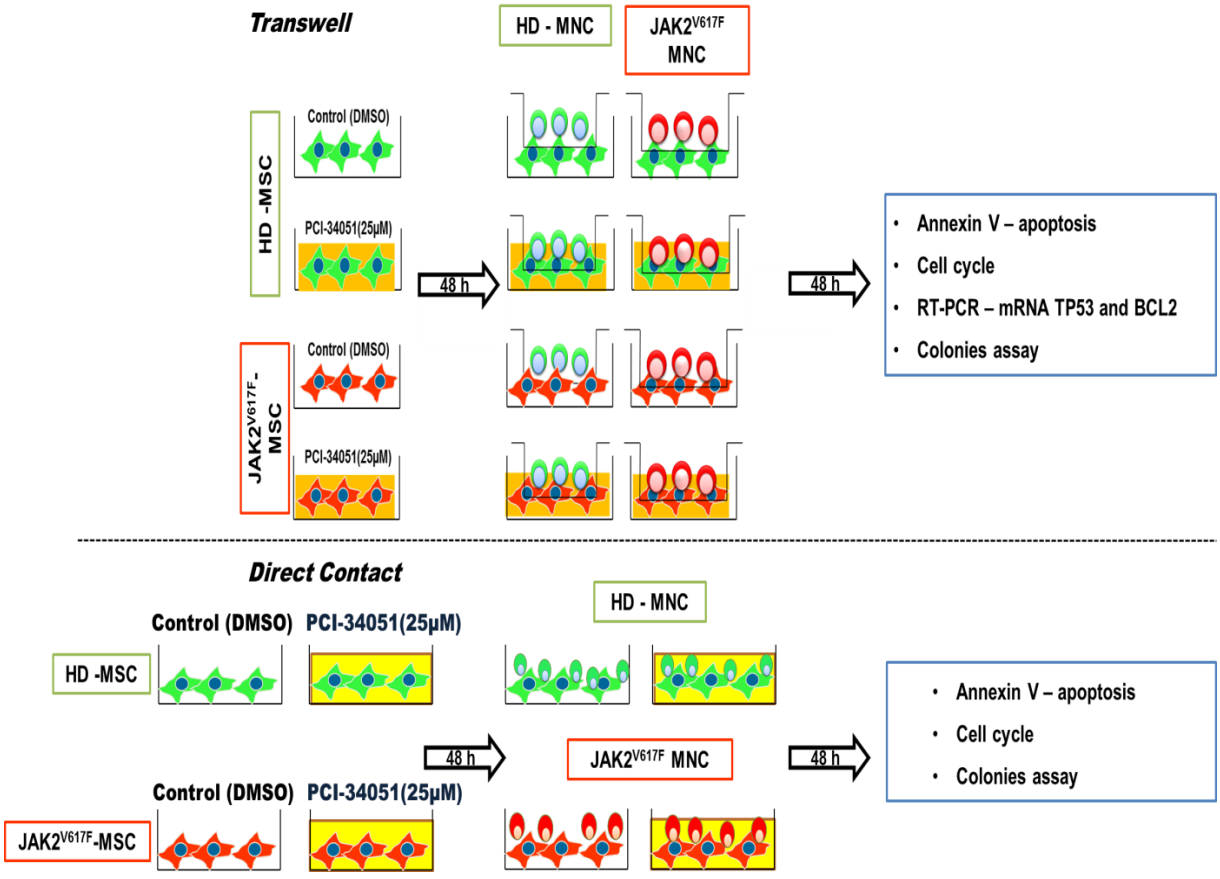

Figure 10: Scheme of hematopoietic supportive capacity of BM-MSC treated (HDAC8i). Hematopoietic cells (CD34^{+} cells and MNC) from HD and JAK2^{V617F} were co-cultured, *transwell* and direct contact, with BM-MSC treated with PCI34051

To study whether or not the stroma protects the leukemic cells from PCI34051 treatment an *in vitro* experimental draw was used, where the BM-MSC and different MPN cell lines were treated at the same time with the specific HDAC8i.

BM-MSC from HD and $JAK2^{V617F}$ patients were cultured until reaching 70% confluence, then MPN cell lines (UKE-1, SET-2 and HEL) were added to the stromal layer at $2x10^5$ cells/mL in culture medium, either in direct contact (cell to cell contact) or separated (by a 3 µm micropore membranes). After 48h of treatment with the specific inhibitor of HDAC8, the cell lines were harvested and assessed as described below for viability, colony assay, and immunoblotting (pSTAT5).

7. Extracellular vesicles

7.1 Isolation of EV from BM-MSC culture medium

The protocol used in our experiments was adapted from Théry et al (2006) *(Thery, et al 2006)* and has been recently published from our group *(Muntion, et al 2016, Ramos, et al 2016)*

BM-MSC culture conditioned media - To prepare the condition media, BM-MSC from HD and MPN patients (ET and PV) were cultured in standard condition until reached a 60-80% of confluence. Then the cultures were washed with PBS twice and cultured, during 24 hours, under starving conditions in RPMI-1640 medium without FBS to induce stress and the release of EV.

The conditioned medium (CM) was collected and centrifuged at 300 *g* for 10 minutes to eliminate the cells, then the supernatant was centrifuged at 2000 *g* for 20 minutes to remove cell debris. To remove large cell organelles and apoptotic vesicles the supernatant was filtered through a 0.22 um filtered (Millipore, Billerica, MA). After filtration the CM was ultracentrifuged at 100,000 *g* for 70 min at 4ºC to obtain the EV. In some cases the EV pellets were washed with doubled filtered PBS and ultracentrifuged at 100,000 *g* for 70 min at 4ºC. The pellets were stored in DMEN with 1% of DMSO at -80ºC until their use or in doubled filtered PBS for other protocols (**Figure 11**).

The samples were ultracentrifuged in polycarbonate tubes (25 mm × 89 mm, Beckman Coulter) that have a volume of 22 ml. A Beckman Coulter ultracentrifuge (Beckman Coulter OptimaL-90K ultracentrifuge; Beckman Coulter, Fullerton, CA, USA) was used with a fixed angle rotor type 70ti.

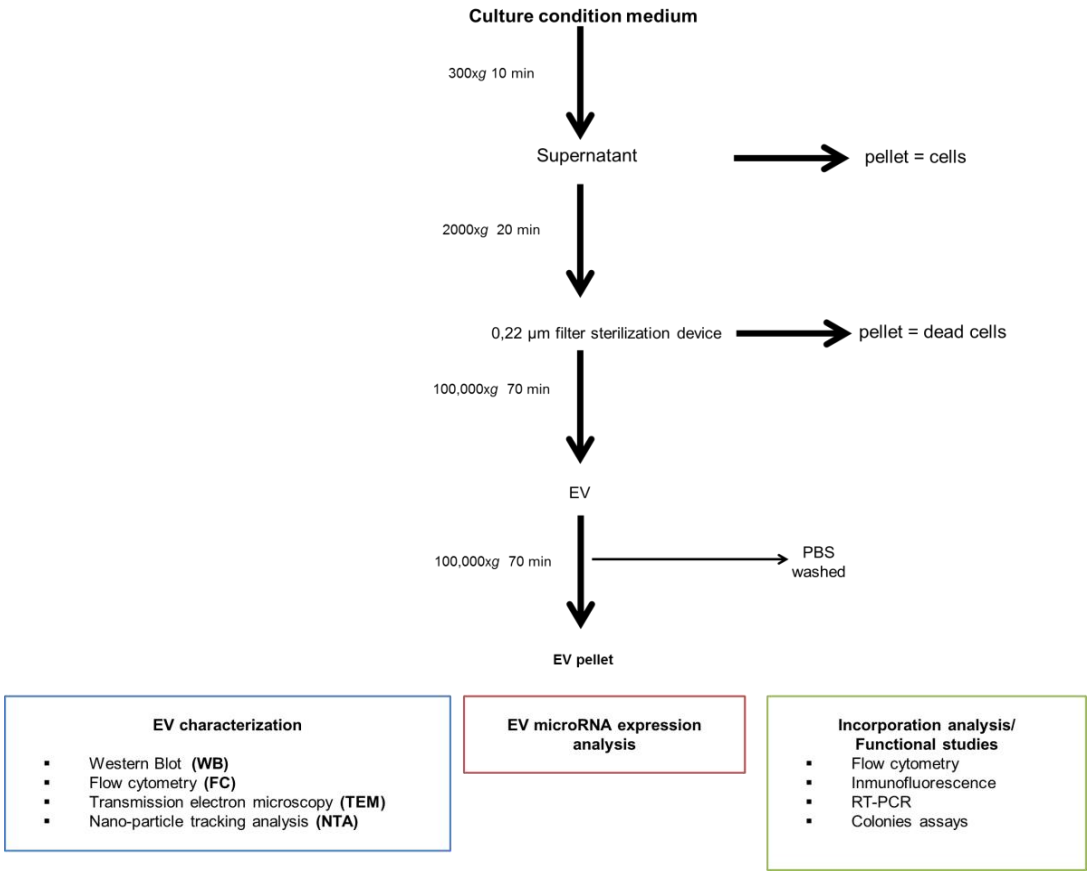

Figure 11*:* **Isolation and characterisation scheme of EV from BM-MSC**

Commercial isolation kits to EV isolation – We also used ExoQuick-TC™ (ExoQuick; System Biosciences, Mountain View, CA, USA), a commercial exosome isolation kit. This kit was used to obtain more EVs from BM-MSC in early passages, to use them for microRNA analysis. The EV from culture medium were isolated according to the manufacturer's instructions.

7.2 EV characterisation

7.2.1 Multiparametric flow cytometry (MFC) analysis - EV from BM-MSC were characterized by MFC following a previously described protocol *(Ramos, et al 2016)*.

After the second ultracentrifugation, the pellet was re-suspended in doubled-filtered PBS and EV were stained with the immunephenotypic panel using human MSC markers (CD90, CD44 and CD73), haematopoietic markers (CD34 and CD45) and EV markers (CD81 and CD63). Samples were incubated using a 6-color combination, set up with the following monoclonal antibody panel: 5 µl of anti-CD90- FITC/ 10 µl of anti-CD73-PE or anti-CD63-PE/ 10 µl of anti-CD34-PerCPCy5.5/ 5 µl of anti-CD44-APC/ 5 µl of anti-CD81-APCH7/ 5 µl of anti-CD45-V500, all of them purchased from BD Biosciences (San José, CA). The stained EV were re-suspended (final volume 700uL) with a mix of fluorescent beads composed of varied diameters (0.5, 0.9 and 3 µm) Megamix (Biocytex, Marseille, France) and perfect-Count Microespheres (Cytognos, Salamanca, Spain) of 6–6.4 µm in size. For EV acquisition we used FACSCanto II flow cytometer (BD Biosciences San Jose, CA) using FACSDiva 6.1 software (BD Biosciences).

A total of 100000 events were acquired (at low speed). Data were analysed using the Infinicyt program (Cytognos, Salamanca, Spain).

7.2.2 Nano-particle tracking analysis (NTA) - Analysis of absolute size distribution of EV was performed using NanoSight NS 300 (NanoSight Ltd., UK) equipped with a sCMOS camera.

After ultracentrifugation, the EV were diluted in 1 ml of doubled filtered PBS. The NTA measurement conditions were as follows: temperature between 21 and 23.6 °C; viscosity between 0.9 and 0.965 cP, frames per second 25, measurement time 60s. Before acquisition the samples were diluted in water (1:1000) due to their high concentration. The detection threshold was similar in all samples. The results indicate the mean sizes and standard deviations of at least three individual measurements. NTA analyses were performed by the *Servicio Científico-Técnico "Soft Materials" Institut de Ciència de Materiales de Barcelona (ICMAB-CSIC)*, Spain.

7.2.3. Transmission electron microscopy (TEM) – The electron microscopy was performed by Dr. Teresa Rejas (Universidad Autónoma de Madrid, Spain). EV pellets were re-suspended in PBS and fixed in 2% of paraformaldehyde and 2.5% of glutaraldehyde, then were added to carbon-coated grids. Uranyl-oxalate solution was used for negative counter-staining. The vesicles were visualized with a transmission electron microscopy (FEITecnai G2 Spirit Biotwin) and the images were captured using a digital camera (Morada, Soft Imaging System, Olympus).

7.2.4. Immunoblotting (WB) – After ultracentrifugation, EV from BM-MSC (patients and donors) were directly re-suspended in lysis buffer, and incubated in ice for 20 minutes. Non-soluble material was eliminated by centrifugation. Primary antibodies were rabbit α-CD63 (EV marker) and rabbit α-CD73 (MSC marker).

7.3. EV microRNA expression analysis

Total RNA (<350 ng) of EV from 8 HD-MSC, 4 PV-MSC and 7 ET-MSC were used to study the microRNA composition. EV were isolated from the supernatant of different samples using a commercial kit for EV isolation (ExoQuick; System Biosiences, Mountain View, CA). Qiagen miRNeasy kit (Qiagen) was used to purify and to conserve the small RNA. Then the RNA from the recruited samples was retro-transcribed (RT) with Megaplex^{TM} RT Primers pool (Applied Biosystems). RT product was loaded in a 384-well microfluidic cards (TaqMan ® Micro RNA Array A) and the PCR runs were performed on a 7900 HT Fats Real-Time PCR system (Applied Biosystems). The panel contains 384 PCR assays enabling accurate quantification of 378 human micro\RNAs and three endogenous controls (RNU44, RNU48 and 4 replicates of RNU6B).

MicroRNAs expression data were processed within the R statistical computing environment (version 2.10.0), using ΔΔCt standard procedures from the *HTqPCR* package. Each microRNA raw Ct value was tagged as undetermined when falling between levels of 36 and 40. Normalization was performed with the raw Ct values of the array endogenous control features according to the equation: $\Delta Ct_{microRNA} = Ct_{microRNA}$ - mean (Ct_{RNUs}). MicroRNA differential expression was extracted according to ΔΔCt calculations, where $\Delta\Delta Ct_{microRNA}$ =

mean($\Delta Ct_{ET\ or\ PV}$) - mean($\Delta Ct_{HealthyDonors}$). Statistical significance was assessed using *limma* package t-tests adjusted for multiple testing.

Hsa−miR−155 expression was studied in 5 EV from HD-MSC and 5 EV from $JAK2^{V617F}$-MSC. EV isolation was performed using the classic ultracentrifugation methodology described above. Isolated EV were re-suspended in 500µl Trizol (Roche Diagnostics GmbH, Mannheim, Germany). RNU43 was used as endogenous control.

7.4. Incorporation analysis and functional studies

7.4.1. Nanoparticle tracking analysis - To study EV uptake into hematopoietic progenitor cells, the EV from 120-160 mL (15-20 flask 75 cm^2) of CM $JAK2^{V617F}$ and HD - MSC were labelled with 2 µl/mL Vybrant Dil cell-labeling solution (Life Technology, NY, USA) according to published works *(Muntion, et al 2016)*. Labelled EV pellets were incubated with $CD34^+$cells ($1X10^5$) for 24 hours. After incubation the cells were recovered and washed with PBS and the incorporation was assessed by flow cytometry and fluorescence microscopy. As negative control, the same quantity of dye used to label the EV was submitted to the same procedure but without the presence of EV.

For immunofluorescence assays the $CD34^+$ cells were first stained with mouse α-CD45 (Biolegend, San Diego, CA) and then with a donkey anti-mouse Alexa Fluor 488 (Invitrogen, Paisley, UK). Cellular nuclei were stained with DAPI (section of methodology 3.2).

7.4.2. MicroRNA-155 expression in HD and $JAK2^{V617F}$ $CD34^+$ cells - $CD34^+$ cells isolated from BM of HD and $JAK2^{V617F}$ patients were maintained in a 96-well plate with RPMI-1640 (with FSB) for 2 hours, and then approximately 70µg/mL of EV from $JAK2^{V617F}$-MSC and HD-MSC (36 mL of CM) were added and maintained for 48 hours in culture. Afterwards, the $CD34^+$ cells were recovered and total RNA was extracted using *Trizol* reagent. $CD34^+$ cells without EV were also maintained in culture as negative control. Individual quantitative PCR was performed for hsa-miR-155-5p and RNU6B, being the latter used as control. Relative quantification was calculated from the $2^{-\Delta\Delta Ct}$ values with the equation: $\Delta Ct = Ct_{microRNA}\text{-}155 - Ct_{RNU6B}$.

7.5 Functional studies

To evaluate if the uptake of EV from normal and leukemic stroma could change the behaviour of the progenitor haematopoietic cells, apoptosis and clonogenic assays were performed. The $CD34^+$ cells from BM and leukapheresis (apoptosis studies) HD and BM-$JAK2^{V617F}$ were incubated with EV from HD-MSC (n=4 in FC assays and n=6 clonogenic assays) and $JAK2^{V617F}$-MSC (n=4 in FC assays and n=6 clonogenic assays). $CD34^+$ cells without EV were used as controls.

8. Statistical Analysis

Statistical analysis was performed using IBM SPSS Statistics 21 (Chicago, IL, USA) and GraphPad Prims version 5.00 for Windows (GraphPad Software). The values reported in the figures are given as median with the interquartile range or with mean ± standard error of the mean (SEM). Differences between populations were calculated using the Mann-Whitney tests with Bonferroni corrections. A p-value <0.05 was considered to be statiscally significant.

1. Myeloproliferative Neoplasms (JAK2^{V617F}): *Mesenchymal Stromal cells*.

1.1. MSC characterisation

1.1.1 Isolation and morphology of BM-MSC in culture

Stromal cells from BM of all groups were isolated and expanded in monolayer of plastic-adherent culture cells. BM-MSC from HD and MPN-JAK2^{V617F} displayed the characteristic fibroblastic-like morphology (**Figure 12**).

BM-MSC from CML (Ph^{+}) showed a heterogeneous morphology, including a mixture of small round-shaped cells and fibroblastic-like cells with aberrant and irregular morphology.

All BM-MSC cultures form HD and MPN (JAK2^{V617F}) were successfully isolated and subcultured reaching 80% confluence, following initial mononuclear cell plating. In the case of cultures from CML patients, one out 14 samples did not expand *in vitro* and other one did not reach passage 3. Because during *in vitro* expansion these cells exhibited an aberrant morphology, ß-Galactosidase staining was performed on 2 CML-MSC and 2 HD-MSC, and the percentage of cells expressing lacZ following transient or stable transfection was determined (**Figure 12**). In (71.9%) of BM-MSC from CML patients, a blue colour was visualised, whereas this never happened in BM-MSC from HD.

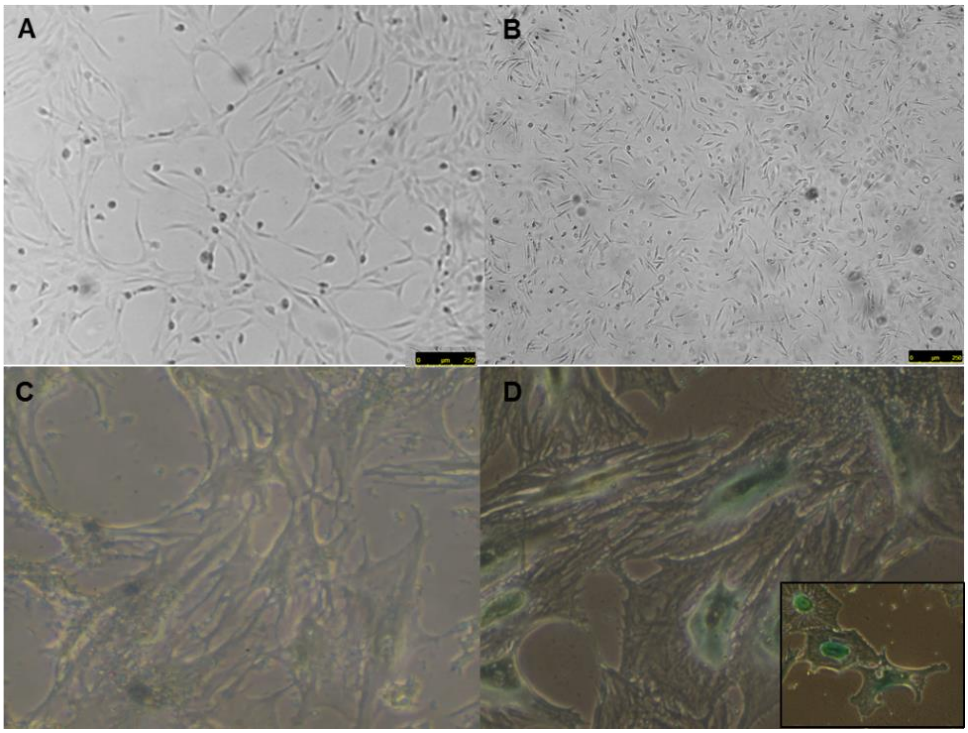

Figure 12: Images of expanded BM-MSC. Initial BM-MSC culture morphology of HD-MSC (A) and JAK2^{V617F}-MSC (B). (C) HD-MSC staining with ß-Galactosidase, where was not observed blue cells (40X). (D) CML-MSC with stained in blue (senescence cells) (40X). Scale bar: 0-250µm

In order to study the growth kinetics, BM-MSC from all groups were plated using the same culture conditions. Population doubling (PD) was calculated through at least 3-4 culture passages. BM-MSC from MPN-JAK2^{V617F} patients showed similar proliferative capacity compared to BM-MSC from HD (**Figure 13**). However, PV-MSC presented the highest proliferative capacity along the passages without statistical significances compared to HD and ET MSC. By the contrast, CML-MSC showed a significantly lower proliferation capacity, as compared with HD-MSC and ET/PV-MSC (**Figure 13**).

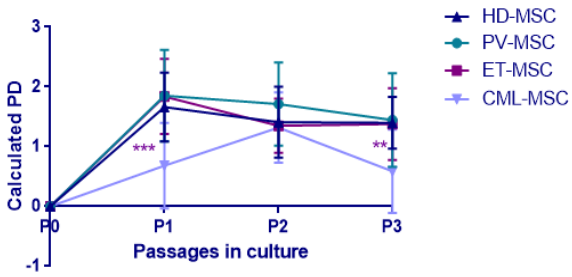

PDs Contrats	p-value	Median and n/ Median and n
PD1 – HD vs PV	0,4710	1,732 n=15/ 1,785 n=12
PD1 – HD vs ET	0,4938	1,732 n=15/ 1,778 n=19
PD1 – HD vs CML	0,0004***	1,732 n=15/ 0,585 n=11
PD2 – HD vs PV	0,42	1,474 n=15/ 1,564 n=12
PD2 – HD vs ET	0,64	1,474 n=15/ 1,352 n=19
PD2 – HD vs CML	0,78	1,474 n=15/ 1,400 n=11
PD3 – HD vs PV	0,9626	1,578 n=15/ 1,152 n=12
PD3 – HD vs ET	0,9171	1,578 n=15/ 1,396 n=19
PD3 – HD vs CML	0,0045**	1,578 n=15/ 0,5443 n=11
PD1 – PV vs CML	0,0004**	1,785 n=12/ 0,5850 n=11
PD1 – ET vs CML	0,0002***	1,778 n=19/ 0,5850 n=11
PD3 – PV vs CML	0,022*	1,152 n=12/ 0,5443 n=11
PD3 – ET vs CML	0,005**	1,396 n=19/ 0,5443 n=11

Figure 13: Analysis of population doubling (PD) - (left) a boxplot of the doublings from P1 to P3 of BM-MSC isolated from HD and from MPN patients. (right) a table with the p values and median results. *, ** and *** statistically significant contrasts (p-value < 0.05, < 0.01 and < 0.001, respectively)

1.1.2 Multiparametric flow cytometry immunophenotyping

To analyse the cell surface phenotype, BM-MSC from HD and JAK2^{V617F} MPN patients (ET and PV) were analysed by flow cytometry in accordance with the criteria established by the ISCT *(Dominici, et al 2006)* **Table 6.**

Table 6: Number (n) of cases which stromal cells were characterised by multiparametric flow cytometry.

Sample	MPN	n
ET	JAK2^{V617F}	23
PV	JAK2^{V617F}	7
CML	BCR-ABL	6
HD	----------	20

In all BM-MSC samples, purity was above 98%, constantly expressed the stromal cell markers CD105, CD90, CD73 and CD166, described as typical surface markers of BM-MSC. Haematopoietic lineage markers were not detected (**Figure 14**).

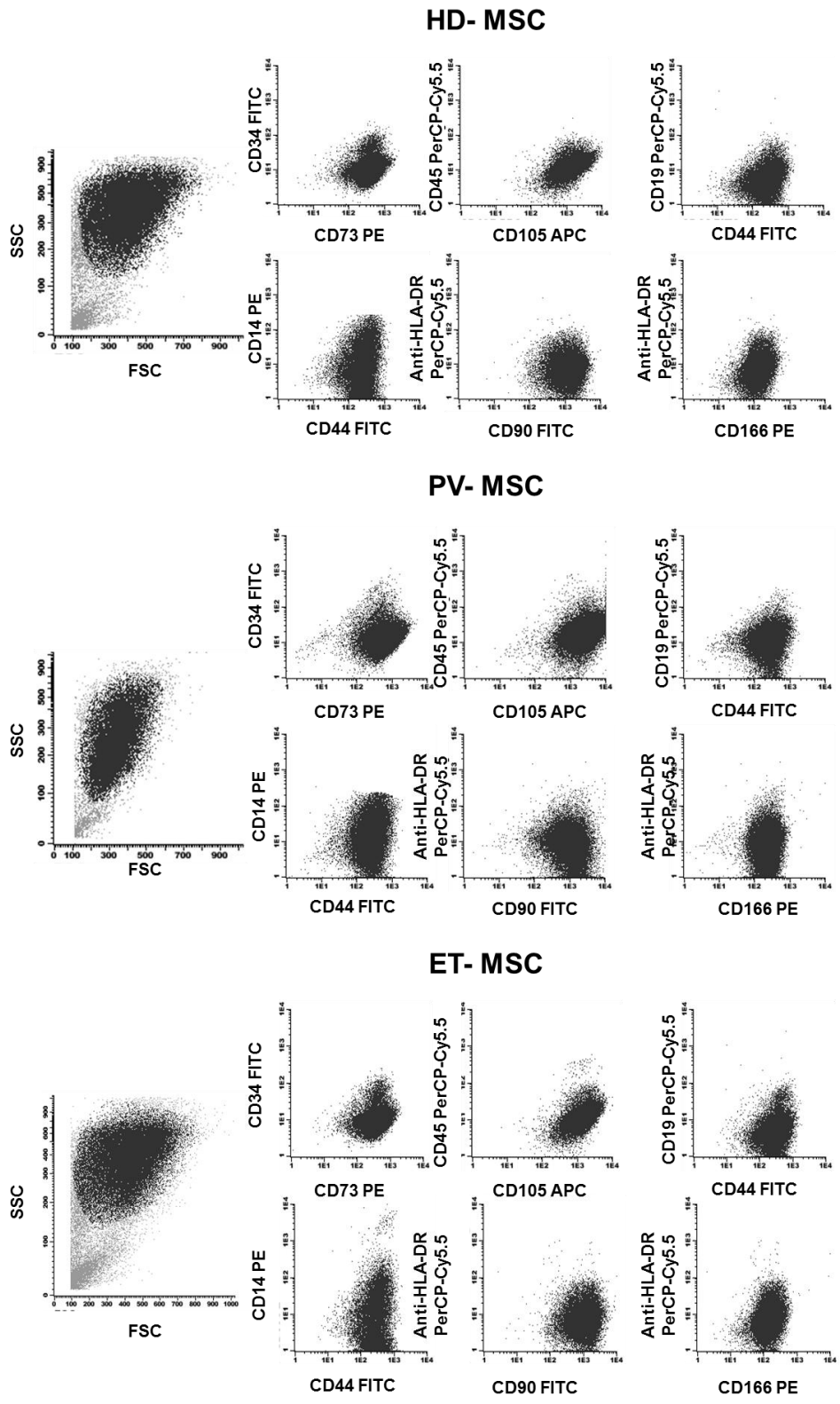

Figure 14: Multiparametric flow cytometry immunophenotyping Representative dot-plots of stained BM-MSC from –HD, -JAK2^{V617F} (PV and ET).

Stroma cell markers were detected in all samples, but different expression levels were observed for each of them. Thus, CD166 was typically dimly expressed, in all BM-MSC, when compared to the other markers. MIF of each marker was set together for comparison into a scatter dot plot (**Figure 15**). BM-MSC from JAK2^{V617F} MPN patients showed an increase expression of the markers CD73, CD90 and CD44, when compared to HD-MSC.

CD105 showed a significant reduction (p=0.03) in its expression in BM-MSC from JAK2^{V617F} patients, both PV and ET, when compared to HD-MSC. However, CD105 expression was increased in BM-MSC from MPN patients without the JAK2^{V617F} mutation (JAK2 negative) compared to BM-MSC from patients JAK2^{V617F}.

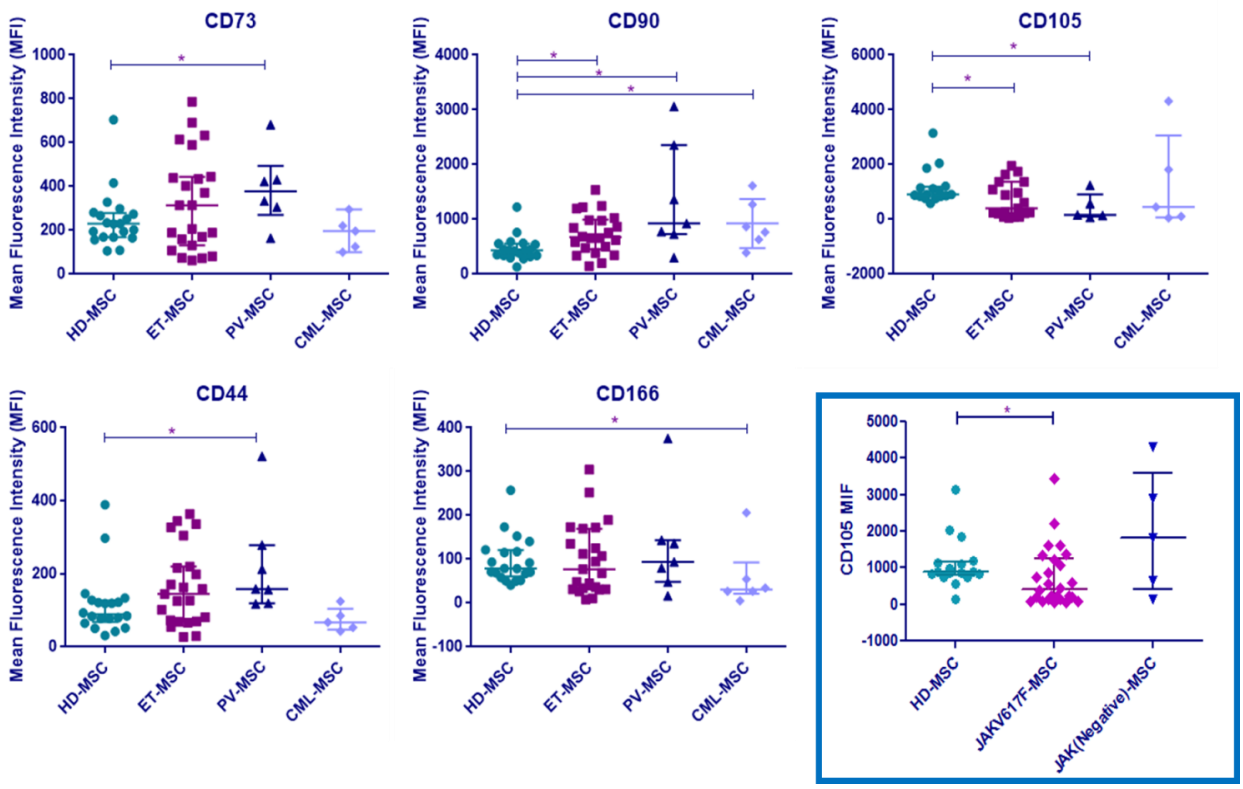

Figure 15: Immunophenotype of BM-MSC from MPN patients *versus* HD. Scatter dot plot of positive surface marker expression of HD-MSC, ET-MSC, PV-MSC and CML-MSC. Differences can be observed between the different stromal population and markers. The line represents the median with interquartile range. MIF – Mean Fluorescence Intensity. (* p<0.05). JAK (Negative)-MSC =4 MSC from MPN without the mutation in JAK2V617F and 1 with the CARL mutation.

1.1.3 Multipotent differentiation potential of BM-MSC

Differentiation assays were performed to fulfil the ISCT *(Dominici, et al 2006)* requirements for MSC definition. After induction with differentiation conditioned media, BM-MSC were able to differentiate into osteoblasts and adipocyte that were identified by positive staining of alkaline phosphatase activity and Oil Red O, respectively (**Figure 16**).

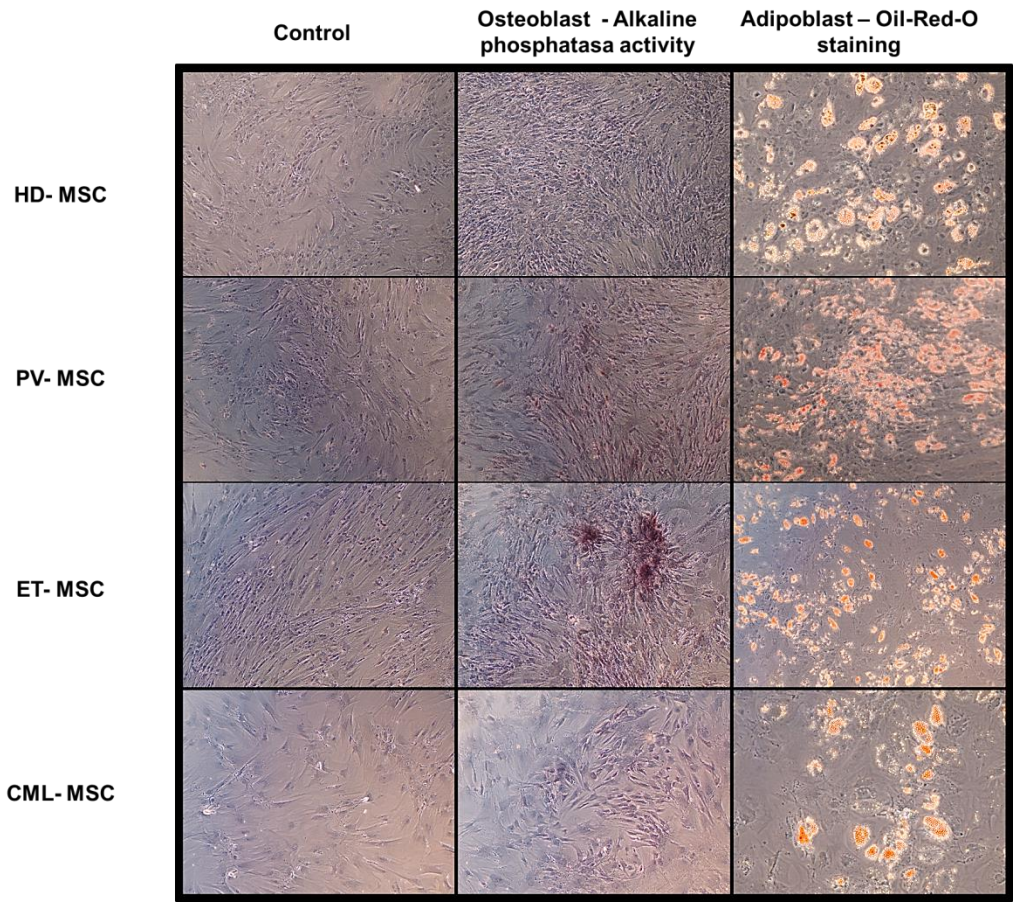

Figure 16: Microscope images of BM-MSC differentiation assays. *In vitro* multipotency by multilineage differentiation assays performed with HD-, ET-, PV-, CML- MSC. Left-handed photos represent the negative controls (no induction medium applied). The photos of the middle show osteogenic differentiation detected by alkaline phosphatase activity. Right -handed photos show adipogenic differentiation detected by fat staining with Oil-Red-O. (20X)

Differentiation capacity was evaluated in BM-MSC from HD (n=21), ET – $JAK2^{V617F}$ (n=22), PV-$JAK2^{V617F}$ (n=13) and from CML – Ph^{+} (n=6). Samples from HD and $JAK2^{V617F}$ patients shared similar capacity of osteoblast and adipocyte differentiation. A reduced time to achieve mature adipocyte lineage in BM-MSC from PV patients was observed when compared to HD-MSC,

although differences were not statistically significant. Whereas all samples from HD-MSC were able to differentiate, the same did not occur with BM-MSC from PV and ET. In detail, in one of the 13 PV-MSC and one of the 22 ET-MSC, adipocyte differentiation could not be documented. Similarly, in one case of ET-MSC samples osteoblast differentiation was not observed (**Figure 17**).

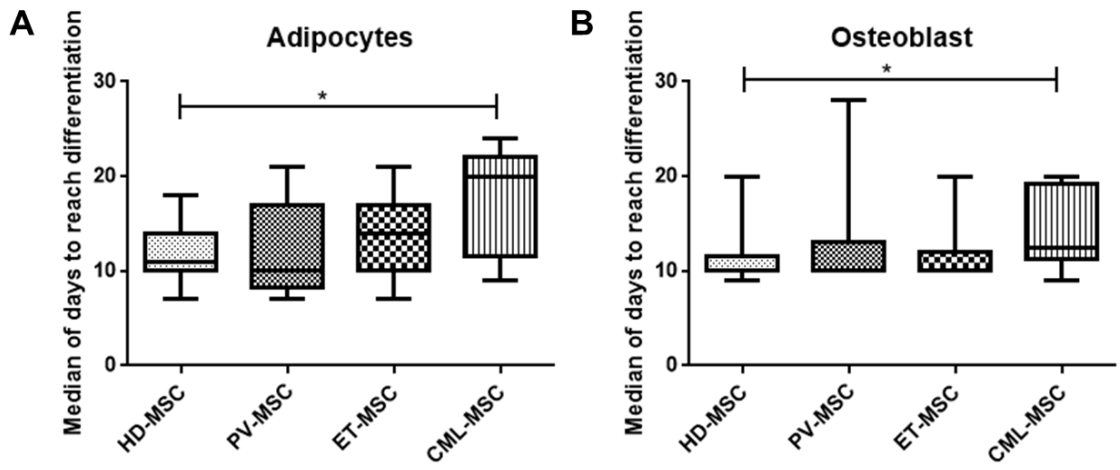

Figure 17: Differentiation capacity of MPN-MSC. Adipogenic (A) and osteogenic differentiation capacity of HD-MSC, JAK2^{V617F} – MSC (PV and ET) and CML-MSC. Boxplot graphics represent the median in days that take the BM-MSC in differentiate into mature adipocytes, which was evaluated by Oil Red O and osteoblasts evaluated by alkaline phosphatase staining.

1.2 Functional and genetic alterations in BM-MSC from JAK2^{V617F} patients

1.2.1 Apoptosis and Cell Cycle of BM-MSC

For these studies, 16 samples from ET, 7 from PV and 15 from HD-MSC were used. As shown in **Figure 18**, the percentage of cells alive (annexinV$^-$/7AAD$^-$) was higher in PV and ET- MSC compared to HD-MSC. The proportion of late apoptosis (AnnexinV$^+$/7AAD$^+$) was increased in the HD when compared to PV-MSC (p=0.02).

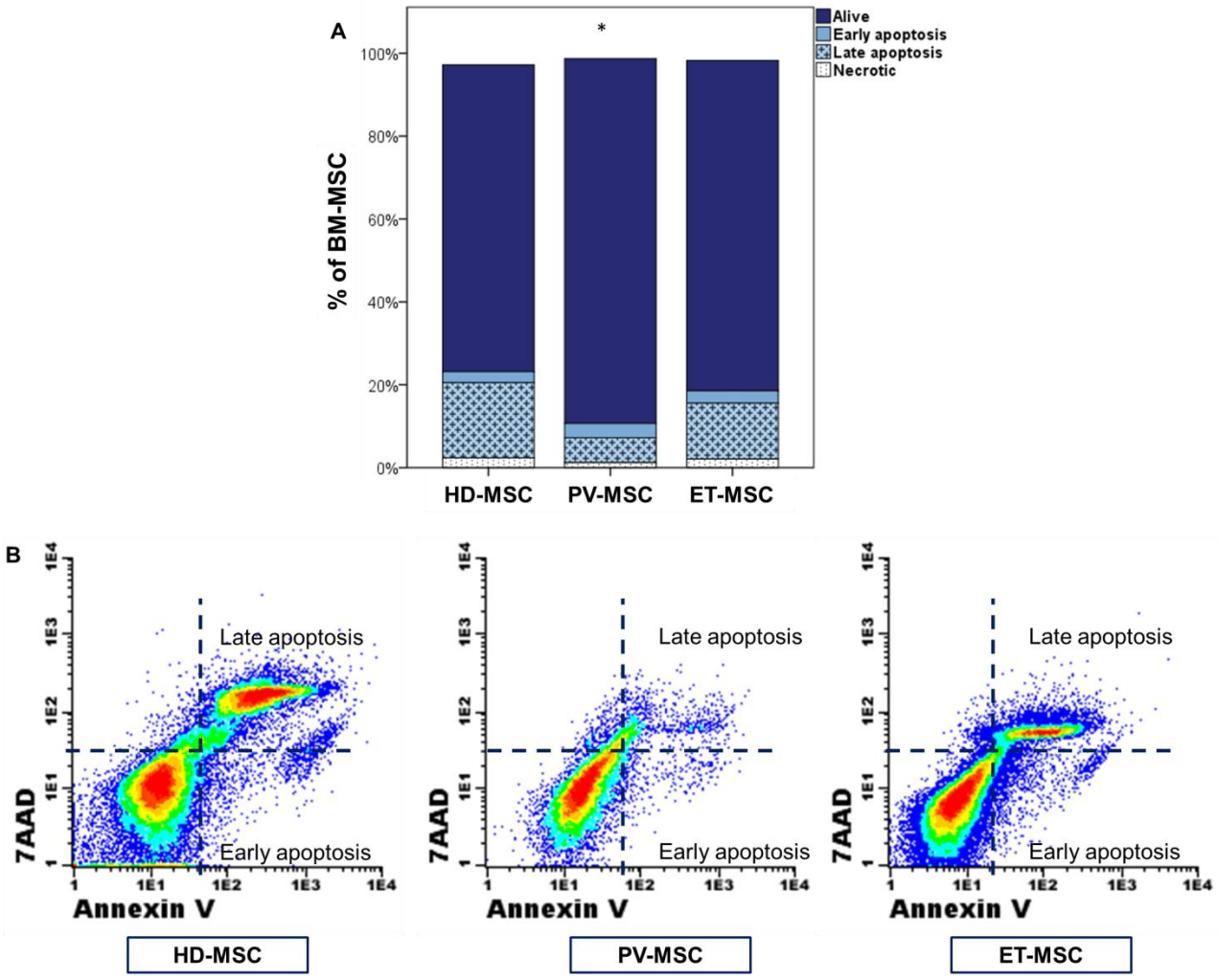

Figure 18: AnnexinV/7AAD analysis of BM-MSC. (A) Stacked bar chart that represents the percentage of viable, apoptotic (early and late apoptosis) and necrotic cells. The percentage of apoptotic cell decrease in the BM-MSC from JAK2^{V617F} patients respect to HD-MSC, statistical significance observed in late apoptosis when compared PV-MSC with HD-MSC (* $p<0.05$). (B) Representative FACS dotplot of annexinV/7AAD staining on BM-MSC.

Additionally, cell cycle was performed in BM-MSC from 10 HD and from 15 JAK2^{V617F}. Only ET-MSC showed a tendency to a higher percentage of cells in S phase (**Figure 19**).

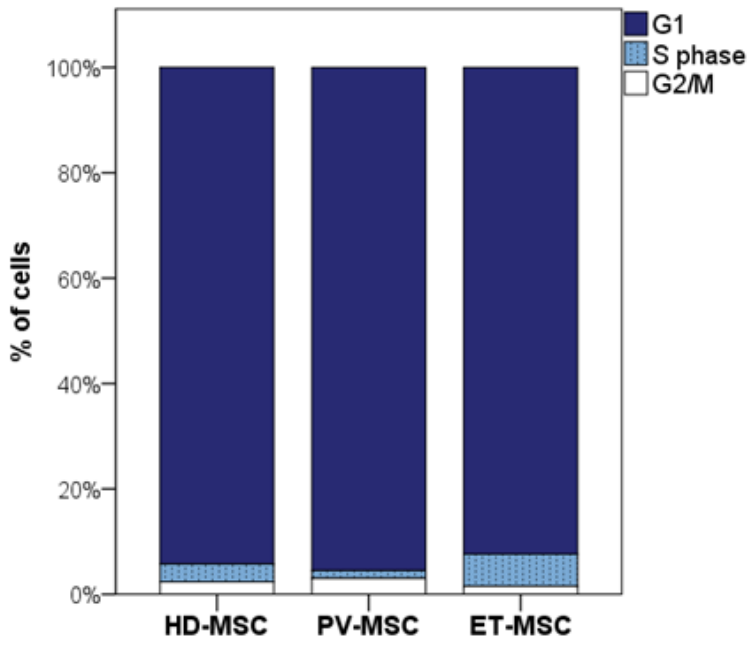

Figure 19: Cell cycle analysis of BM-MSC. Stacked bar chart represents the percentage of cells in G1, S and G2/M phase from HD-MSC, PV-MSC and ET-MSC. No differences were observed between groups.

1.2.2 Gene expression profile of BM-MSC from MPN patients

We analysed the gene expression profile of BM-MSC from 6 CML, 8 $JAK2^{V617F}$ (4 PV/4 TE) patients and 10 HD, using Affymetrix Oligoarrays (human Gene 1.0 ST arrays). Compared to HD, a total of 596 and 33 genes were differentially expressed in BM-MSC from $JAK2^{V617F}$ and CML patients, respectively.

Compared to HD, in PV-MSC 141 genes were up-regulated and 16 genes down-regulated, in ET-MSC 24 genes up-regulated and 12 down-regulated, and in CML 31 genes up-regulated and 20 genes were down-regulated. As it can be observed in **Figure 20**, 19 dysregulated genes were common in all the diseases (**Table 7**).

Myeloid-associated differentiation marker (MYADM) gene and myeloid leukaemia factor 2 (MLF2) genes were constantly overexpressed in the BM-MSC from MPN patients (CML, PV and ET) compared to BM-MSC from HD (Adjusted.p. value <0.01).

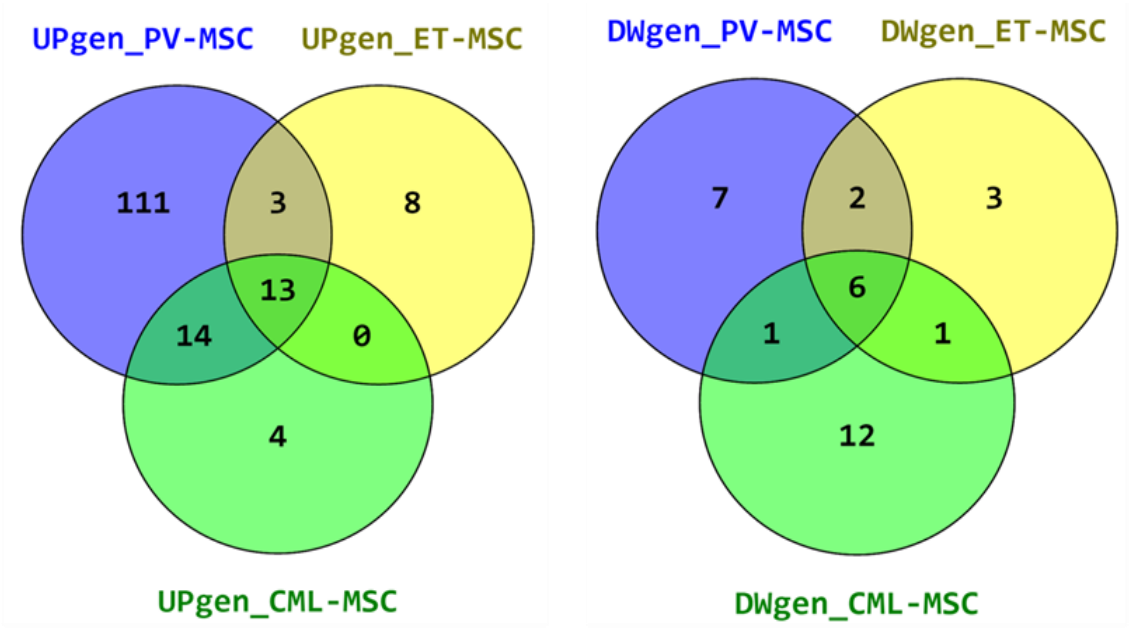

Adj. P. Val <0,05	Up- Regulated genes expression	Down-Regulated genes expression
	HD-MSC	
JAK2V617F-MSC	447	149
ET-MSC	24	12
PV-MSC	141	16
CML-MSC	31	20

Figure 20: Gene expression profile of BM-MSC from CML and JAK2^{V617F} (ET and PV) patients contrasted with BM-MSC of HD. Table represents the number of genes Up and Down regulated in each group when contrasted against HD group.

Table 7: Differential Up/Down – regulated expression genes in BM-MSC from MPN patients contrasted against HD.

Chronic Myeloid leukaemia

UP- regulated: SNORD29, DCAKD, **RP11-249L21.3**, **MYADM**, EMD, PLEKHO1, C16orf57, **RP11-369J21.2,** TAGLN2, RBMS2, **MLF2**, PIGS, KDELR3, **PIGU,** PLSCR3, **SDHC**, **GMEB1**, **SPRYD4,** DAG1, ABHD5, **PPP6C**, **SCAMP2,** RNASEK, RWDD2B, ALG8, DAZAP2, **ASB8**, **RBM4B**, DIRC2, UBE2Q1, **GORASP2.**

Down- regulated: AP000351.2, AC107956.1, SAFB2, ZNF498, **SURF6**, **TRIM56**, SART3, SPAG7, RP11-342F17.1, **RPL23,** AC009963.3, AC005154.6, AD000090.2, J01415.28, **AC097526.11**, J01415.10, AC025627.1, **AC131055.17**, **AC073869.19**, J01415.25

Polycythemia Vera
UP-regulated: RAC2, PRPS1, SLC16A2, ADAM19, RP11-354P17.1, TMEM106A, RAB15, RPS26, ATP6V1G2, TGFBI, TMEM173, LDOC1, **RP11-249L21.3**, C16orf57, PRAF2, MEOX2, AC004967.6, TMEM104, EMD, PPT2, COX8A, **PIGU**, **MYADM**, KDELR3, DCAKD, **MLF2**, CDA, TAGLN2, RBMS2, AC007842.1, PPME1, ATP5J2, PLSCR3, CYB561D2, AC084031.2, **SPRYD4**, PEX11B, PLEKHO1, ALG3, OAZ2, PLP2, RAB1B, G6PC3, PLEK2, ZYX, DAG1, PIGS, TNFAIP1, **RP11-369J21.2**, **SDHC,** C16orf70, ZC4H2, **SCAMP2**, TMEM110, RHOG, LYPLA2P1, ZDHHC12, ANO10, SLC9A3R1, TRAPPC1, ABHD5, KIAA1191, C12orf32, RHOC, TEX261, WSB2, PFN1, OBFC2B, SLC4A8, UBE2A, EYA3, PTPRB, PDZD11, TMEM127, PTMS, C18orf10, **RBM4B**, SUOX, C16orf61, C17orf63, C16orf13, RPL10, TXNL4B, HOXA1, HDAC8, ORMDL2, SAP130, PSME3, TPI1, TMEM177,KDELR1, ARF3, GNG5, TIMM22, ATP5SL**, PPP6C**, CINP, TRMT2B, ZSWIM3, S100A11, TMEM214, POLR2D, CFL1, GRPEL1, SSBP3, AC012652.1, NCSTN, CS, ALG8, **GORASP2**, SAE1, BFAR, KIAA0090, TM9SF4, CRADD, **GMEB1,** RNF34, FKBP10, **ASB8,** UBAP2, WRAP53, RNASEK, DYNLRB1, VAPB, KDELR2, KPNA6, PSMB2, COPS3, FDXACB1, EIF2C1, RAB5C, UBE2Q1, GSTTP2, STT3A, MYL12B, EXT2, AL079307.1, EXD2, Y_RNA, OR5H1, OR1E2
Down-regulated: **SURF6,** NTN1, AC137932.3, **RPL23**, 5S_rRNA, **TRIM56**, CDYL, TBCEL, H3F3C, PRDM5, PARD3B, SFRS5, **AC097526.11**, AC025627.1, **AC131055.17**, **AC073869.19**
Essential thrombocythemia
UP-regulated: HIP1, **RP11-249L21.3**, AL122001.1, **PIGU, SDHC, RP11-369J21.2**, **MYADM**, CCDC92, **MLF2**, **SPRYD4, RBM4B**, **SCAMP2**, AC012652.1, **GMEB1**, C18orf10, PCDHGC5, **PPP6C**, **ASB8**, AL161756.1, COPS3, **GORASP2**, CPA6, SNORA25, OR8J1
Down-regulated: AC107956.1, AC087885.1, C7orf46, CDYL, GOLGA2L1, **TRIM56**, **SURF6**, AC137932.3, **RPL23**, **AC097526.11**, **AC131055.17**, **AC073869.19**.

**In black is represented the genes that are common in the three pathologies*

1.2.3 Differential biological processes between BM-MSC from MPN patients and HD

The differential signal pathways are shown according to the enrichment score value in **Table 8** (just represent the DAVID results, however the clusters are similar between data bases). Total genes in respective signal pathways are also shown. The differential signal pathways included in BM-MSC from $JAK2^{V617F}$ are mainly related with endoplasmatic reticulum, protein transport, GTPase activity and transmembrane/membrane region. However, the main pathways in CML-MSC are: glycerophospholipid biosynthetic process, nuclear envelope-endoplasmic reticulum network, organelle membrane, and intrinsic to membrane/ transmembrane region (**Table 9**).

Table 8: Functional enrichment on the differential Up/Down – regulated genes expressed in BM-MSC from JAK2^{V617F} patients (PV and ET). Enrichment Score: the overall enrichment score for the group based on the EASE scores of each term members. Analyses were performed using DAVID web tool.

Pathways UP- regulated genes	Total genes	Enrichment Score	Representative gene title
Endoplasmatic reticulum	76	4.3	CYB5R3, SLC36A1, VAPB, MRVI1, ALG3, RCE1, ALG8, C14ORF1, CANT1, TAPBP, ELOVL1, TMEM173, PLOD1, PIGB, RPL10, PSENEN, KDELR1, AGPAT1, KDELR3, PGAP2, KDELR2, PIGU, PIGS, TECR, LPCAT4, UGT2B11, ASPHD1, ORMDL2, LEPREL1, FKBP10, TRAPPC1, EXT2, SLC27A2, SEC61G, CLN6, EXTL3, DERL1, CACNB1, UBE2V1, PPT2, CTSA, TRAM2, STT3A, SHISA5, EMD, PLP2, NPLOC4, ICMT, PORCN, NCSTN, BFAR, C3ORF52, TXNDC11, LASS2, DPM2, TAPBP, BFAR, NRBP1, SLC22A18, C16ORF70, COPZ1, TAGLN2, SLC35A4, NUP214, NECAP1, QSOX1, AP2M1, HIP1, SCAMP2, NRM, KPNA6, VAMP2, FAF1, MGAT5, PEX11B, MPV17
Protein transport	75	3,15	SNAP29, RAB7A, DERL1, RAB5C, COPZ1, VPS52, RAB1C, RAB1B, NUP214, TRAM2, NECAP1, KDELR1, SCAMP4, AP2M1, KDELR3, KDELR2, PRAF2, RAB8A, SCAMP2, RABIF, RAB4B, STXBP1, TIMM22, TOM1L2, ARF3, ARF4, KPNA6, RAB15, SEC61G, VPS25 GRPEL1, C16ORF70, CACNB1, CTSA, TRAM2, TOMM34, GDI1, ICMT, YWHAE, YWHAH, YWHAQ, PAX6, FAF1, SLC16A13, SLC36A1, SLC22A18, SLC35A4, GOT2, DIRC2, NDUFS4, ANO10, CYB5B, ATP6V1F, SLC35E1, TRAPPC1, RBP4, SLC39A11, CACNB3, FXYD5, CYB561D2, TRAM2, SLC35B4, SLC4A8, SLC25A44, TCIRG1, ATP5J2, NDUFA2, ATP5F1, SLC16A2, AFM, LASP1, SDHC, TAPBP, MAP1S, VAMP2.
GTPase activity	47	2,99	RAB7A, RAB5C, RAB4B, TUBB, GNB1, ARF3, ARF4, RAC1, RRAS, TUBA3D, RHOC, TUBG1, TUBG2, GNG5, NKIRAS2, TUBB3, RHOG, RAB8A, KIF3C, RAB1C, RAB1B, RAB15, GDI1, RABIF, ARHGAP1, CFL1, YWHAQ, ARHGDIA, ACTB, CRYAB, HIST1H2BM, GORASP2, CALM3, PRPS1, CYB5R3, COPZ1, CACNB1, ILK, MSN, AP2M1, TOMM34, MUC1, APOBEC3C, GOLGA7, PLSCR3, DYM, PRKACA
Membrane/Transmembrane region	191	2,55	TGOLN2, SLC36A1, **RNASEK**, NRBP1, SLC22A18, PEAR1, VAPB, CSPG4, RAB1C, VPS52, RAB1B, MPV17, RCE1, FAM119B, C14ORF1, COX5A, SLC35A4, TAPBP, GOT2, OR8K1, ELOVL1, **DIRC2**, PLOD1, ILK, RRAS, PSENEN, TMEM185B, RNF34, GNG5, SCAMP4, **SCAMP2**, C1ORF212, TECR, SIRPA, LPCAT4, MARK2, C1ORF85, OR8J1, KIAA0090, TMEM106A, MGAM, RAB15, ASPHD1, NRSN2, TMEM184B, VAMP2, MGAT5, NEU3, FAM171A2, EXT2, SEC61G, FAM171A1, MAVS, EXTL3, DERL1, TMEM214, COPZ1, **DAG1**, CACNB1, UBE2V1, FXYD5, MANSC1, TRAM2, TMEM127, **GORASP2,** RAC1, PTPLA, **EMD**, AP2M1, HIP1, MUC1, RAB8A, PRAF2, ATP5J2, C17ORF101, COX8A, CD276, PPAPDC1A, ICMT, TMEM110, GPR137C, TMEM179B, PORCN, BFAR, EI24, TXNDC11, LASS2, TBXA2R, ENG, PIP4K2C, DCXR, NYNRIN, SLC16A13, CYB5R3, OR10A3, OR5H1, LRRC8A, GPR160, RAB5C, MRVI1, ALG3, TMEM62, **ALG8**, FAM57A, CANT1, TMEM175, CD97, EFHD2, TMEM173, GOLGA7, NDUFS4, SMAGP, PIGB, NECAP1, RHOC, MSN, TM9SF4, KDELR1, RHOG, COX16, TUBB3, TMEM104, ANO10, AGPAT1, TOMM34, **KDELR3,** KDELR2, PGAP2, FLOT2, RAB4B, **PIGU**, STXBP1, **PIGS,** CYB5B, SLC9A3R1, **MYADM**, TIMM22, PRKD1, KIAA1161, CLECL1, NRM, SLC35E1, ZDHHC12, UGT2B11, MOSPD3, ORMDL2, MFSD11, C2ORF24, SLC27A2, CLN6, SNAP29, USP30, SLC39A11, SAMM50, CD248, PCDHGC5, ZDHHC18, ITM2C, CYB561D2, STT3A, SHISA4, SLC35B4, SHISA5, PLEKHO1, SLC4A8, HRCT1, SLC25A44, MANBAL, SELPLG, QSOX1, TEX261, GBA, TCIRG1, PTPRB, PLP2, NDUFA2, ATP5F1, TMEM53, AXL, NLGN2, CBARA1, NID2, NCSTN, PEX11B, SLC16A2, C3ORF52, **SDHC**, **PLSCR3,** DPM2, CMTM7, VPS25

Pathways Down- regulated genes	Total genes	Enrichment Score	Representative gene title
RNA binding/ RNA recognition motif, RNP-1	9	1,46	DDX55, SFRS5, SURF6, ZMAT3, RPS14, SART3, EWSR1, RPS3, SAFB2
structural molecule activity	8	1,32	ISCU, RPL23, COL21A1, RPS14, RPL7L1, COL24A1, COL16A1, RPS3
zinc finger region	8	1,08	ZNF516, ZNF236, ZNF274, KLF9, YY1, PRDM5, ZNF460, ZNF498
extracellular matrix/ biological adhesion	10	1,06	SMOC2, COL24A1, COL16A1, NTN1, COL21A1, IL16, ADAM17, PARD3, TNFRSF10B, GABRB3

Table 9: Functional enrichment on the differential up-regulated genes expressed in BM-MSC from CML Enrichment Score: the overall enrichment score for the group based on the EASE scores of each term members. Analyses were performed using DAVID web tool.

Pathways UP- regulated genes	Total genes	Enrichment Score	Representative gene title
Glycerophospholipid biosynthetic process	3	1.77	ABHD5, PIGU, PIGS
Nuclear envelope-endoplasmic reticulum network	8	1.70	SCAMP2, SDHC, PIGU, PIGS, TAGLN2, ALG8, EMD, KDELR3
Organelle membrane	7	1.28	SCAMP2, SDHC, PIGU, PIGS, TAGLN2, ALG8, EMD
Intrinsic to membrane/ transmembrane region		1.22	KDELR3, SCAMP2, RNASEK, DAG1, PIGU, PIGS, ALG8, MYADM, DIRC2, SDHC, GORASP2, PLSCR3, EMD

1.2.4 Gene expression by Real Time (RT) - PCR

Based on the gene expression profile results from human Gene 1.0 ST arrays, we studied two genes that were up-regulated in the BM-MSC from the different MPN subtypes. The first gene studied was MYADM, which was overexpressed in the BM-MSC from the three diseases (PV, ET and CML, p=0.003, 0.004 and 0.0002, respectively). The second studied gene was class 1 histone deacetylate 8 (HDAC8), which was overexpressed in BM-MSC from PV patients.

In the majority of the groups the overexpression of MYADM was confirmed by RT-PCR, excepted for BM-MSC from PV patients (**Figure 21 A**). Furthermore, BM-MSC from other MPN patients were also studied. As shown in **Figure 21**, 3 MPN patients negative for $JAK2^{V617F}$, and 2 MPN patients with the CARL mutation also presented higher MYADM expression (p=0.003). By contrast, the human cell lines (hTERT and HS5) showed lower expression of MYADM with significant differences (p=0.02), when compared to HD-MSC.

Regarding the MYADM expression in BM-MNC from PV and ET patients, a significant overexpression was observed (p=0.016) when compared with HD-MNC.

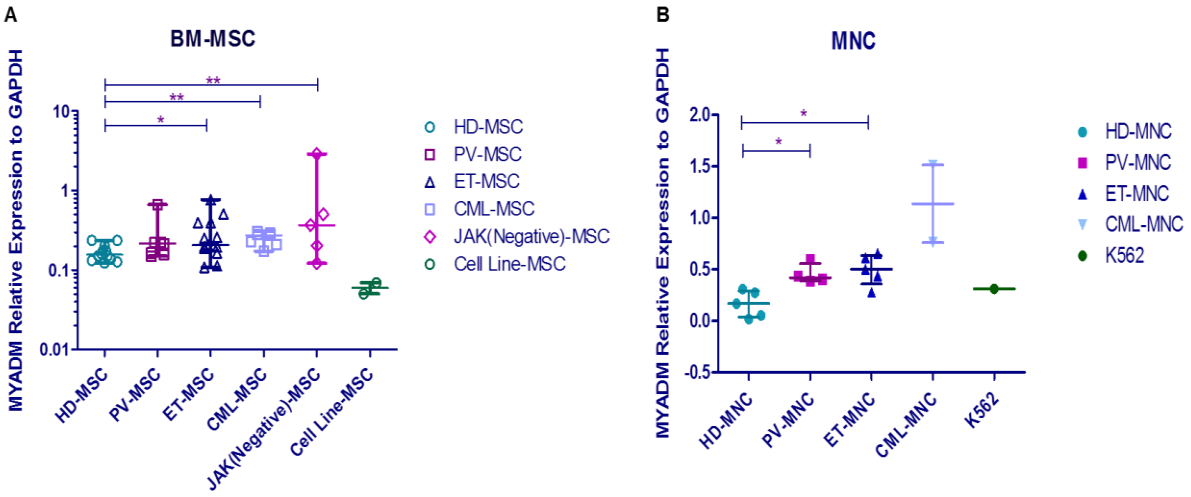

Figure 21: Gene expression of MYADM gene tested in BM-MSC (A) and MNC (B) from MPN patients and HD. Results were normalized with the housekeeping gene GAPDH. HD-MSC=12; PV-MSC=7; ET-MSC=14; CML-MSC=7 and JAK (negative)-MSC=5; MSC cell line =2. For MNC: 6 HD, 4 PV, 5 ET and 2 CML * p<0.05 and ** p<0.01. Results are represented by the median and the interquartile range.

HDAC8 expression was significantly increased (p=0.0025) in $JAK2^{V617F}$-MSC compared to HD-MSC (**Figure 22**), mainly in PV-MSC and ET-MSC (p=0.005). BM-MSC from the others MPN patients (negative for JAK2) showed similar HDAC8 expression compared with HD-MSC. Furthermore, the expression of this gene in the MNC from 7 HD, 4 PV, 10 ET, 12 JAK (negative) and 7 CML was also studied. As shown in **Figure 22**, HDAC8 expression was similar among the different MNC groups. Cell line K562 showed the higher HDAC8 expression.

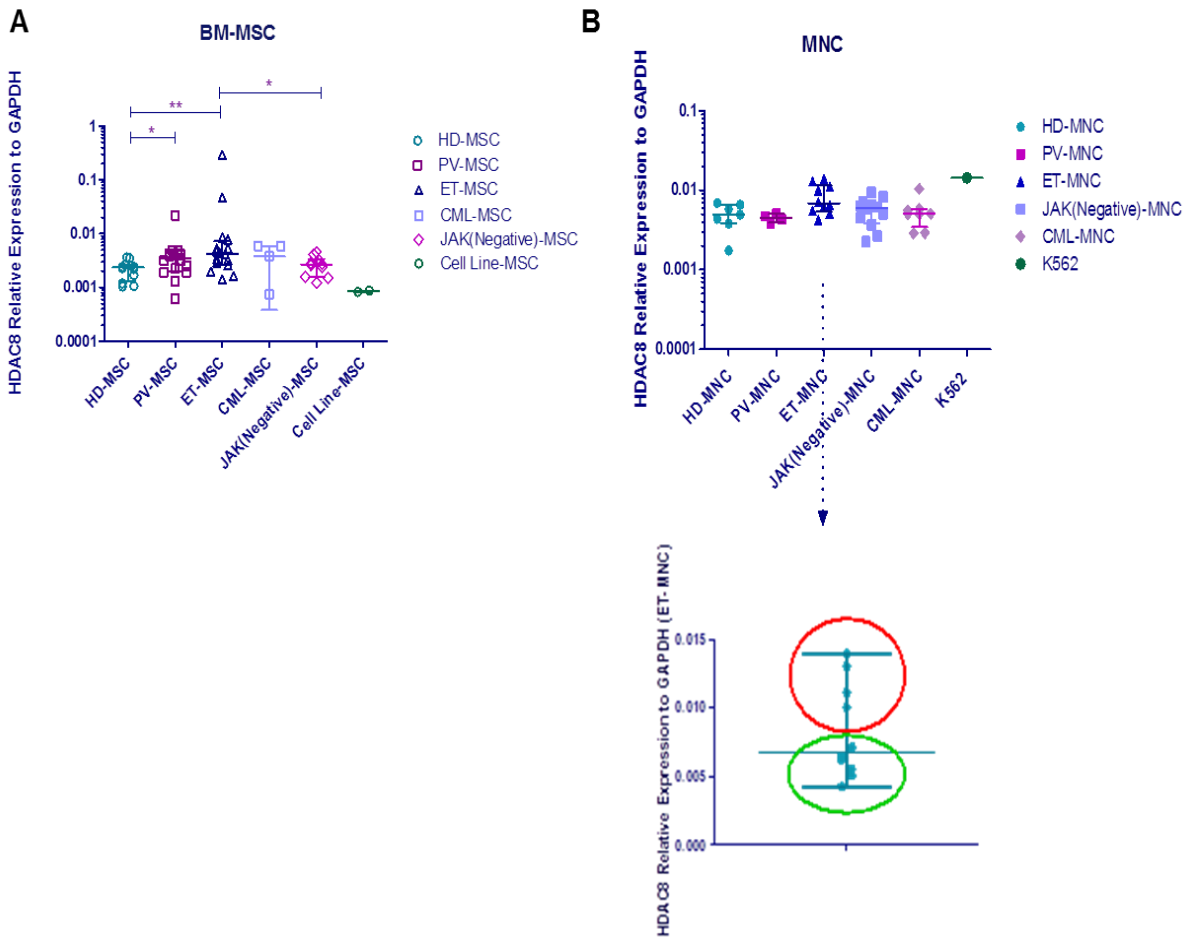

Figure 22: Gene expression of HDAC8 gene tested in BM-MSC (A) and MNC (B) from MPN patients and HD. Results were normalized with the housekeeping gene GAPDH. HD-MSC=12; PV-MSC=7; ET-MSC=14; CML-MSC=7 and JAK (negative)-MSC=5; MSC cell line =2. For MNC: 8 HD, 4 PV, 10 ET, 12 JAK (negative), 8 CML.* $p<0.05$ and ** $p<0.01$ Results are represented by the median and the range.

Within the $JAK2^{V617F}$ group, ET-MNC showed higher expression of HDAC8, almost reaching significant differences when compared with HD-MNC ($p=0.056$). Among the ET groups, we observed two subsets, one with increased expression of HDAC8 and the other with an expression similar to the control group. To understand this difference we studied the correlation between HDAC8 expression and percentage of $JAK2^{V617F}$ mutation, platelets count, WBC and age. As show in **Figure 23**, a correlation between expression of this gene and the different variables studied was not observed.

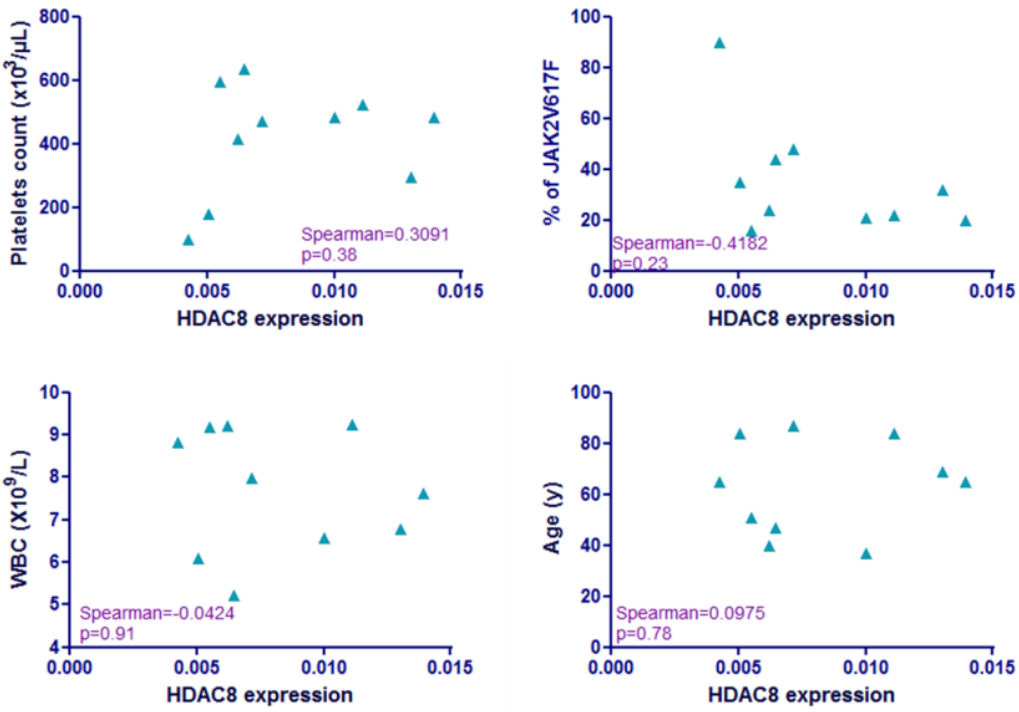

Figure 23: Correlation coefficient graph. Correlation between the HDAC8 expression in the MNC from ET patients with the % of JAK2V617F, platelets count, WBC and age.

1.3 Haematopoietic supportive capacity of JAK2^{V617F} - MSC

1.3.1 JAK2 ^{V617F}-MSC differentially supports the clonogenic capacity of healthy and leukaemia cell progenitors.

The ability of BM-MSC from HD and MPN patients to support (short-time) haematopoiesis *in vitro* was assessed in a co-culture system. CD34^{+} cells freshly isolated from BM of HD and MPN patients presented a purity superior to 90% (n=2 JAK2^{V617F}-BM and n=3 HD-BM).

Co-cultures were performed using as feeder layers BM-MSC derived from HD (n=10) and JAK2^{V617F} patients (n=9). As represented in **Figure 24**, the total number of colonies was similar when healthy haematopoietic progenitors were co-cultured with HD-MSC or JAK2^{V617F}-MSC. However, when CD34^{+} cells from JAK2^{V617F} patients were cultured with JAK2^{V617F}-MSC, the total number of colonies increased significantly (p=0.03), when compared with the HD-MSC co-cultures (**Figure 24**).

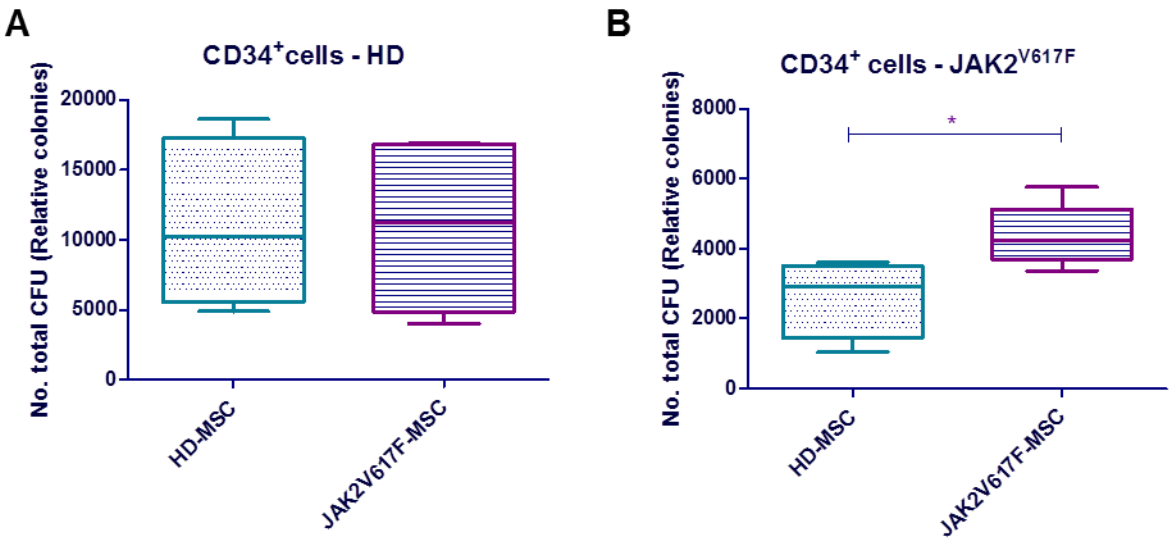

Figure 24: Selective protection of leukemic haematopoiesis by JAK2^{V617F}-MSC. (A) Total colony-forming unit (CFU) from HD-CD34^{+} cells after 48h of culture with HD-MSC (n=7) and JAK2^{V617F}-MSC (n=7), no differences were observed between groups. (B) CFU from JAK2^{V617F}-CD34^{+} cells after culture with HD-MSC (n=4) and JAK2^{V617F}-MSC (n=6), significant increase was observed when leukemic progenitor cells were in cultured with pathologic stroma. * p<0.05

1.3.2 Long-term BM culture (LT-BMC) assays

To evaluate the ability of HD-MSC (n=7) and JAK2^{V617F}-MSC (n=7) to maintain and expand HD HPC, long-term BM cultures were performed. Our data, suggest that CD34^{+} cells co-cultured with stroma from both origins produce similar number of CFU-GM and BFU-e during the first two weeks. However, at the 3rd and 4th week a significant increase of CFU production was observed (week 3: p=0.021 and week 4: p=0.028, respectively), when co-cultured with MPN-MSC (**Figure 25**). No differences were detected in the total number of colonies produced during the 5 weeks, when HD-HPC were co-cultured with HD-MSC and JAK2^{V617F}-MSC.

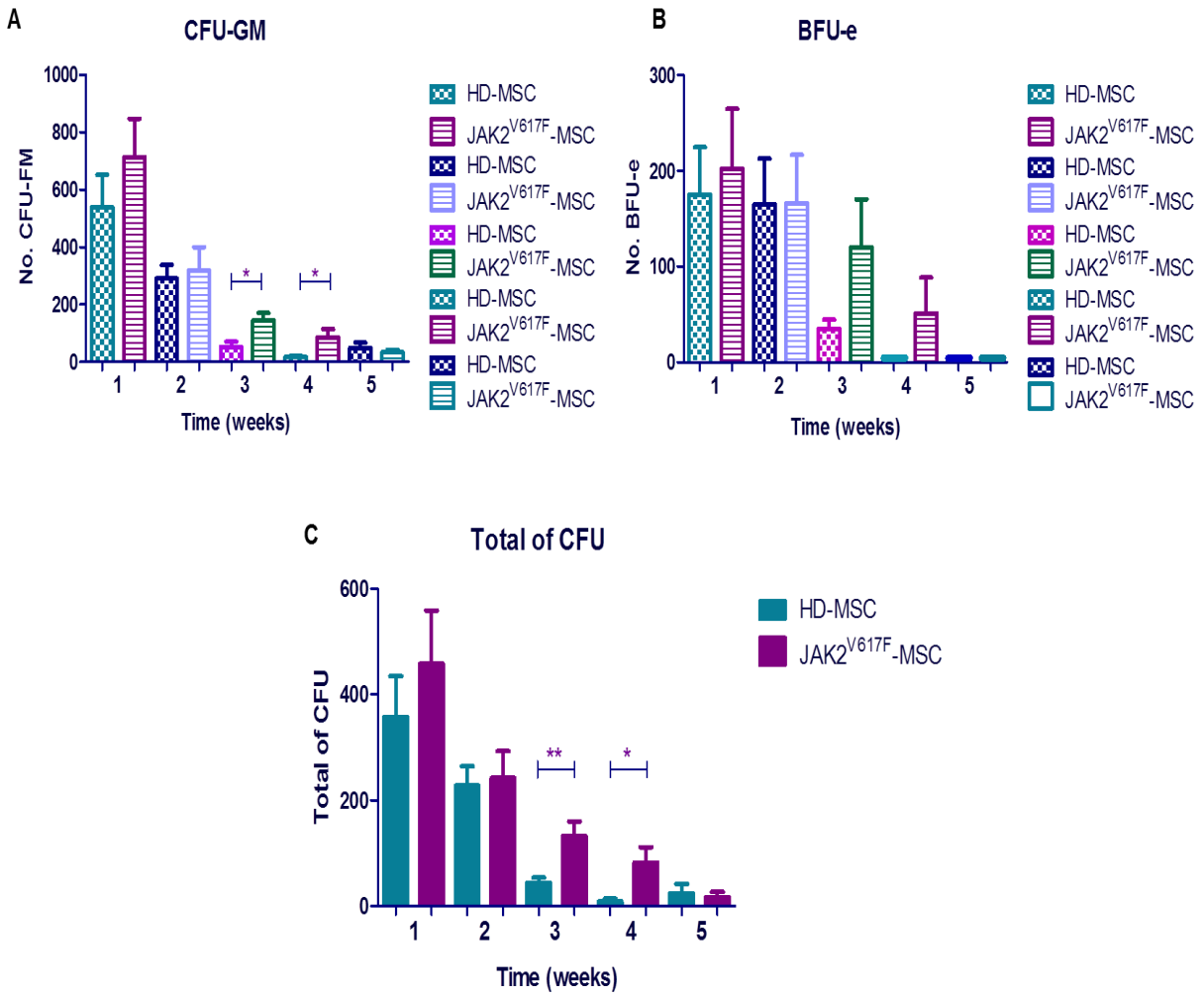

Figure 25: Capacity to MPN-MSC to maintain HD-HPC in LTBMC (A) Total colony-forming unit - granulocyte/macrophage (CFU-GM) from HD-CD34^{+} cells after 5 weeks in co-culture with HD-MSC (n=7) and JAK2^{V617F}-MSC (n=7). (B) Total of Burst-Forming Unit – Erythroid (BFU-e); (C) Total of colonies (CFU), results shown are expressed as the mean of CFU±SD from adherent and nonadherent cell fraction co-cultured over a period of 5 weeks in controls (blue bars) and patients (pink bars) * $p<0.05$ ** $p<0.01$

1.3.3. Expression pattern of genes related with haematopoiesis regulation

Due to the changes observed in the capacity of JAK2^{V617F}-MSC to maintain healthy and pathologic haematopoiesis, RT-PCR was performed to assess the expression of genes related to MSC differentiation/proliferation, and the maintenance of haematopoiesis. The studied genes were SDF1-α or CXCL12, TP53, Angiopoetin-1 (ANGPT1), nuclear factor kappa B (NF-kB),

Jagged-1 (JAG-1), bone morphogenetic protein 2 (BMP-2), osteopontin or secreted phospho-protein 1 (SPP1), thrombopoietin (THPO), pro-oncogene c-KIT, and tumour necrosis factor (TNF).

As showed in **Figure 26,** regarding the expression of CXCL12, the BM-MSC from JAK2^{V617F} patients presented similar expression of this gene compared to controls. When the expression of this gene in the MNC was studied, similar results between HD and MPN were observed (**Figure 26 B**). However, we detected a significant decrease in the expression of CXCL12 in the CML-MNC compared to HD-MNC (p=0.038).

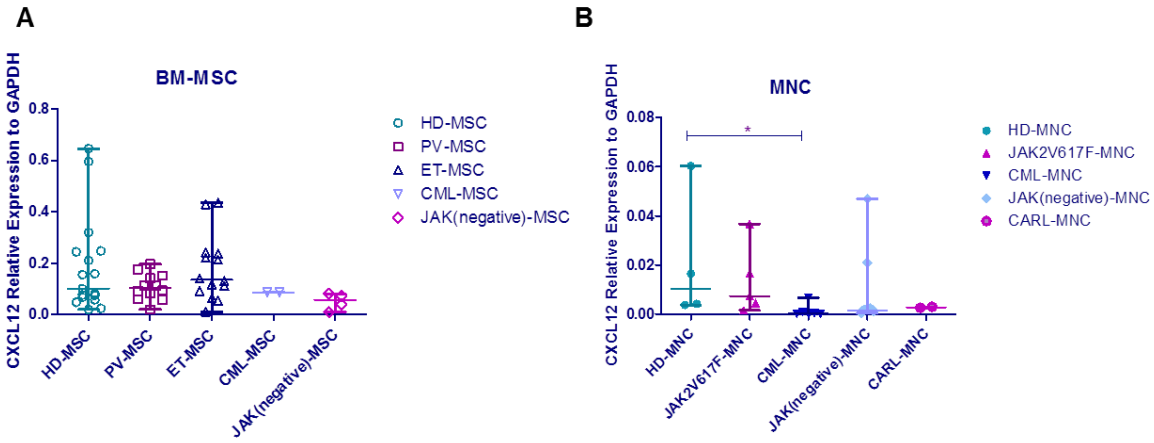

Figure 26: CXCL12 expression in BM-MSC (A) and MNC (B) from MPN patients and HD. Results were normalized with the housekeeping gene GAPDH. For BM-MSC: HD-MSC=17; PV-MSC=13; ET-MSC=15; CML-MSC=2 and JAK (negative)-MSC=4. For MNC: HD=4, JAK2V617F=6, CML=6, JAK(negative)=8 and CARL=2 . * p<0.05 Results are represented by the median and the range.

Another gene studied was TP53, which has been shown as a critical gene in MSC function. As shown in **Figure 27**, no significant differences in the BM-MSC from the different groups were observed. A decrease in TP53 expression was observed in all MNC groups, with significant differences in CML-MNC when compared to HD-MNC (p=0.0043) (**Figure 27 B**).

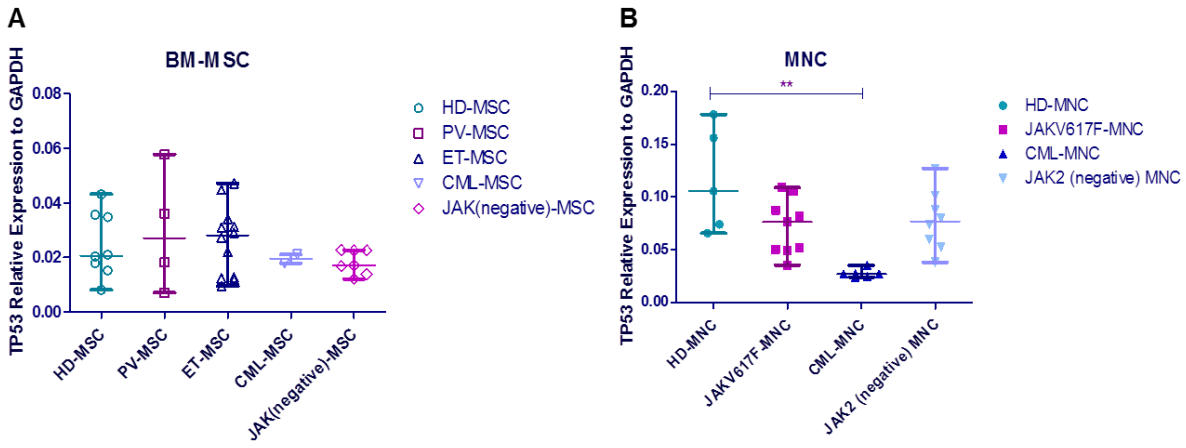

Figure 27: Gene expression of TP53 gene studied in BM-MSC (A) and MNC (B) from MPN patients and HD. Results were normalized with the housekeeping gene GAPDH. HD-MSC=10; PV-MSC=4; ET-MSC=13; CML-MSC=3 and JAK (negative)-MSC=10. For MNC: HD=5; PV=9; ET=7; CML=8. ** p<0.01 Results are represented by the median and the range.

Because the expression of TP53 in ET-MSC and PV-MSC presented a high coefficient of variation, we analysed the correlation between TP53 expression and the percentage of $JAK2^{V617F}$ mutation, haemoglobin (Hb), platelet count, WBC and age (**Supplementary Figure 1**). As observed in the **Figure 28**, a correlation between the expression of TP53 in the BM-MSC from ET patients and $JAK2^{V617F}$ mutation allele burden of in MNC was found, with higher expression levels of TP53 correlated with lower percentage of $JAK2^{V617F}$. No correlation was observed in PV-MSC group.

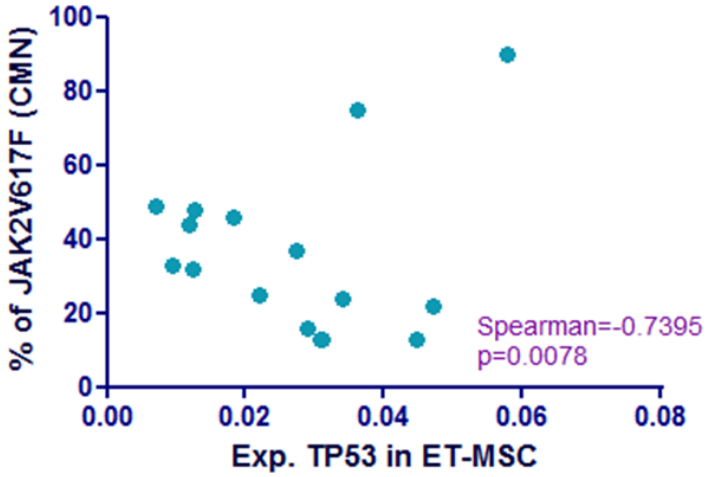

Figure 28: Correlation coefficient graph . Correlation between the TP53 expressions in the MSC from ET with the % of $JAK2^{V617F}$.

We also analysed the expression other key genes (**Figure 29**) involved in the maintenance of haematopoiesis. We restricted the study to the $JAK2^{V617F}$-MSC to analyse potential differences between normal and myeloproliferative microenvironment.

The expression level of the quiescence regulator ANGPT1 was significantly decreased in ET and PV-MSC compared to control MSC (p=0.04 for ET and 0.02 for PV).

Regarding to the expression of NF-kB, THPO and SPP1 an increase in the expression levels in the ET and PV-MSC was observed when compared to HD-MSC, with differences reaching statistical significance in PV-MSC (NF-kB p=0.027 and THPO p=0.028). No significant differences were observed in the expression of the other analysed genes.

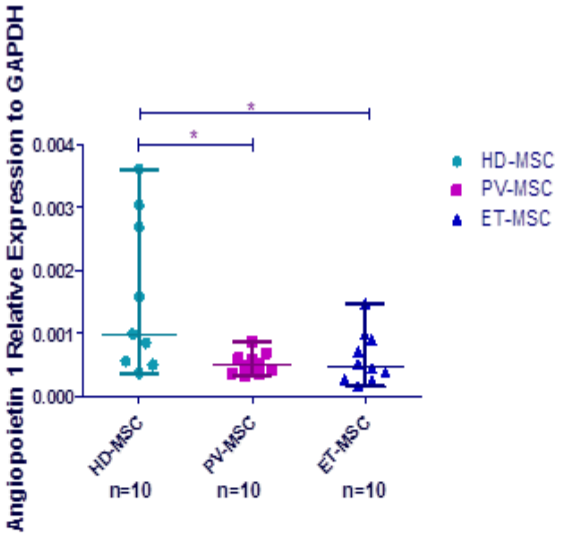
Angiopoietin 1 Relative Expression to GAPDH
0.004
0.003
0.002
0.001
0.000
*
*
HD-MSC
PV-MSC
ET-MSC
HD-MSC
PV-MSC
ET-MSC
n=10
n=10
n=10

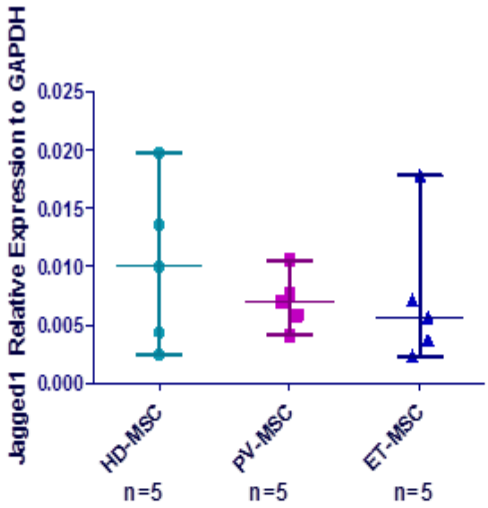
Jagged1 Relative Expression to GAPDH
0.025
0.020
0.015
0.010
0.005
0.000
HD-MSC
PV-MSC
ET-MSC
n=5
n=5
n=5

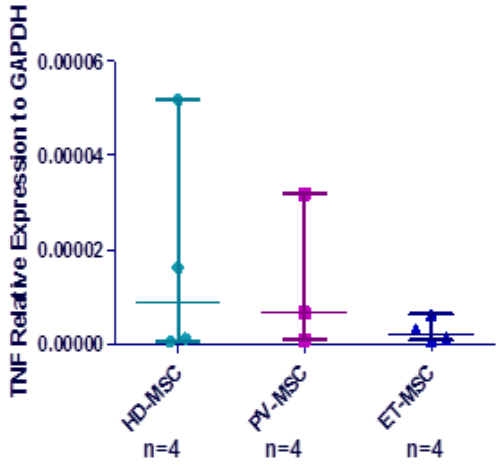
TNF Relative Expression to GAPDH
0.00006
0.00004
0.00002
0.00000
HD-MSC
PV-MSC
ET-MSC
n=4
n=4
n=4

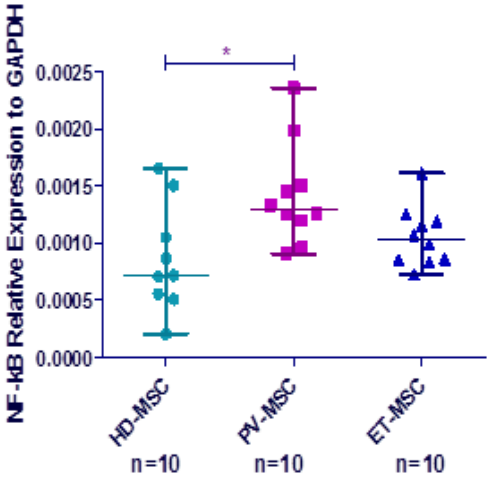
NF-kB Relative Expression to GAPDH
0.0025
0.0020
0.0015
0.0010
0.0005
0.0000
*
HD-MSC
PV-MSC
ET-MSC
n=10
n=10
n=10

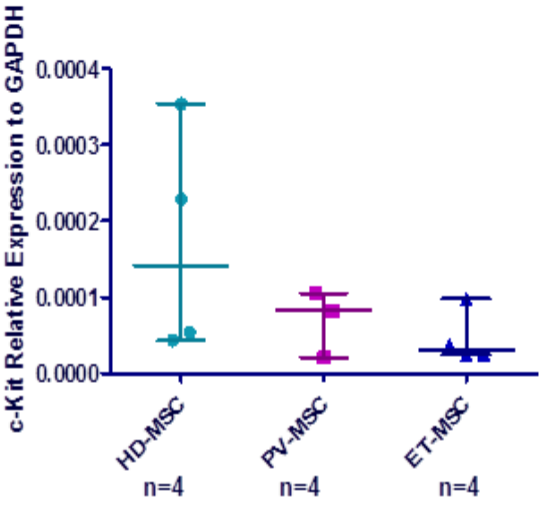
c-Kit Relative Expression to GAPDH
0.0004
0.0003
0.0002
0.0001
0.0000
HD-MSC
PV-MSC
ET-MSC
n=4
n=4
n=4

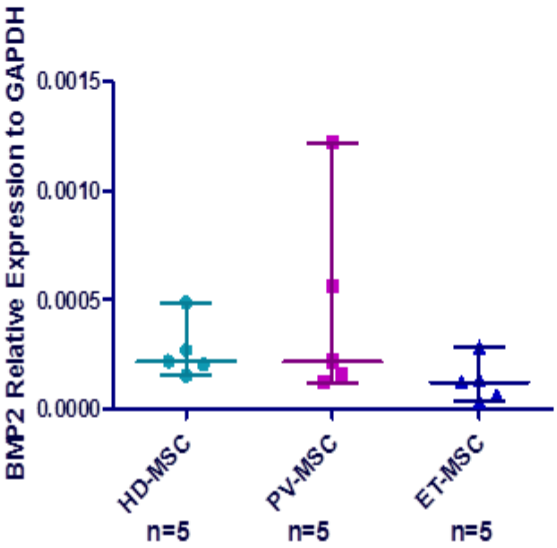
BMP2 Relative Expression to GAPDH
0.0015
0.0010
0.0005
0.0000
HD-MSC
PV-MSC
ET-MSC
n=5
n=5
n=5

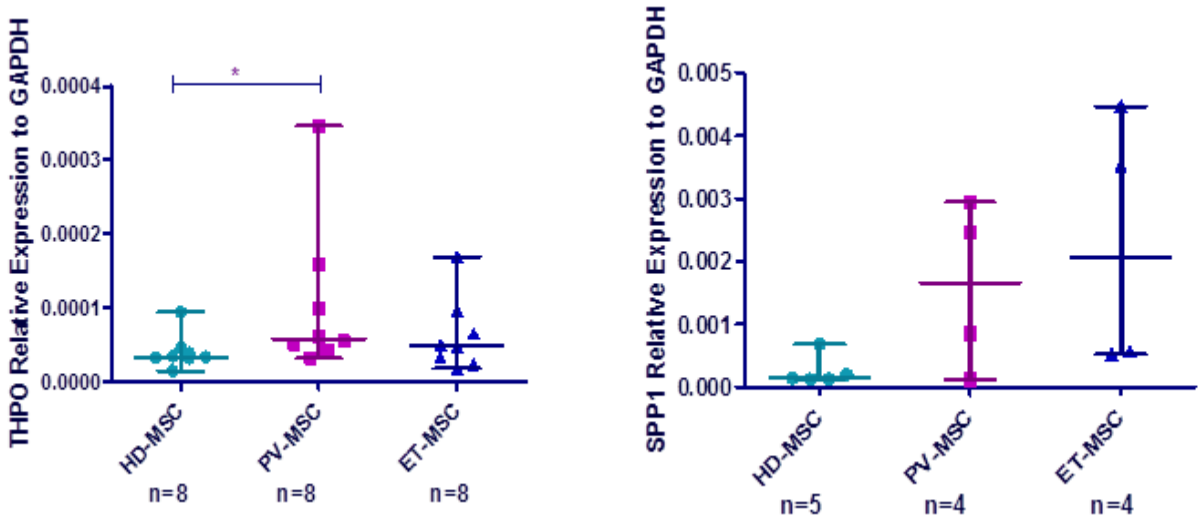

Figure 29: Differential expression in JAK2^{V617F}-MSC of genes related to haematopoiesis. RT-PCR was used to determine the expression level of the different genes associated with maintenance of haematopoiesis. GAPDH was used as housekeeping to normalize the results. In the scatter plot graphic are represented by the median and the range.

1.4 HDAC8, SDF-1 and MYADM protein expression in BM-MSC

In order to study the protein expression of CXCL12, HDAC8 and MYADM, western blot and immunofluorescence assays were performed.

As shown in **Figure 30 A**, BM-MSC from JAK2^{V617F}-MSC showed higher MYADM protein expression compared to HD-MSC. Regarding to HDAC8 protein expression, ET-MSC and PV-MSC showed an increase in the expression of this protein when compared to HD-MSC, confirming the RT-PCR results. However, a higher expression of HDAC8 was observed in the ET-MSC (**Figure 30 B**).

CXCL12 was analysed by immunofluorescent assays (**Figure 30 C**), HD-MSC showed higher expression of this protein compared to Hela cells (positive control). The BM-MSC from JAK2^{V617F} patients showed a decrease in the expression of CXCL12 compared to HD-MSC.

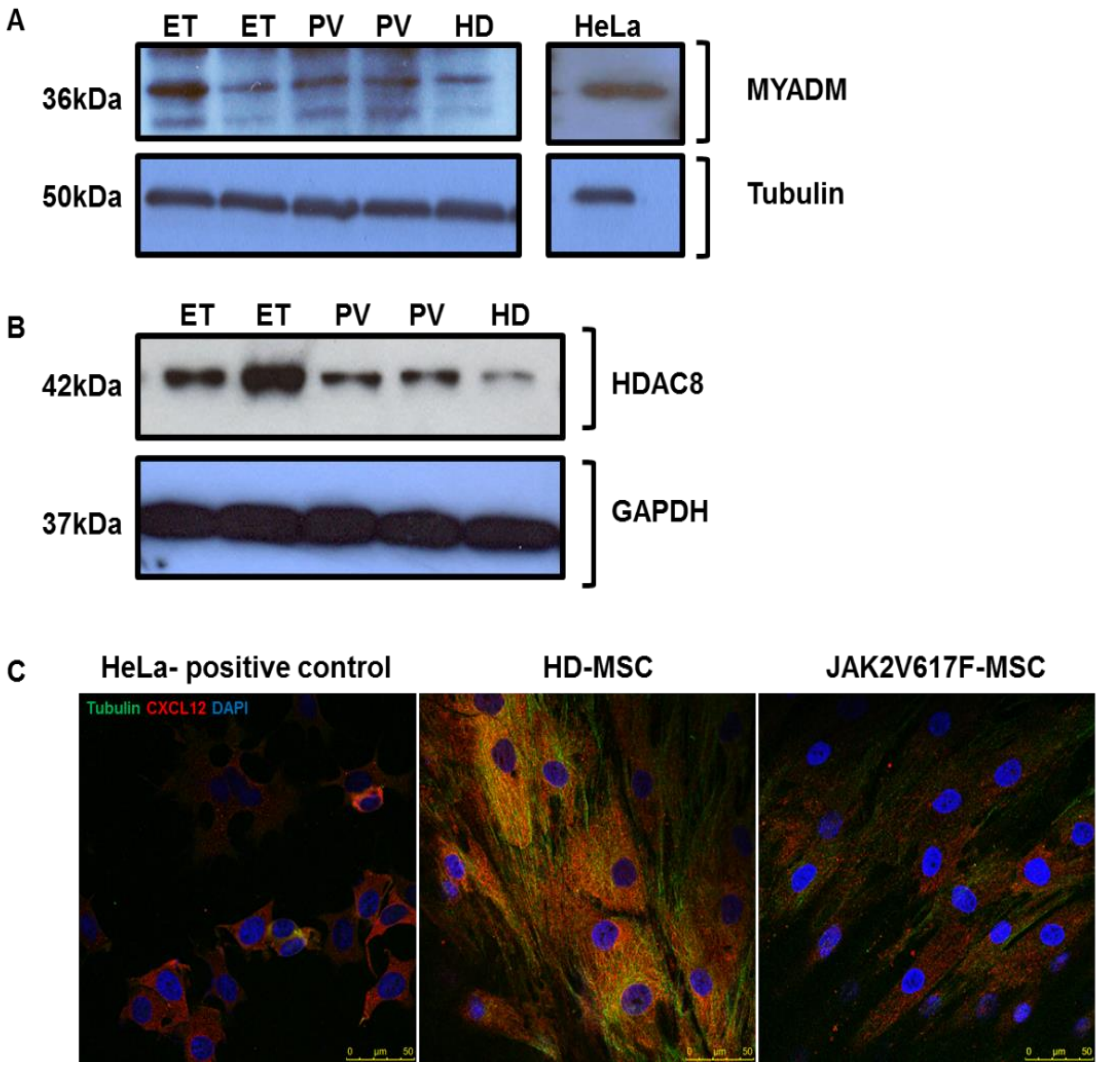

Figure 30: Western blot analysis of MYADM, HDAC8 protein and immunofluorescence of CXCL12. The Up-panel represents the expression of MYADM in ET, PV and HD-MSC, HeLa cells were used as positive control. Myeloproliferative mesenchymal have more expression than HD-MSC, mainly the ET-MSC. The middle panel represents the HDAC8 expression, where can be observed an up-expression in the MSC from JAK2^{V617F} patients (principally in ET-MSC). The lower panel is a representative image of CXCL12 expression in the MSC by immunofluorescence. HD-MSC shows more CXCL12 (red) then the positive control (HeLa cells) and the JAK2^{V617F}-MSC. In green shows tubulin. Scale: 0-50µm

1.5 HDAC8 as a therapeutic target (*in vitro* studies)

1.5.1 PCI34051 decrease HDAC8 expression in JAK2^{V617F}-MSC, modifying their cell proliferative capacity.

First of all, we evaluated the effect of the specific HDAC8 inhibitor (HDACi) in BM-MSC cell growth of HD (n=4), ET (n=4) and PV (n=4). PCI34051 induced a decrease in cell growth on the BM-MSC from JAK2^{V617F} patients after 24 hours of treatment. However, at 48 hours of treatment, a wider decrease in cell proliferation in ET and PV-MSC was observed. The treatment of HD-MSC with PCI34051 had no effect on the cell proliferation (**Figure 31**).

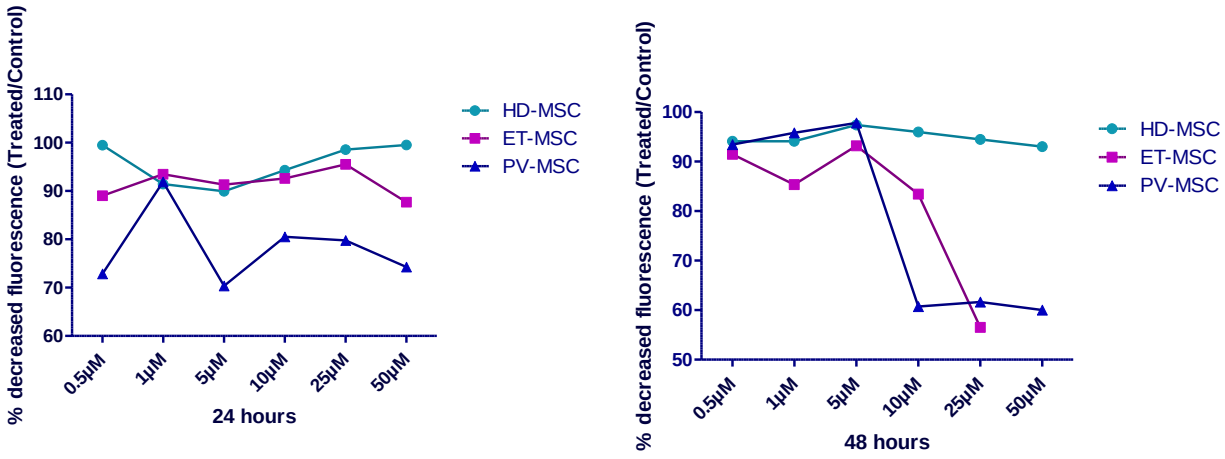

Figure 31: PCI34051 reduces the viability of BM-MSC from JAK2^{V617F} patients. HDAC8 inhibitor treatment for 24 hours (A) and 48 hours (B) reduce the percentage of viable cells that was evaluated with alamarBlue assays. PCI34051 reduces the viability of ET and PV – MSC, at concentrations superiors to 10 µM, but not in HD-MSC.

Next, we aimed to determine whether HDAC8i could modify the expression of HDAC8 in BM-MSC. As illustrated in **Figure 32**, after 48 hours of exposure the BM-MSC to 25 µM of PCI34051 a decrease of HDAC8 mRNA in PV and ET-MSC was observed that was followed by a decreased in the protein expression (**Figure 32 C**). In HD-MSC, this behaviour was not observed, since PCI34051 treatment did not affect the expression of HDAC8 (mRNA and protein).

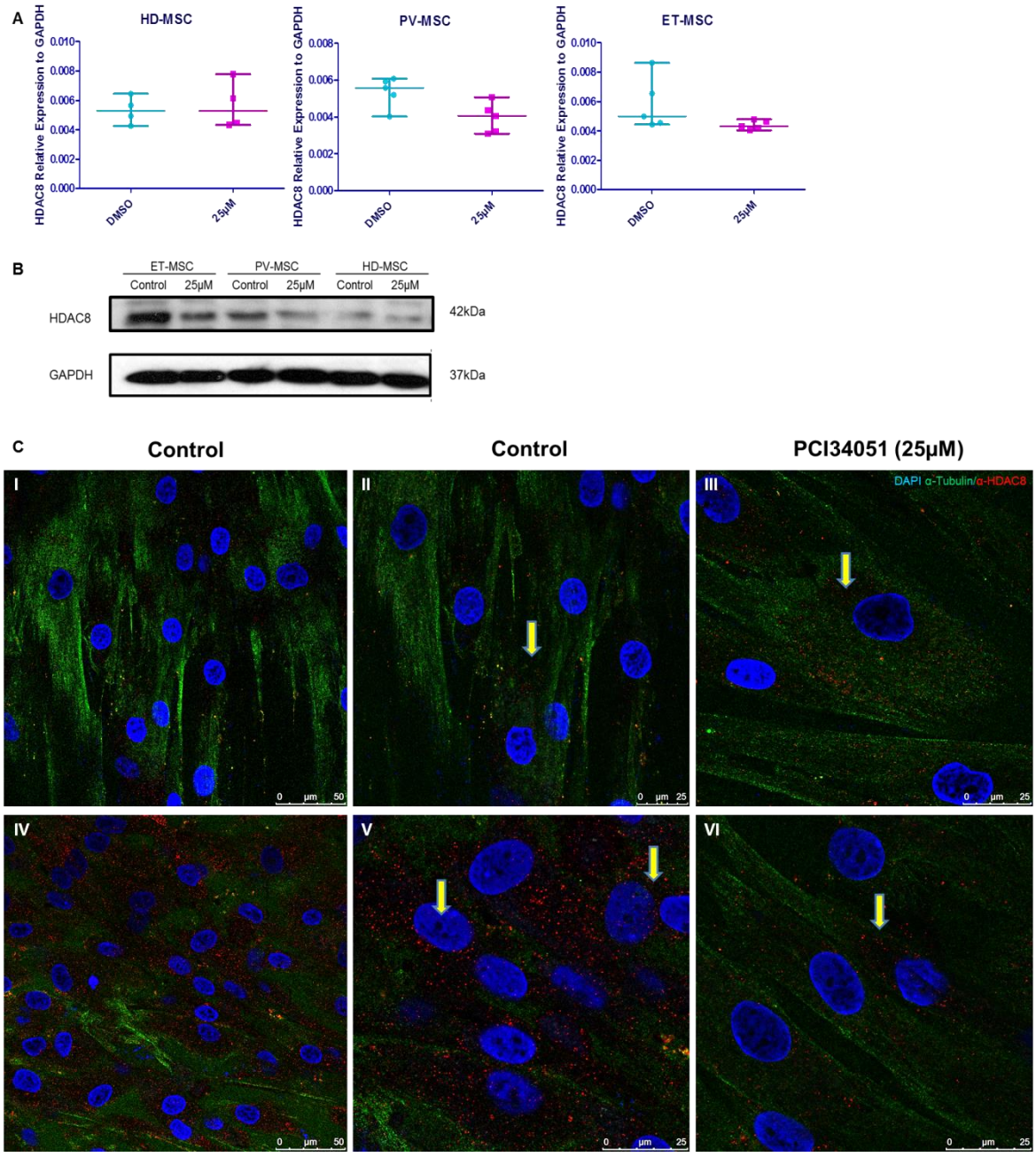

Figure 32: HDAC8i decrease the expression of HDAC8 in BM-MSC from JAK2^{V617F} patients. (A) RT-PCR showing that the treatment for 48h with PCI34051 (25μM) decrease HDAC8 mRNA expression in PV and ET-MSC and maintaining the expression in HD-MSC. Was also observed a decrease of HDAC8 protein expression, (c) WB analysis showing the decrease in the expression of HDAC8 in BM-MSC from ET and PV treated with HDAC8i, no protein changes were observed in BM-MSC from HD after treatment; (C) representative images of HD-MSC (up panel) and MPN-MSC (down-panel) without treatment (I-II and IV-V) and after treatment (III and VI). The red shows the localization of HDAC8 in the cells, where can be found mainly in the cytoplasm but also in the nucleus. The scale bar represents 50 and 25 μm.

To further investigate the role of HDAC8 inhibition on BM-MSC, its effects on apoptosis was studied by treating BM-MSC with different doses of PCI34051 (5µM and 25µM). As illustrated in **Figure 33**, when the cells were treated with a high dose (25µM) of the inhibitor, a significant decrease (p=0.02) in the percentage of alive ET-MSC (AnnexinV$^-$/7AAD$^-$) was observed. That was a consequence of a significant increase in the percentage of early and late apoptosis (p=0.002 and p=0.001, respectively) in ET-MSC, when compared to control cells (DMSO).

Regarding the effect of PCI34051 in the PV-MSC, a higher sensitivity to the compound was observed. Lower doses (5µM) of HDAC8i were able to induce a decrease in the percentage of alive PV-MSC (p=0.03), and this effect was increased (p=0.008) with higher concentrations. The drug increase the percentage of annexinV positive cells (p=0.03) and annexinV$^+$/7AAD$^+$ cells (p=0.04), in both neoplastic BM-MSC (ET and PV). Treating HD-MSC with PCI34051 produced no observable effects in its apoptosis.

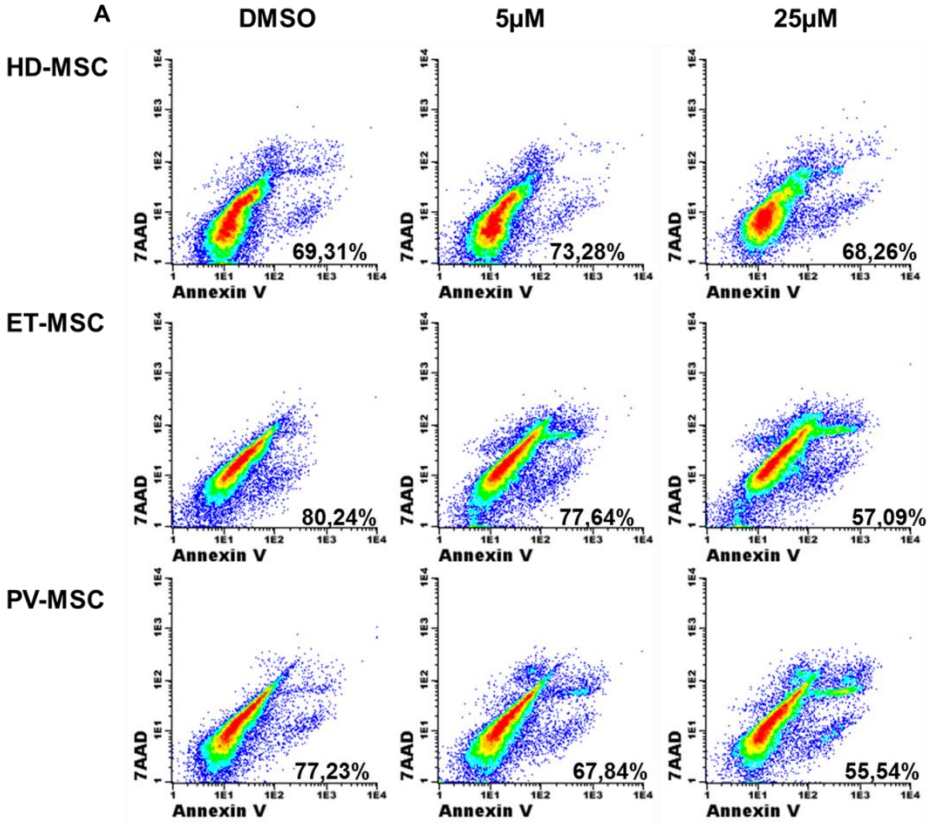

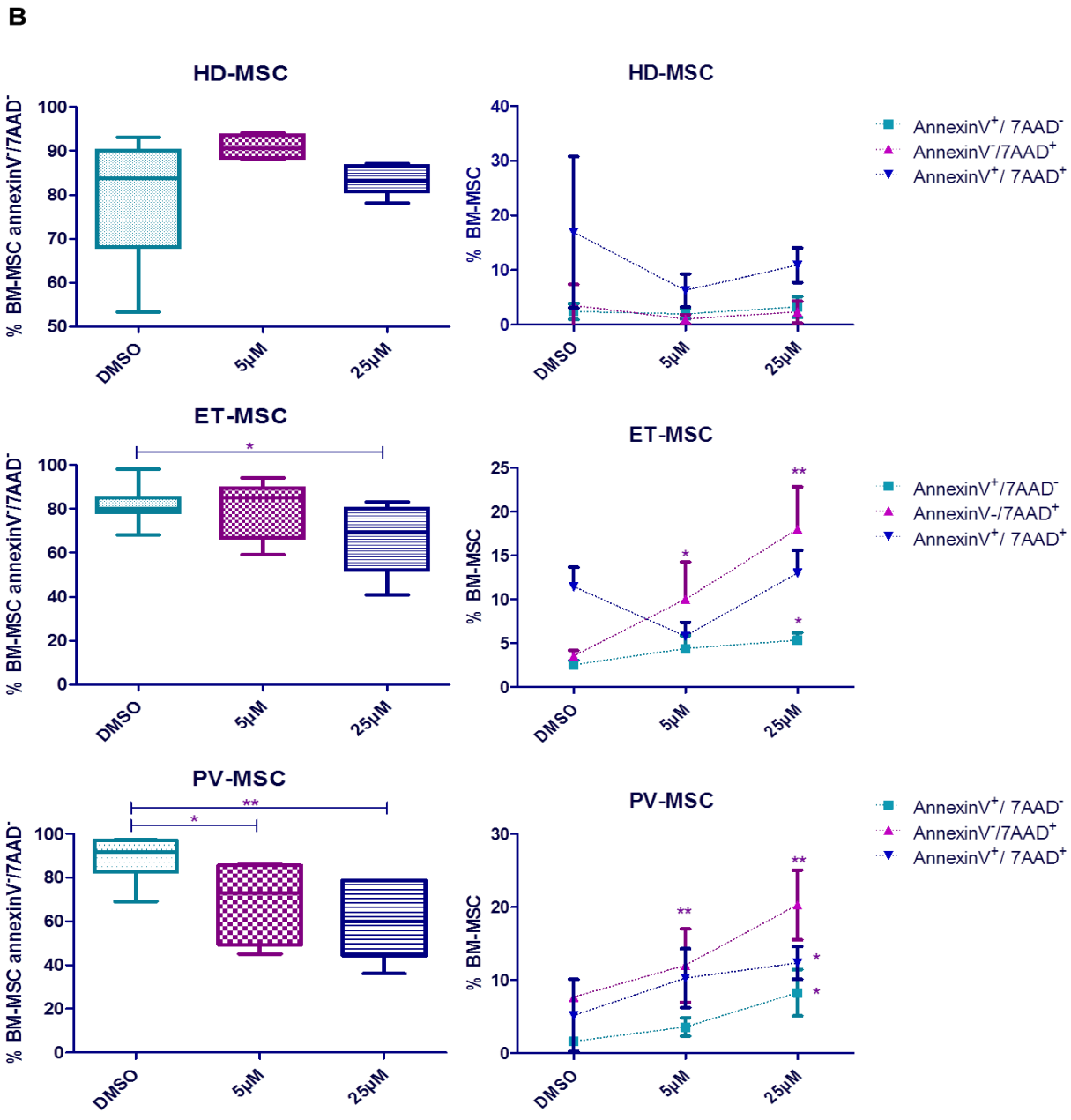

Figure 33: PCI34051 treatment decrease the viability of BM-MSC from JAK2^{V617F}. (A) Dotplot results (B) Boxplot showing the viability of BM-MSC by annexinV assay. ET-MSC and PV-MSC showed a significant decrease of viable cells at concentration of 25µM with significant increase of apoptotic cells. At concentration of 5µM was observed a significant decrease of viable cells only in PV-MSC. * p<0.05 and ** p<0.01

When cell cycle studies were performed, 48 hours after treatment with PCI34051, an increase in the percentage of cells in G1/G2 phase of cell cycle together with a decrease in the percentage of cells in S phase was observed. These results were more pronounced in the JAK2^{V617F}-

MSC, mainly in ET-MSC p=0.056. Higher concentrations of the inhibitor (50µM), produced a significant decrease in the percentage of S-phase on PV-MSC (p=0.025) and ET-MSC (p=0.020) (**Figure 34**).

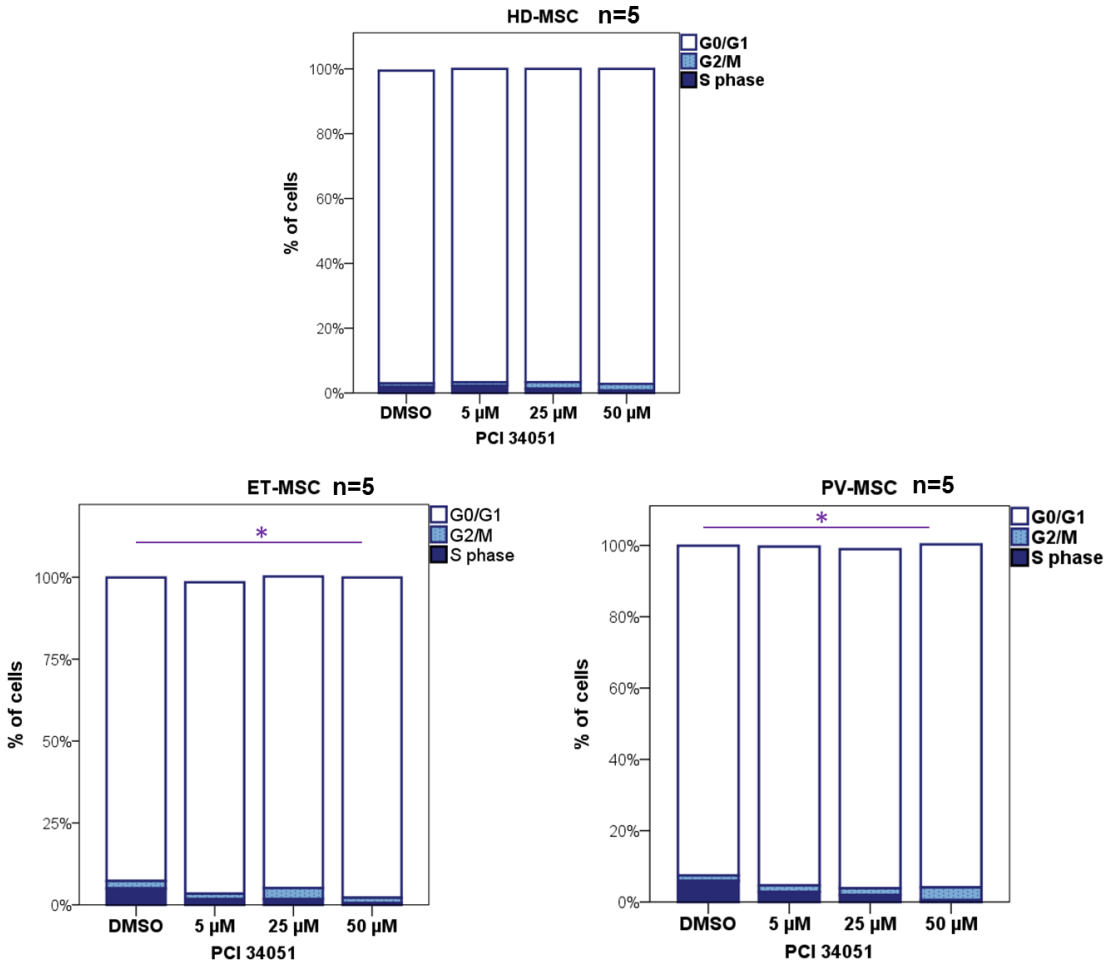

Figure 34: Cell cycle profiling on BM-MSC after 48 hours of drug incubation. Cell cycle profiling on the HD-MSC, ET-MSC and PV-MSC after 48 hours of HDAC8i incubation with different concentrations. The agent induces S-phase reduction when compared to the untreated condition (DMSO). The graphics represent the percentage of cells in G2/M, S and G0/G1 phases of the cell cycle. Data are represented as median of 5 experiments for each group. * p<0.05.

1.5.2 HDAC8i changes the capacity to maintain the myeloproliferative haematopoiesis of MSC-JAK2^{V617F}.

Because BM-MSC from JAK2^{V617F} patients seemed to have increased capacity to maintain clonal haematopoiesis, we wanted to know if the HDAC8 inhibitor could interfere with it.

Our results suggest that the inhibition of HDAC8 in JAK2^{V617F}-MSC significantly decrease (p=0.0006) the viability of the JAK2^{V617F}-MNC (**Figure 35**), with a significant increase in early apoptosis (p=0.0001), **Figure 35 B**. But no effect was observed, when treated JAK2^{V617F}-MSC were co-culture with HD-MNC (**Figure 35 C**). Treatment of HD-MSC did not affect JAK2^{V617F} and HD MNC viability (p=0.1431) (**Figure 35 D**).

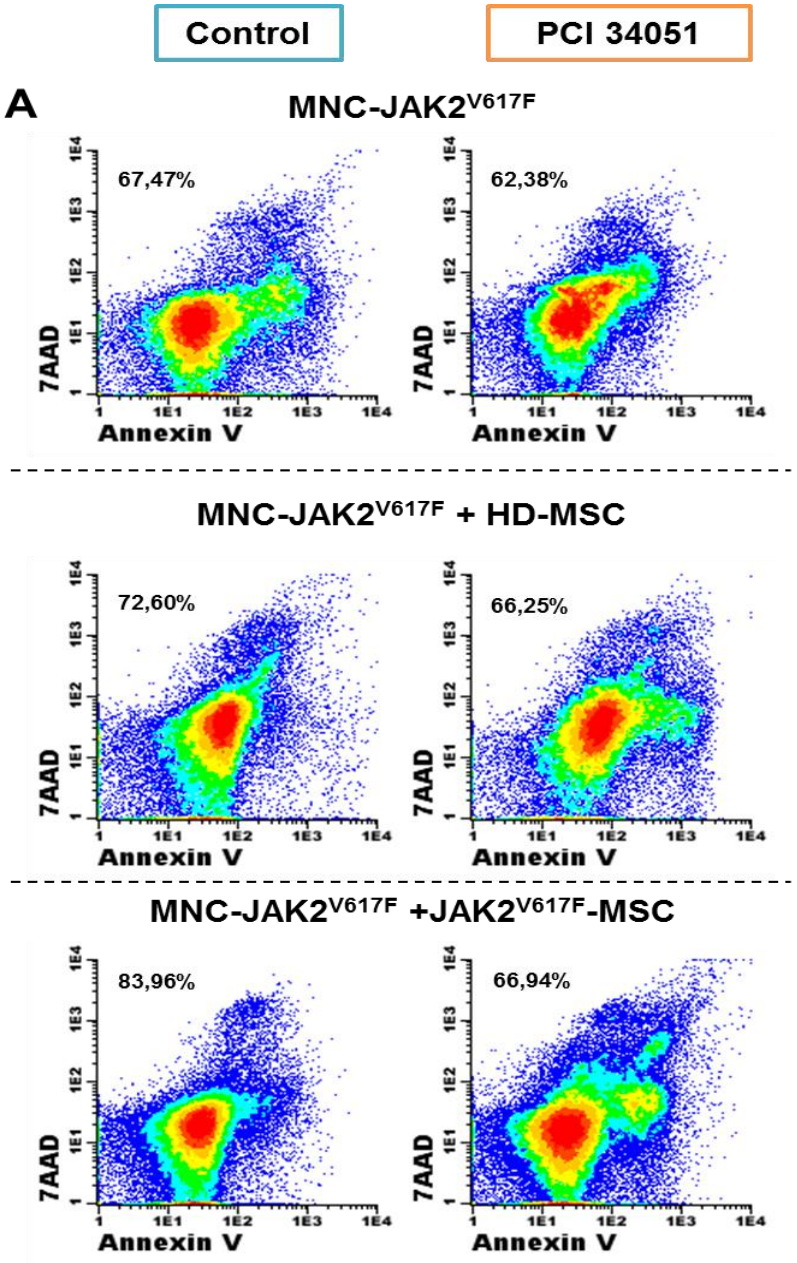

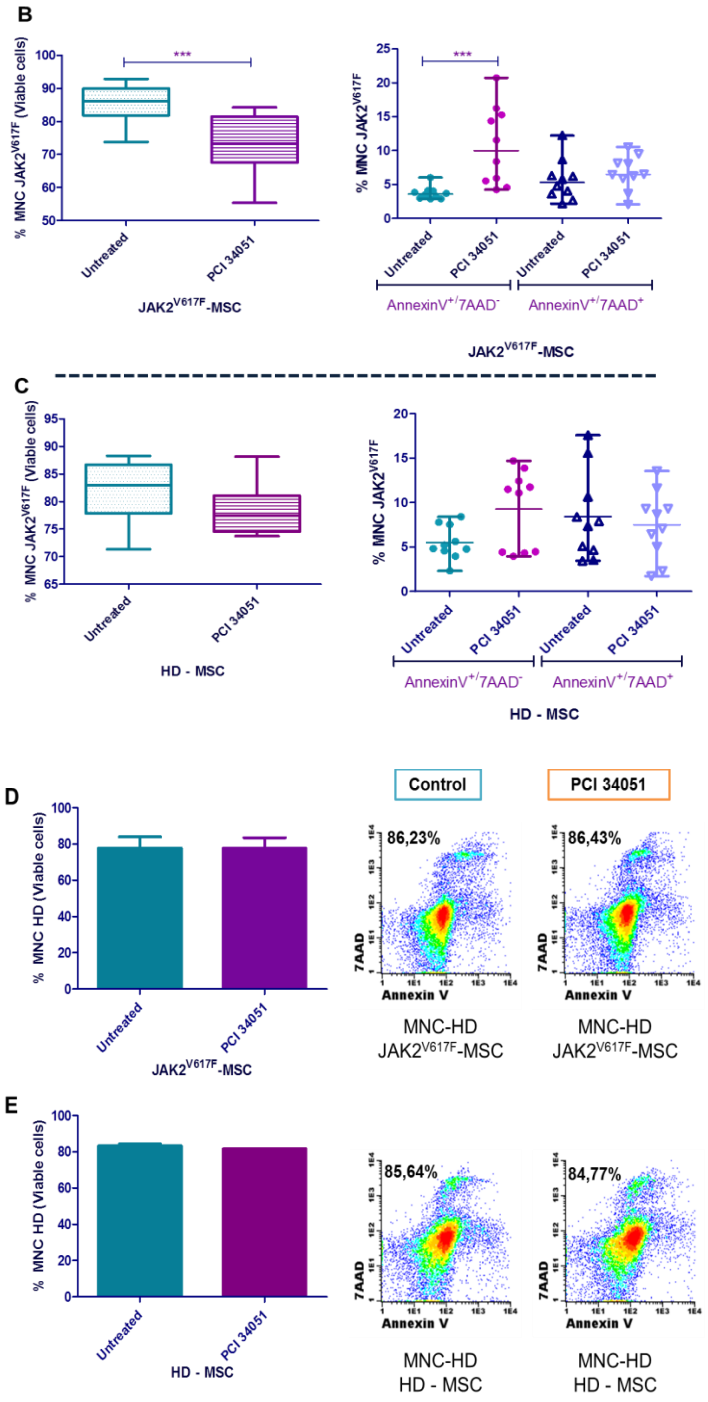

Figure 35: HDAC8i in JAK2^{V617F}-MSC increases the apoptosis of pathologic MNC in co-culture systems. (B) A significant increase of early apoptosis was observed in the JAK2^{V617F}-MNC when co-cultured with JAK2^{V617F}-MSC treated with PCI34051 (n=10). (C) Was not observed differences when the pathologic MNC were co-cultured with HD-MSC treated with HDAC8i (n=10). No difference in apoptosis was observed when HD-MNC were co-cultured with HD and JAK2-MSC with or without treatment (n=4). * p<0.05.*** p<0.001. Data are represented as median and range.

To analyse whether HDAC8i induced apoptosis was due to abrogated cell cycle progression, we co-cultured MNC with treated BM-MSC (HD and JAK2). No differences in MNC cell cycle was observed, when they were co-cultured with treated HD or MPN-MSC.

Because these studies were performed with MNC, we wanted to know if similar results could be achieved with HPC. For this propose $CD34^+$ cells were used.

As seen in the **Figure 36**, we observed that the inhibition of HDAC8 in $JAK2^{V617F}$-MSC induce significant decrease of alive HPC (Annexin V^-/$7AAD^-$) from both HD (p=0.028) and $JAK2^{V617F}$ $CD34^+$ cells (p=0.015). The treatment of HD-MSC has no effect in the viability of $CD34^+$ cells, both from HD and $JAK2^{V617F}$ patients.

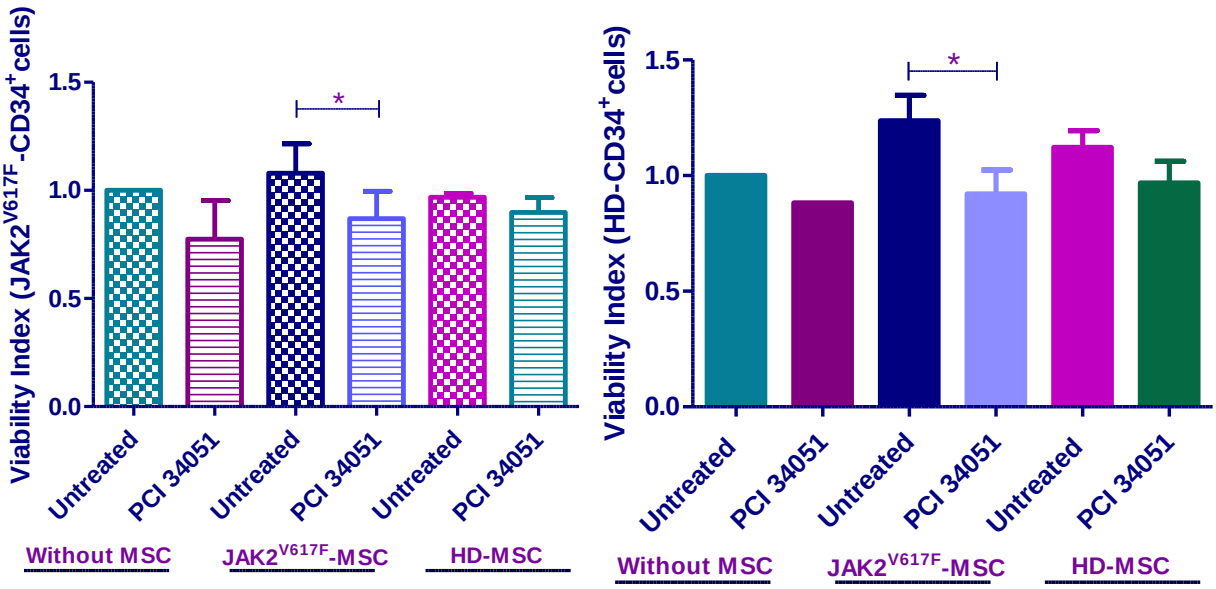

Figure 36: HDAC8i in $JAK2^{V617F}$-MSC decrease the viability of progenitor hematopoietic cells. The left column bar graph represents the viability of $CD34^+$ cells from BM of MPN patients (n=5) and the right column bar graph represents the BM from HD (n=4). The treatment with PCI34051 in the $JAK2^{V617F}$-MSC decrease significantly the viability of $CD34^+$ cells from HD (n=4) and $JAK2^{V617F}$ patients (n=5). * p<0.05. Data are represented as median and range.

To study which mechanisms could be involved in the increase of apoptosis, TP53 and BAD expression in the MNC was also studied. We observed an increase in the expression of TP53 with a decrease in the expression of BAD in JAK2^{V617F}-MNC co-cultured with JAK2^{V617F}-MSC where HDAC8 had been inhibited, although differences did not reach significance (**Figure 37**).

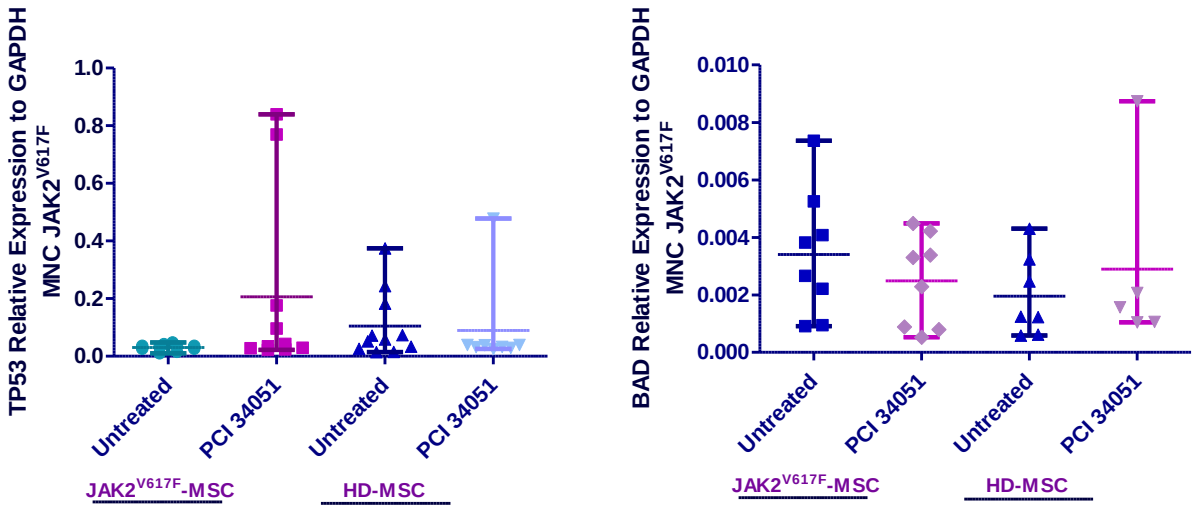

Figure 37: Gene expression of TP53 and BAD gene in MNC from JAK2^{V617F} patients. The left scatter plot shows an increase of TP53 in the MNC when co-cultured with JAK2^{V617F}-MSC that was treated with PCI 34051. The expression of TP53 is followed with a decrease of BAD (right graphic). Results were normalized with the housekeeping gene GAPDH. Scatter plots are represented by the median and the range.

We also evaluated if the observed effects were maintained, when stroma and haematopoietic cells were co-cultured in direct contact (**DC**). MNC from BM of JAK2^{V617F} patients were co-cultured in **DC** (n=19) and in *transwell* - **T** (n=19) with MSC from HD (n=9) and JAK2^{V617F} (n=10) previously treated with PCI34051, and MNC viability was evaluated. The percentage of alive JAK2-MNC was significant decreased, when they were cultured, in DC and T, with treated JAK2-MSC (**Figure 38**).

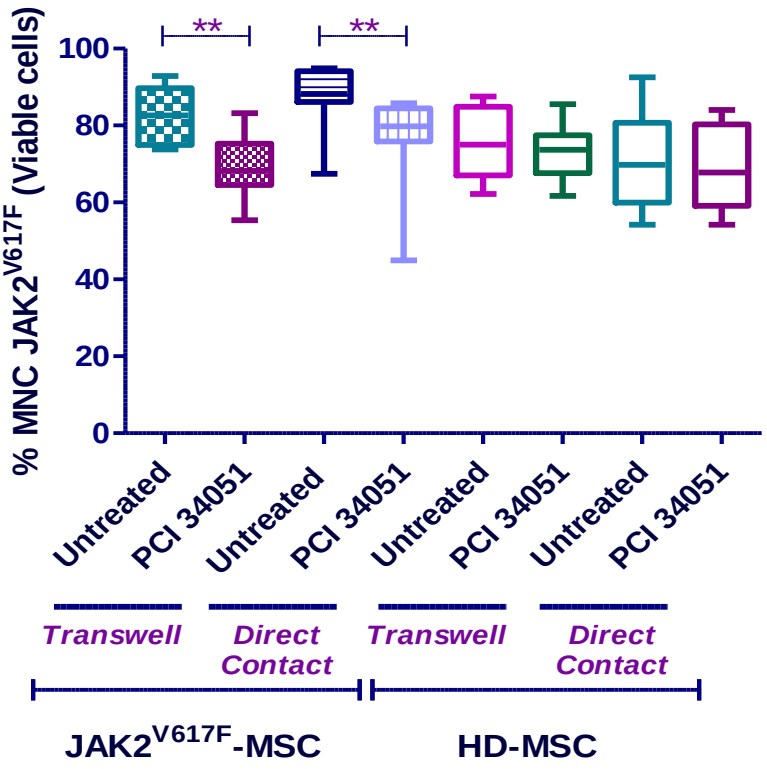

Figure 38: HDAC8i in JAK2^{V617F}-MSC increase the apoptosis of pathologic MNC in co-culture systems (direct contact vs *transwell*). A significant decrease of alive JAK2^{V617F}-MNC was observed when were co-cultured with JAK2^{V617F}-MSC treated with PCI34051 in direct contact (n=9) or by *transwell* (n=10). Was not observed differences when the pathologic MNC were co cultured with HD-MSC treated with PCI 34051 in direct contact (n=9) or in *transwell* (n=10) * p<0.05. Data are represented as median.

Because we observed an increase in the colony formation when co-culturing MNC-JAK2^{V617F} with JAK2^{V617F}-MSC, we wanted to analyse if treating BM-MSC with HDAC8 inhibitor diminished this capacity. As can be observed (**Figure 39 A**), this capacity of the myeloproliferative MSC to maintain the malignant MNC was reverted when the MPN-MSC were treated with PCI34051 (p=0.0086). No differences in the production of malignant colonies (MPN-CFU-GM) were observed, when HDAC8 was inhibited in HD-MSC (n=5).

In order to confirm that the effect was done on HPC the same experiments were performed using HD and JAK2 -CD34^{+} cells (n=2). A decrease in CFU-GM was observed when JAK2-CD34^{+} cells were maintained with the JAK2^{V617F}-MSC treated with HDAC8i (**Figure 39 B**).

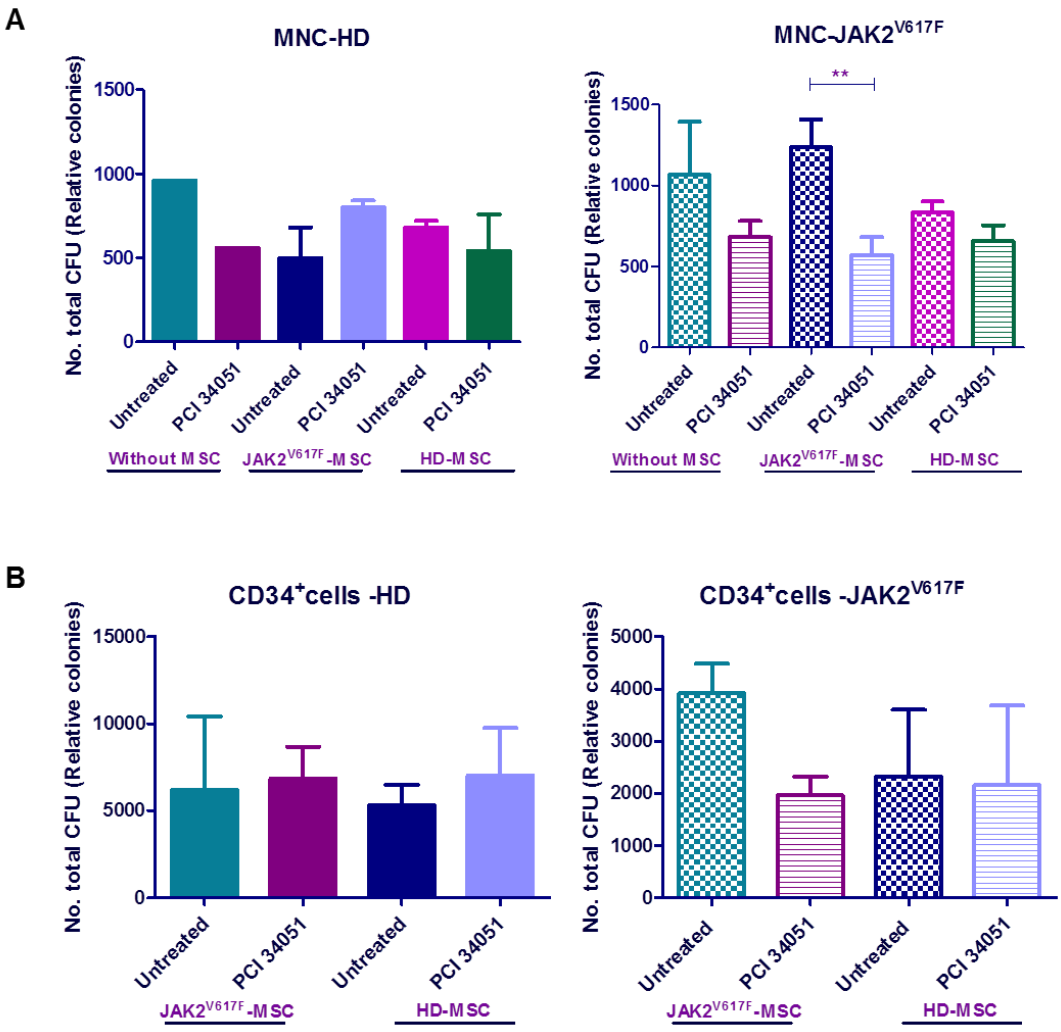

Figure 39: HDAC8 inhibition in JAK2^{V617F}-MSC decreases the colony-formation of myeloproliferative haematopoietic cells. (A) Relative numbers of CFU-GM from JAK2^{V617F}-MNC and HD-MNC that were co-cultured with HD (n=6) and JAK2-MSC (n=10) treated with PCI 34051. (B) Relative numbers of CFU-GM from JAK2^{V617F}-CD34^{+} cells and HD-CD34^{+} cells that were co-cultured with HD (n=2) and JAK2-MSC (n=2) treated with PCI 34051.** p<0.01.

Data are represented as median and interquartile range. CFU-GM: colony-forming unit-granulocyte macrophage.

1.5.3 HDAC8i induces apoptosis in myeloproliferative cell lines HEL, SET-2 and UKE-1

To determine if HDAC8 inhibition by PCI34051 affects the apoptosis of myeloproliferative cell lines, three different cell lines (HEL, UKE-1 and SET-2) were treated for 72 hours with various concentrations of inhibitor. As shown in **Figure 40**, the inhibitor induces cell death at higher concentrations (25 and 50µM). HEL was the cell line more sensitive to the HDAC8i, so that after only 24 hours of treatment with PCI34051 at concentrations 25 and 50µM the percentage of alive cells was inferior to 50%. After 48 and 72 hours of culture with these concentrations of the drug almost all cells were dead.

SET-2 and UKE-1 were less sensitive to the inhibitor, although we observed a marked decrease of viable cells 72 hours after treatment with this compound at a concentration of 50µM.

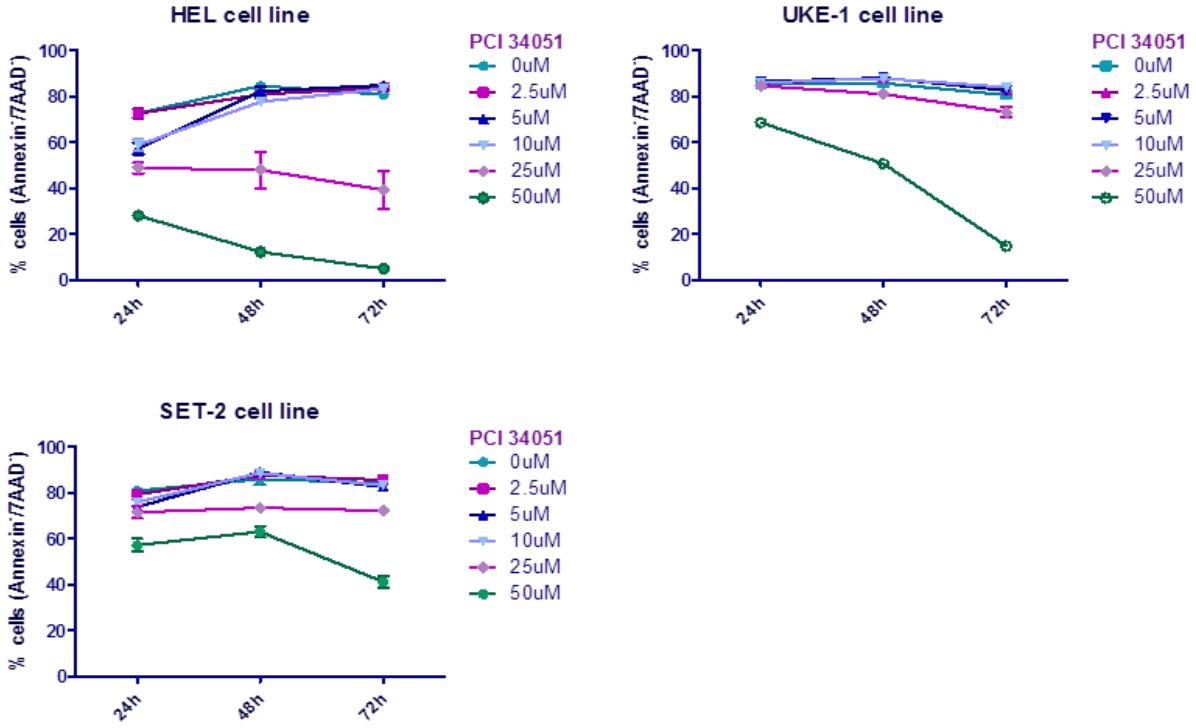

Figure 40: HADC8i in myeloproliferative cell lines (SET-2, UKE-1 and HEL) decrease the cell viability. Cell lines were cultured in vitro and treated with the indicated concentrations of PCI34051 during 72h. At higher concentrations (25µM and 50µM) have effect in the percentage of viable cells (annexin$^-$/7AAD$^-$)

Moreover, we analysed if the capacity of PCI34051 to induce cell apoptosis was maintained in the presence of MSC from HD and JAK2^{V617F} patients. To address this question, co-culture assays were performed. The different cell lines were cultured by *transwell* (3 µm) or in direct contact with BM-MSC, and treated with PCI34051. After 48h, the haematopoietic cell lines were recovered and the percentage of apoptotic cells analysed. The presence of BM-MSC from HD and JAK2^{V617F} patients did not change the cell viability of the different cell lines.

The three JAK2^{+} cell lines showed a significant decrease in alive cells when treated with PCI34051. However, this decrease was enhanced in the presence of JAK2^{V617F}-MSC, both in direct contact and in *transwell* (**Figure 41 and 42**).

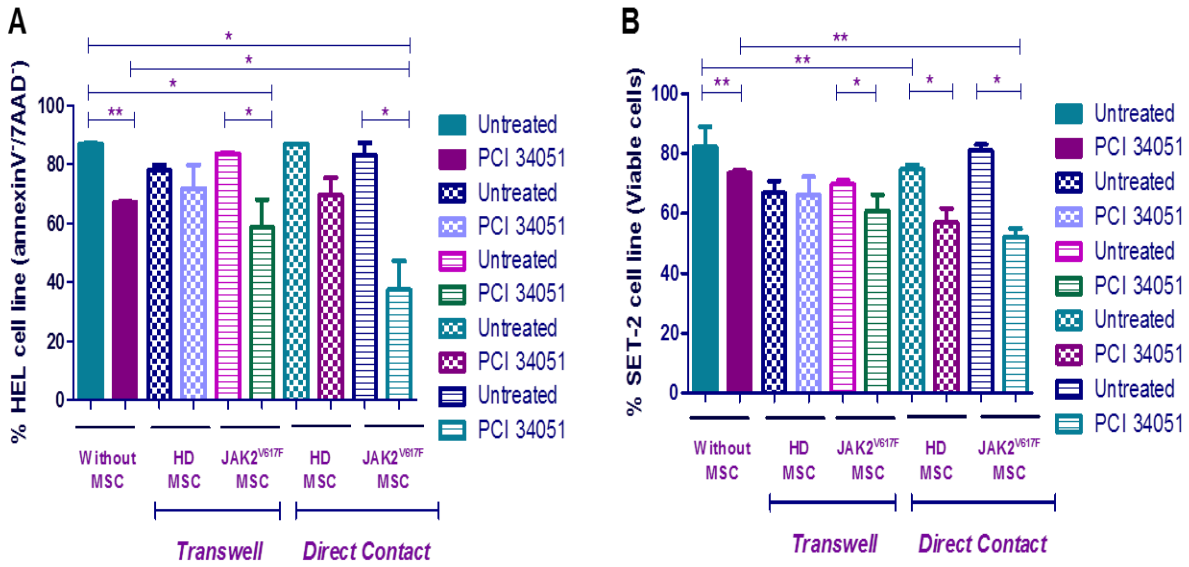

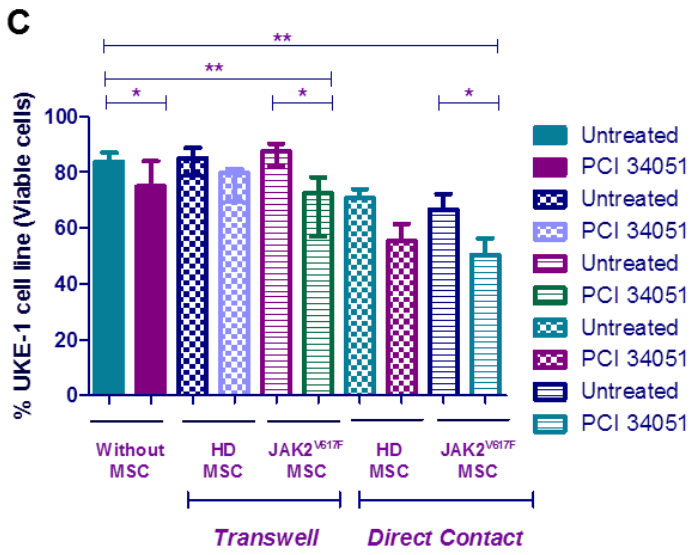

Figure 41: HDAC8 inhibition in JAK2^{V617F}-MSC induces apoptosis in the different myeloproliferative cell lines . HEL (A), SET-2 (B) and UKE-1 (C) were cultured *in vitro* (no stroma) and co-cultured separated by 3µm micropore membranes (*transwell*) or by direct contact. The different cell lines without stroma were incubated for 48h with PCI34051 (25µM). When co-cultured with the stroma, the BM-MSC were previously treated with PCI34051 and then were co-cultured with the treated stroma during 48h. After that time the cells were harvested, stained with CD45 and Annexin-V/7AAD and analysed the apoptosis by flow cytometry. Values indicate the median with the interquartile range of 4 experiments for each condition.*p<0.05 ** p<0.01.

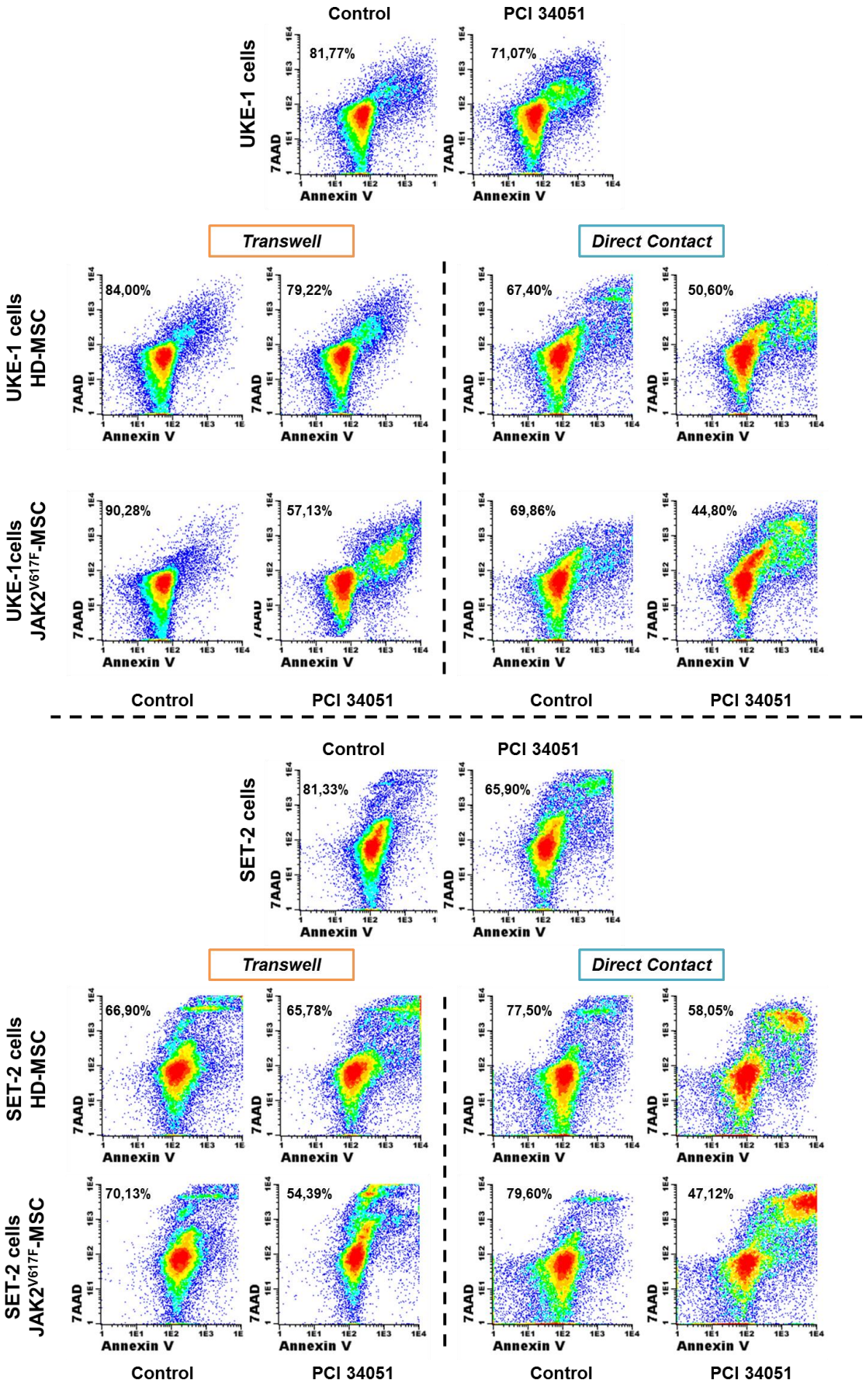
Control
PCI 34051
UKE-1 cells
81,77%
71,07%
Transwell
Direct Contact
UKE-1 cells
HD-MSC
84,00%
79,22%
67,40%
50,60%
UKE-1cells
JAK2V617F-MSC
90,28%
57,13%
69,86%
44,80%
Control
PCI 34051
Control
PCI 34051
SET-2 cells
81,33%
65,90%
SET-2 cells
HD-MSC
66,90%
65,78%
77,50%
58,05%
SET-2 cells
JAK2V617F-MSC
70,13%
54,39%
79,60%
47,12%
Control
PCI 34051
Control
PCI 34051
7AAD
Annexin V

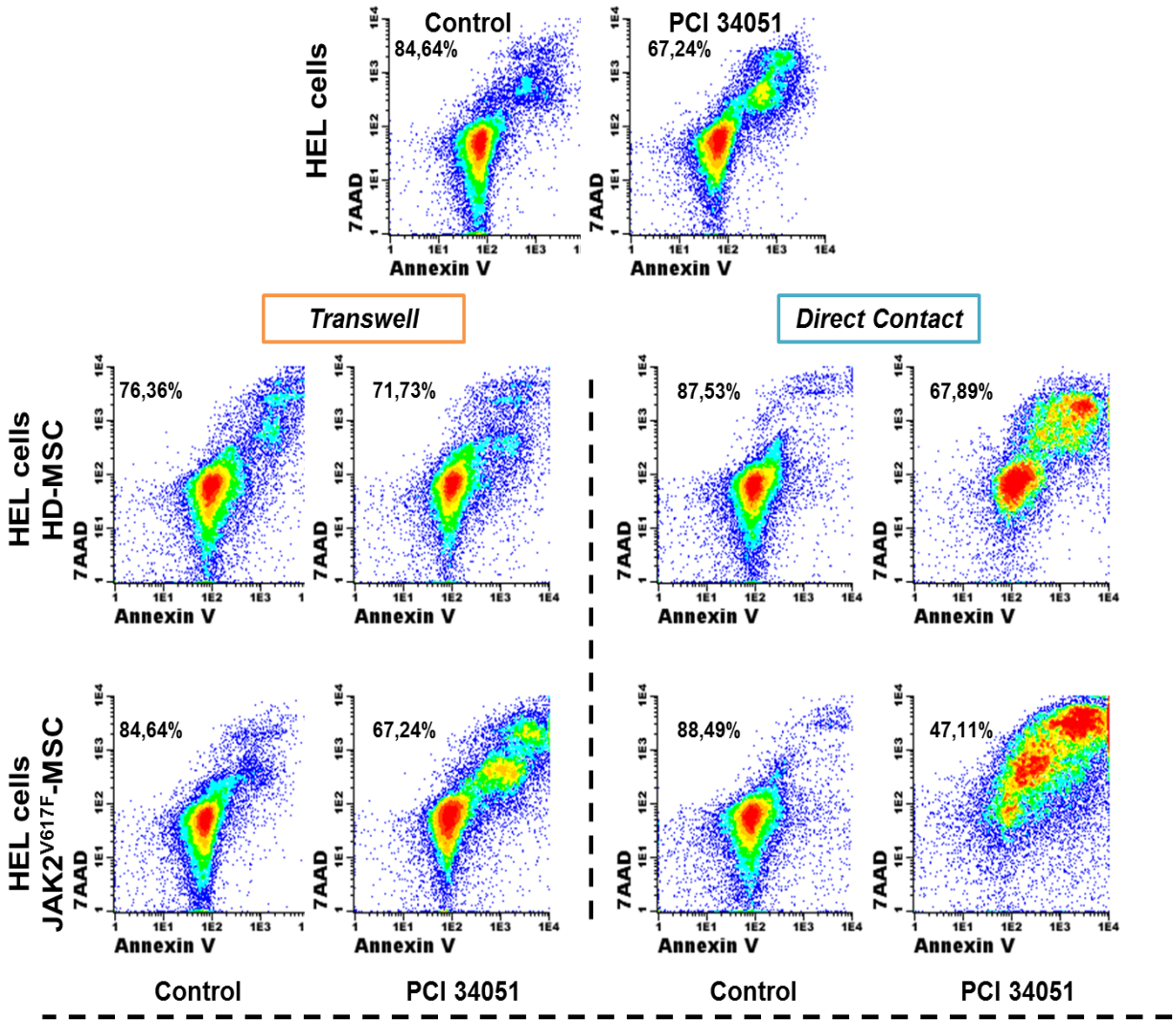

Figure 42: Flow Cytometry dot plot images. Apoptosis of the different cell lines (UKE-1, SET-2 and HEL) that were co-cultured with stroma (HD and JAK2^{V617F}) treated with PCI34051 for 48h was evaluated by flow cytometry.

Later on, the clonogenic capacity of UKE-1 cells treated with PCI34051 and co-cultured with BM-MSC (HD and JAK2), was evaluated. Despite the capacity of PCI34051 to induce apoptosis in UKE-1, no differences regarding to colony formation were observed (**Figure 43**). When UKE-1 cells were co-cultured MPN-MSC, an increase in the total number of colonies was observed. This increase was reversed when the UKE-1 cells were treated with PCI34051 whith the pres-

ence of JAK2^{V617F}-MSC. The **Figure 43** shows that the treatment with PCI34051, induces changes in the morphology of the colonies, with the development of smaller colonies size.

In other to understand if the inhibition of cell growth was induced by the STAT5 changes, the phosphorylation of STAT5 was analysed after being treated in the different conditions.

The **Figure 43 B**, shows a decrease of pSTAT5 when the UKE-1 cells were treated with HDAC8i in the presence of JAK2^{V617F}-MSC.

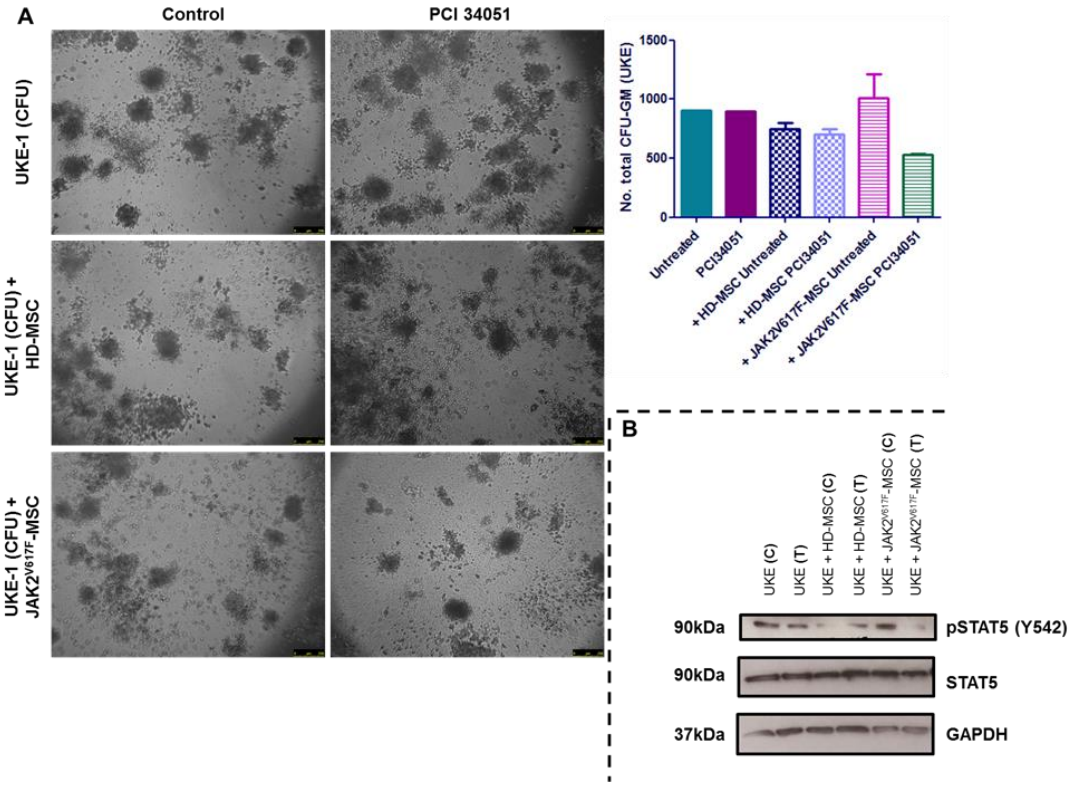

Figure 43: HDAC8i reduces colony-formation in the presence of pathologic stroma. (A) A decrease of colony-forming unit-granulocyte-macrophage (CFU-GM) was observed, without significant differences, when the UKE-1 cells and the pathologic stroma were treated with PCI34051 (n=3)**.** (B) A decrease of pSTAT 5 when UKE-1 cells were treated with HDAC8i in present of pathologic stroma.

2. Biological properties of extracellular vesicles released by mesenchymal stromal cells from MPN patients and their role in the pathophysiology

2.1 Isolation and characterisation of EV from JAK2^{V617F}-MSC

In order to investigate if the extracellular vesicles released from JAK2^{V617F}-MSC have different vesicular cargo, we isolated and characterised EV from HD-MSC (n=19) and MPN-MSC (n=22). Regarding to EV characterisation, TEM revealed no differences in the morphology and size of EV from JAK2^{V617F}-MSC and HD-MSC. **Figure 44** shows a typical bilayer-membrane vesicle population with heterogeneous size with a diameter < 200nm.

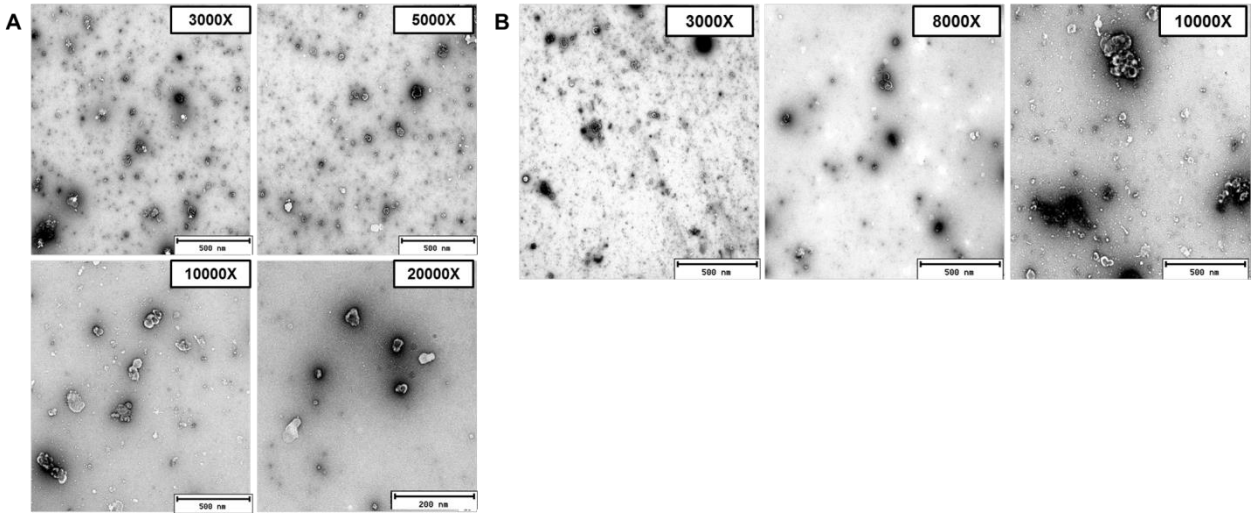

Figure 44: Representative TEM images of JAK2^{V617F}-MSC (A) and HD-MSC (B) the preparation showing the characteristic rounded morphology with a hypodense centre. Both groups were observed vesicles with heterogeneous size. (Scale bars: 500 and 200 nm).

These preparations were also analysed for the expression of the known EV marker protein (CD63), which was present in all samples, as well as the mesenchymal marker CD73 (**Figure 45**).

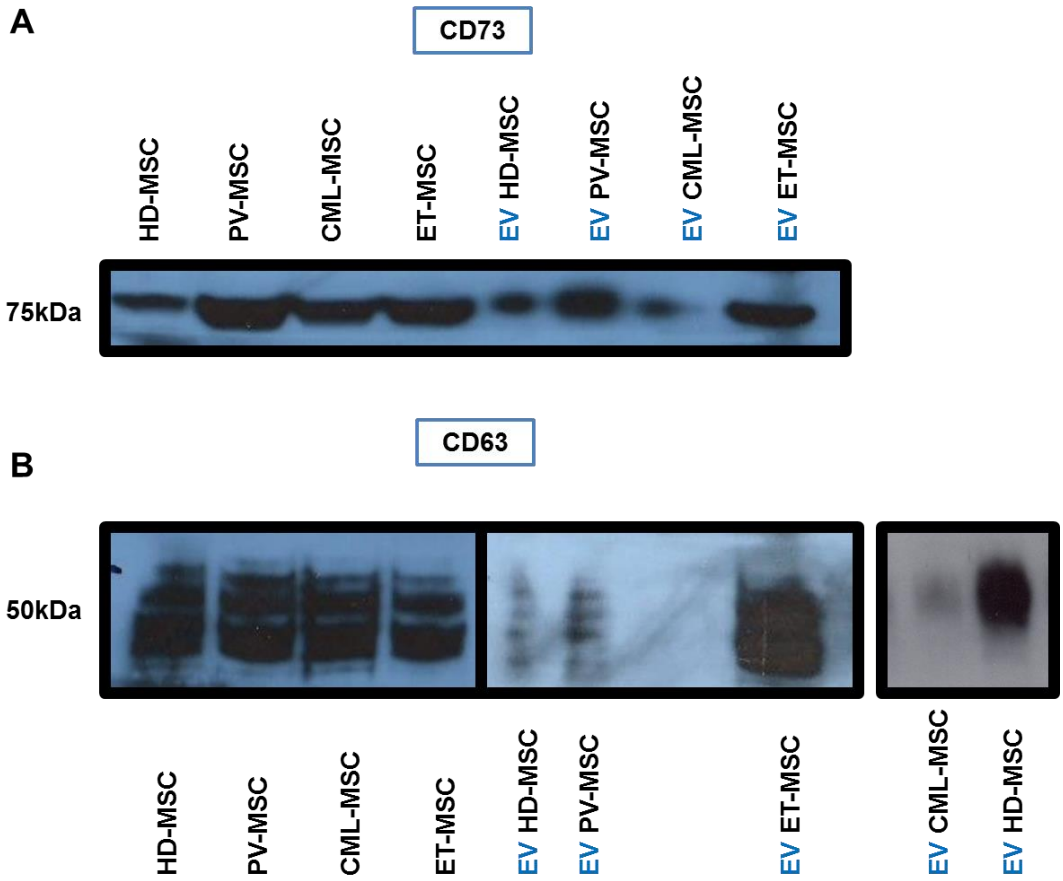

Figure 45: MSC and EV western blot (WB) images. WB analysis of human mesenchymal protein CD73 (A) and expression of EV protein CD63 (B) analysed on EV from ET-, PV-, CML- and HD-MSC in comparison to whole cell lysates.

Next, we analysed the EV released from BM-MSC by nano-particle tracking analysis (NTA). As shown in **Figure 46**, EV from both groups display similar size distribution profile, always inferior to 500nm.

Regarding the concentration, a higher particle concentration of EV released by MPN-MSC ($5.56X10^{10}$±$5.60X10^{8}$ particles/mL) was observed compared with EV from HD-MSC ($6.40X10^{8}$±$1.0X10^{7}$ particles/mL).

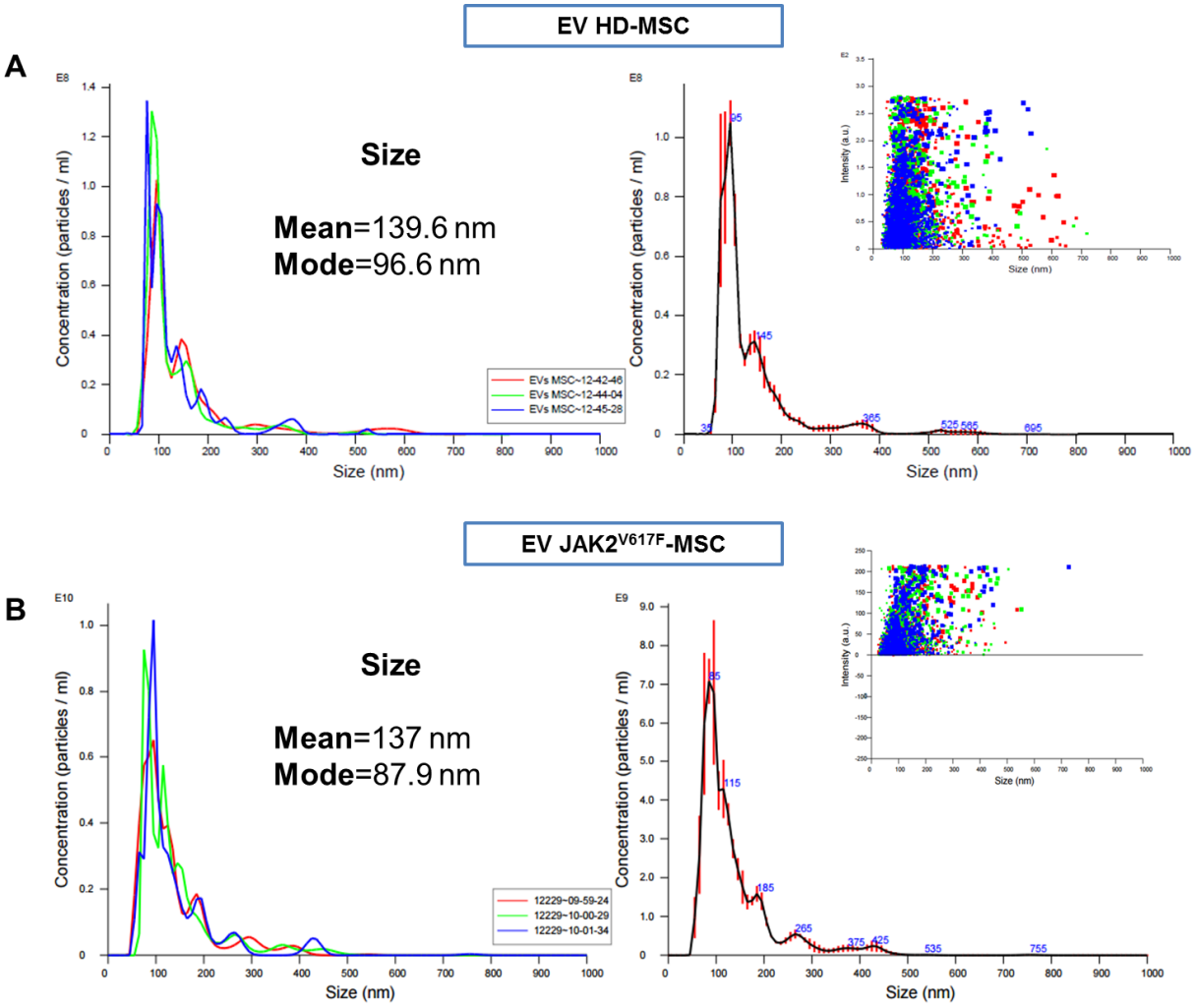

Figure 46: EV quantification using Nanosight nanoparticle tracking analysis. (A) EV from HD-MSC and (B) EV from JAK2^{V617F}-MSC.

EV characterisation by multiparametric flow cytometry was also performed as previously described *(Ramos, et al 2016)*. After EV isolation, the samples from HD (n=3) and JAK2^{V617F} patients (n=3) were labelled with the same panel of monoclonal antibodies.

As observed in the dot-plots in **Figure 47**, we were able to characterise EV released from BM-MSC of both groups (HD and JAK2), defined as particles less than 0.9 µM, positive for CD90, CD44 and CD73 and for EV markers, and negative for CD34 and CD45.

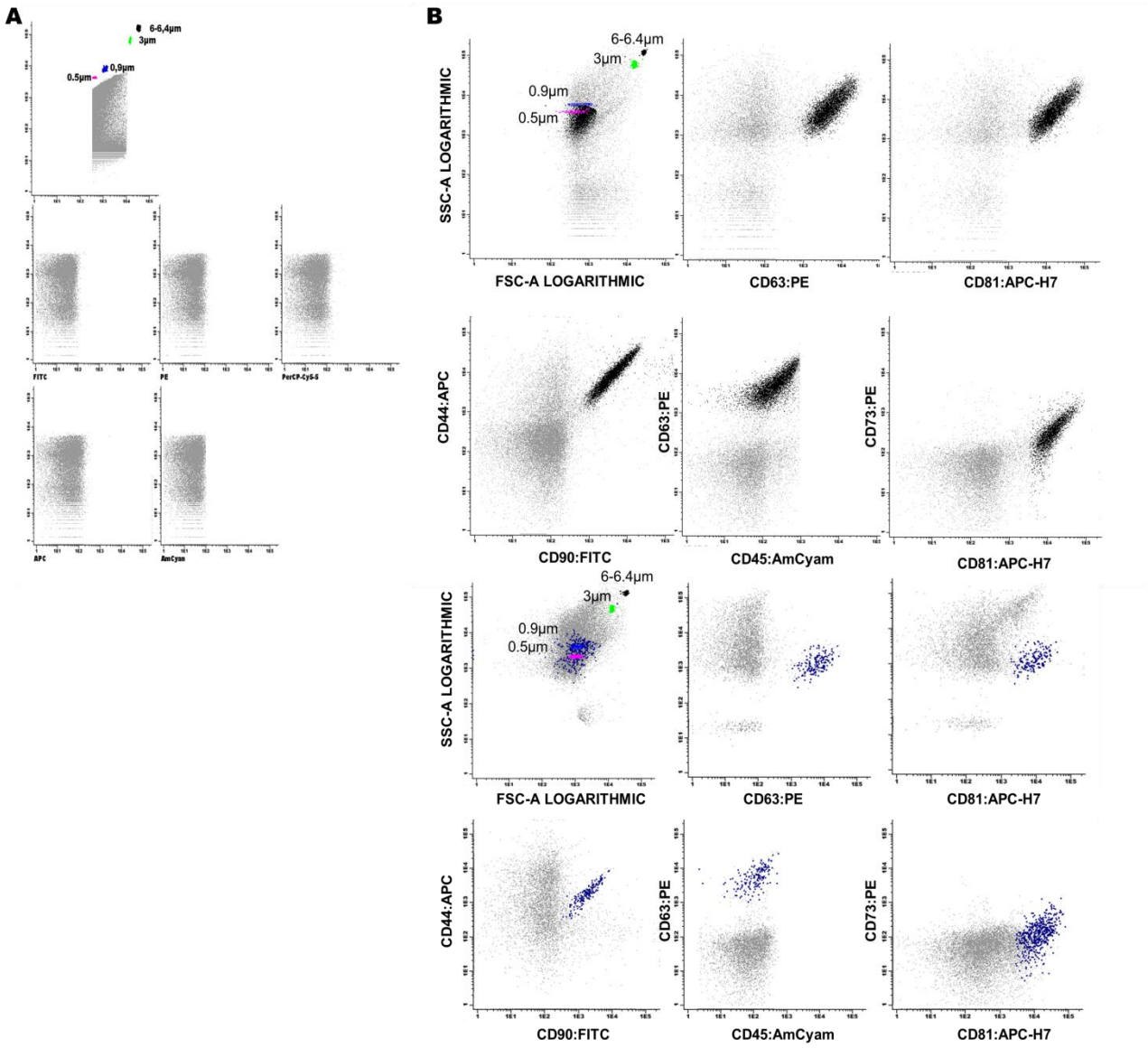

Figure 47: Representative MFC density plot showing (A) acquired PBS 0.22µm doubled filtered and PBS doubled filtered with beads (0.5, 0.9, 3, 6-6.4µm) and (B, C) the gate of EV from HD-MSC (A) and JAK2^{V617F}-MSC (B). Standard microbeads with a diameter of 0.9µm were used to set the upper size limit for the EV and were used to gate them. EV from BM-MSC were negative hematopoietic markers (CD34 and CD45) and positive for MSC markers (CD90, CD44, CD73) and for EV markers (CD81 and CD63). In gray represents the control (unstained EV) and in black/blue the EV stained with the different antibodies

2.2 MicroRNAs expression analysis in EV from JAK2^{V617F}-MSC

We analysed the microRNA compostition of the released EV from 8 HD-MSC, 4 PV-MSC and 7 ET-MSC, usinig a quantitative PCR *TaqMan* array platform.

As shown in **Figure 48**, no differences were observed between JAK2^{V617F} -MSC- and HD-MSC EV-microRNA profiling. However, when CT values were analysed, 283 out of all the 380 tested microRNAs showed increased expression, with a tendency to a significant overexpression of miRNA155 in the EV from ET and PV MSC patients (**Figure 49**).

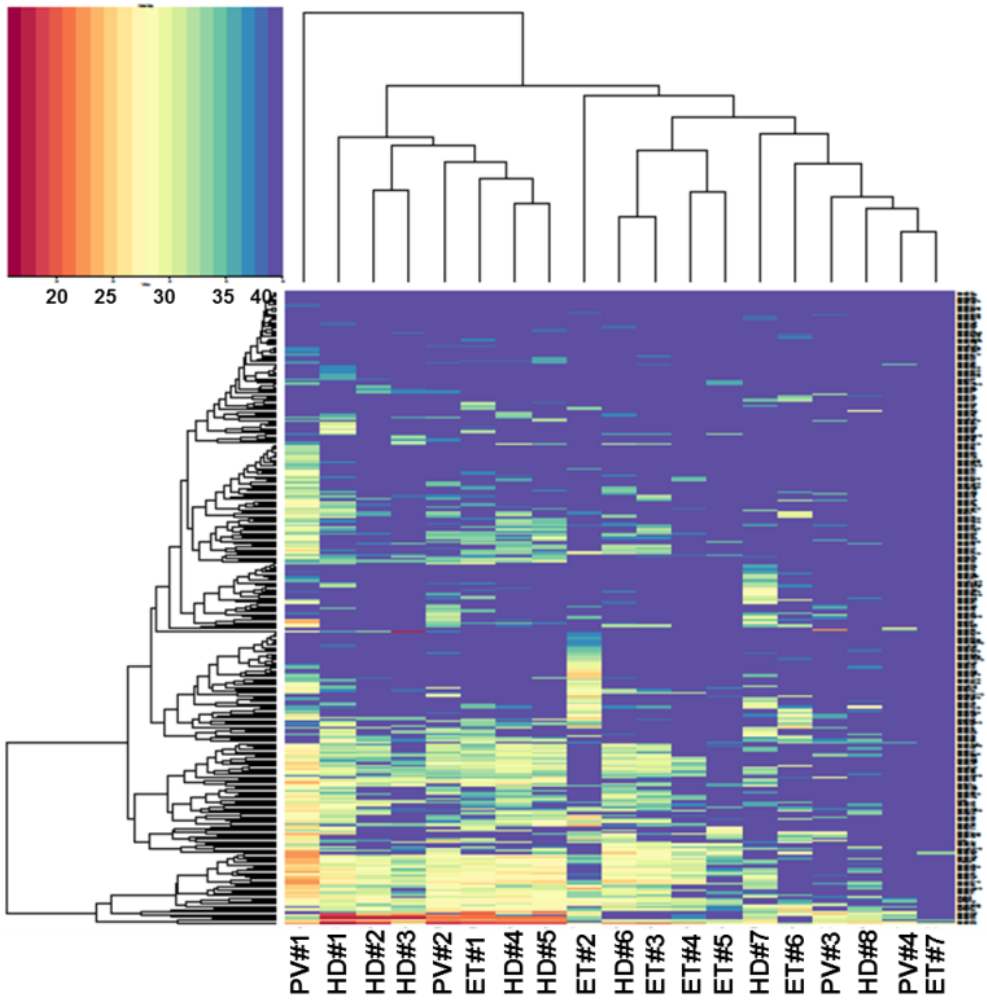

Figure 48: Heatmap based on Raw CT values of 384 microRNAs from 19 EV-MSC samples. At the left side, a dendrogram of microRNA Euclidean distances. At the top, a dendrogram of Euclidean distances of EV-MSC samples. HD – healthy donors, ET – essential thrombocythemia and PV – polycythemia vera. A colour scale legend is at the top-left panel.

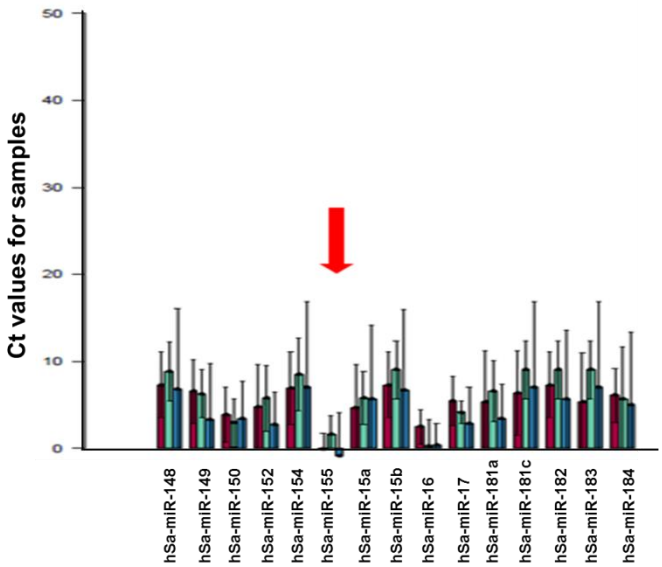

Figure 49: MicroRNA expression pattern by TaqMan® MicroRNA Arrays. A sectioned barplot representing the microRNAs. Bars represent individual microRNA normalized Delta Ct mean values of EV from PV-MSC (pink), HD-MSC (green) and ET-MSC (blue).

When hsa-miR-155 RT-PCR was performed (2 PV and 3 ET patients) a significant overexpression (p=0.032) was observed in EV from MPN-MSC, when compared to EV from HD-MSC (p=0.032) (**Figure 50**).

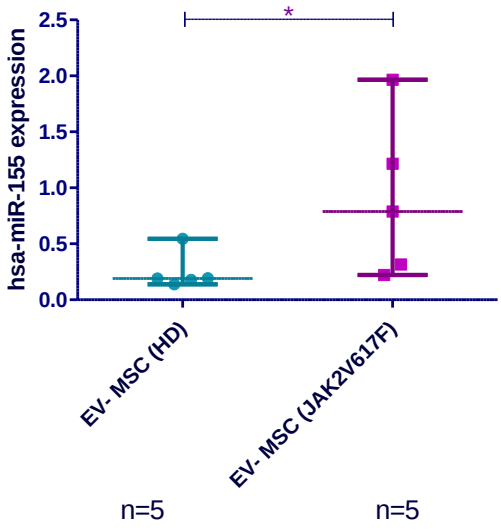

Figure 50: Expression of miR-155. RT-PCR from 5 EV released from HD-MSC and 5 EV from JAK2^{V617F}-MSC. Values are expressed by median and interquartile range. *p<0.05

2.3 Release of EV from stromal cells and transference to haematopoietic progenitors cells.

To study if EV released from MPN-MSC can be up taken by $CD34^+$ cells, EV were labelled with Vybrant-Dil dye cell-labelling solution (red), and then co-cultured with $CD34^+$ cells. Using fluorescent microscopy, we were able to detect red signals in the membrane of $CD34^+$ cells that engulfed EV from $JAK2^{V617F}$-MSC (n=2) and also by HD-MSC (n=2) (**Figure 51**). Flow cytometry showed (**Figure 51**) a displacement of $CD34^+$ cells after 24 hours of co-culture with $JAK2^{V617F}$-EV (labelled with vibrant-dil dye).

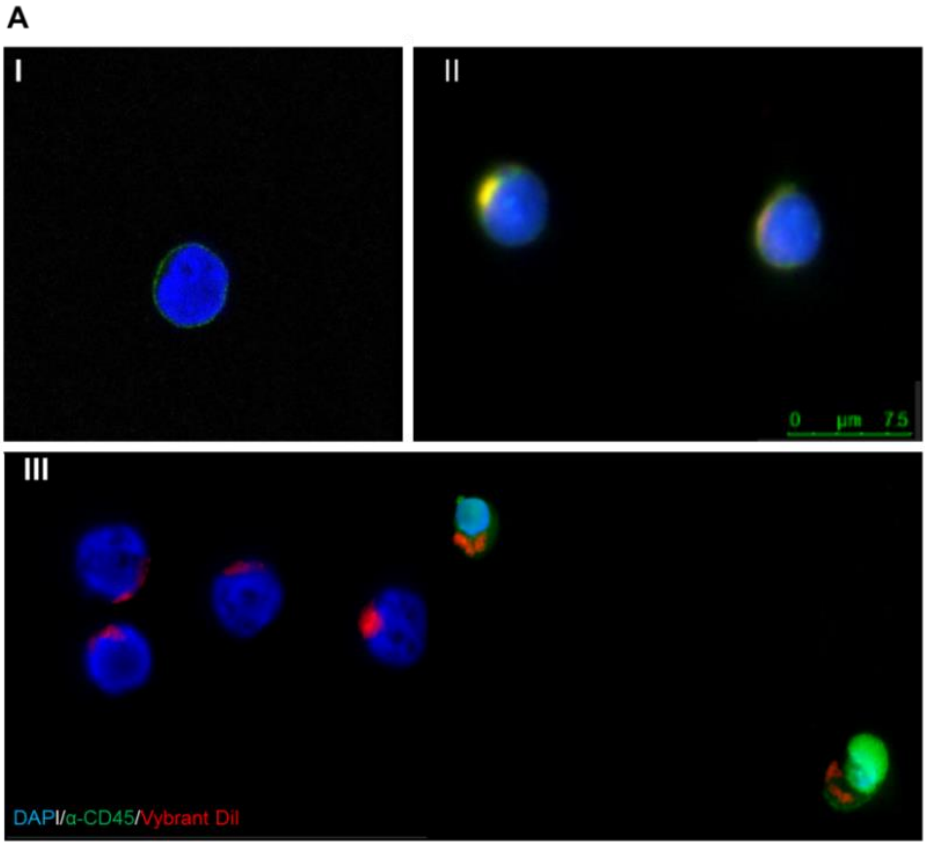

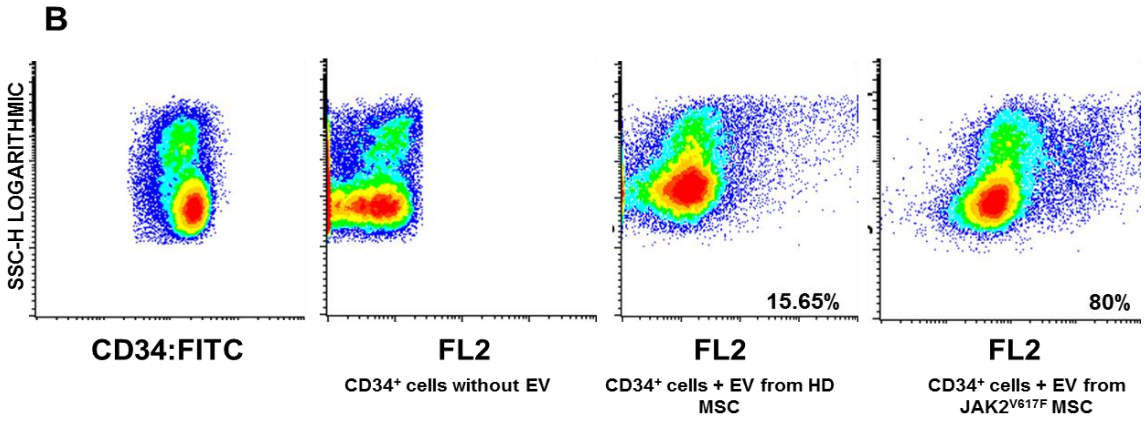

Figure 51: Incorporation of EV from JAK2^{V617F}-MSC and HD-MSC into CD34^{+} cells. (A) Representative images of EV previously libelled with Vybrant-Dil cell-labelling solution (red) that were incorporated into CD34^{+} cells and stained with anti-CD45 Ab (green). (I) CD34^{+} cells without EV, (II) CD34^{+} cells with EV from HD-MSC and (III) CD34^{+} cells co-cultured with EV from JAK2^{V617F}-MSC. (B) Images represent the CD34^{+} cells that were incubated with EV libelled with Vybrant Dil cell-labelling solution and evaluated 24 hours by FC

Since we verified the overexpression of miR-155 in the EV released from JAK2^{V617F}-MSC, we further examined the expression of this micro-RNA in the CD34^{+} cells after EV incorporation. CD34^{+} cells were isolated from BM of HD (n=2) and JAK2^{V617F} patients (n=2) and incubated with EV from HD-MSC and JAK2^{V617F}-MSC for 48 hours. The expression of miR-155 was higher in the CD34^{+} cells from myeloproliferative patients compared to CD34^{+} cells from HD.

The incorporation of EV from the different stroma sources increased the expression of miR-155 in the HD CD34^{+} cells (**Figure 52**), expression that became significantly higher after uptaking EV from JAK2^{V617F}-MSC ($p=0.04$), but not in CD34^{+} cells from JAK2^{V617F} patients.

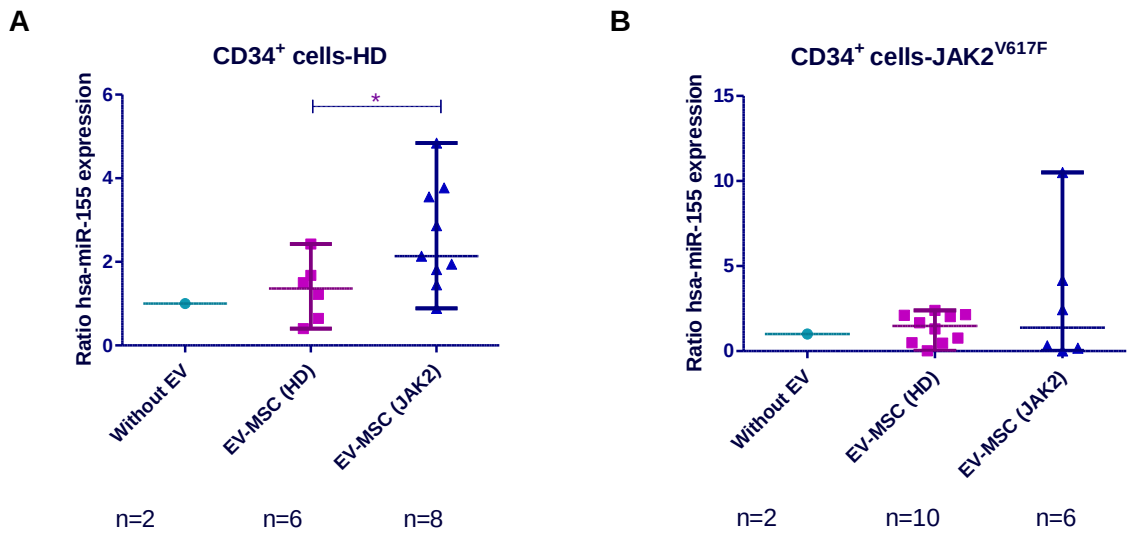

Figure 52: Levels of miR-155 by RT-PCR in BM CD34^{+} cells incubated with EV from BM-MSC. Variation of the miR-155 expression when CD34^{+} cells from BM of HD (A) and JAK2^{V617F} patients (B) were incubated with HD-EV and JAK2^{V617}-EV. RNU6B was used as an internal standard. Ratio was calculated dividing the each result from CD34^{+} cells with EV for CD34^{+} cells without EV. Results are expressed as medians and interquartile range. *p < 0.05

Subsequently the expression of miR-155 in HD-HPC and myeloproliferative haematopoietic progenitor cells after 48 hours co-culture (*transwell*) with BM-MSC (HD and JAK2) was analysed. The expression levels (**Figure 53**) of miR-155 in CD34^{+} cells (HD and JAK2^{V617F}) increased, when the HPC were co-cultured with JAK2-MSC, but did not reach significant differences.

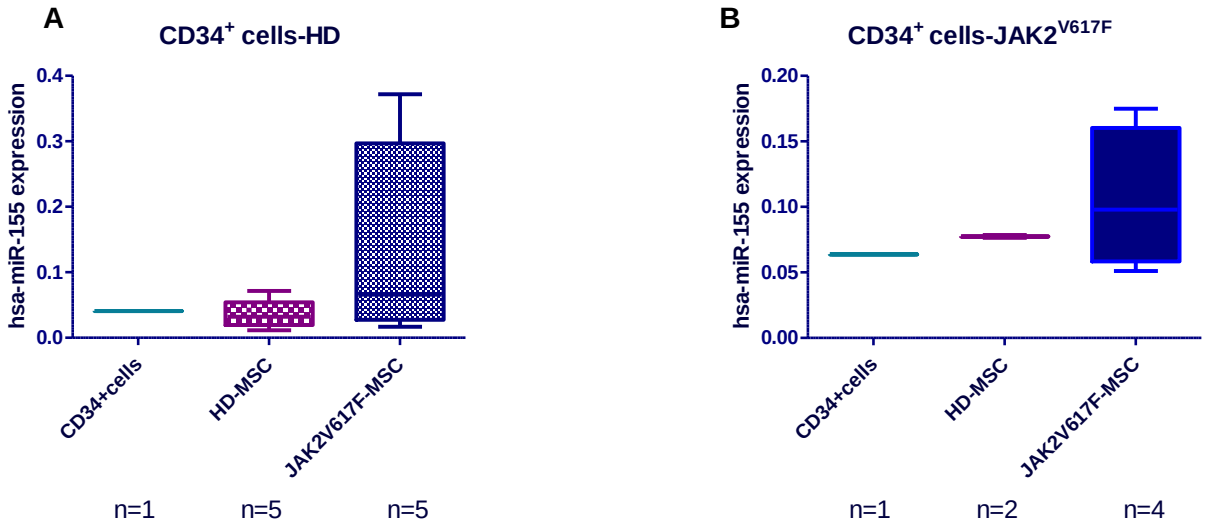

Figure 53: Levels of miR-155 were analysed by RT-PCR in BM CD34$^+$ cells co-cultured with BM-MSC. Variation of the miR-155 expression when CD34$^+$ cells from BM of HD (A) and JAK2^{V617F} patients (B) were co-cultured separated by 0.4µm micropore membranes (*transwell*) with HD-MSC and JAK2^{V617}-MSC. RNU6B was used as an internal standard. Results are expressed as medians and interquartile range.

2.4 Haematopoietic progenitor capacity evaluation after the uptake of EV from JAK2^{V617F}-MSC

Once we demonstrated that the incorporation of EV from JAK2^{V617F} increased the expression of miR-155, we analysed if the clonogenic capacity of CD34$^+$cells from HD and JAK2^{V617F} patients showed any variation. We observed (**Figure 55**) that in most cases there was an increase in the total number of CFU when the haematopoietic progenitors incorporated the EV. The incorporation of EV from JAK2-MSC was associated with a higher number of colonies in both groups (HD and patients). Results of specific subtypes of colonies are shown in **Figure 54**. We observed an increase in the number of BFU-e when the CD34$^+$ cells from an ET-patient (JAK2 mutated) incorporated EV from JAK2^{V617F}-MSC (2 ET and 1 PV).

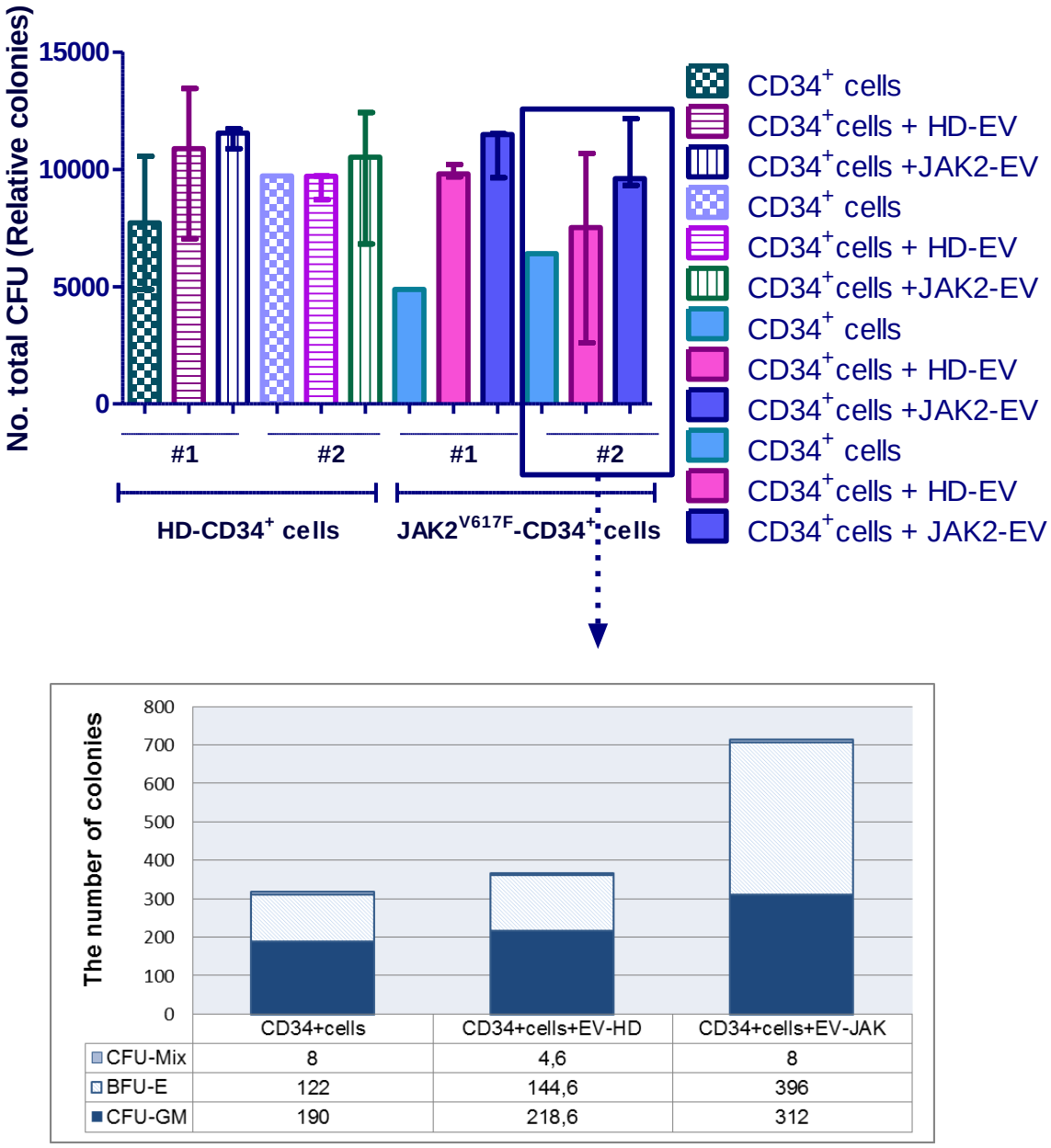

Figure 54: Clonogenic capacity after incorporation of EV from the stroma into HD and leukemic CD34$^+$ cells. Total colony-forming unit (CFU) from HD-CD34$^+$ cells and JAK2^{V617F}-CD34$^+$cells after 48h of culture with EV from HD-MSC and JAK2^{V617F}-MSC. The lower image represent the number of colonies (CFU-GM, BFU-e and CFU-Mix) from CD34$^+$cells without EV and incubated with EV from HD-MSC (n=3) and JAK2^{V617F}-MSC (n=3) of the case #2 (CD34$^+$ cells from a ET patient)

In order to normalise and compare the results, we analysed the ratio of CFU. This was calculated dividing the number of CFU from CD34$^+$ cells incubated with EV by the number of CD34$^+$

cells without EV. As shown in **Figure 55**, we observed a tendency to an increase in clonogenic production (p=0.056) of JAK2^{V617F}-CD34^{+} cells when incorporated EV from JAK2-MSC.

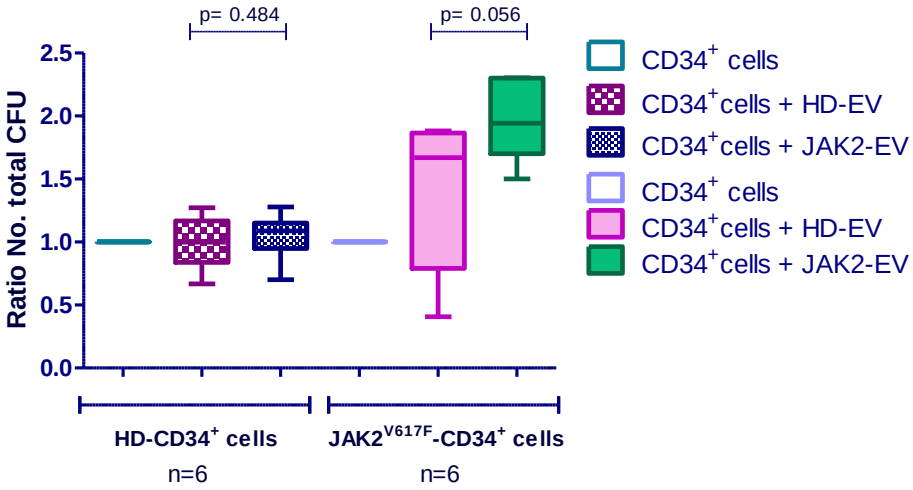

Figure 56: Clonogenic assays. Results are expressed as the ratio between the total CFU from CD34^{+}cells that were incubated with EV and CD34^{+} cells without EV.

To evaluate if the incorporation of the different EV modifies the viability of the progenitor haematopoietic cells, apoptosis assays were performed. As can be seen in the **Figure 56**, there was a decrease in the percentage of dead CD34^{+} cells in both groups (HD and JAK2) with the incorporation of EV from HD-MSC and JAK2^{V617F}-MSC, without differences between them.

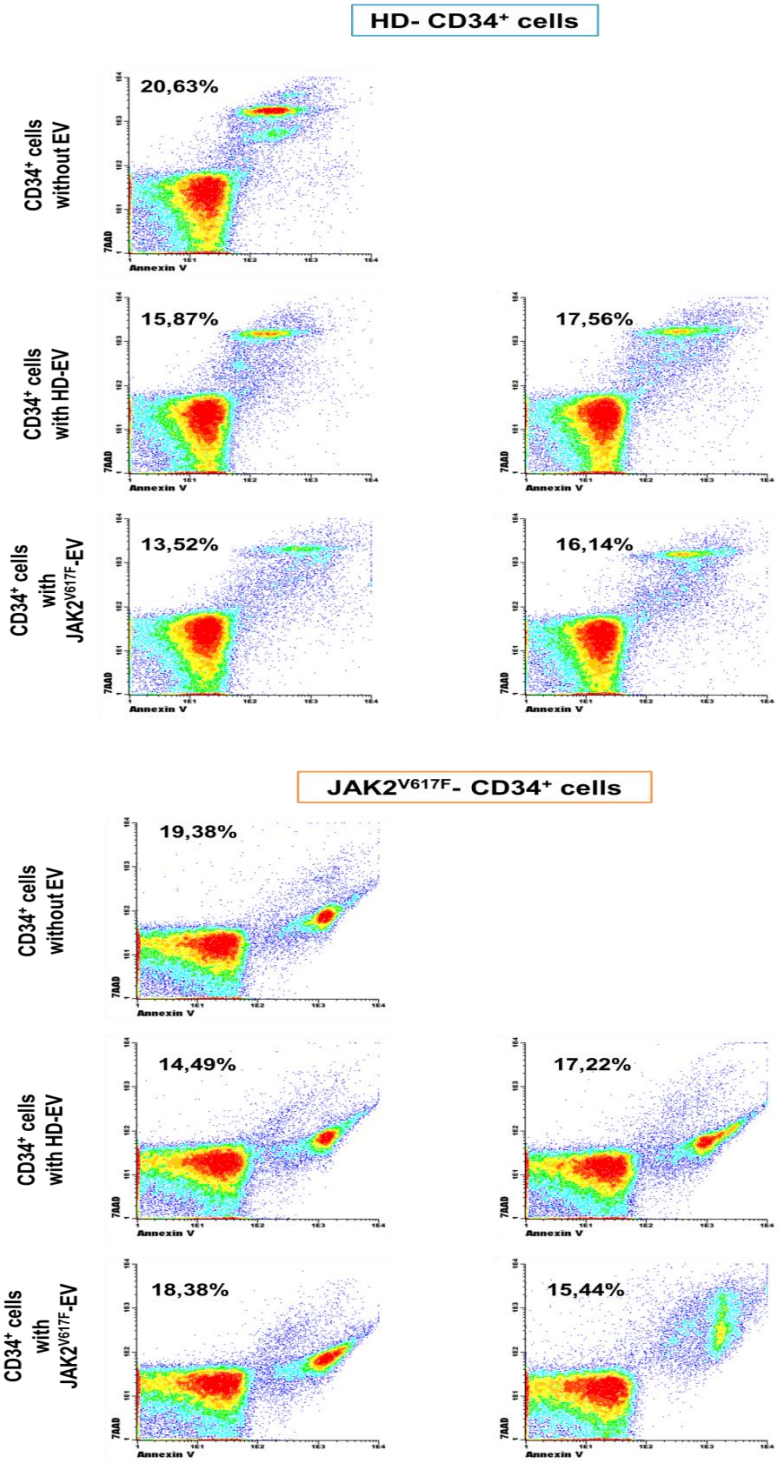

Figure 56: Flow Cytometry dot plot images. (left panel) Apoptosis of HD-CD34^{+} cells without EV and EV from HD-MSC and JAK2^{V617F}-MSC. The right panel represent the CD34^{+} cells from BM of MPN patients without EV and with HD-EV and JAK2^{V617F}-EV. (n=2 for each condition). The percentage showed represents the total of dead cells.

The notion that bone marrow stroma provides important cues for homing, quiescence, maintenance and proliferation of haematopoietic stem/progenitor cells has been well documented in recent years. Under pathological conditions (leukaemia), it has also been demonstrated that HSC niche is compromised.

Myeloproliferative neoplasms are a group of related haematological disorders characterised by the overproduction of mature blood cells. Depending on the predominant myeloid cell lineage in the peripheral blood, they can be classified in Polycythemia Vera (elevated red cell mass), Essential Thrombocythemia (elevated platelet numbers) and Primary Myelofibrosis (BM fibrosis). The most recurrent clonal mutation in MPN is $JAK2^{V617F}$, a point mutation that activates the JAK2 tyrosine kinase leading to a clonal proliferation without control. An increasing number of publications support the fact that the mutated HSC can modify the BM stroma, and these modifications create a positive feedback loop that plays an essential role in MPN progression. The interactions between mutant HSC and the BM create a vicious circle that blocks the maintenance of normal haematopoiesis, allowing the expansion and progression of MPN clones.

Aiming to put into place one more piece of this complicated puzzle, we focused this thesis in studying the genetic alterations in the BM-MSC from MPN, and the communications established between the stroma and the haematopoietic system, by means of the transference of biological material in nano-particles known as extracellular vesicles.

Characterisation of BM-MSC

With that aim, we started focusing in the characterisation of BM-MSC from $JAK2^{V617F}$ patients. We adopted the consensus criteria endorsed by the International Society for Cellular Therapy (ISCT) to characterise MSC from bone marrow of MPN patients and healthy donors *(Dominici, et al 2006)*. Regarding the proliferative and differentiation capabilities of MPN-MSC, we did not observe any glaring differences with HD-MSC, except for some cases of PV-MSC, which presented a higher proliferative capacity. These results are in agreement with previously published data *(Martinaud, et al 2015)*. However, some studies reported that MSC from PMF patients showed slower proliferation rate and reached senescence at earlier passages *(Avanzini, et al*

2014). The differences between their results and ours can be due to the fact that we isolated and characterised MSC from BM of patients where the fibrotic state was not established.

In order to analyse the differences in BM-MSC among all the MPN, we also characterised BM-MSC from chronic myeloid leukaemia (CML), using the same isolation methodology. The proliferative capacity of CML-MSC was reduced when compared to HD-MSC and MPN-MSC, as well as the capacity to differentiate into osteoblast and adipocyte. By contrast, other authors have previously reported that CML $Flk1^{+}CD31^{-}CD34^{-}$ MSC had morphology and proliferation capacity similar to controls *(Xishan, et al 2011)*, although, their immunomodulatory function was impaired, showing once again that these cells do not show a normal behaviour.

Regarding the immunophenotypic characterisation of MPN-MSC the CD90, CD73 and CD105, the typical MSC markers were positive in all cases and as expected they did not express haematopoietic markers. These results are in agreement with previous publications *(Lopez-Villar, et al 2009, Sanchez-Guijo, et al 2009)*. However, as previously stated in the results chapter, MIF expression from some molecules was different, increased for CD73, CD90 and CD44, and decreased for the adhesion molecule CD105 in MPN-MSC as compared to HD-MSC. Numerous studies have previously described discrepancies in the expression of these markers in the MSC from other haematological disorders *(Campioni, et al 2006, Chandran, et al 2015, Flores-Figueroa, et al 2005, Lopez-Villar, et al 2009)*. As far as we know, it is the first time that these differences have been observed, because few studies investigating the immunophenotypic expression of BM-MSC in MPN have been published. Only a brief report in 2014, reported no differences in the immunophenotype when compared to HD-MSC *(Avanzini, et al 2014)*. It should be stressed that in the present work, we not only observed differences compared to HD-MSC, but also observed that the expression of CD105 was higher in MSC from BM of patients JAK2-negative, when compared to those patients with JAK2 mutated, although differences did not reach statistical significance, probably because the low number of cases without JAK2 mutation. This warrants further studies to explain the impact of this adhesion molecule CD105 expression in the alterations of BM stroma in MPN. The endoglin CD105 is an important molecule in osteoblast and adipocyte differentiation process *(Levi, et al 2011)*.

In order to deep into the differences between MPN-MSC and HD-MSC, we performed functional and genomic studies in BM-MSC from both groups.

Because differences in proliferative capacity were observed in BM-MSC from our patients, cell cycle and apoptosis studies were carried out. No differences were observed in the cell cycle distribution. By contrast, we could ascertain that among MPN-MSC the percentage of apoptotic cells were decreased compared to HD-MSC, mainly in PV-MSC.

Genomic Studies

Gene expression arrays studies showed a differential expression pattern in PV-, ET- and CML-MSC when compared to HD-MSC. Specially, PV-MSC showed the highest number of overexpressed genes. Biological analysis showed that these genes are related to endoplasmic reticulum processing, protein transport and GTPase activity. These signal pathways are important in cell differentiation, organisation and dynamics of actin cytoskeleton, and cell migration *(Chung, et al 2014, Qu, et al 2016)*.

When specific differentially expressed genes were revised, we could ascertain that some of them could be involved in the pathophysiology of myeloid neoplasms, and two of them were selected for other studies: MYADM and HDAC8:

- MYADM is a gene involved in the process of haematopoiesis, being up-regulated during myeloid differentiation *(Pettersson, et al 2000, Wang, et al 2007)*. Thus, MYADM overexpression has been proposed as a marker of myeloid differentiation in myeloid leukaemic cells *(Wang, et al 2007).* We have observed an overexpression of MYADM in the BM-MSC obtained from ET, PV and CML patients, results that were subsequently confirmed by RT-PCR and WB assays. Furthermore, we also observed an increase of MYADM expression in BM-MSC from MPN Ph-negative/JAK2^{V617F} negative, suggesting that this gene is up regulated in the BM-MSC from MPN patients, independently of the clonal genomic alteration affecting the HSC. More work is warranted to understand the role of the overexpression of MYADM in the BM-MSC from patients with the full spectrum of MPN. MYADM is a MAL (myelin and lymphocyte) family protein, with eight transmembrane regions localised at the plasma membrane. Several lines of evi-

dence support a role for these proteins in events related to the reorganisation of membrane domains in response to extracellular signalling *(Anton, et al 2008, Aranda, et al 2011).* It is well know that membrane rafts are cholesterol-enriched ordered domains that regulate a plethora of signalling pathways, such as pro-inflammatory signals that can be activated by cytokines like TNF-α and IL-1β or bacterial ligands of Toll-like-receptors *(Muppidi, et al 2004, Oakley, et al 2009, Triantafilou, et al 2011).* As part of these endothelial surface rafts, MYADM has the capacity to regulate the connections between the plasma membrane and the cortical cytoskeleton, changing the migration capacity of these cells and controlling the endothelial inflammatory response *(Aranda, et al 2013).*

- The second selected gene was HDAC8, previously reports as implicated this gene in MPN development. In these studies, HDAC8 knockdown resulted in increased expression of the suppressor of cytokine signalling 1/3 (SOCS1/3), thus leading to a change in JAK2 signal, that translated in a reduced cell growth and clonogenic activity of haematopoietic cells derived from patients with MPN *(Chen, et al 2013, Gao, et al 2013)*.

In other to know whether this gene was overexpressed in BM-MSC from patients, we performed RT-PCR and WB assays. Among $JAK2^{V617F}$ positive samples, the group that presented the highest expression of this gene as well as the protein was ET-MSC. When we analysed PV-MSC samples, we also found significantly higher expression of HDAC8 as compared to HD-MSC. By contrast, when CML-MSC or JAK2 (negative)-MSC, unlike the results observed with MYADM, we could observe that HDAC8 was not overexpressed, suggesting that the overexpression of HDAC8 could be a characteristic feature of MPN ($JAK2^{V617F}$)-MSC.

Haematopoiesis support capacity

One of the most important functional properties of BM-MSC is their capacity to support haematopoiesis. One of our objectives was to analyse whether BM-MSC from MPN-patients maintain this capacity similar to normal BM-MSC. Two set of experiments were performed: firstly we analysed the capacity of BM-MSC to promote clonogenic growth of HPC. Curiously, we observed that BM-MSC from patients increased the number of colonies derived from $JAK2^{V617F}$ haemato-

poietic progenitor cells. Results from other groups have suggested that malignant stroma promotes the survival and proliferation of mutated haematopoietic progenitor cells *(Schepers, et al 2015, Schepers, et al 2013)*. Secondly, we assessed MPN-MSC capacity to maintain HD-HPC in a long-term culture system. Although we did not observe differences in the total number of CFU-GM produced. During the weekly evaluation of the number of colonies produced, a significantly higher number of CFU-GM were obtained at third and fourth weeks for the HD-HPC that were co-cultured with JAK2-MSC.

Previous studies in this setting have shown contradictory results. There are some reports describing a severely compromised ability to maintain HD-HSC in MPN-expanded osteoblasts and in human MSC from patients with classical Philadelphia-negative MPN (with or without the mutation $JAK2^{V617F}$) *(Avanzini, et al 2014, Schepers, et al 2013)*. Conversely, others have indicated that MPN-MSC exhibit a similar long-term haematopoiesis support ability compared to HD-MSC *(Martinaud, et al 2015)*.

Results from the present work suggest that BM-MSC from patients promote higher cell growth, preferentially in clonal HPC. In order to analyse which mechanism could be involved in this increased functional capacity, we analysed the expression of some genes known to be directly or indirectly related with haematopoiesis support.

The first selected gene was CXCL12. This protein is required for haematopoietic stem-cell maintenance in early mesenchymal progenitor cells. In MPN, decreased expression of CXCL12 by osteoblasts or by $Nestin^{+}$ cells has been associated to enhanced the mobilisation and loss of normal HSC *(Arranz, et al 2014, Greenbaum, et al 2013, Krause, et al 2014)*. We did not observe differences in CXCL12 expression by RT-PCR between HD and MPN-MSC. However, using immunofluorescence studies, we observed a decrease in the expression of this protein in the MPN-MSC, showing that our results are in agreement with data from other authors.

The expression of TP53 in MSC has been recognised as a negative regulator factor during osteogenic differentiation. It has also been described as an inhibitor of MSC migration in response to tumour cells, in conjunction with a decrease in CXCL12 *(Lin, et al 2013, Velletri, et al 2016).*

In the present work we did not observe significant differences in the expression of TP53 in the

BM-MSC and BM-MNC from the patients (JAK2^{V617F}) compared to the control group (HD). Because a high amplitude in the results from BM-MSC was observed, ranging from high to low TP53 expression, correlation studies were performed. Interestingly, we found a significant inverse correlation between TP53 expression in the BM-MSC and the percentage of JAK2^{V617F} mutation in MNC, with lower TP53 expression in ET-MSC associated to higher percentages of JAK2 mutation. In the PV-MSC this correlation was not observed. However, it should be taken into account the low number of cases (n=4), and the higher allele burden (>50% JAK2^{V617F}) in MNC-PV patients.

Other genes related to haematopoiesis support were also analysed. A decrease in the expression of ANGPT1 and an increase of NF-KB and THPO expression in MPN-MSC were observed. ANGPT1 is a gene that regulates angiogenesis, which in the haematopoiesis context it has been associated with the induction of quiescence in HSC through the interaction with the Tie-2 (CD90) receptor, increasing the adhesion of HSC to osteoblasts in the BM *(Arai, et al 2004)*. The nuclear factor (ƙB) is an important rapid acting transcription factor found in all cell types. In MSC, NF-ƙB induces the expression of other factors such as VEGF, FGF2 and HGF, which are involved in cellular response to stress, inducing the proliferation, migration and differentiation *(Chang, et al 2013)*. Recent studies reported that BM-MSC from leukaemic patients express NF-ƙB at higher levels than normal BM-MSC *(Jacamo, et al 2014)*. They also showed that the activation of NF-ƙB signalling can be induced by the leukemic cell, playing a pivotal role in the development of leukaemia chemoresistance. Other important HSC-maintenance transcription factor, THPO, was also differentially expressed in the BM-MSC from MPN patients. THPO is a very important cytokine in the regulation of megakaryocyte development and platelet production, and it is also involved in the regulation of HSC survival and proliferation *(Qian, et al 2007)*. THPO/ MPL signalling is involved in the HSC niche regulation, maintaining the LT-HSC in quiescence state on the osteoblastic niche *(Yoshihara, et al 2007)*. In the study reported by Schepers, they identified the role of THPO and CCL3 by which leukemic myeloid cells stimulate MSC to overproduce osteoblasts during BM remodelling in the MPN development *(Schepers, et al 2013)*.

During the last years, it has been discussed how leukemic haematopoiesis could affect the BM-stroma to create a self-reinforcing leukemic niche that promotes leukaemia progression, while negatively affecting normal HSC function. Our findings in the present work show a deregulated expression profile affecting some genes involved in HSC maintenance. In contrast to what has been reported, a profound deregulation of these genes was found in the MSC from patients with PMF, where the fibrotic state it is well established. In our study, the majority of MSC were isolated from BM of MPN at diagnosis, suggesting that during MPN evolution there are genetic alterations involving BM-MSC, which likely influence the disease behaviour. It will be interesting to follow up the expression of these genes, and to study if they change during disease progression.

HDAC8: A new therapeutic target?

As opposed to what happens with CML, therapeutic strategies for the classic Philadelphia-Negative MPN are currently limited. JAK inhibitors ameliorate symptoms and reduce splenomegaly, but cannot control the disease burden. Given the limitation of JAK inhibition as monotherapy *(Kaplan, et al 2016)*, novel treatment strategies are needed.

Post-translational protein modifications such as acetylation or methylation plays an important role during epigenetic regulation *(Wolfson, et al 2013)*. Histone deacetylases (HDACs) have gained particular interest as potential targets for novel therapeutic drugs in cancer. HDACs not only are involved in deacetylation of chromatin that can regulate gene-transcription regulation, but also are involved in the deacetylation of non-histone protein, which regulate cellular homeostasis (cell-cycle, differentiation and apoptosis)*(Minucci and Pelicci 2006)*. Eighteen mammalian HDACs enzymes have been identified so far, which can be subdivided into two classes, according to their homology.

An increase in HDAC activity has been shown to be elevated in PMF patients compared to other MPN patients and healthy donors. Results from a small cohort of MF patients (n=17) had showed aberrant HDAC expression profile in their $CD34^+$ cells when compared to controls, with

heterogeneous alterations in HDAC subgroups, mainly in HDAC1, 2, 8 and class II HDACs, which were upregulated, whereas HDAC4 and 5 were downregulated *(Wang, et al 2008)*.

HDAC inhibitors (HADCi) induce a complex cellular response involving both transcriptional and posttranscriptional modulation *(Falkenberg and Johnstone 2014)*. Two pan-HDACi are currently under clinical investigations. Panobinostat induced dose-dependent apoptosis of HEL cells (JAK2^{V617F}) by inhibiting the autophosphorylation and expression levels of JAK2^{V617F}, which is followed by a reduced phosphorylation of STAT3, STAT5, ERK1/2 and AKT proteins *(Wang, et al 2009)*. The tolerability of this pan-inhibitor in two *in vivo* studies, allowed the establishment of a phase Ib trial using the combination of a JAK2 specific inhibitor (TG101209) with panobinostat in MPN patients *(Evrot, et al 2013)*.

The other agent also under investigation is the pan-HDACi vorinostat, which has also the capacity to reduce the proliferation and to increase the apoptosis of HEL cells. Cardoso *et al.*, have recently confirmed that the combination of vorinostat and ruxolitinib inhibited the differentiation, induced apoptosis and decreased reactive oxygen species production in MPN-cell lines and primary MPN samples *(Cardoso, et al 2015)*. The authors also highlighted that these effects were attenuated in the presence of the HS-5 marrow stromal cells, by the up-regulation of antiapoptotic genes and pro-survival pathways (PI3K-AKT). These results show how bone-marrow niche can protect MPN cells from apoptosis of HDACi or JAK2i *(Cardoso, et al 2015).*

Importantly, the most significant side effects of these pan-HDACi are those related with myelotoxicity, that were thrombocytopenia, neutropenia and anaemia *(Mottamal, et al 2015)*.

Given the seemingly low therapeutic index of HDACis with associated toxicity, and considering our initial observation of the increased expression of HDAC8 characteristically in MSC-MPN JAK2^{V617F,} we decided to further investigate the effects of HDAC8 inhibition with a specific inhibitor PCI34051. HDAC8 is a class I histone deacetylase, which has emerged as an attractive target for drug development in cancer. It has been demonstrated that the overexpression of these protein in multiple tumour types, including neuroblastoma, glioma and childhood acute lymphoblastic leukaemia, where the use of isoform-specific or selective HDAC8i showed relevant therapeutic results.

We found that HDAC8 mRNA expression is selectively higher in BM-MSC from MPN-JAK2^{V617F} patients, compared to other MPN. Furthermore, we studied the impact in the BM-MSC the inhibition of HDAC8 using a selective inhibitor, PCI34051. This compound was demonstrated to induce caspase-dependent apoptosis in cell lines derived from T-cell lymphomas *(Balasubramanian, et al 2008)*.

In a set of experiments, we inhibited the expression of HDAC8 in the MPN-MSC using this specific HADC8i. We observed a decrease in cell proliferation, which was followed by an increase in apoptosis of BM-MSC from JAK2^{V617F} treated samples. Nevertheless, in BM-MSC from HD, treatment with PCI34051 did not induce significant apoptosis. These data suggests that the PCI34051 acts specifically in neoplastic BM-MSC, likely due to the overexpression of HDAC8 in these cells.

Then, we studied the impact of HDAC8 inhibition in one of the main functions of BM-MSC, which is the capacity to support haematopoiesis. After treating BM-MSC from HD and MPN-JAK2^{V617F} with PCI34051, we performed co cultures with MNC and HPC from HD and MPN patients. We observed that MPN-MSC treated with PCI34051 enhanced the apoptosis of JAK2^{V617F}-MNC, and decrease their clonogenic capacity. Our data suggest that PCI34051 treatment is able to reverse the advantageous effect conferred by neoplastic-MSC in MPN haematopoiesis maintenance. Studies over the past few years have shown that class 1 HDACs, as HDAC8, are involved in regulation or suppression of gene expression, which can be subject to modulation by intra and extracellular signals *(Qi, et al 2015)*. Then, we assessed the effects of HDAC8 inhibition in the JAK2^{V617F}-MSC when co-cultured with HPC. Similarly, we observed a decrease in MPN-CD34^{+} cell viability and a decrease in CFU-GM formation. By contrast, no significant changes in HD-HPC viability and CFU-GM formation were observed. The observed results could be related to the increase (without significant differences) in TP53 expression, when the JAK2^{V617F}-MNC were co cultured with MPN-MSC previously treated with HDAC8i.

The performed *in vitro* culture model was based on the inhibition of HDAC8 expression in the BM-MSC from MPN patients, and the effects in the maintenance of the normal and pathologic haematopoiesis. We then planned to study if the previously described effects were maintained,

when MPN-cell lines (haematopoietic component) and MPN-MSC were treated with HDAC8i simultaneously. A decrease in the viability of HEL, SET-2 and UKE-1 (all $JAK2^{V617F}$ cell lines) was shown when treated with PCI34051, which was increased when co-cultured with MPN-MSC. An increase in the apoptosis of these MPN cell lines was associated to a decrease in colony-formation and to a decrease in pSTAT5. $JAK2^{V617F}$ mutation in haematopoietic stem and progenitor cells confers hypersensitivity to cytokines, which leads to a constitutive JAK2 tyrosine kinase signalling. The activated signalling activates downstream pathways, in particular the phosphorylation of transcription factors STAT3 and STAT5 *(Vu, et al 2016)*. Previous studies have demonstrated that STAT5 loss prevents the development of $JAK2^{V617F}$-induced MPN and is dispensable in normal haematopoiesis *(Yan, et al 2012)*.

Finally, the current findings provide possible new pathways to understand the biological role of BM-MSC in the pathophysiology of MPN-$JAK2^{V617F}$. MPN-MSC display different proliferative rate, immunophenotype expression (CD105) and gene expression profile with HDAC8 overexpression. The inhibition of HDAC8 expression by its specific inhibitor decreases the capacity of the BM-stroma to support MPN haematopoiesis, suggesting that HDAC8 may be a potential therapeutic target in this setting (**Figure 58**).

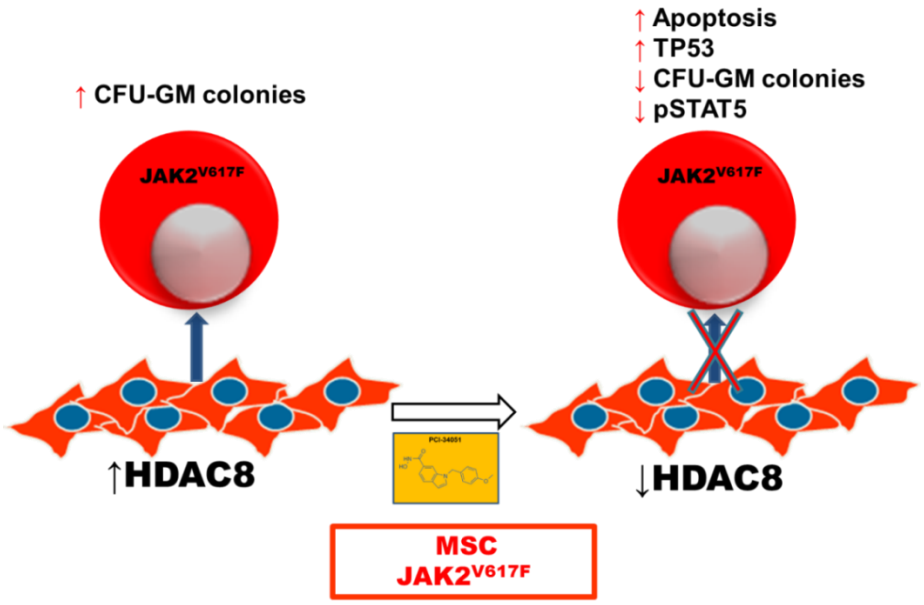

Figure 58: Schematic effects of PCI34051 treatment in MPN-MSC.

Having comprehensively characterised BM-MSC from human MPN patients with the mutation in $JAK2^{V617F}$, and described a new therapeutic target, HDAC8, our data support the idea that the treatment *in vitro* with a specific compound is capable of inhibiting leukemic stem cells, but not normal haematopoietic or stromal cells. Therefore, *in vivo* studies will be required to demonstrate the action of HDAC8i in MPN context. Murine studies of neuroblastoma have demonstrated that the selective inhibition of HDAC8 exhibits antineuroblastoma activity, inducing cell cycle arrest and differentiation, without toxicity *(Rettig, et al 2015)*.

Extracellular Vesicles from BM-MSC

The last aim in our investigation was to explore the crosstalk between neoplastic stroma and HPC, by analysing the role of extracellular vesicles. In recent years, it has been recognised the importance of tumour microenvironment for cancer progression *(Raimondo, et al 2015).* The bidirectional signals established between both compounds are crucial in maintaining tissue architecture, control of cell growth and differentiation. *In vivo* models have hypothesised that incorrect signals from the microenvironment may lead to a destabilisation in haematopoiesis homeostasis, enabling the initiation/promotion of normal cells to malignant *(Bissell and Hines 2011, Muralidharan-Chari, et al 2010)*. In myelodysplastic syndromes we have shown that microvesicles from MSC of these patients change HPC properties, modifying the expression of important genes (MDM2 and TP53), and increasing their clonogenic capacity *(Muntion, et al 2016).* Recently we also have shown that CML cells derived EV, which carry the transcript BCR-ABL that can be incorporated in endothelial cells, leading to the expression of the oncogene and oncoprotein in these cells *(Ramos, et al 2015)*. Other studies showed that the transference of the BCR-ABL gene from CML-derived EV to neutrophils may provide *in vivo* transformation of normal cells *(Cai, et al 2014)*.

In the present work, we hypothesised that EV released by the BM-MSC from MPN could be involved in the progression of the mutated HPC. To assess this intercellular communication system, we obtained and characterised EV from MSC from MPN patients and HD. EV can be isolated by different methods, and their characterisation in most experiments is based on their

structure/morphology or on the tetraspanin expression. In this study, we observed that EV from MPN-MSC presented their characteristic morphology (TEM), expressed the typical tetraspanin CD63 and had a size around 137 nm (NTA). Furthermore, we also characterised the EV from MPN-MSC by MFC, that were defined as particles less than 0.9µm, positive for the human MSC markers (CD90, CD44 and CD73) and negative for CD34 and CD45 (haematopoietic markers). No differences were observed between EV from HD and MPN MSC, but MPN-MSC released higher quantity of EV.

In addition, we studied the microRNA cargo of EV released from MSC of both groups (HD and JAK2^{V617F}). Although no significant differences were found, we observed an overall increase of microRNA expression in the EV released by MPN-MSC. Since increased evidence suggests the involvement of the miR-155 in numerous biological processes, including haematopoiesis and inflammation, it was selected for further studies. It has been previously shown that transient induction of miR-155 in mouse bone marrow induced granulocyte/monocyte expansion with features characteristic of myeloid neoplasia *(O'Connell, et al 2008).* It has also been shown that the overexpression of miR-155-5p results in the downregulation of JARID2, contributing to megakaryocyte hyperplasia characterized in PMF patients *(Norfo, et al 2014)*. Other study also showed a relationship between miR-155 and MPN, where the loss of the Notch/RBPJ (a non-redundant downstream effector of the canonical Notch signalling cascade) axis increased the over-expression of miR-155 and induced a persistent proinflammatory state of the BM niche leading to a myeloproliferative-like disease (Carter, *et al* 2016). All these features point to a role of this microRNA into MPN pathophysiology. The overexpression of miR-155 in the BM-MSC-derived EV from MPN patients suggest that this microRNA could play a role in the development or in the maintenance of clonal progenitors.

In order to verify this hypothesis, incorporation assays were carried out. We observed that the incorporation of EV from MPN-MSC increased the expression of the miR-155 in the HD-CD34^{+} cells. However, when the incorporation analysis was performed in HPC JAK2^{V617F} an increase of miR-155 was not observed, probably because these cells show a high expression of this microRNA.

We found that EV from MPN-MSC increased the clonogenic capacity of MPN-CD34$^+$ cells, with an increase not only in CFU-GM but also BFU-e, but this increase was not observed when the recipient was HD-CD34$^+$ cells. These results suggest that these structures act as a survival mechanism selectively for MPN haematopoietic progenitor cells.

As far as we know, this is the first time that it has been shown that EV can act as intercellular mediators between HPC from MPN patients and BM-MSC, showing once again the important role that microenvironment can have in these disorders. More research is warranted to scrutinize other mechanisms that could be involved in this interplay.

1. Regarding the characterisation of BM-MSC from MPN patients with JAK2 (JAK2^{V617F}) mutation, we observed:

1.1 BM-MSC from MPN patients displayed the characteristic fibroblastic-like morphology with similar proliferation rate compared to HD-MSC.

1.2 Cell surface immunophenotype of BM-MSC from MPN patients were in accordance to the criteria established by the international Society of Cellular Therapy. However, a higher expression of CD90 with a decrease of CD105 expression was observed.

1.3 BM-MSC from MPN patients displayed similar *in vitro* ability to differentiate into osteoblasts and adipocytes compared to HD-MSC.

2. Regarding the functional and genomic alterations of *in vitro*-cultured BM-MSC from MPN with JAK2^{V617F} mutation:

2.1 MPN-MSC showed lower apoptosis compared to HD-MSC, without differences in their cell cycle.

2.2 BM-MSC from MPN patients showed alterations in their gene expression profile compared to HD-MSC and, MSC from PV patients was the entity with more over-expressed genes.

2.3 Confirming gene expression by RT-PCR showed higher expression of two genes, MYADM and HDAC8 in the BM-MSC from MPN patients. HDAC8 overexpression was shown to be specific of BM-MSC of JAK2^{V617F} patients.

2.4 MPN-MSC selectively protected myeloproliferative haematopoiesis, increasing their clonogenic capacity *in vitro*.

2.5 BM-MSC from MPN patients showed similar capacity, compared to HD-MSC, to maintain HD-CD34^{+}cells in long-term BM culture assays.

2.6 MPN-MSC showed a deregulation of genes involved in haematopoiesis regulation, with a decrease of Angiopoetin-1 and an increase of NF-ƙB and THPO expression.

2.7 The inhibition of HDAC8 expression by its specific inhibitor (PCI34051) decreases the capacity of the MPN stroma to support haematopoietic cells from MPN patients, suggesting that HDAC8 may be a potential therapeutic target in this setting.

3. Regarding the biological properties of extracellular vesicles released by BM-MSC from MPN patients and the role in the pathophysiology of this diseases:

3.1 EV derived from MPN-MSC isolated by ultracentrifugation displayed the EV characteristic described by the International Society of Extracellular Vesicles, with a size < 1µm, round morphology and the expressing of the tetraspanin CD63.

3.2 EV released by MPN-MSC were defined by flow cytometry, as particles less than 1µm, positive for human MSC markers (CD90, CD44 and CD73), for EV markers (CD81 and CD63) and negative for haematopoietic markers (CD45 and CD34).

3.3 Results from microRNA arrays did not show differences in the microRNA cargo of EV released by HD and MPN-MSC.

3.4 RT-PCR showed an overexpression of miR-155 in the BM-MSC-derived EV from MPN patients when compared to EV from HD-MSC.

3.5 The incorporation of EV from MPN-MSC in HD-$CD34^+$ cells increases the expression of miR-155 in these cells.

3.6 Clonogenic capacity is enhanced when $CD34^+$ cells from patients with the JAK2 mutation incorporate EV from MPN-MSC.

Abkowitz, J.L., Linenberger, M.L., Newton, M.A., Shelton, G.H., Ott, R.L. & Guttorp, P. (1990) Evidence for the maintenance of hematopoiesis in a large animal by the sequential activation of stem-cell clones. *Proc Natl Acad Sci U S A,* **87,** 9062-9066.

Adams, G.B., Chabner, K.T., Alley, I.R., Olson, D.P., Szczepiorkowski, Z.M., Poznansky, M.C., Kos, C.H., Pollak, M.R., Brown, E.M. & Scadden, D.T. (2006) Stem cell engraftment at the endosteal niche is specified by the calcium-sensing receptor. *Nature,* **439,** 599-603.

Anton, O., Batista, A., Millan, J., Andres-Delgado, L., Puertollano, R., Correas, I. & Alonso, M.A. (2008) An essential role for the MAL protein in targeting Lck to the plasma membrane of human T lymphocytes. *J Exp Med,* **205,** 3201-3213.

Arai, F., Hirao, A., Ohmura, M., Sato, H., Matsuoka, S., Takubo, K., Ito, K., Koh, G.Y. & Suda, T. (2004) Tie2/angiopoietin-1 signaling regulates hematopoietic stem cell quiescence in the bone marrow niche. *Cell,* **118,** 149-161.

Aranda, J.F., Reglero-Real, N., Kremer, L., Marcos-Ramiro, B., Ruiz-Saenz, A., Calvo, M., Enrich, C., Correas, I., Millan, J. & Alonso, M.A. (2011) MYADM regulates Rac1 targeting to ordered membranes required for cell spreading and migration. *Mol Biol Cell,* **22,** 1252-1262.

Aranda, J.F., Reglero-Real, N., Marcos-Ramiro, B., Ruiz-Saenz, A., Fernandez-Martin, L., Bernabe-Rubio, M., Kremer, L., Ridley, A.J., Correas, I., Alonso, M.A. & Millan, J. (2013) MYADM controls endothelial barrier function through ERM-dependent regulation of ICAM-1 expression. *Mol Biol Cell,* **24,** 483-494.

Arranz, L., Sanchez-Aguilera, A., Martin-Perez, D., Isern, J., Langa, X., Tzankov, A., Lundberg, P., Muntion, S., Tzeng, Y.S., Lai, D.M., Schwaller, J., Skoda, R.C. & Mendez-Ferrer, S. (2014) Neuropathy of haematopoietic stem cell niche is essential for myeloproliferative neoplasms. *Nature,* **512,** 78-81.

Asada, N., Katayama, Y., Sato, M., Minagawa, K., Wakahashi, K., Kawano, H., Kawano, Y., Sada, A., Ikeda, K., Matsui, T. & Tanimoto, M. (2013) Matrix-embedded osteocytes regulate mobilization of hematopoietic stem/progenitor cells. *Cell Stem Cell,* **12,** 737-747.

Avanzini, M.A., Bernardo, M.E., Novara, F., Mantelli, M., Poletto, V., Villani, L., Lenta, E., Ingo, D.M., Achille, V., Bonetti, E., Massa, M., Campanelli, R., Fois, G., Catarsi, P., Gale, R.P., Moretta, A., Aronica, A., Maccario, R., Acquafredda, G., Lisini, D., Zecca, M., Zuffardi, O., Locatelli, F., Barosi, G. & Rosti, V. (2014) Functional and genetic aberrations of in vitro-cultured marrow-derived mesenchymal stromal cells of patients with classical Philadelphia-negative myeloproliferative neoplasms. *Leukemia,* **28,** 1742-1745.

Bakker, S.T. & Passegue, E. (2013) Resilient and resourceful: genome maintenance strategies in hematopoietic stem cells. *Exp Hematol,* **41,** 915-923.

Balasubramanian, S., Ramos, J., Luo, W., Sirisawad, M., Verner, E. & Buggy, J.J. (2008) A novel histone deacetylase 8 (HDAC8)-specific inhibitor PCI-34051 induces apoptosis in T-cell lymphomas. *Leukemia,* **22,** 1026-1034.

Barbui, T., Thiele, J., Vannucchi, A.M. & Tefferi, A. (2015) Rationale for revision and proposed changes of the WHO diagnostic criteria for polycythemia vera, essential thrombocythemia and primary myelofibrosis. *Blood Cancer J,* **5,** e337.

Baxter, E.J., Scott, L.M., Campbell, P.J., East, C., Fourouclas, N., Swanton, S., Vassiliou, G.S., Bench, A.J., Boyd, E.M., Curtin, N., Scott, M.A., Erber, W.N. & Green, A.R. (2005) Acquired mutation of the tyrosine kinase JAK2 in human myeloproliferative disorders. *Lancet,* **365,** 1054-1061.

Bissell, M.J. & Hines, W.C. (2011) Why don't we get more cancer? A proposed role of the microenvironment in restraining cancer progression. *Nat Med,* **17,** 320-329.

Blau, O., Baldus, C.D., Hofmann, W.K., Thiel, G., Nolte, F., Burmeister, T., Turkmen, S., Benlasfer, O., Schumann, E., Sindram, A., Molkentin, M., Mundlos, S., Keilholz, U., Thiel, E. & Blau, I.W. (2011) Mesenchymal stromal cells of myelodysplastic syndrome and acute myeloid leukemia patients have distinct genetic abnormalities compared with leukemic blasts. *Blood,* **118,** 5583-5592.

Blau, O., Hofmann, W.K., Baldus, C.D., Thiel, G., Serbent, V., Schumann, E., Thiel, E. & Blau, I.W. (2007) Chromosomal aberrations in bone marrow mesenchymal stroma cells from patients with myelodysplastic syndrome and acute myeloblastic leukemia. *Exp Hematol,* **35,** 221-229.

Brandt, J.E., Bartholomew, A.M., Fortman, J.D., Nelson, M.C., Bruno, E., Chen, L.M., Turian, J.V., Davis, T.A., Chute, J.P. & Hoffman, R. (1999) Ex vivo expansion of autologous bone marrow CD34(+) cells with porcine microvascular endothelial cells results in a graft capable of rescuing lethally irradiated baboons. *Blood,* **94,** 106-113.

Buors, C., Douet-Guilbert, N., Morel, F., Lecucq, L., Cassinat, B. & Ugo, V. (2012) Clonal evolution in UKE-1 cell line leading to an increase in JAK2 copy number. *Blood Cancer J,* **2,** e66.

Cai, J., Wu, G., Tan, X., Han, Y., Chen, C., Li, C., Wang, N., Zou, X., Chen, X., Zhou, F., He, D., Zhou, L., Jose, P.A. & Zeng, C. (2014) Transferred BCR/ABL DNA from K562 extracellular vesicles causes chronic myeloid leukemia in immunodeficient mice. *PLoS One,* **9,** e105200.

Calvi, L.M., Adams, G.B., Weibrecht, K.W., Weber, J.M., Olson, D.P., Knight, M.C., Martin, R.P., Schipani, E., Divieti, P., Bringhurst, F.R., Milner, L.A., Kronenberg, H.M. &

Scadden, D.T. (2003) Osteoblastic cells regulate the haematopoietic stem cell niche. *Nature,* **425,** 841-846.

Calvi, L.M., Bromberg, O., Rhee, Y., Weber, J.M., Smith, J.N., Basil, M.J., Frisch, B.J. & Bellido, T. (2012) Osteoblastic expansion induced by parathyroid hormone receptor signaling in murine osteocytes is not sufficient to increase hematopoietic stem cells. *Blood,* **119,** 2489-2499.

Campioni, D., Moretti, S., Ferrari, L., Punturieri, M., Castoldi, G.L. & Lanza, F. (2006) Immunophenotypic heterogeneity of bone marrow-derived mesenchymal stromal cells from patients with hematologic disorders: correlation with bone marrow microenvironment. *Haematologica,* **91,** 364-368.

Cardoso, B.A., Belo, H., Barata, J.T. & Almeida, A.M. (2015) The Bone Marrow-Mediated Protection of Myeloproliferative Neoplastic Cells to Vorinostat and Ruxolitinib Relies on the Activation of JNK and PI3K Signalling Pathways. *PLoS One,* **10,** e0143897.

Carrancio, S., Blanco, B., Romo, C., Muntion, S., Lopez-Holgado, N., Blanco, J.F., Brinon, J.G., San Miguel, J.F., Sanchez-Guijo, F.M. & del Canizo, M.C. (2011) Bone marrow mesenchymal stem cells for improving hematopoietic function: an in vitro and in vivo model. Part 2: Effect on bone marrow microenvironment. *PLoS One,* **6,** e26241.

Carrancio, S., Lopez-Holgado, N., Sanchez-Guijo, F.M., Villaron, E., Barbado, V., Tabera, S., Diez-Campelo, M., Blanco, J., San Miguel, J.F. & Del Canizo, M.C. (2008) Optimization of mesenchymal stem cell expansion procedures by cell separation and culture conditions modification. *Exp Hematol,* **36,** 1014-1021.

Carter, B.Z., Mak, P.Y., Chen, Y., Mak, D.H., Mu, H., Jacamo, R., Ruvolo, V., Arold, S.T., Ladbury, J.E., Burks, J.K., Kornblau, S. & Andreeff, M. (2016) Anti-apoptotic ARC protein confers chemoresistance by controlling leukemia-microenvironment interactions through a NFkappaB/IL1beta signaling network. *Oncotarget*.

Casanova-Acebes, M., Pitaval, C., Weiss, L.A., Nombela-Arrieta, C., Chevre, R., N, A.G., Kunisaki, Y., Zhang, D., van Rooijen, N., Silberstein, L.E., Weber, C., Nagasawa, T., Frenette, P.S., Castrillo, A. & Hidalgo, A. (2013) Rhythmic modulation of the hematopoietic niche through neutrophil clearance. *Cell,* **153,** 1025-1035.

Chandran, P., Le, Y., Li, Y., Sabloff, M., Mehic, J., Rosu-Myles, M. & Allan, D.S. (2015) Mesenchymal stromal cells from patients with acute myeloid leukemia have altered capacity to expand differentiated hematopoietic progenitors. *Leuk Res,* **39,** 486-493.

Chang, J., Liu, F., Lee, M., Wu, B., Ting, K., Zara, J.N., Soo, C., Al Hezaimi, K., Zou, W., Chen, X., Mooney, D.J. & Wang, C.Y. (2013) NF-kappaB inhibits osteogenic differentiation of mesenchymal stem cells by promoting beta-catenin degradation. *Proc Natl Acad Sci U S A,* **110,** 9469-9474.

Chen, C.Q., Yu, K., Yan, Q.X., Xing, C.Y., Chen, Y., Yan, Z., Shi, Y.F., Zhao, K.W. & Gao, S.M. (2013) Pure curcumin increases the expression of SOCS1 and SOCS3 in myeloproliferative neoplasms through suppressing class I histone deacetylases. *Carcinogenesis,* **34,** 1442-1449.

Chung, K.M., Hsu, S.C., Chu, Y.R., Lin, M.Y., Jiaang, W.T., Chen, R.H. & Chen, X. (2014) Fibroblast activation protein (FAP) is essential for the migration of bone marrow mesenchymal stem cells through RhoA activation. *PLoS One,* **9,** e88772.

Cipolleschi, M.G., Dello Sbarba, P. & Olivotto, M. (1993) The role of hypoxia in the maintenance of hematopoietic stem cells. *Blood,* **82,** 2031-2037.

Costa, G., Kouskoff, V. & Lacaud, G. (2012) Origin of blood cells and HSC production in the embryo. *Trends Immunol,* **33,** 215-223.

Dameshek, W. (1951) Some speculations on the myeloproliferative syndromes. *Blood,* **6,** 372-375.

Del Canizo, M.C., Fernandez, M.E., Lopez, A., Vidriales, B., Villaron, E., Arroyo, J.L., Ortuno, F., Orfao, A. & San Miguel, J.F. (2003) Immunophenotypic analysis of myelodysplastic syndromes. *Haematologica,* **88,** 402-407.

Ding, L. & Morrison, S.J. (2013) Haematopoietic stem cells and early lymphoid progenitors occupy distinct bone marrow niches. *Nature,* **495,** 231-235.

Ding, L., Saunders, T.L., Enikolopov, G. & Morrison, S.J. (2012) Endothelial and perivascular cells maintain haematopoietic stem cells. *Nature,* **481,** 457-462.

Dominici, M., Le Blanc, K., Mueller, I., Slaper-Cortenbach, I., Marini, F., Krause, D., Deans, R., Keating, A., Prockop, D. & Horwitz, E. (2006) Minimal criteria for defining multipotent mesenchymal stromal cells. The International Society for Cellular Therapy position statement. *Cytotherapy,* **8,** 315-317.

Doulatov, S., Notta, F., Laurenti, E. & Dick, J.E. (2012) Hematopoiesis: a human perspective. *Cell Stem Cell,* **10,** 120-136.

Emerson, S.G., Sieff, C.A., Gross, R.G., Rozans, M.K., Miller, R.A., Rappeport, J.M. & Nathan, D.G. (1987) Decreased hematopoietic accessory cell function following bone marrow transplantation. *Exp Hematol,* **15,** 1013-1021.

Evrot, E., Ebel, N., Romanet, V., Roelli, C., Andraos, R., Qian, Z., Dolemeyer, A., Dammassa, E., Sterker, D., Cozens, R., Hofmann, F., Murakami, M., Baffert, F. & Radimerski, T. (2013) JAK1/2 and Pan-deacetylase inhibitor combination therapy yields improved efficacy in preclinical mouse models of JAK2V617F-driven disease. *Clin Cancer Res,* **19,** 6230-6241.

Falkenberg, K.J. & Johnstone, R.W. (2014) Histone deacetylases and their inhibitors in cancer, neurological diseases and immune disorders. *Nat Rev Drug Discov,* **13,** 673-691.

Fisher, J.W. (2010) Landmark advances in the development of erythropoietin. *Exp Biol Med (Maywood),* **235,** 1398-1411.

Flores-Figueroa, E., Arana-Trejo, R.M., Gutierrez-Espindola, G., Perez-Cabrera, A. & Mayani, H. (2005) Mesenchymal stem cells in myelodysplastic syndromes: phenotypic and cytogenetic characterization. *Leuk Res,* **29,** 215-224.

Fontanillo, C., Nogales-Cadenas, R., Pascual-Montano, A. & De las Rivas, J. (2011) Functional analysis beyond enrichment: non-redundant reciprocal linkage of genes and biological terms. *PLoS One,* **6,** e24289.

Fujita, T., Azuma, Y., Fukuyama, R., Hattori, Y., Yoshida, C., Koida, M., Ogita, K. & Komori, T. (2004) Runx2 induces osteoblast and chondrocyte differentiation and enhances their migration by coupling with PI3K-Akt signaling. *J Cell Biol,* **166,** 85-95.

Gadina, M., Hilton, D., Johnston, J.A., Morinobu, A., Lighvani, A., Zhou, Y.J., Visconti, R. & O'Shea, J.J. (2001) Signaling by type I and II cytokine receptors: ten years after. *Curr Opin Immunol,* **13,** 363-373.

Galloway, J.L. & Zon, L.I. (2003) Ontogeny of hematopoiesis: examining the emergence of hematopoietic cells in the vertebrate embryo. *Curr Top Dev Biol,* **53,** 139-158.

Gao, S.M., Chen, C.Q., Wang, L.Y., Hong, L.L., Wu, J.B., Dong, P.H. & Yu, F.J. (2013) Histone deacetylases inhibitor sodium butyrate inhibits JAK2/STAT signaling through upregulation of SOCS1 and SOCS3 mediated by HDAC8 inhibition in myeloproliferative neoplasms. *Exp Hematol,* **41,** 261-270 e264.

Gattazzo, F., Urciuolo, A. & Bonaldo, P. (2014) Extracellular matrix: a dynamic microenvironment for stem cell niche. *Biochim Biophys Acta,* **1840,** 2506-2519.

Gianelli, U., Bossi, A., Cortinovis, I., Sabattini, E., Tripodo, C., Boveri, E., Moro, A., Valli, R., Ponzoni, M., A, M.F., G, F.O., Ascani, S., Bonoldi, E., Iurlo, A., Gugliotta, L. & Franco, V. (2014) Reproducibility of the WHO histological criteria for the diagnosis of Philadelphia chromosome-negative myeloproliferative neoplasms. *Mod Pathol,* **27,** 814-822.

Gianelli, U., Vener, C., Bossi, A., Cortinovis, I., Iurlo, A., Fracchiolla, N.S., Savi, F., Moro, A., Grifoni, F., De Philippis, C., Radice, T., Bosari, S., Lambertenghi Deliliers, G. & Cortelezzi, A. (2012) The European Consensus on grading of bone marrow fibrosis allows a better prognostication of patients with primary myelofibrosis. *Mod Pathol,* **25,** 1193-1202.

Gordon, M.Y., Riley, G.P. & Clarke, D. (1988) Heparan sulfate is necessary for adhesive interactions between human early hemopoietic progenitor cells and the extracellular matrix of the marrow microenvironment. *Leukemia,* **2,** 804-809.

Greenbaum, A., Hsu, Y.M., Day, R.B., Schuettpelz, L.G., Christopher, M.J., Borgerding, J.N., Nagasawa, T. & Link, D.C. (2013) CXCL12 in early mesenchymal progenitors is required for haematopoietic stem-cell maintenance. *Nature,* **495,** 227-230.

Greenbaum, A.M., Revollo, L.D., Woloszynek, J.R., Civitelli, R. & Link, D.C. (2012) N-cadherin in osteolineage cells is not required for maintenance of hematopoietic stem cells. *Blood,* **120,** 295-302.

Huang da, W., Sherman, B.T. & Lempicki, R.A. (2009) Bioinformatics enrichment tools: paths toward the comprehensive functional analysis of large gene lists. *Nucleic Acids Res,* **37,** 1-13.

Huang, L.J., Constantinescu, S.N. & Lodish, H.F. (2001) The N-terminal domain of Janus kinase 2 is required for Golgi processing and cell surface expression of erythropoietin receptor. *Mol Cell,* **8,** 1327-1338.

Huber, T.L. (2010) Dissecting hematopoietic differentiation using the embryonic stem cell differentiation model. *Int J Dev Biol,* **54,** 991-1002.

Ihle, J.N., Stravapodis, D., Parganas, E., Thierfelder, W., Feng, J., Wang, D. & Teglund, S. (1998) The roles of Jaks and Stats in cytokine signaling. *Cancer J Sci Am,* **4 Suppl 1,** S84-91.

Irizarry, R.A., Bolstad, B.M., Collin, F., Cope, L.M., Hobbs, B. & Speed, T.P. (2003) Summaries of Affymetrix GeneChip probe level data. *Nucleic Acids Res,* **31,** e15.

Jacamo, R., Chen, Y., Wang, Z., Ma, W., Zhang, M., Spaeth, E.L., Wang, Y., Battula, V.L., Mak, P.Y., Schallmoser, K., Ruvolo, P., Schober, W.D., Shpall, E.J., Nguyen, M.H., Strunk, D., Bueso-Ramos, C.E., Konoplev, S., Davis, R.E., Konopleva, M. & Andreeff, M. (2014) Reciprocal leukemia-stroma VCAM-1/VLA-4-dependent activation of NF-kappaB mediates chemoresistance. *Blood,* **123,** 2691-2702.

James, C., Ugo, V., Le Couedic, J.P., Staerk, J., Delhommeau, F., Lacout, C., Garcon, L., Raslova, H., Berger, R., Bennaceur-Griscelli, A., Villeval, J.L., Constantinescu, S.N., Casadevall, N. & Vainchenker, W. (2005) A unique clonal JAK2 mutation leading to constitutive signalling causes polycythaemia vera. *Nature,* **434,** 1144-1148.

Jatiani, S.S., Baker, S.J., Silverman, L.R. & Reddy, E.P. (2010) Jak/STAT pathways in cytokine signaling and myeloproliferative disorders: approaches for targeted therapies. *Genes Cancer,* **1,** 979-993.

Kaplan, J.B., Stein, B.L., McMahon, B., Giles, F.J. & Platanias, L.C. (2016) Evolving Therapeutic Strategies for the Classic Philadelphia-Negative Myeloproliferative Neoplasms. *EBioMedicine,* **3,** 17-25.

Kiel, M.J., Acar, M., Radice, G.L. & Morrison, S.J. (2009) Hematopoietic stem cells do not depend on N-cadherin to regulate their maintenance. *Cell Stem Cell,* **4,** 170-179.

Kiel, M.J. & Morrison, S.J. (2008) Uncertainty in the niches that maintain haematopoietic stem cells. *Nat Rev Immunol,* **8,** 290-301.

Kim, Y.W., Koo, B.K., Jeong, H.W., Yoon, M.J., Song, R., Shin, J., Jeong, D.C., Kim, S.H. & Kong, Y.Y. (2008) Defective Notch activation in microenvironment leads to myeloproliferative disease. *Blood,* **112,** 4628-4638.

Kinder, S.J., Tsang, T.E., Quinlan, G.A., Hadjantonakis, A.K., Nagy, A. & Tam, P.P. (1999) The orderly allocation of mesodermal cells to the extraembryonic structures and the anteroposterior axis during gastrulation of the mouse embryo. *Development,* **126,** 4691-4701.

Kleppe, M., Kwak, M., Koppikar, P., Riester, M., Keller, M., Bastian, L., Hricik, T., Bhagwat, N., McKenney, A.S., Papalexi, E., Abdel-Wahab, O., Rampal, R., Marubayashi, S., Chen, J.J., Romanet, V., Fridman, J.S., Bromberg, J., Teruya-Feldstein, J., Murakami, M., Radimerski, T., Michor, F., Fan, R. & Levine, R.L. (2015) JAK-STAT pathway activation in malignant and nonmalignant cells contributes to MPN pathogenesis and therapeutic response. *Cancer Discov,* **5,** 316-331.

Kode, A., Manavalan, J.S., Mosialou, I., Bhagat, G., Rathinam, C.V., Luo, N., Khiabanian, H., Lee, A., Murty, V.V., Friedman, R., Brum, A., Park, D., Galili, N., Mukherjee, S., Teruya-Feldstein, J., Raza, A., Rabadan, R., Berman, E. & Kousteni, S. (2014) Leukaemogenesis induced by an activating beta-catenin mutation in osteoblasts. *Nature,* **506,** 240-244.

Kralovics, R., Passamonti, F., Buser, A.S., Teo, S.S., Tiedt, R., Passweg, J.R., Tichelli, A., Cazzola, M. & Skoda, R.C. (2005a) A gain-of-function mutation of JAK2 in myeloproliferative disorders. *N Engl J Med,* **352,** 1779-1790.

Kralovics, R., Teo, S.S., Buser, A.S., Brutsche, M., Tiedt, R., Tichelli, A., Passamonti, F., Pietra, D., Cazzola, M. & Skoda, R.C. (2005b) Altered gene expression in myeloproliferative disorders correlates with activation of signaling by the V617F mutation of Jak2. *Blood,* **106,** 3374-3376.

Krause, D.S., Fulzele, K., Catic, A., Sun, C.C., Dombkowski, D., Hurley, M.P., Lezeau, S., Attar, E., Wu, J.Y., Lin, H.Y., Divieti-Pajevic, P., Hasserjian, R.P., Schipani, E., Van Etten, R.A. & Scadden, D.T. (2013) Differential regulation of myeloid leukemias by the bone marrow microenvironment. *Nat Med,* **19,** 1513-1517.

Krause, D.S., Lazarides, K., Lewis, J.B., von Andrian, U.H. & Van Etten, R.A. (2014) Selectins and their ligands are required for homing and engraftment of BCR-ABL1+ leukemic stem cells in the bone marrow niche. *Blood,* **123,** 1361-1371.

Laemmli, U.K. (1970) Cleavage of structural proteins during the assembly of the head of bacteriophage T4. *Nature,* **227,** 680-685.

Larsson, J. & Karlsson, S. (2005) The role of Smad signaling in hematopoiesis. *Oncogene,* **24,** 5676-5692.

Lemieux, J.M., Horowitz, M.C. & Kacena, M.A. (2010) Involvement of integrins alpha(3)beta(1) and alpha(5)beta(1) and glycoprotein IIb in megakaryocyte-induced osteoblast proliferation. *J Cell Biochem,* **109,** 927-932.

Levesque, J.P., Winkler, I.G., Hendy, J., Williams, B., Helwani, F., Barbier, V., Nowlan, B. & Nilsson, S.K. (2007) Hematopoietic progenitor cell mobilization results in hypoxia with increased hypoxia-inducible transcription factor-1 alpha and vascular endothelial growth factor A in bone marrow. *Stem Cells,* **25,** 1954-1965.

Levi, B., Wan, D.C., Glotzbach, J.P., Hyun, J., Januszyk, M., Montoro, D., Sorkin, M., James, A.W., Nelson, E.R., Li, S., Quarto, N., Lee, M., Gurtner, G.C. & Longaker, M.T. (2011) CD105 protein depletion enhances human adipose-derived stromal cell osteogenesis through reduction of transforming growth factor beta1 (TGF-beta1) signaling. *J Biol Chem,* **286,** 39497-39509.

Levine, R.L., Wadleigh, M., Cools, J., Ebert, B.L., Wernig, G., Huntly, B.J., Boggon, T.J., Wlodarska, I., Clark, J.J., Moore, S., Adelsperger, J., Koo, S., Lee, J.C., Gabriel, S., Mercher, T., D'Andrea, A., Frohling, S., Dohner, K., Marynen, P., Vandenberghe, P., Mesa, R.A., Tefferi, A., Griffin, J.D., Eck, M.J., Sellers, W.R., Meyerson, M., Golub, T.R., Lee, S.J. & Gilliland, D.G. (2005) Activating mutation in the tyrosine kinase JAK2 in polycythemia vera, essential thrombocythemia, and myeloid metaplasia with myelofibrosis. *Cancer Cell,* **7,** 387-397.

Levy, D.E. & Darnell, J.E., Jr. (2002) Stats: transcriptional control and biological impact. *Nat Rev Mol Cell Biol,* **3,** 651-662.

Li, W., Johnson, S.A., Shelley, W.C. & Yoder, M.C. (2004) Hematopoietic stem cell repopulating ability can be maintained in vitro by some primary endothelial cells. *Exp Hematol,* **32,** 1226-1237.

Lin, S.Y., Dolfi, S.C., Amiri, S., Li, J., Budak-Alpdogan, T., Lee, K.C., Derenzo, C., Banerjee, D. & Glod, J. (2013) P53 regulates the migration of mesenchymal stromal cells in response to the tumor microenvironment through both CXCL12-dependent and -independent mechanisms. *Int J Oncol,* **43,** 1817-1823.

Lo Celso, C., Fleming, H.E., Wu, J.W., Zhao, C.X., Miake-Lye, S., Fujisaki, J., Cote, D., Rowe, D.W., Lin, C.P. & Scadden, D.T. (2009) Live-animal tracking of individual haematopoietic stem/progenitor cells in their niche. *Nature,* **457,** 92-96.

Lopez-Holgado, N., Arroyo, J.L., Pata, C., Villaron, E., Sanchez Guijo, F., Martin, A., Hernandez Rivas, J.M., Orfao, A., San Miguel, J.F. & Del Canizo Fernandez-Roldan, M.C. (2004) Analysis of hematopoietic progenitor cells in patients with myelodysplastic syndromes according to their cytogenetic abnormalities. *Leuk Res,* **28,** 1181-1187.

Lopez-Holgado, N., Pata, C., Villaron, E., Sanchez-Guijo, F., Alberca, M., Martin, A., Corral, M., Sanchez-Abarca, I., Perez-Simon, J.A., San Miguel, J.F. & del Canizo, M.C. (2005) Long-term bone marrow culture data are the most powerful predictor of peripheral blood progenitor cell mobilization in healthy donors. *Haematologica,* **90,** 353-359.

Lopez-Villar, O., Garcia, J.L., Sanchez-Guijo, F.M., Robledo, C., Villaron, E.M., Hernandez-Campo, P., Lopez-Holgado, N., Diez-Campelo, M., Barbado, M.V., Perez-Simon, J.A., Hernandez-Rivas, J.M., San-Miguel, J.F. & del Canizo, M.C. (2009) Both expanded and uncultured mesenchymal stem cells from MDS patients are genomically abnormal, showing a specific genetic profile for the 5q- syndrome. *Leukemia,* **23,** 664-672.

Lu, L.L., Liu, Y.J., Yang, S.G., Zhao, Q.J., Wang, X., Gong, W., Han, Z.B., Xu, Z.S., Lu, Y.X., Liu, D., Chen, Z.Z. & Han, Z.C. (2006) Isolation and characterization of human umbilical cord mesenchymal stem cells with hematopoiesis-supportive function and other potentials. *Haematologica,* **91,** 1017-1026.

Lucas, D., Battista, M., Shi, P.A., Isola, L. & Frenette, P.S. (2008) Mobilized hematopoietic stem cell yield depends on species-specific circadian timing. *Cell Stem Cell,* **3,** 364-366.

Ludin, A., Itkin, T., Gur-Cohen, S., Mildner, A., Shezen, E., Golan, K., Kollet, O., Kalinkovich, A., Porat, Z., D'Uva, G., Schajnovitz, A., Voronov, E., Brenner, D.A., Apte, R.N., Jung, S. & Lapidot, T. (2012) Monocytes-macrophages that express alpha-smooth muscle actin preserve primitive hematopoietic cells in the bone marrow. *Nat Immunol,* **13,** 1072-1082.

Mansour, A., Abou-Ezzi, G., Sitnicka, E., Jacobsen, S.E., Wakkach, A. & Blin-Wakkach, C. (2012) Osteoclasts promote the formation of hematopoietic stem cell niches in the bone marrow. *J Exp Med,* **209,** 537-549.

Martinaud, C., Desterke, C., Konopacki, J., Pieri, L., Torossian, F., Golub, R., Schmutz, S., Anginot, A., Guerton, B., Rochet, N., Albanese, P., Henault, E., Pierre-Louis, O., Souraud, J.B., de Revel, T., Dupriez, B., Ianotto, J.C., Bourgeade, M.F., Vannucchi, A.M., Lataillade, J.J. & Le Bousse-Kerdiles, M.C. (2015) Osteogenic Potential of Mesenchymal Stromal Cells Contributes to Primary Myelofibrosis. *Cancer Res,* **75,** 4753-4765.

Mendez-Ferrer, S., Battista, M. & Frenette, P.S. (2010a) Cooperation of beta(2)- and beta(3)-adrenergic receptors in hematopoietic progenitor cell mobilization. *Ann N Y Acad Sci,* **1192,** 139-144.

Mendez-Ferrer, S., Chow, A., Merad, M. & Frenette, P.S. (2009) Circadian rhythms influence hematopoietic stem cells. *Curr Opin Hematol,* **16,** 235-242.

Mendez-Ferrer, S., Garcia-Fernandez, M. & de Castillejo, C.L. (2015) Convert and conquer: the strategy of chronic myelogenous leukemic cells. *Cancer Cell,* **27,** 611-613.

Mendez-Ferrer, S., Michurina, T.V., Ferraro, F., Mazloom, A.R., Macarthur, B.D., Lira, S.A., Scadden, D.T., Ma'ayan, A., Enikolopov, G.N. & Frenette, P.S. (2010b) Mesenchymal and haematopoietic stem cells form a unique bone marrow niche. *Nature,* **466,** 829-834.

Minucci, S. & Pelicci, P.G. (2006) Histone deacetylase inhibitors and the promise of epigenetic (and more) treatments for cancer. *Nat Rev Cancer,* **6,** 38-51.

Morrison, S.J. & Scadden, D.T. (2014) The bone marrow niche for haematopoietic stem cells. *Nature,* **505,** 327-334.

Mostafa, S.S., Miller, W.M. & Papoutsakis, E.T. (2000) Oxygen tension influences the differentiation, maturation and apoptosis of human megakaryocytes. *Br J Haematol,* **111,** 879-889.

Mottamal, M., Zheng, S., Huang, T.L. & Wang, G. (2015) Histone deacetylase inhibitors in clinical studies as templates for new anticancer agents. *Molecules,* **20,** 3898-3941.

Muntion, S., Ramos, T.L., Diez-Campelo, M., Roson, B., Sanchez-Abarca, L.I., Misiewicz-Krzeminska, I., Preciado, S., Sarasquete, M.E., de Las Rivas, J., Gonzalez, M., Sanchez-Guijo, F. & Del Canizo, M.C. (2016) Microvesicles from Mesenchymal Stromal Cells Are Involved in HPC-Microenvironment Crosstalk in Myelodysplastic Patients. *PLoS One,* **11,** e0146722.

Muppidi, J.R., Tschopp, J. & Siegel, R.M. (2004) Life and death decisions: secondary complexes and lipid rafts in TNF receptor family signal transduction. *Immunity,* **21,** 461-465.

Muralidharan-Chari, V., Clancy, J.W., Sedgwick, A. & D'Souza-Schorey, C. (2010) Microvesicles: mediators of extracellular communication during cancer progression. *J Cell Sci,* **123,** 1603-1611.

Nangalia, J., Massie, C.E., Baxter, E.J., Nice, F.L., Gundem, G., Wedge, D.C., Avezov, E., Li, J., Kollmann, K., Kent, D.G., Aziz, A., Godfrey, A.L., Hinton, J., Martincorena, I., Van Loo, P., Jones, A.V., Guglielmelli, P., Tarpey, P., Harding, H.P., Fitzpatrick, J.D., Goudie, C.T., Ortmann, C.A., Loughran, S.J., Raine, K., Jones, D.R., Butler, A.P., Teague, J.W., O'Meara, S., McLaren, S., Bianchi, M., Silber, Y., Dimitropoulou, D., Bloxham, D., Mudie, L., Maddison, M., Robinson, B., Keohane, C., Maclean, C., Hill, K., Orchard, K., Tauro, S., Du, M.Q., Greaves, M., Bowen, D., Huntly, B.J., Harrison, C.N., Cross, N.C., Ron, D., Vannucchi, A.M., Papaemmanuil, E., Campbell, P.J. & Green, A.R. (2013) Somatic CALR mutations in myeloproliferative neoplasms with nonmutated JAK2. *N Engl J Med,* **369,** 2391-2405.

Nombela-Arrieta, C., Pivarnik, G., Winkel, B., Canty, K.J., Harley, B., Mahoney, J.E., Park, S.Y., Lu, J., Protopopov, A. & Silberstein, L.E. (2013) Quantitative imaging of haematopoietic stem and progenitor cell localization and hypoxic status in the bone marrow microenvironment. *Nat Cell Biol,* **15,** 533-543.

Norfo, R., Zini, R., Pennucci, V., Bianchi, E., Salati, S., Guglielmelli, P., Bogani, C., Fanelli, T., Mannarelli, C., Rosti, V., Pietra, D., Salmoiraghi, S., Bisognin, A., Ruberti, S., Rontauroli, S., Sacchi, G., Prudente, Z., Barosi, G., Cazzola, M., Rambaldi, A., Bortoluzzi, S., Ferrari, S., Tagliafico, E., Vannucchi, A.M. & Manfredini, R. (2014) miRNA-mRNA integrative analysis in primary myelofibrosis CD34+ cells: role of miR-155/JARID2 axis in abnormal megakaryopoiesis. *Blood,* **124,** e21-32.

Notta, F., Doulatov, S., Laurenti, E., Poeppl, A., Jurisica, I. & Dick, J.E. (2011) Isolation of single human hematopoietic stem cells capable of long-term multilineage engraftment. *Science,* **333,** 218-221.

Nowell, P.C. (1962) The minute chromosome (Phl) in chronic granulocytic leukemia. *Blut,* **8,** 65-66.

Nowell, P.C. & Hungerford, D.A. (1960) Chromosome studies on normal and leukemic human leukocytes. *J Natl Cancer Inst,* **25,** 85-109.

O'Connell, R.M., Rao, D.S., Chaudhuri, A.A., Boldin, M.P., Taganov, K.D., Nicoll, J., Paquette, R.L. & Baltimore, D. (2008) Sustained expression of microRNA-155 in hematopoietic stem cells causes a myeloproliferative disorder. *J Exp Med,* **205,** 585-594.

Oakley, F.D., Smith, R.L. & Engelhardt, J.F. (2009) Lipid rafts and caveolin-1 coordinate interleukin-1beta (IL-1beta)-dependent activation of NFkappaB by controlling endocytosis of Nox2 and IL-1beta receptor 1 from the plasma membrane. *J Biol Chem,* **284,** 33255-33264.

Omatsu, Y., Sugiyama, T., Kohara, H., Kondoh, G., Fujii, N., Kohno, K. & Nagasawa, T. (2010) The essential functions of adipo-osteogenic progenitors as the hematopoietic stem and progenitor cell niche. *Immunity,* **33,** 387-399.

Osawa, M., Hanada, K., Hamada, H. & Nakauchi, H. (1996) Long-term lymphohematopoietic reconstitution by a single CD34-low/negative hematopoietic stem cell. *Science,* **273,** 242-245.

Pan, B.T., Blostein, R. & Johnstone, R.M. (1983) Loss of the transferrin receptor during the maturation of sheep reticulocytes in vitro. An immunological approach. *Biochem J,* **210,** 37-47.

Pan, B.T. & Johnstone, R.M. (1983) Fate of the transferrin receptor during maturation of sheep reticulocytes in vitro: selective externalization of the receptor. *Cell,* **33,** 967-978.

Papayannopoulou, T., Nakamoto, B., Yokochi, T., Chait, A. & Kannagi, R. (1983) Human erythroleukemia cell line (HEL) undergoes a drastic macrophage-like shift with TPA. *Blood,* **62,** 832-845.

Parganas, E., Wang, D., Stravopodis, D., Topham, D.J., Marine, J.C., Teglund, S., Vanin, E.F., Bodner, S., Colamonici, O.R., van Deursen, J.M., Grosveld, G. & Ihle, J.N. (1998) Jak2 is essential for signaling through a variety of cytokine receptors. *Cell,* **93,** 385-395.

Park, O.K., Schaefer, T.S. & Nathans, D. (1996) In vitro activation of Stat3 by epidermal growth factor receptor kinase. *Proc Natl Acad Sci U S A,* **93,** 13704-13708.

Passamonti, F., Cervantes, F., Vannucchi, A.M., Morra, E., Rumi, E., Pereira, A., Guglielmelli, P., Pungolino, E., Caramella, M., Maffioli, M., Pascutto, C., Lazzarino, M., Cazzola, M. & Tefferi, A. (2010) A dynamic prognostic model to predict survival in primary myelofibrosis: a study by the IWG-MRT (International Working Group for Myeloproliferative Neoplasms Research and Treatment). *Blood,* **115,** 1703-1708.

Passamonti, F., Maffioli, M., Caramazza, D. & Cazzola, M. (2011) Myeloproliferative neoplasms: from JAK2 mutations discovery to JAK2 inhibitor therapies. *Oncotarget,* **2,** 485-490.

Pettersson, M., Dannaeus, K., Nilsson, K. & Jonsson, J.I. (2000) Isolation of MYADM, a novel hematopoietic-associated marker gene expressed in multipotent progenitor cells and up-regulated during myeloid differentiation. *J Leukoc Biol,* **67,** 423-431.

Qi, J., Singh, S., Hua, W.K., Cai, Q., Chao, S.W., Li, L., Liu, H., Ho, Y., McDonald, T., Lin, A., Marcucci, G., Bhatia, R., Huang, W.J., Chang, C.I. & Kuo, Y.H. (2015) HDAC8 Inhibition Specifically Targets Inv(16) Acute Myeloid Leukemic Stem Cells by Restoring p53 Acetylation. *Cell Stem Cell,* **17,** 597-610.

Qian, H., Buza-Vidas, N., Hyland, C.D., Jensen, C.T., Antonchuk, J., Mansson, R., Thoren, L.A., Ekblom, M., Alexander, W.S. & Jacobsen, S.E. (2007) Critical role of thrombopoietin in maintaining adult quiescent hematopoietic stem cells. *Cell Stem Cell,* **1,** 671-684.

Qu, P., Wang, L., Min, Y., McKennett, L., Keller, J.R. & Lin, P.C. (2016) Vav1 regulates mesenchymal stem cell differentiation decision between adipocyte and chondrocyte via Sirt1. *Stem Cells*.

Raaijmakers, M.H., Mukherjee, S., Guo, S., Zhang, S., Kobayashi, T., Schoonmaker, J.A., Ebert, B.L., Al-Shahrour, F., Hasserjian, R.P., Scadden, E.O., Aung, Z., Matza, M., Merkenschlager, M., Lin, C., Rommens, J.M. & Scadden, D.T. (2010) Bone progenitor dysfunction induces myelodysplasia and secondary leukaemia. *Nature,* **464,** 852-857.

Rafii, S., Shapiro, F., Pettengell, R., Ferris, B., Nachman, R.L., Moore, M.A. & Asch, A.S. (1995) Human bone marrow microvascular endothelial cells support long-term proliferation and differentiation of myeloid and megakaryocytic progenitors. *Blood,* **86,** 3353-3363.

Raimondo, S., Corrado, C., Raimondi, L., De Leo, G. & Alessandro, R. (2015) Role of Extracellular Vesicles in Hematological Malignancies. *Biomed Res Int,* **2015,** 821613.

Ramalho-Santos, M. & Willenbring, H. (2007) On the origin of the term "stem cell". *Cell Stem Cell,* **1,** 35-38.

Ramos, T.L., Sanchez-Abarca, L.I., Lopez-Ruano, G., Muntion, S., Preciado, S., Hernandez-Ruano, M., Rosado, B., de las Heras, N., Chillon, M.C., Hernandez-Hernandez, A., Gonzalez, M., Sanchez-Guijo, F. & Del Canizo, C. (2015) Do endothelial cells belong to the primitive stem leukemic clone in CML? Role of extracellular vesicles. *Leuk Res,* **39,** 921-924.

Ramos, T.L., Sanchez-Abarca, L.I., Muntion, S., Preciado, S., Puig, N., Lopez-Ruano, G., Hernandez-Hernandez, A., Redondo, A., Ortega, R., Rodriguez, C., Sanchez-Guijo, F. & del Canizo, C. (2016) MSC surface markers (CD44, CD73, and CD90) can identify human MSC-derived extracellular vesicles by conventional flow cytometry. *Cell Commun Signal,* **14,** 2.

Raposo, G., Nijman, H.W., Stoorvogel, W., Liejendekker, R., Harding, C.V., Melief, C.J. & Geuze, H.J. (1996) B lymphocytes secrete antigen-presenting vesicles. *J Exp Med,* **183,** 1161-1172.

Reissmann, K.R. (1950) Studies on the mechanism of erythropoietic stimulation in parabiotic rats during hypoxia. *Blood,* **5,** 372-380.

Rettig, I., Koeneke, E., Trippel, F., Mueller, W.C., Burhenne, J., Kopp-Schneider, A., Fabian, J., Schober, A., Fernekorn, U., von Deimling, A., Deubzer, H.E., Milde, T., Witt, O. & Oehme, I. (2015) Selective inhibition of HDAC8 decreases neuroblastoma growth in vitro and in vivo and enhances retinoic acid-mediated differentiation. *Cell Death Dis,* **6,** e1657.

Reynaud, D., Pietras, E., Barry-Holson, K., Mir, A., Binnewies, M., Jeanne, M., Sala-Torra, O., Radich, J.P. & Passegue, E. (2011) IL-6 controls leukemic multipotent progenitor cell fate and contributes to chronic myelogenous leukemia development. *Cancer Cell,* **20,** 661-673.

Risueno, A., Fontanillo, C., Dinger, M.E. & De Las Rivas, J. (2010) GATExplorer: genomic and transcriptomic explorer; mapping expression probes to gene loci, transcripts, exons and ncRNAs. *BMC Bioinformatics,* **11,** 221.

Roccaro, A.M., Sacco, A., Maiso, P., Azab, A.K., Tai, Y.T., Reagan, M., Azab, F., Flores, L.M., Campigotto, F., Weller, E., Anderson, K.C., Scadden, D.T. & Ghobrial, I.M. (2013) BM mesenchymal stromal cell-derived exosomes facilitate multiple myeloma progression. *J Clin Invest,* **123,** 1542-1555.

Rowley, J.D. (1973) Letter: A new consistent chromosomal abnormality in chronic myelogenous leukaemia identified by quinacrine fluorescence and Giemsa staining. *Nature,* **243,** 290-293.

Rupec, R.A., Jundt, F., Rebholz, B., Eckelt, B., Weindl, G., Herzinger, T., Flaig, M.J., Moosmann, S., Plewig, G., Dorken, B., Forster, I., Huss, R. & Pfeffer, K. (2005) Stroma-

mediated dysregulation of myelopoiesis in mice lacking I kappa B alpha. *Immunity,* **22,** 479-491.

S, E.L.A., Mager, I., Breakefield, X.O. & Wood, M.J. (2013) Extracellular vesicles: biology and emerging therapeutic opportunities. *Nat Rev Drug Discov,* **12,** 347-357.

Sacchetti, B., Funari, A., Michienzi, S., Di Cesare, S., Piersanti, S., Saggio, I., Tagliafico, E., Ferrari, S., Robey, P.G., Riminucci, M. & Bianco, P. (2007) Self-renewing osteoprogenitors in bone marrow sinusoids can organize a hematopoietic microenvironment. *Cell,* **131,** 324-336.

Saez, B., Ferraro, F., Yusuf, R.Z., Cook, C.M., Yu, V.W., Pardo-Saganta, A., Sykes, S.M., Palchaudhuri, R., Schajnovitz, A., Lotinun, S., Lymperi, S., Mendez-Ferrer, S., Toro, R.D., Day, R., Vasic, R., Acharya, S.S., Baron, R., Lin, C.P., Yamaguchi, Y., Wagers, A.J. & Scadden, D.T. (2014) Inhibiting stromal cell heparan sulfate synthesis improves stem cell mobilization and enables engraftment without cytotoxic conditioning. *Blood,* **124,** 2937-2947.

Salter, A.B., Meadows, S.K., Muramoto, G.G., Himburg, H., Doan, P., Daher, P., Russell, L., Chen, B., Chao, N.J. & Chute, J.P. (2009) Endothelial progenitor cell infusion induces hematopoietic stem cell reconstitution in vivo. *Blood,* **113,** 2104-2107.

Sanchez-Abarca, L.I., Alvarez-Laderas, I., Diez Campelo, M., Caballero-Velazquez, T., Herrero, C., Muntion, S., Calderon, C., Garcia-Guerrero, E., Sanchez-Guijo, F., Del Canizo, C., San Miguel, J. & Perez-Simon, J.A. (2013) Uptake and delivery of antigens by mesenchymal stromal cells. *Cytotherapy,* **15,** 673-678.

Sanchez-Guijo, F.M., Blanco, J.F., Cruz, G., Muntion, S., Gomez, M., Carrancio, S., Lopez-Villar, O., Barbado, M.V., Sanchez-Abarca, L.I., Blanco, B., Brinon, J.G. & del Canizo, M.C. (2009) Multiparametric comparison of mesenchymal stromal cells obtained from trabecular bone by using a novel isolation method with those obtained by iliac crest aspiration from the same subjects. *Cell Tissue Res,* **336,** 501-507.

Sanchez-Guijo, F.M., Sanchez-Abarca, L.I., Villaron, E., Lopez-Holgado, N., Alberca, M., Vazquez, L., Perez-Simon, J.A., Lopez-Fidalgo, J., Orfao, A., Caballero, M.D., Del Canizo, M.C. & San Miguel, J.F. (2005) Posttransplant hematopoiesis in patients undergoing sibling allogeneic stem cell transplantation reflects that of their respective donors although with a lower functional capability. *Exp Hematol,* **33,** 935-943.

Schepers, K., Campbell, T.B. & Passegue, E. (2015) Normal and leukemic stem cell niches: insights and therapeutic opportunities. *Cell Stem Cell,* **16,** 254-267.

Schepers, K., Pietras, E.M., Reynaud, D., Flach, J., Binnewies, M., Garg, T., Wagers, A.J., Hsiao, E.C. & Passegue, E. (2013) Myeloproliferative neoplasia remodels the endosteal bone marrow niche into a self-reinforcing leukemic niche. *Cell Stem Cell,* **13,** 285-299.

Schmitt-Graeff, A.H., Nitschke, R. & Zeiser, R. (2015) The Hematopoietic Niche in Myeloproliferative Neoplasms. *Mediators Inflamm,* **2015,** 347270.

Schofield, R. (1978) The relationship between the spleen colony-forming cell and the haemopoietic stem cell. *Blood Cells,* **4,** 7-25.

Semenza, G.L., Jiang, B.H., Leung, S.W., Passantino, R., Concordet, J.P., Maire, P. & Giallongo, A. (1996) Hypoxia response elements in the aldolase A, enolase 1, and lactate dehydrogenase A gene promoters contain essential binding sites for hypoxia-inducible factor 1. *J Biol Chem,* **271,** 32529-32537.

Simsek, T., Kocabas, F., Zheng, J., Deberardinis, R.J., Mahmoud, A.I., Olson, E.N., Schneider, J.W., Zhang, C.C. & Sadek, H.A. (2010) The distinct metabolic profile of hematopoietic stem cells reflects their location in a hypoxic niche. *Cell Stem Cell,* **7,** 380-390.

Smyth, G.K., Michaud, J. & Scott, H.S. (2005) Use of within-array replicate spots for assessing differential expression in microarray experiments. *Bioinformatics,* **21,** 2067-2075.

Staerk, J. & Constantinescu, S.N. (2012) The JAK-STAT pathway and hematopoietic stem cells from the JAK2 V617F perspective. *JAKSTAT,* **1,** 184-190.

Starr, R. & Hilton, D.J. (1999) Negative regulation of the JAK/STAT pathway. *Bioessays,* **21,** 47-52.

Steensma, D.P., Dewald, G.W., Lasho, T.L., Powell, H.L., McClure, R.F., Levine, R.L., Gilliland, D.G. & Tefferi, A. (2005) The JAK2 V617F activating tyrosine kinase mutation is an infrequent event in both "atypical" myeloproliferative disorders and myelodysplastic syndromes. *Blood,* **106,** 1207-1209.

Sugiyama, T., Kohara, H., Noda, M. & Nagasawa, T. (2006) Maintenance of the hematopoietic stem cell pool by CXCL12-CXCR4 chemokine signaling in bone marrow stromal cell niches. *Immunity,* **25,** 977-988.

Takubo, K., Goda, N., Yamada, W., Iriuchishima, H., Ikeda, E., Kubota, Y., Shima, H., Johnson, R.S., Hirao, A., Suematsu, M. & Suda, T. (2010) Regulation of the HIF-1alpha level is essential for hematopoietic stem cells. *Cell Stem Cell,* **7,** 391-402.

Taverna, S., Amodeo, V., Saieva, L., Russo, A., Giallombardo, M., De Leo, G. & Alessandro, R. (2014) Exosomal shuttling of miR-126 in endothelial cells modulates adhesive and migratory abilities of chronic myelogenous leukemia cells. *Mol Cancer,* **13,** 169.

Tefferi, A., Thiele, J., Orazi, A., Kvasnicka, H.M., Barbui, T., Hanson, C.A., Barosi, G., Verstovsek, S., Birgegard, G., Mesa, R., Reilly, J.T., Gisslinger, H., Vannucchi, A.M., Cervantes, F., Finazzi, G., Hoffman, R., Gilliland, D.G., Bloomfield, C.D. & Vardiman, J.W. (2007) Proposals and rationale for revision of the World Health Organization diagnostic criteria for polycythemia vera, essential thrombocythemia, and primary myelofibrosis: recommendations from an ad hoc international expert panel. *Blood,* **110,** 1092-1097.

Thery, C., Amigorena, S., Raposo, G. & Clayton, A. (2006) Isolation and characterization of exosomes from cell culture supernatants and biological fluids. *Curr Protoc Cell Biol,* **Chapter 3,** Unit 3 22.

Thiele, J., Kvasnicka, H.M., Facchetti, F., Franco, V., van der Walt, J. & Orazi, A. (2005) European consensus on grading bone marrow fibrosis and assessment of cellularity. *Haematologica,* **90,** 1128-1132.

Till, J.E. & Mc, C.E. (1961) A direct measurement of the radiation sensitivity of normal mouse bone marrow cells. *Radiat Res,* **14,** 213-222.

Triantafilou, M., Lepper, P.M., Olden, R., Dias, I.S. & Triantafilou, K. (2011) Location, location, location: is membrane partitioning everything when it comes to innate immune activation? *Mediators Inflamm,* **2011,** 186093.

Ungureanu, D., Wu, J., Pekkala, T., Niranjan, Y., Young, C., Jensen, O.N., Xu, C.F., Neubert, T.A., Skoda, R.C., Hubbard, S.R. & Silvennoinen, O. (2011) The pseudokinase domain of JAK2 is a dual-specificity protein kinase that negatively regulates cytokine signaling. *Nat Struct Mol Biol,* **18,** 971-976.

Uozumi, K., Otsuka, M., Ohno, N., Moriyama, T., Suzuki, S., Shimotakahara, S., Matsumura, I., Hanada, S. & Arima, T. (2000) Establishment and characterization of a new human megakaryoblastic cell line (SET-2) that spontaneously matures to megakaryocytes and produces platelet-like particles. *Leukemia,* **14,** 142-152.

Vannucchi, A.M., Lasho, T.L., Guglielmelli, P., Biamonte, F., Pardanani, A., Pereira, A., Finke, C., Score, J., Gangat, N., Mannarelli, C., Ketterling, R.P., Rotunno, G., Knudson, R.A., Susini, M.C., Laborde, R.R., Spolverini, A., Pancrazzi, A., Pieri, L., Manfredini, R., Tagliafico, E., Zini, R., Jones, A., Zoi, K., Reiter, A., Duncombe, A., Pietra, D., Rumi, E., Cervantes, F., Barosi, G., Cazzola, M., Cross, N.C. & Tefferi, A. (2013) Mutations and prognosis in primary myelofibrosis. *Leukemia,* **27,** 1861-1869.

Vardiman, J.W., Thiele, J., Arber, D.A., Brunning, R.D., Borowitz, M.J., Porwit, A., Harris, N.L., Le Beau, M.M., Hellstrom-Lindberg, E., Tefferi, A. & Bloomfield, C.D. (2009) The 2008 revision of the World Health Organization (WHO) classification of myeloid neoplasms and acute leukemia: rationale and important changes. *Blood,* **114,** 937-951.

Velletri, T., Xie, N., Wang, Y., Huang, Y., Yang, Q., Chen, X., Chen, Q., Shou, P., Gan, Y., Cao, G., Melino, G. & Shi, Y. (2016) P53 functional abnormality in mesenchymal stem cells promotes osteosarcoma development. *Cell Death Dis,* **7,** e2015.

Villaron, E.M., Almeida, J., Lopez-Holgado, N., Alcoceba, M., Sanchez-Abarca, L.I., Sanchez-Guijo, F.M., Alberca, M., Perez-Simon, J.A., San Miguel, J.F. & Del Canizo, M.C. (2004) Mesenchymal stem cells are present in peripheral blood and can engraft after allogeneic hematopoietic stem cell transplantation. *Haematologica,* **89,** 1421-1427.

Vu, T., Austin, R., Kuhn, C.P., Bruedigam, C., Song, A., Guignes, S., Jacquelin, S., Ramshaw, H.S., Hill, G.R., Lopez, A.F. & Lane, S.W. (2016) Jak2V617F driven myeloproliferative neoplasm occurs independently of interleukin-3 receptor beta common signaling. *Haematologica,* **101,** e77-80.

Walkley, C.R., Olsen, G.H., Dworkin, S., Fabb, S.A., Swann, J., McArthur, G.A., Westmoreland, S.V., Chambon, P., Scadden, D.T. & Purton, L.E. (2007a) A microenvironment-induced myeloproliferative syndrome caused by retinoic acid receptor gamma deficiency. *Cell,* **129,** 1097-1110.

Walkley, C.R., Shea, J.M., Sims, N.A., Purton, L.E. & Orkin, S.H. (2007b) Rb regulates interactions between hematopoietic stem cells and their bone marrow microenvironment. *Cell,* **129,** 1081-1095.

Wang, J.C., Chen, C., Dumlao, T., Naik, S., Chang, T., Xiao, Y.Y., Sominsky, I. & Burton, J. (2008) Enhanced histone deacetylase enzyme activity in primary myelofibrosis. *Leuk Lymphoma,* **49,** 2321-2327.

Wang, L., Zhang, H., Rodriguez, S., Cao, L., Parish, J., Mumaw, C., Zollman, A., Kamoka, M.M., Mu, J., Chen, D.Z., Srour, E.F., Chitteti, B.R., HogenEsch, H., Tu, X., Bellido, T.M., Boswell, H.S., Manshouri, T., Verstovsek, S., Yoder, M.C., Kapur, R., Cardoso, A.A. & Carlesso, N. (2014) Notch-dependent repression of miR-155 in the bone marrow niche regulates hematopoiesis in an NF-kappaB-dependent manner. *Cell Stem Cell,* **15,** 51-65.

Wang, Q., Li, N., Wang, X., Shen, J., Hong, X., Yu, H., Zhang, Y., Wan, T., Zhang, L., Wang, J. & Cao, X. (2007) Membrane protein hMYADM preferentially expressed in myeloid cells is up-regulated during differentiation of stem cells and myeloid leukemia cells. *Life Sci,* **80,** 420-429.

Wang, Y., Fiskus, W., Chong, D.G., Buckley, K.M., Natarajan, K., Rao, R., Joshi, A., Balusu, R., Koul, S., Chen, J., Savoie, A., Ustun, C., Jillella, A.P., Atadja, P., Levine, R.L. & Bhalla, K.N. (2009) Cotreatment with panobinostat and JAK2 inhibitor TG101209 attenuates JAK2V617F levels and signaling and exerts synergistic cytotoxic effects against human myeloproliferative neoplastic cells. *Blood,* **114,** 5024-5033.

Webber, J., Yeung, V. & Clayton, A. (2015) Extracellular vesicles as modulators of the cancer microenvironment. *Semin Cell Dev Biol,* **40,** 27-34.

Welch, J.S., Ley, T.J., Link, D.C., Miller, C.A., Larson, D.E., Koboldt, D.C., Wartman, L.D., Lamprecht, T.L., Liu, F., Xia, J., Kandoth, C., Fulton, R.S., McLellan, M.D., Dooling, D.J., Wallis, J.W., Chen, K., Harris, C.C., Schmidt, H.K., Kalicki-Veizer, J.M., Lu, C., Zhang, Q., Lin, L., O'Laughlin, M.D., McMichael, J.F., Delehaunty, K.D., Fulton, L.A., Magrini, V.J., McGrath, S.D., Demeter, R.T., Vickery, T.L., Hundal, J., Cook, L.L., Swift, G.W., Reed, J.P., Alldredge, P.A., Wylie, T.N., Walker, J.R., Watson, M.A., Heath, S.E.,

Shannon, W.D., Varghese, N., Nagarajan, R., Payton, J.E., Baty, J.D., Kulkarni, S., Klco, J.M., Tomasson, M.H., Westervelt, P., Walter, M.J., Graubert, T.A., DiPersio, J.F., Ding, L., Mardis, E.R. & Wilson, R.K. (2012) The origin and evolution of mutations in acute myeloid leukemia. *Cell,* **150,** 264-278.

Welner, R.S., Amabile, G., Bararia, D., Czibere, A., Yang, H., Zhang, H., Pontes, L.L., Ye, M., Levantini, E., Di Ruscio, A., Martinelli, G. & Tenen, D.G. (2015) Treatment of chronic myelogenous leukemia by blocking cytokine alterations found in normal stem and progenitor cells. *Cancer Cell,* **27,** 671-681.

Winkler, I.G., Barbier, V., Nowlan, B., Jacobsen, R.N., Forristal, C.E., Patton, J.T., Magnani, J.L. & Levesque, J.P. (2012) Vascular niche E-selectin regulates hematopoietic stem cell dormancy, self renewal and chemoresistance. *Nat Med,* **18,** 1651-1657.

Winkler, I.G., Barbier, V., Wadley, R., Zannettino, A.C., Williams, S. & Levesque, J.P. (2010a) Positioning of bone marrow hematopoietic and stromal cells relative to blood flow in vivo: serially reconstituting hematopoietic stem cells reside in distinct nonperfused niches. *Blood,* **116,** 375-385.

Winkler, I.G., Sims, N.A., Pettit, A.R., Barbier, V., Nowlan, B., Helwani, F., Poulton, I.J., van Rooijen, N., Alexander, K.A., Raggatt, L.J. & Levesque, J.P. (2010b) Bone marrow macrophages maintain hematopoietic stem cell (HSC) niches and their depletion mobilizes HSCs. *Blood,* **116,** 4815-4828.

Wolfson, N.A., Pitcairn, C.A. & Fierke, C.A. (2013) HDAC8 substrates: Histones and beyond. *Biopolymers,* **99,** 112-126.

Xishan, Z., Guangyu, A., Yuguang, S. & Hongmei, Z. (2011) The research on the immuno-modulatory defect of mesenchymal stem cell from Chronic Myeloid Leukemia patients. *J Exp Clin Cancer Res,* **30,** 47.

Yamaoka, K., Saharinen, P., Pesu, M., Holt, V.E., 3rd, Silvennoinen, O. & O'Shea, J.J. (2004) The Janus kinases (Jaks). *Genome Biol,* **5,** 253.

Yamazaki, S., Ema, H., Karlsson, G., Yamaguchi, T., Miyoshi, H., Shioda, S., Taketo, M.M., Karlsson, S., Iwama, A. & Nakauchi, H. (2011) Nonmyelinating Schwann cells maintain hematopoietic stem cell hibernation in the bone marrow niche. *Cell,* **147,** 1146-1158.

Yan, D., Hutchison, R.E. & Mohi, G. (2012) Critical requirement for Stat5 in a mouse model of polycythemia vera. *Blood,* **119,** 3539-3549.

Yanez-Mo, M., Siljander, P.R., Andreu, Z., Zavec, A.B., Borras, F.E., Buzas, E.I., Buzas, K., Casal, E., Cappello, F., Carvalho, J., Colas, E., Cordeiro-da Silva, A., Fais, S., Falcon-Perez, J.M., Ghobrial, I.M., Giebel, B., Gimona, M., Graner, M., Gursel, I., Gursel, M., Heegaard, N.H., Hendrix, A., Kierulf, P., Kokubun, K., Kosanovic, M., Kralj-Iglic, V., Kramer-Albers, E.M., Laitinen, S., Lasser, C., Lener, T., Ligeti, E., Line, A., Lipps, G., Llorente, A., Lotvall, J., Mancek-Keber, M., Marcilla, A., Mittelbrunn, M., Nazarenko, I.,

Nolte-'t Hoen, E.N., Nyman, T.A., O'Driscoll, L., Olivan, M., Oliveira, C., Pallinger, E., Del Portillo, H.A., Reventos, J., Rigau, M., Rohde, E., Sammar, M., Sanchez-Madrid, F., Santarem, N., Schallmoser, K., Ostenfeld, M.S., Stoorvogel, W., Stukelj, R., Van der Grein, S.G., Vasconcelos, M.H., Wauben, M.H. & De Wever, O. (2015) Biological properties of extracellular vesicles and their physiological functions. *J Extracell Vesicles,* **4,** 27066.

Yoshihara, H., Arai, F., Hosokawa, K., Hagiwara, T., Takubo, K., Nakamura, Y., Gomei, Y., Iwasaki, H., Matsuoka, S., Miyamoto, K., Miyazaki, H., Takahashi, T. & Suda, T. (2007) Thrombopoietin/MPL signaling regulates hematopoietic stem cell quiescence and interaction with the osteoblastic niche. *Cell Stem Cell,* **1,** 685-697.

Zhang, J., Niu, C., Ye, L., Huang, H., He, X., Tong, W.G., Ross, J., Haug, J., Johnson, T., Feng, J.Q., Harris, S., Wiedemann, L.M., Mishina, Y. & Li, L. (2003) Identification of the haematopoietic stem cell niche and control of the niche size. *Nature,* **425,** 836-841.

Zhao, R., Xing, S., Li, Z., Fu, X., Li, Q., Krantz, S.B. & Zhao, Z.J. (2005) Identification of an acquired JAK2 mutation in polycythemia vera. *J Biol Chem,* **280,** 22788-22792.

Supplementary Appendix

Supplementary Table 1: Differential Up (red) Down (green) – regulated expression genes in BM-MSC from CML patients contrasted against HD.

ID	logFC	AveExpr	P.Value	adj.P.Val	gene_symbol	biotype
ENSG00000206653	-1,198	10,74441	0,0001	0,0455	SNORD29	snoRNA
ENSG00000172992	-0,878	11,05065	0,0000	0,0312	DCAKD	protein_coding
ENSG00000228834	-0,856	10,69114	0,0000	0,0174	RP11-249L21.3	pseudogene
ENSG00000179820	-0,807	12,30798	0,0000	0,0002	MYADM	protein_coding
ENSG00000102119	-0,785	10,65757	0,0000	0,0375	EMD	protein_coding
ENSG00000023902	-0,746	9,272683	0,0000	0,0320	PLEKHO1	protein_coding
ENSG00000103005	-0,731	9,106761	0,0001	0,0423	C16orf57	protein_coding
ENSG00000133678	-0,703	10,96507	0,0000	0,0051	RP11-369J21.2	protein_coding
ENSG00000158710	-0,695	11,47564	0,0000	0,0305	TAGLN2	protein_coding
ENSG00000076067	-0,684	11,53077	0,0000	0,0317	RBMS2	protein_coding
ENSG00000089693	-0,651	12,10153	0,0000	0,0172	MLF2	protein_coding
ENSG00000087111	-0,642	10,40432	0,0000	0,0317	PIGS	protein_coding
ENSG00000100196	-0,642	12,1138	0,0001	0,0473	KDELR3	protein_coding
ENSG00000101464	-0,635	10,25713	0,0001	0,0425	PIGU	protein_coding
ENSG00000187838	-0,62	10,2464	0,0001	0,0455	PLSCR3	protein_coding
ENSG00000143252	-0,61	8,910272	0,0000	0,0317	SDHC	protein_coding
ENSG00000162419	-0,601	8,964494	0,0000	0,0053	GMEB1	protein_coding
ENSG00000176422	-0,598	8,523831	0,0000	0,0211	SPRYD4	protein_coding
ENSG00000173402	-0,59	10,38109	0,0001	0,0493	DAG1	protein_coding
ENSG00000011198	-0,56	10,3454	0,0001	0,0403	ABHD5	protein_coding
ENSG00000119414	-0,524	12,22531	0,0000	0,0053	PPP6C	protein_coding
ENSG00000140497	-0,498	11,21762	0,0001	0,0433	SCAMP2	protein_coding
ENSG00000219200	-0,488	13,24832	0,0000	0,0161	RNASEK	protein_coding
ENSG00000156253	-0,476	10,5179	0,0001	0,0425	RWDD2B	protein_coding
ENSG00000159063	-0,442	10,96351	0,0000	0,0317	ALG8	protein_coding
ENSG00000183283	-0,426	11,7132	0,0000	0,0317	DAZAP2	protein_coding
ENSG00000177981	-0,419	11,19727	0,0000	0,0172	ASB8	protein_coding
ENSG00000173914	-0,397	10,28316	0,0000	0,0375	RBM4B	protein_coding
ENSG00000138463	-0,373	10,75682	0,0001	0,0450	DIRC2	protein_coding
ENSG00000160714	-0,359	11,46092	0,0001	0,0403	UBE2Q1	protein_coding
ENSG00000115806	-0,347	11,79658	0,0001	0,0416	GORASP2	protein_coding
ENSG00000240339	0,2254	4,705539	0,0001	0,0455	AP000351.2	Mt_tRNA_pseudogene
ENSG00000243202	0,2507	5,577353	0,0001	0,0473	AC107956.1	scRNA_pseudogene
ENSG00000130254	0,2925	8,630656	0,0000	0,0317	SAFB2	protein_coding
ENSG00000197037	0,2936	7,984107	0,0001	0,0493	ZNF498	protein_coding
ENSG00000148296	0,3656	7,257902	0,0000	0,0195	SURF6	protein_coding
ENSG00000169871	0,3807	8,175019	0,0000	0,0317	TRIM56	protein_coding
ENSG00000075856	0,4308	8,758453	0,0000	0,0195	SART3	protein_coding
ENSG00000091640	0,4639	8,908877	0,0001	0,0409	SPAG7	protein_coding
ENSG00000213755	0,5124	5,806739	0,0000	0,0305	RP11-342F17.1	pseudogene
ENSG00000125691	0,5418	12,39951	0,0000	0,0051	RPL23	protein_coding
ENSG00000237745	0,5692	12,05774	0,0000	0,0174	AC009963.3	pseudogene
ENSG00000196295	0,7743	7,020675	0,0000	0,0174	AC005154.6	processed_transcript
ENSG00000242944	0,9253	10,66072	0,0001	0,0450	AD000090.2	rRNA_pseudogene
ENSG00000210140	1,232	11,61962	0,0001	0,0493	J01415.28	Mt_tRNA
ENSG00000242900	1,3361	6,165952	0,0000	0,0161	AC097526.11	Mt_tRNA_pseudogene

ENSG00000210144	1,429	11,43491	0,0001	0,0388	J01415.10	Mt_tRNA
ENSG00000242752	1,4811	5,997306	0,0000	0,0195	AC025627.1	Mt_tRNA_pseudogene
ENSG00000240234	2,0012	8,531542	0,0000	0,0030	AC131055.17	Mt_tRNA_pseudogene
ENSG00000242240	2,3795	9,57558	0,0000	0,0005	AC073869.19	Mt_tRNA_pseudogene
ENSG00000210117	3,1647	9,575726	0,0000	0,0172	J01415.25	Mt_tRNA

Supplementary Table 2: Differential Up (red) Down (green) – regulated expression genes in BM-MSC from PV patients contrasted against HD.

ID	logFC	AveExpr	P.Value	adj.P.Val	gene_symbol	biotype
ENSG00000179820	-0,913	12,308	0,0000	0,0003	MYADM	**protein_coding**
ENSG00000089693	-0,88	12,1015	0,0000	0,0077	MLF2	protein_coding
ENSG00000173914	-0,619	10,2832	0,0000	0,0077	RBM4B	protein_coding
ENSG00000103005	-1,03	9,10676	0,0000	0,0097	C16orf57	protein_coding
ENSG00000115806	-0,51	11,7966	0,0000	0,0114	GORASP2	protein_coding
ENSG00000176422	-0,781	8,52383	0,0000	0,0114	SPRYD4	protein_coding
ENSG00000101464	-0,915	10,2571	0,0000	0,0114	PIGU	protein_coding
ENSG00000158825	-0,871	7,14014	0,0000	0,0114	CDA	protein_coding
ENSG00000184584	-1,088	9,88173	0,0000	0,0114	TMEM173	protein_coding
ENSG00000228834	-1,041	10,6911	0,0000	0,0114	RP11-249L21.3	pseudogene
ENSG00000140497	-0,707	11,2176	0,0000	0,0114	SCAMP2	protein_coding
ENSG00000100196	-0,913	12,1138	0,0000	0,0114	KDELR3	protein_coding
ENSG00000125149	-0,712	9,8079	0,0000	0,0114	C16orf70	protein_coding
ENSG00000119414	-0,551	12,2253	0,0000	0,0114	PPP6C	protein_coding
ENSG00000133678	-0,719	10,9651	0,0000	0,0114	RP11-369J21.2	protein_coding
ENSG00000158710	-0,869	11,4756	0,0000	0,0114	TAGLN2	protein_coding
ENSG00000086848	-0,404	9,2107	0,0000	0,0133	FDXACB1	protein_coding
ENSG00000177981	-0,475	11,1973	0,0000	0,0146	ASB8	protein_coding
ENSG00000076067	-0,867	11,5308	0,0000	0,0146	RBMS2	protein_coding
ENSG00000105991	-0,601	7,19679	0,0000	0,0146	HOXA1	protein_coding
ENSG00000170043	-0,679	12,1044	0,0000	0,0160	TRAPPC1	protein_coding
ENSG00000162736	-0,523	11,5362	0,0000	0,0160	NCSTN	protein_coding
ENSG00000139998	-1,259	7,98604	0,0000	0,0160	RAB15	protein_coding
ENSG00000187838	-0,816	10,2464	0,0000	0,0160	PLSCR3	protein_coding
ENSG00000147403	-0,61	12,8932	0,0000	0,0160	RPL10	protein_coding
ENSG00000134779	-0,62	11,4564	0,0000	0,0160	C18orf10	protein_coding
ENSG00000141756	-0,477	12,6345	0,0000	0,0160	FKBP10	protein_coding
ENSG00000147099	-0,598	9,87112	0,0000	0,0160	HDAC8	protein_coding
ENSG00000120509	-0,639	8,17884	0,0000	0,0166	PDZD11	protein_coding
ENSG00000144043	-0,653	11,2335	0,0000	0,0180	TEX261	protein_coding
ENSG00000103429	-0,505	10,7062	0,0000	0,0180	BFAR	protein_coding
ENSG00000180304	-0,773	9,58422	0,0000	0,0190	OAZ2	protein_coding
ENSG00000188917	-0,546	8,11408	0,0000	0,0196	TRMT2B	protein_coding
ENSG00000134287	-0,564	12,0757	0,0000	0,0201	ARF3	protein_coding
ENSG00000124164	-0,426	9,98444	0,0000	0,0201	VAPB	protein_coding
ENSG00000143252	-0,716	8,91027	0,0000	0,0203	SDHC	protein_coding
ENSG00000102119	-0,934	10,6576	0,0000	0,0224	EMD	protein_coding
ENSG00000158161	-0,646	8,72548	0,0000	0,0224	EYA3	protein_coding
ENSG00000168227	-0,306	4,99745	0,0000	0,0227	AL079307.1	pseudogene
ENSG00000011198	-0,678	10,3454	0,0000	0,0227	ABHD5	protein_coding

ENSG00000213760	-1,151	7,79946	0,0000	0,0227	ATP6V1G2	protein_coding
ENSG00000087111	-0,727	10,4043	0,0000	0,0227	PIGS	protein_coding
ENSG00000159063	-0,511	10,9635	0,0000	0,0227	ALG8	protein_coding
ENSG00000025800	-0,419	11,359	0,0000	0,0227	KPNA6	protein_coding
ENSG00000214160	-0,773	11,2461	0,0001	0,0245	ALG3	protein_coding
ENSG00000173402	-0,736	10,3811	0,0001	0,0246	DAG1	protein_coding
ENSG00000131779	-0,78	10,7443	0,0001	0,0246	PEX11B	protein_coding
ENSG00000134910	-0,356	12,7155	0,0001	0,0246	STT3A	protein_coding
ENSG00000206697	-0,247	4,70656	0,0001	0,0246	Y_RNA	misc_RNA
ENSG00000127463	-0,502	10,1881	0,0001	0,0246	KIAA0090	protein_coding
ENSG00000109066	-0,951	9,28432	0,0001	0,0246	TMEM104	protein_coding
ENSG00000144231	-0,535	9,86265	0,0001	0,0246	POLR2D	protein_coding
ENSG00000159840	-0,738	12,0045	0,0001	0,0246	ZYX	protein_coding
ENSG00000177105	-0,705	10,8891	0,0001	0,0246	RHOG	protein_coding
ENSG00000171792	-0,664	10,4625	0,0001	0,0246	C12orf32	protein_coding
ENSG00000100865	-0,548	10,0112	0,0001	0,0246	CINP	protein_coding
ENSG00000105341	-0,552	9,89154	0,0001	0,0246	ATP5SL	protein_coding
ENSG00000126970	-0,71	8,36453	0,0001	0,0246	ZC4H2	protein_coding
ENSG00000214517	-0,844	11,5372	0,0001	0,0246	PPME1	protein_coding
ENSG00000176871	-0,652	11,7434	0,0001	0,0246	WSB2	protein_coding
ENSG00000173065	-0,614	9,15411	0,0001	0,0250	C17orf63	protein_coding
ENSG00000108518	-0,651	12,5405	0,0001	0,0274	PFN1	protein_coding
ENSG00000237758	-0,783	11,2674	0,0001	0,0274	AC084031.2	pseudogene
ENSG00000109519	-0,529	9,76648	0,0001	0,0274	GRPEL1	protein_coding
ENSG00000184988	-1,278	8,74942	0,0001	0,0283	TMEM106A	protein_coding
ENSG00000177370	-0,558	10,6932	0,0001	0,0284	TIMM22	protein_coding
ENSG00000122203	-0,666	11,0962	0,0001	0,0286	KIAA1191	protein_coding
ENSG00000103121	-0,617	11,7125	0,0001	0,0301	C16orf61	protein_coding
ENSG00000139579	-0,65	10,74	0,0001	0,0305	OBFC2B	protein_coding
ENSG00000126067	-0,419	11,9904	0,0001	0,0305	PSMB2	protein_coding
ENSG00000183444	-0,975	9,90172	0,0001	0,0305	AC004967.6	pseudogene
ENSG00000213533	-0,706	10,0429	0,0001	0,0310	TMEM110	protein_coding
ENSG00000102007	-0,772	12,4461	0,0001	0,0310	PLP2	protein_coding
ENSG00000131467	-0,583	11,4473	0,0001	0,0316	PSME3	protein_coding
ENSG00000187446	-0,527	12,3693	0,0001	0,0316	AC012652.1	protein_coding
ENSG00000163191	-0,538	13,0987	0,0001	0,0328	S100A11	protein_coding
ENSG00000171889	-1,383	9,35891	0,0001	0,0333	RP11-354P17.1	processed_transcript
ENSG00000130731	-0,611	8,98163	0,0001	0,0335	C16orf13	protein_coding
ENSG00000176340	-0,926	11,1231	0,0001	0,0349	COX8A	protein_coding
ENSG00000140830	-0,605	8,6955	0,0001	0,0355	TXNL4B	protein_coding
ENSG00000174903	-0,745	12,1389	0,0001	0,0355	RAB1B	protein_coding
ENSG00000160746	-0,682	10,8961	0,0001	0,0355	ANO10	protein_coding
ENSG00000147100	-1,411	9,59391	0,0001	0,0355	SLC16A2	protein_coding
ENSG00000147224	-1,437	10,5916	0,0001	0,0355	PRPS1	protein_coding
ENSG00000219200	-0,448	13,2483	0,0001	0,0355	RNASEK	protein_coding
ENSG00000050438	-0,648	6,32168	0,0001	0,0355	SLC4A8	protein_coding
ENSG00000106511	-0,984	8,48998	0,0001	0,0355	MEOX2	protein_coding
ENSG00000221988	-0,932	7,7227	0,0001	0,0362	PPT2	protein_coding
ENSG00000172992	-0,904	11,0507	0,0001	0,0362	DCAKD	protein_coding
ENSG00000109062	-0,682	9,35106	0,0001	0,0362	SLC9A3R1	protein_coding
ENSG00000114395	-0,799	8,19884	0,0001	0,0362	CYB561D2	protein_coding
ENSG00000127329	-0,64	5,85214	0,0002	0,0362	PTPRB	protein_coding

ENSG00000172757	-0,531	13,0548	0,0002	0,0362	CFL1	protein_coding
ENSG00000141030	-0,413	10,7665	0,0002	0,0362	COPS3	protein_coding
ENSG00000108774	-0,382	12,9279	0,0002	0,0362	RAB5C	protein_coding
ENSG00000101337	-0,497	10,8953	0,0002	0,0371	TM9SF4	protein_coding
ENSG00000160446	-0,7	10,4786	0,0002	0,0371	ZDHHC12	protein_coding
ENSG00000136240	-0,422	12,5765	0,0002	0,0375	KDELR2	protein_coding
ENSG00000141499	-0,463	7,89447	0,0002	0,0381	WRAP53	protein_coding
ENSG00000023902	-0,778	9,27268	0,0002	0,0381	PLEKHO1	protein_coding
ENSG00000111669	-0,582	10,4189	0,0002	0,0381	TPI1	protein_coding
ENSG00000243279	-1,024	11,0704	0,0002	0,0387	PRAF2	protein_coding
ENSG00000241468	-0,83	10,9631	0,0002	0,0387	ATP5J2	protein_coding
ENSG00000135956	-0,635	11,4194	0,0002	0,0387	TMEM127	protein_coding
ENSG00000162419	-0,48	8,96449	0,0002	0,0399	GMEB1	protein_coding
ENSG00000139531	-0,618	8,13392	0,0002	0,0407	SUOX	protein_coding
ENSG00000160714	-0,379	11,4609	0,0002	0,0417	UBE2Q1	protein_coding
ENSG00000120708	-1,129	12,7278	0,0002	0,0420	TGFBI	protein_coding
ENSG00000157216	-0,528	10,1115	0,0002	0,0420	SSBP3	protein_coding
ENSG00000187534	-0,851	10,5616	0,0002	0,0422	AC007842.1	pseudogene
ENSG00000125971	-0,43	10,4283	0,0002	0,0423	DYNLRB1	protein_coding
ENSG00000105438	-0,573	11,8186	0,0002	0,0425	KDELR1	protein_coding
ENSG00000170633	-0,48	9,2245	0,0002	0,0425	RNF34	protein_coding
ENSG00000144120	-0,582	8,25572	0,0002	0,0425	TMEM177	protein_coding
ENSG00000197728	-1,21	9,39335	0,0002	0,0425	RPS26	protein_coding
ENSG00000062485	-0,523	11,6361	0,0002	0,0425	CS	protein_coding
ENSG00000128340	-1,56	9,07757	0,0002	0,0425	RAC2	protein_coding
ENSG00000135074	-1,409	8,65956	0,0002	0,0425	ADAM19	protein_coding
ENSG00000228285	-0,702	8,81161	0,0002	0,0430	LYPLA2P1	pseudogene
ENSG00000169372	-0,485	8,62715	0,0002	0,0430	CRADD	protein_coding
ENSG00000123353	-0,597	11,0127	0,0002	0,0435	ORMDL2	protein_coding
ENSG00000155366	-0,654	12,183	0,0002	0,0435	RHOC	protein_coding
ENSG00000132801	-0,542	6,9645	0,0002	0,0438	ZSWIM3	protein_coding
ENSG00000141349	-0,742	10,8263	0,0002	0,0445	G6PC3	protein_coding
ENSG00000127780	-0,215	4,88522	0,0002	0,0445	OR1E2	protein_coding
ENSG00000142230	-0,505	10,7459	0,0003	0,0453	SAE1	protein_coding
ENSG00000239334	-0,36	5,61432	0,0003	0,0453	GSTTP2	processed_transcript
ENSG00000136715	-0,595	10,4446	0,0003	0,0453	SAP130	protein_coding
ENSG00000109079	-0,721	10,8449	0,0003	0,0453	TNFAIP1	protein_coding
ENSG00000137073	-0,469	10,1549	0,0003	0,0467	UBAP2	protein_coding
ENSG00000092847	-0,399	10,0216	0,0003	0,0467	EIF2C1	protein_coding
ENSG00000182195	-1,059	10,0649	0,0003	0,0467	LDOC1	protein_coding
ENSG00000100558	-0,74	6,59212	0,0003	0,0469	PLEK2	protein_coding
ENSG00000231192	-0,221	4,32163	0,0003	0,0475	OR5H1	protein_coding
ENSG00000174021	-0,559	10,8632	0,0003	0,0475	GNG5	protein_coding
ENSG00000077721	-0,646	11,0012	0,0003	0,0475	UBE2A	protein_coding
ENSG00000119777	-0,536	11,4247	0,0003	0,0476	TMEM214	protein_coding
ENSG00000151348	-0,332	11,846	0,0003	0,0476	EXT2	protein_coding
ENSG00000118680	-0,333	13,0533	0,0003	0,0490	MYL12B	protein_coding
ENSG00000159335	-0,625	11,2267	0,0003	0,0490	PTMS	protein_coding
ENSG00000081177	-0,279	9,43746	0,0003	0,0499	EXD2	protein_coding
ENSG00000138738	0,645	8,29697	0,0003	0,0467	PRDM5	protein_coding
ENSG00000199438	0,457	6,28652	0,0003	0,0466	5S_rRNA	rRNA
ENSG00000116117	0,725	8,80956	0,0003	0,0451	PARD3B	protein_coding

ENSG00000065320	0,393	8,13004	0,0002	0,0423	NTN1	protein_coding
ENSG00000125691	0,422	12,3995	0,0002	0,0391	RPL23	protein_coding
ENSG00000148296	0,347	7,2579	0,0002	0,0375	SURF6	protein_coding
ENSG00000242900	1,257	6,16595	0,0001	0,0314	AC097526.11	Mt_tRNA_pseudogene
ENSG00000100650	0,775	10,7951	0,0001	0,0305	SFRS5	protein_coding
ENSG00000154114	0,537	10,1584	0,0001	0,0305	TBCEL	protein_coding
ENSG00000188375	0,552	11,1899	0,0001	0,0274	H3F3C	protein_coding
ENSG00000244577	0,416	8,56961	0,0000	0,0227	AC137932.3	scRNA_pseudogene
ENSG00000242752	1,652	5,99731	0,0000	0,0192	AC025627.1	Mt_tRNA_pseudogene
ENSG00000169871	0,471	8,17502	0,0000	0,0160	TRIM56	protein_coding
ENSG00000240234	1,952	8,53154	0,0000	0,0114	AC131055.17	Mt_tRNA_pseudogene
ENSG00000242240	2,152	9,57558	0,0000	0,0114	AC073869.19	Mt_tRNA_pseudogene
ENSG00000153046	0,515	8,95551	0,0000	0,0077	CDYL	protein_coding

Supplementary Table : Differential Up (red) Down (green) – regulated expression genes in BM-MSC from ET patients contrasted against HD.

ID	logFC	AveExpr	P.Value	adj.P.Val	gene_symbol	biotype
ENSG00000127946	-0,972	8,408285	0,0000	0,0257	HIP1	protein_coding
ENSG00000228834	-0,906	10,69114	0,0000	0,0315	RP11-249L21.3	pseudogene
ENSG00000243685	-0,833	5,752575	0,0000	0,0026	AL122001.1	scRNA_pseudogene
ENSG00000101464	-0,814	10,25713	0,0000	0,0257	PIGU	protein_coding
ENSG00000143252	-0,772	8,910272	0,0000	0,0257	SDHC	protein_coding
ENSG00000133678	-0,76	10,96507	0,0000	0,0185	RP11-369J21.2	protein_coding
ENSG00000179820	-0,744	12,30798	0,0000	0,0041	MYADM	protein_coding
ENSG00000119242	-0,724	11,01909	0,0001	0,0467	CCDC92	protein_coding
ENSG00000089693	-0,714	12,10153	0,0000	0,0257	MLF2	protein_coding
ENSG00000176422	-0,682	8,523831	0,0000	0,0257	SPRYD4	protein_coding
ENSG00000173914	-0,609	10,28316	0,0000	0,0124	RBM4B	protein_coding
ENSG00000140497	-0,601	11,21762	0,0000	0,0394	SCAMP2	protein_coding
ENSG00000187446	-0,591	12,36932	0,0000	0,0266	AC012652.1	protein_coding
ENSG00000162419	-0,578	8,964494	0,0000	0,0257	GMEB1	protein_coding
ENSG00000134779	-0,566	11,4564	0,0001	0,0463	C18orf10	protein_coding
ENSG00000081853	-0,557	8,182415	0,0000	0,0257	PCDHGC5	protein_coding
ENSG00000119414	-0,532	12,22531	0,0000	0,0257	PPP6C	protein_coding
ENSG00000177981	-0,513	11,19727	0,0000	0,0185	ASB8	protein_coding
ENSG00000214770	-0,457	5,461314	0,0000	0,0256	AL161756.1	protein_coding
ENSG00000141030	-0,457	10,76647	0,0000	0,0391	COPS3	protein_coding
ENSG00000115806	-0,456	11,79658	0,0000	0,0257	GORASP2	protein_coding
ENSG00000165078	-0,429	5,3891	0,0000	0,0256	CPA6	protein_coding
ENSG00000201957	-0,201	4,51223	0,0000	0,0257	SNORA25	snoRNA
ENSG00000172487	-0,197	4,686754	0,0001	0,0488	OR8J1	protein_coding
ENSG00000243202	0,3146	5,577353	0,0000	0,0266	AC107956.1	scRNA_pseudogene
ENSG00000244112	0,3729	6,051949	0,0000	0,0266	AC087885.1	scRNA_pseudogene
ENSG00000188732	0,3816	5,597397	0,0001	0,0467	C7orf46	protein_coding
ENSG00000153046	0,4092	8,955514	0,0000	0,0266	CDYL	protein_coding
ENSG00000120853	0,4245	6,254706	0,0000	0,0257	GOLGA2L1	protein_coding
ENSG00000169871	0,4251	8,175019	0,0001	0,0467	TRIM56	protein_coding
ENSG00000148296	0,4255	7,257902	0,0000	0,0257	SURF6	protein_coding
ENSG00000244577	0,4482	8,569607	0,0000	0,0257	AC137932.3	scRNA_pseudogene

ENSG00000125691	0,5036	12,39951	0,0000	0,0257	RPL23	protein_coding
ENSG00000242900	1,3902	6,165952	0,0000	0,0278	AC097526.11	Mt_tRNA_pseudogene
ENSG00000240234	1,8453	8,531542	0,0000	0,0257	AC131055.17	Mt_tRNA_pseudogene
ENSG00000242240	2,0915	9,57558	0,0000	0,0185	AC073869.19	Mt_tRNA_pseudogene

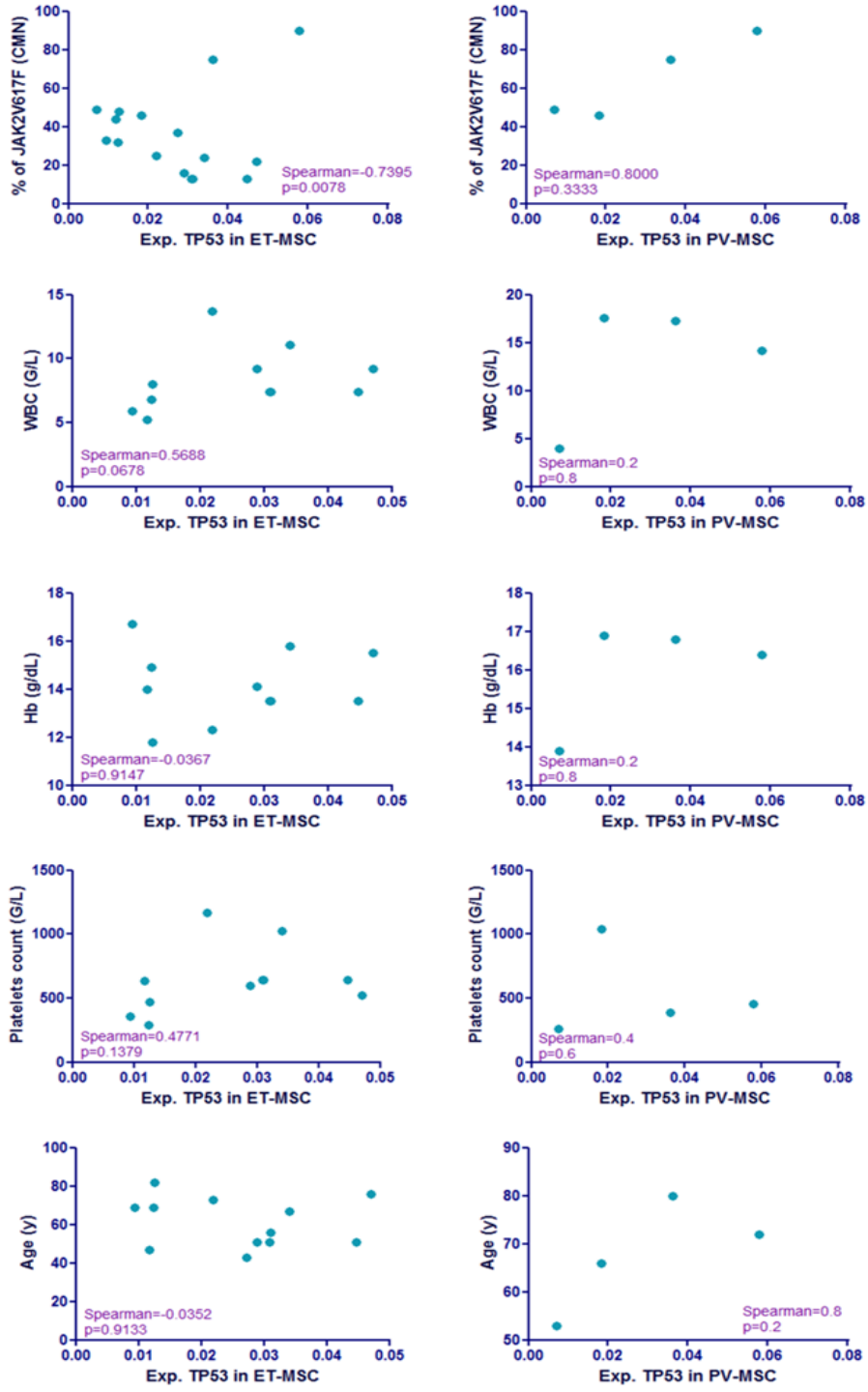

Supplementary Figure 1: Correlation coefficient graph. Correlation between the TP53 expression in the MSC from ET with the % of JAK2^{V617F}, Hb (Hemoglobin), Age (y-years), Platelets Count and WBC (With Blood Count)